

学位論文

Two-Particle Channels in Lattice QCD
(格子QCDにおける二粒子チャンネル)

平成26年7月博士(理学)申請
東京大学大学院理学系研究科
物理学専攻

シャロン ブリュノー アンドレ

Abstract

The de facto standard method for the study of two-particle channels from lattice QCD consists in first extracting the finite-volume spectrum from lattice correlators using the variational method and then relating it to the infinite-volume scattering phase shifts using the finite-size formula introduced by Lüscher or one of its generalizations. This approach has been applied successfully to a large number of two-particle channels, paving the way for a complete ab-initio description of hadron physics. The HAL QCD method is a more recent addition to this field and proposes an alternative way to extract the scattering phase shifts of a two-particle system from lattice QCD simulations. Wave function-like correlators are computed on the lattice which can be related to the scattering phase shifts in infinite volume. The energy-dependence of these wave functions is modeled by a non-local kernel through the Schrödinger equation and this kernel is approximated from lattice input, leading to predictions for the scattering phase shifts in the whole elastic energy region.

A part of this thesis is dedicated to the numerical application of the HAL QCD method to various meson-meson channels. In particular, we study the pion-pion channel in the isospin $I = 1$ and $I = 2$ channels. For $I = 2$, the HAL QCD method allows us to extract the scattering phase shifts from simulations at a pion mass of $m_\pi = 700$ MeV. The $I = 1$ P-wave channel contains the rho meson and is particularly challenging. The HAL QCD method is found to face difficulties in this channels which only allows us to acquire a qualitative understanding of the interaction. We also study several charmed meson-meson channels which have been predicted to host tetraquark bound states by some quark model calculations. No bound state is found in the pion mass range $m_\pi = 410 \sim 700$ MeV and the quark-mass dependence of the results hints at the absence of bound states at the physical point.

Another part of this thesis is dedicated to improve the theoretical tools available for the study of two-particle channels in lattice QCD. We first show how the HAL QCD method can be extended to treat the interaction above the inelastic threshold for both coupled two-particle channels and channels with more than two particles. We then go on to propose two new methods which address some of the criticisms of the HAL QCD method while retaining its core ideas. Firstly, the effective potential method is a new way to extract the finite-volume spectrum for two-particle channels. It extends the variational method to rectangular correlation matrices which are used to parameterize an effective Hamiltonian operator. The finite-volume spectrum is then related to the spectrum of this operator. Secondly, the kernel approximation method is a rigorous alternative to the HAL QCD method based on an extensive study of the finite-volume effects. It relies on the same wave function-like correlators in finite volume, which we directly relate to the infinite-volume Bethe-Salpeter kernel. The properties of this kernel are then used to study the energy-dependence of the correlators as well as the

mixing of their angular momentum components by the cubic group. This leads to a well-defined strategy to extract the scattering phase shifts. Our two newly proposed methods are compared numerically to the previously available ones and are found to be both correct and efficient.

Contents

Abstract	ii
Contents	v
1 Introduction	1
2 Lattice quantum chromodynamics	5
2.1 Quantum field theory	5
2.1.1 Wick rotation	5
2.1.2 Path integral	6
2.2 QCD on a computer	8
2.2.1 QCD in the continuum	8
2.2.2 QCD on a lattice	10
2.2.3 Computation	13
2.3 Lattice spectroscopy	14
2.3.1 Euclidean correlators	14
2.3.2 Spectrum extraction	15
3 Two-particle channels	17
3.1 Scattering theory	17
3.1.1 Classical mechanics	17
3.1.2 Quantum mechanics	19
3.1.3 Quantum field theory	22
3.2 Finite-size method	24
3.2.1 Two-particle states on a torus	25
3.2.2 Potential in QFT	30
3.3 HAL QCD method	33
3.3.1 Bethe-Salpeter wave function	33
3.3.2 Energy-independent potential	37
4 Towards better methods	41
4.1 HAL QCD method above the inelastic threshold	41
4.1.1 Multi-particle channels	41
4.1.2 Coupled two-particle channels	47
4.2 Effective potential method	48
4.2.1 Effective Hamiltonian	49
4.2.2 Effective potential	52

4.2.3	<i>Qualitative comparison with other methods</i>	54
4.3	Kernel approximation method	54
4.3.1	<i>The 4-point function</i>	55
4.3.2	<i>Finite-volume spectrum</i>	61
4.3.3	<i>Description of the method</i>	69
5	Numerical applications	75
5.1	Comparing the methods in the two-pion $I = 2$ channel	75
5.1.1	<i>Simulations details</i>	75
5.1.2	<i>HAL QCD method</i>	76
5.1.3	<i>Kernel approximation method</i>	82
5.1.4	<i>Variational and effective potential methods</i>	84
5.2	Study of the rho meson channel	87
5.2.1	<i>Computation method</i>	88
5.2.2	<i>Simulation results</i>	91
5.3	Search for tetraquark bound states	93
5.3.1	<i>Quark model predictions</i>	93
5.3.2	<i>Simulation details</i>	94
5.3.3	<i>Numerical results</i>	95
6	Summary	101
	Acknowledgments	104
A	Details for the effective potential method	107
A.1	Effective Hamiltonian perturbation	107
A.1.1	<i>Notations and preliminary result</i>	107
A.1.2	<i>General case</i>	108
A.1.3	<i>Effective Hamiltonian</i>	109
A.2	Lattice operators and cubic symmetry	110
A.2.1	<i>Open boundary conditions</i>	110
A.2.2	<i>Periodic boundary conditions</i>	111
A.3	Inversion problems	112
A.3.1	<i>Basic strategy</i>	112
A.3.2	<i>Inversion with locality constraint</i>	113
A.3.3	<i>Inversion with Hermiticity and locality constraints</i>	114
B	Details for the kernel approximation method	117
B.1	Fourier transform of a 3D compactly supported function	117
B.2	Relation between the finite- and infinite-volume 4-point functions	118
	Bibliography	121

Introduction

Physics, as a science, finds value in its predictions of the natural phenomena of our world. Probably the first and simplest phenomenon that a student in Physics learns to describe mathematically, hence becoming capable to derive quantitative predictions, is the motion of a body in free fall. It is simple because it only involves two bodies: the Earth and, say, a ball which interact in a well-known manner. However, the ball and the Earth are not elementary objects but composed of many subcomponents so that a more accurate description of the phenomenon is theoretically possible. A calculation from first-principles, or *ab-initio*, is a prediction for some phenomenon which considers directly the interaction of its elementary subcomponents. This thesis attempts to contribute towards an ideal of Physics which is to describe any physical system from the very basic constituents of the universe: elementary particles.

To date, the known elementary particles are 6 flavors of quarks (up, down, strange, charm, bottom, top), as many leptons (electron, electron neutrino, muon, muon neutrino, tau, tau neutrino), the antiparticle partners of the quarks and leptons as well as 5 gauge bosons (photon, gluon, W^+ , W^- and Z^0). The Standard Model (SM) of particle physics is a theory which attempts to describe the properties of these elementary particles and their interactions through all the known elementary forces but gravity: electromagnetism, the weak force and the strong force. Since its finalization in the mid-1970s, it has found unprecedented success in the experimental validation of its prediction so that it is generally accepted as a correct representation of our world, at least within the energy scales currently accessible by experiments.

Any natural phenomenon will unavoidably be the combined result of the four elementary interactions. At the scales considered in particle physics, gravity is completely negligible. As for electromagnetism and the weak force, we will only consider in this thesis phenomena for which their contributions are also negligible compared to that of the strong force at the currently accessible degree of accuracy.

Quantum chromodynamics (QCD) is the subset of the SM that attempts to explain the strong force, i.e. the force which in particular helps keep the atomic nuclei bound in spite of the electromagnetic repulsion between protons. While the theoretical formulation of QCD is quite concise, it leads to a very rich array of natural phenomena. A characteristic feature of QCD is asymptotic freedom [5], which implies that the strong interaction actually becomes weaker and weaker as the energy increases. At large energies (compared to $\Lambda_{\text{QCD}} \sim 200$ MeV) such as the ones encountered in collision experiments, the theory can therefore be treated perturbatively in a numerically efficient way and the success of the resulting predictions so far have established the correctness of QCD.

As the energy goes below Λ_{QCD} , the interaction in QCD becomes too strong to be treated as a perturbation and non-perturbative calculations are needed to extract any quantitative predictions. This corresponds to distances at or above $\Lambda_{\text{QCD}}^{-1} \sim 1 \text{ fm}$ ($= 10^{-15} \text{ m}$), which is around the size of the nucleons. Until recently, the physics at these scales was mostly described by phenomenological models fitted to experimental values. The advent of lattice QCD, a fully non-perturbative quantitative treatment of QCD pioneered by Wilson [6], has opened the way to ab-initio predictions of nuclear physics and in general any phenomenon dominated by the strong interaction.

Due to confinement, another characteristic feature of QCD, the quarks and anti-quarks cannot be observed in isolation but only in certain composite particles called hadrons. The experimentally established hadrons can be grouped into two categories: the baryons (which include the nuclei) are composed of three quarks and the mesons are composed of a quark and an antiquark. This thesis is dedicated to apply and improve the methods for the non-perturbative, ab-initio study using lattice QCD of the interaction between hadrons. Although the methods can be generalized to any hadrons, the applications considered in this thesis are restricted to the interaction between two mesons.

While many physicists or engineers routinely tackle highly complexified versions of the Earth and ball problem involving a huge number of subcomponents, it may seem that the interaction of two mesons is not much of a challenge. The difficulty arises in the fact that a meson is actually not simply composed of a quark and an antiquark and that the quarks and antiquarks are not particles in the classical sense. As a quantum field theory (QFT), QCD describes the quarks, antiquarks and gluons in the form of quantized fields, the physical particles being identified with the excited states of their associated field.

In the path integral formalism, quantitative predictions of a QFT for some physical process are obtained by summing the contribution to this process of all the possible states of the fields of the theory. Schematically, this leads to two principal difficulties: (i) the sum is performed over an infinite number of degrees of freedom because the fields take values at each position in space-time and (ii) the contributions are all of the same order, meaning that the final result is only finite if all the contributions (an infinity) are considered. Lattice QCD overcomes these issues by (i) restricting the space-time to a finite lattice so that the theory has a finite number of degrees of freedom and (ii) considering imaginary (Euclidean) times so that the contributions are exponentially suppressed in some functional of the fields and only the most important ones need to be considered.

The discretization and restriction of space-time to a finite lattice induces corrections which need to be treated carefully but disappear as the continuum and infinite-volume limits are taken. However, the fact that lattice QCD calculations are in Euclidean space (imaginary time) severely restricts the set of possible predictions for real-world phenomena. Indeed, it is well-known that a finite set of predictions in Euclidean space cannot be analytically continued to predictions at real (Minkowski) times. Predictions which are actually accessible to lattice QCD calculations include the spectrum of the theory and some matrix elements.

Lattice spectroscopy is the name of the field concerned by the study of the spectrum in lattice QCD, which has already encountered great success towards reproducing the mass spectrum of QCD [7]. The light hadron masses, computed from the spectrum of single-particle channels, are probably the simplest observables to extract from lattice QCD with quarks but precision calculations still require very large computational

resources. It is then no surprise that the extraction of the spectrum of two-particle channels is even more demanding and that real-world predictions still lie ahead for most channels of interest. However, due to technical reasons that we will see later, lattice QCD computations are less demanding if the quark masses are set to larger-than-physical values and the resulting predictions for two-particle channels are very promising.

The systematic study of two-particle channels in lattice QCD became possible with the seminal work of Lüscher [8, 9]. He derived a direct relation between the discrete spectrum of two-particle channels in finite volume and the scattering phase shifts of the theory in infinite volume. The former is accessible to lattice calculations while the latter can be directly compared to experimental values, thereby making a bridge between theory and experiments. This formula has been the basis of most of the lattice studies of two-particle channels in the past two decades although some alternative methods have been formulated. In particular, we will discuss the HAL QCD method [10–12], named after the HAL QCD collaboration which has been formed around the initiators of the method to improve and apply it to various systems¹.

Instead of the finite-volume spectrum, the HAL QCD method is based on the computation through lattice QCD of some matrix elements reminiscent of quantum mechanical wave functions. These matrix elements, called the Bethe-Salpeter (BS) wave functions, can be related to the scattering phase shifts in infinite volume. Furthermore, a non-local but energy-independent potential can be constructed such that the BS wave functions at all energies below the inelastic threshold satisfy the Schrödinger equation for this potential. This potential and its properties are unknown but some physical arguments suggest that it could be approximated by truncation of its velocity expansion, an expansion in non-locality valid with some assumptions on the potential. Once the potential is approximated with lattice QCD inputs, the Schrödinger equation can be solved at any energy. In other words, a finite number of BS wave functions computed in lattice QCD can lead to the scattering phase shifts at any energy in the domain of validity of the approximation.

The HAL QCD method relies on a certain number of assumptions and approximations. While these have been shown to be reasonable in a few channels [13, 14], they may have hindered a wider adoption of the method outside of the HAL QCD collaboration. The HAL QCD method is often deemed too complex and not well-justified theoretically compared to Lüscher’s approach. However, it is based on the enticing idea that even in quantum field theory the interaction is “well-behaved” and may be approximated in the form of a simple kernel. In contrast, Lüscher’s formula stems less from the properties of a system than from geometric considerations arising when it is restricted to a finite box. Because it does not make assumptions on the system, it gives rigorous but limited predictions. Combining the rigor of Lüscher’s approach with the ideas of the HAL QCD method has been a central theme of this work.

The work compiled in this thesis is the result of a certain number of investigations, both theoretical and numerical, in the wide field of study of two-particle channels from lattice QCD. As its name suggests (Hadron to Atomic nuclei from Lattice QCD), the HAL QCD collaboration was created with a particular focus on the nuclear interaction. By its importance, the nuclear interaction has attracted a lot of interest but there is a large number of hadronic channels with interesting properties which could benefit from ab-initio calculations using lattice QCD. A part of this thesis is dedicated to the application of the HAL QCD method to new two-particle channels, including the

¹ The author of this thesis is a member of the HAL QCD collaboration.

challenging isospin $I = 1$ two-pion channel which required the development of new numerical techniques and several charmed meson-meson channels. Another part of this thesis stems from a reflection on the method itself and has led to an extension of the method, as well as the proposition of two new methods aiming to mitigate the shortcomings of the HAL QCD method while retaining its powerful core ideas.

* * *

This thesis is organized as follows. In Chapter 2, we explain the basics of lattice QCD. Starting with some notations and reminders in several topics of quantum field theory, we go on to describe the formulation of quantum chromodynamics as well as how this theory can be expressed in a way amenable to computer calculations. The chapter ends with a brief treatment of lattice spectroscopy which shows how physical information can be extracted from numerical results.

Chapter 3 is dedicated to the methods involved in the study of two-particle channels. We first introduce the basics of scattering theory, exploring its evolution from classical mechanics to quantum mechanics and finally quantum field theory. These basics then allow us to easily present the two currently dominant approaches to the study of two-particle channels in lattice QCD: Lüscher's formula and the HAL QCD method.

After these review chapters, Chapter 4 presents the theoretical contributions of this thesis. The first section describes how the HAL QCD method can be extended to study the properties of a system above its inelastic threshold. In the second section, we present a new method, called the effective potential method, to extract the finite-size spectrum of a theory from lattice simulations. It is a generalization of the usual variational method which incorporates the ideas of the HAL QCD method for increased efficiency but retains Lüscher's formula for the link to the scattering phase shifts. The last section introduces another new method, called the kernel approximation method, to directly extract scattering phase shifts. It is based on an extensive study of the lattice correlators in two-particle channels using the theoretical tools used to derive Lüscher's formula. By generalizing these tools, we arrive at a strategy to model the interaction in a rigorous and efficient way.

In Chapter 5, we show our numerical results for the study of several two-particle channels using lattice QCD. The first application is a comparison of all the methods presented thus far in the context of the two-pion channel with isospin $I = 2$. We then go on to the study of the more challenging two-pion channel with isospin $I = 1$ using the HAL QCD method. Finally, we show the result of an investigation of possible tetraquark bound states, again using the HAL QCD method.

A summary of this work and some concluding remarks are presented in Chapter 6. Appendices A and B provide technical details related to section 4.2, on the effective potential method, and section 4.3, on the kernel approximation method, respectively.

Lattice quantum chromodynamics

2.1 QUANTUM FIELD THEORY

Before tackling QCD, we will first introduce some notions of quantum field theory (QFT) in the context of the simpler example of a scalar field theory. QFT is a difficult framework, with still uncertain mathematical foundations and many of its subtleties are beyond the scope of this thesis. A more rigorous treatment of the objects discussed in this section can be found in standard textbooks or may be yet to be discovered. We will mainly follow ref. [15].

2.1.1 Wick rotation

Let us consider a quantum field theory of a real scalar field $\phi(x)$ which describes the physics of a particle of mass m and spin 0. In Minkowski space, the theory is characterized by the Hilbert space \mathcal{H} of physical states, containing a vacuum state $|0\rangle$ invariant under the transformations of the Poincaré group. All the information of the Hilbert space and thus the physical content of the theory can be recovered from the knowledge of the n -point correlation functions

$$\mathcal{W}(x_1, \dots, x_n) \equiv \langle 0 | \hat{\phi}(x_1) \cdots \hat{\phi}(x_n) | 0 \rangle, \quad (2.1)$$

also called Wightman functions, where $\hat{\phi}(x)$ is the quantized field which acts as an operator on \mathcal{H} and x_i are 4-dimensional vectors in Minkowski space.

While the physical theory is defined in Minkowski space, it will prove useful to consider its extension to Euclidean space for actual calculations. Continuing the coordinates to complex values, both spaces represent the same space-time. To distinguish the two, the coordinates in Minkowski space will be noted $(x^0, \mathbf{x}) = (x^0, \dots, x^3)$ while those in Euclidean space will be noted $(\mathbf{x}, x^4) = (x^1, \dots, x^4)$. The correspondence is then given by $x^0 = -ix^4$ and the spatial components left unchanged. We will call *Euclidean points* the space-time points with real Euclidean coordinates, i.e. $(x^1, \dots, x^4) \in \mathbb{R}^4$.

Provided the spectral condition, an axiom of scalar quantum field theory related to causality, the Wightman functions can be continued analytically in some region of the space with complex coordinates. In particular, we can define the Schwinger functions as the restriction of this continuation on Euclidean points,

$$\mathcal{S}(\dots, (\mathbf{x}_k, x_k^4), \dots) \equiv \mathcal{W}(\dots, (-ix_k^4, \mathbf{x}_k), \dots), \quad (x_k^1, \dots, x_k^4) \in \mathbb{R}^4, \quad (2.2)$$

with the constraint that

$$x_1^4 > x_2^4 > \dots > x_n^4. \quad (2.3)$$

The Schwinger functions can actually be shown to be defined on a much larger domain, in particular on all non-coinciding Euclidean points

$$x_j \neq x_k \quad \text{for } j \neq k. \quad (2.4)$$

Furthermore, they have the nice property to be symmetric in their arguments, which is not the case for the Wightman functions. Conversely, the Wightman functions can be recovered from the Schwinger functions.

Another important class of functions, as we will see in section 3.1.3, are the time-ordered Wightman functions

$$\mathcal{W}^T(x_1, \dots, x_n) \equiv \langle 0 | T \hat{\phi}(x_1) \cdots \hat{\phi}(x_n) | 0 \rangle, \quad (2.5)$$

where the time-ordering operator T orders the field operators $\hat{\phi}(x_k)$ from left to right by decreasing time coordinate x_k^0 . These functions can be shown to be related with the Schwinger functions by the so-called *Wick rotation*,

$$\mathcal{W}^T(\dots, (x_k^0, \mathbf{x}_k), \dots) = \lim_{\theta \rightarrow (\frac{\pi}{2})^-} \mathcal{S}(\dots, (\mathbf{x}_k, e^{i\theta} x_k^0), \dots). \quad (2.6)$$

In the following, we will write the Schwinger functions, or *Euclidean correlation functions*, as

$$\langle \hat{\phi}(x_1) \cdots \hat{\phi}(x_n) \rangle \equiv \mathcal{S}(x_1, \dots, x_n), \quad (2.7)$$

for Euclidean coordinates x_k , in contrast to the notation on the right-hand side of (2.1) where Minkowski coordinates are implied.

2.1.2 Path integral

Generating functional

The generating functional of the Euclidean correlation functions is defined as

$$Z[J] \equiv \sum_{n=0}^{\infty} \frac{1}{n!} \int d^4x_1 \cdots d^4x_n J(x_1) \cdots J(x_n) \langle \hat{\phi}(x_1) \cdots \hat{\phi}(x_n) \rangle \quad (2.8)$$

which acts on a *source* J , a classical real scalar field. The correlation functions are then simply recovered using functional derivatives as

$$\langle \hat{\phi}(x_1) \cdots \hat{\phi}(x_n) \rangle = \left. \frac{\delta^n Z[J]}{\delta J(x_1) \cdots \delta J(x_n)} \right|_{J=0} \quad (2.9)$$

The functional derivatives act as

$$\frac{\delta}{\delta f(y)} f(x) = \delta(x - y) \quad (2.10)$$

and satisfies the usual rules of differential operators. Note that (2.8) can be formally written as

$$Z[J] = \langle e^{(J, \hat{\phi})} \rangle \quad \text{with} \quad (J, f) \equiv \int d^4x J(x) f(x). \quad (2.11)$$

The connected Euclidean correlation functions $\langle \hat{\phi}(x_1) \cdots \hat{\phi}(x_n) \rangle_C$ are defined recursively by $\langle \hat{\phi}(x_1) \rangle_C \equiv \langle \hat{\phi}(x_1) \rangle$ and

$$\langle \hat{\phi}(x_1) \cdots \hat{\phi}(x_n) \rangle_C \equiv \sum_{\mathcal{P}} \langle \hat{\phi}(x_i) \cdots \hat{\phi}(x_j) \rangle_C \cdots \langle \hat{\phi}(x_k) \cdots \hat{\phi}(x_l) \rangle_C \quad (2.12)$$

where the sum is over all partitions \mathcal{P} of the set $\{1, \dots, n\}$. They can also be recovered from the generating functional as

$$\langle \hat{\phi}(x_1) \cdots \hat{\phi}(x_n) \rangle_C = \left. \frac{\delta^n \log Z[J]}{\delta J(x_1) \cdots \delta J(x_n)} \right|_{J=0} \quad (2.13)$$

Free scalar field

We will first look at the generating functional in the theory of a free scalar field, which is particularly simple. It can be shown axiomatically that the Euclidean 2-point correlation function is then

$$G(x, y) \equiv \langle \hat{\phi}(x) \hat{\phi}(y) \rangle = \int \frac{d^4 p}{(2\pi)^4} \frac{e^{ip \cdot (x-y)}}{p^2 + m^2}. \quad (2.14)$$

We recognize the Green function of the Klein-Gordon equation

$$(\partial_\mu \partial^\mu - m^2)G(x, y) = -\delta(x - y). \quad (2.15)$$

Furthermore, the only non-zero Euclidean connected correlation function in the free theory is

$$\langle \hat{\phi}(x) \hat{\phi}(y) \rangle_C = G(x, y). \quad (2.16)$$

We then deduce from (2.13) that the generating functional of the free theory is equal to

$$Z[J] = \exp \left\{ \frac{1}{2} \int d^4 x d^4 y J(x) G(x, y) J(y) \right\}. \quad (2.17)$$

For a $k \times k$ symmetric, positive-definite covariance matrix A and an arbitrary vector J , the following gaussian integral is well-known

$$\int d^k \phi \exp \left\{ -\frac{1}{2} (\phi, A \phi) + (J, \phi) \right\} = \sqrt{\frac{(2\pi)^n}{\det A}} \exp \left\{ \frac{1}{2} (J, A^{-1} J) \right\}. \quad (2.18)$$

The integration is over vectors $\phi \in \mathbb{R}^k$ on the left-hand side. If we think of a field as a vector in an infinite space, we can make an analogy between the right-hand sides of (2.17) and (2.18) to write formally

$$Z[J] = \frac{1}{Z[0]} \int \prod_x d\phi(x) \exp \left\{ -\frac{1}{2} (\phi, (-\partial_\mu \partial^\mu + m^2) \phi) + (J, \phi) \right\}. \quad (2.19)$$

Of course, the continuous space-time is not only infinite but also uncountable so the product \prod_x is formal and this integral is clearly not well-defined. We will take care of this when we put the theory on a finite lattice.

Interacting scalar field

We now consider the case of an interacting quantum scalar field, with a classical Euclidean action given by

$$S[\phi] = \frac{1}{2} (\phi, (-\partial_\mu \partial^\mu + m^2) \phi) + S_I[\phi] \quad (2.20)$$

where S_I is the part describing the interaction.

Dyson's formula relate the generating formula for the free and the interacting theories. In Euclidean space, it reads

$$Z[J] \propto \langle \exp \{ -S_I[\hat{\phi}_{\text{in}}] + (J, \hat{\phi}_{\text{in}}) \} \rangle_{\text{in}} \quad (2.21)$$

where the subscript in refers to the free field theory (standing incoming as will be made clear in section 3.1.3). Combining this equation with our results for the free theory, we deduce a formal expression for the generating function of the interacting theory

$$Z[J] = \frac{1}{Z} \int \prod_x d\phi(x) e^{-S[\phi] + (J, \phi)}, \quad (2.22)$$

where $Z = Z[0]$. This translates to the correlation functions as

$$\langle \hat{\phi}(x_1) \cdots \hat{\phi}(x_n) \rangle = \frac{1}{Z} \int \prod_x d\phi(x) e^{-S[\phi]} \phi(x_1) \cdots \phi(x_n). \quad (2.23)$$

We have thus reached an explicit expression of the Euclidean correlation functions using the Euclidean action of the theory. The left-hand side of (2.23) is the expectation value of a product of operators $\hat{\phi}$ acting on the Hilbert space of physical states \mathcal{H} while on the right-hand side, ϕ is a classical field and there is no mention of the Hilbert space (remember (2.18), the field ϕ is simply introduced as a mathematical device). This relation is called the functional integral or *path integral* of the theory. We remind that this expression is formal and will require some regularization, on the lattice in our case.

2.2 QCD ON A COMPUTER

We have seen in the previous section how the physical content of a quantum field theory is encoded in the Euclidean correlation functions and how these can be expressed as an integral over classical fields. Integrals are precisely something computers can compute so that after extending the previous argument to QCD, we will see how these integrals can be prepared for computation. A more extensive treatment can be found in many books, e.g. ref. [15–18].

2.2.1 QCD in the continuum

Fields

QCD describes the physics of the *quarks*, elementary particles of spin $\frac{1}{2}$ coming in $N_f = 6$ flavors (with bare masses m^f) and $N_c = 3$ colors (degenerate masses), as well as the *antiquarks*, their antiparticle partners. We will note the quark field ψ_c^f , and the antiquark field $\bar{\psi}_c^f$, with f (resp. c) the flavor (resp. color) index and the spin indices kept implicit. QCD is a Yang-Mills theory for the color gauge group $SU(3)_c$. This means that the quark and antiquark fields are required to transform covariantly under local gauge transformations as

$$\psi^f(x) \rightarrow \Omega(x)\psi^f(x), \quad \bar{\psi}^f(x) \rightarrow \psi^f(x)\Omega(x)^{-1} \quad (2.24)$$

where $\Omega(x) \in SU(3)$ acts on the color degrees of freedom (d.o.f.) of ψ^f differently at each position x .

QCD is invariant under local gauge transformations thanks to the existence of gauge fields of spin 1, the *gluons*, which come in 8 types and will be noted A_μ^a for $a = 1, \dots, 8$. It is convenient to define the gluon field as a field of 3×3 matrices $A_\mu(x) = \sum_{a=1}^8 A_\mu^a t^a$, where t^a are the generators of the Lie algebra $\mathfrak{su}(3)$, normalized by $\text{Tr } t^a t^b = \frac{1}{2} \delta_{ab}$. The gluon field transforms under local gauge transformations as

$$A_\mu \rightarrow \Omega(x)A_\mu(x)\Omega(x)^{-1} + i\partial_\mu\Omega(x)\Omega(x)^{-1}. \quad (2.25)$$

Action

We can now introduce the action of QCD in Euclidean space as

$$S[\psi, \bar{\psi}, A] = S_F[\psi, \bar{\psi}, A] + S_G[A]. \quad (2.26)$$

The fermionic part of the action is

$$S_F[\psi, \bar{\psi}, A] = \sum_{f=1}^{N_f} \int d^4x \bar{\psi}^f(x) (\gamma_\mu [\partial_\mu + igA_\mu(x)] + m^f) \psi^f(x). \quad (2.27)$$

where the constant g is the bare gauge coupling and γ_μ are the Euclidean Dirac matrices. Note that γ_μ implicitly acts on the spin d.o.f. and A_μ on the color d.o.f. The gauge part of the action is

$$S_G[A] = \frac{1}{2g^2} \int d^4x \text{Tr} [F_{\mu\nu}(x) F_{\mu\nu}(x)] \quad (2.28)$$

where the field strength tensor is defined from the gluon field as

$$F_{\mu\nu}(x) \equiv \partial_\mu A_\nu - \partial_\nu A_\mu + ig[A_\mu, A_\nu]. \quad (2.29)$$

Provided (2.24) and (2.25), the action S thus constructed is invariant under local gauge transformation.

Similarly as was discussed in the previous section, QCD is characterized by the Hilbert space \mathcal{H} of physical states after quantization. The Euclidean space path integral for QCD will be written by analogy as

$$\langle F[\hat{\psi}, \hat{\bar{\psi}}, \hat{A}] \rangle = \frac{1}{Z} \int \prod_x \{d\psi(x) d\bar{\psi}(x) dA(x)\} e^{-S[\psi, \bar{\psi}, A]} F[\psi, \bar{\psi}, A]. \quad (2.30)$$

with $Z = \langle 1 \rangle$ and $d\psi(x)$ a measure taking into account flavor, spin and color indices. On the left-hand side, F is a functional of the field operators $\hat{\psi}, \dots$ acting on \mathcal{H} which also returns an operator. On the right-hand side, F is the same functional but taking as arguments the classical fields ψ, \dots and thus returning a classical field. Note that this infinite-dimensional integral is still formal.

Parallel transporter

For any path \mathcal{C}_{xy} between two space-time points x and y , define the parallel transporter $U(\mathcal{C}_{xy}) \in SU(3)$ as

$$U(\mathcal{C}_{xy}) = P \exp \left\{ ig \int_{\mathcal{C}_{xy}} A_\mu ds^\mu \right\}. \quad (2.31)$$

where P is the path ordering operator. It follows from (2.25) that it transforms under local gauge transformations simply as

$$U(\mathcal{C}_{xy}) \rightarrow \Omega(x) U(\mathcal{C}_{xy}) \Omega(y)^{-1}. \quad (2.32)$$

The parallel transporter and the gluon field are equivalent as can be seen by taking infinitesimal paths in (2.31). This means that the action could be equivalently written as a function of the parallel transporter. Indeed, with $\hat{\mu}$ the unit vector in the direction μ , we have for the straight curve $\mathcal{C}_{x, x+a\hat{\mu}}$ between x and $x+a\hat{\mu}$

$$(\partial_\mu + igA_\mu(x)) \psi^f(x) = \lim_{a \rightarrow 0} \frac{U(\mathcal{C}_{x, x+a\hat{\mu}}) \psi^f(x+a\hat{\mu}) - U(\mathcal{C}_{x, x-a\hat{\mu}}) \psi^f(x-a\hat{\mu})}{2a}. \quad (2.33)$$

Similarly, for the closed path $\mathcal{C}_{x,x} = \mathcal{C}_{x, x+a\hat{\mu}} \circ \mathcal{C}_{x+a\hat{\mu}, x+a\hat{\mu}+a\hat{\nu}} \circ \mathcal{C}_{x+a\hat{\mu}+a\hat{\nu}, x+a\hat{\nu}} \circ \mathcal{C}_{x+a\hat{\nu}, x}$ following the edges of a square, we have

$$\text{Tr} [F_{\mu\nu}(x) F_{\mu\nu}(x)] = \lim_{a \rightarrow 0} \frac{2}{a^4} \text{Re} \text{Tr} [\mathbf{1} - U(\mathcal{C}_{x,x})]. \quad (2.34)$$

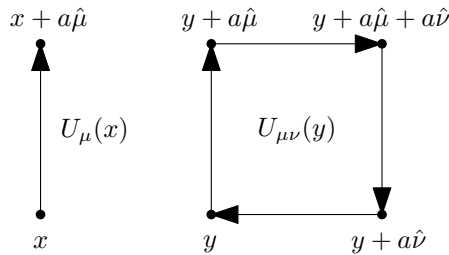


Figure 2.1: Gauge links $U_\mu(x)$ and plaquettes $U_{\mu\nu}(x)$ on the lattice.

With such identities we can write the QCD action as $S[\psi, \bar{\psi}, U]$ where the parallel transporters replace the gluon field. The path integral would then be written as

$$\langle F[\hat{\psi}, \hat{\bar{\psi}}, \hat{U}] \rangle = \frac{1}{Z} \int \mathcal{D}U \prod_x \{d\psi(x) d\bar{\psi}(x)\} e^{-S[\psi, \bar{\psi}, U]} F[\psi, \bar{\psi}, U] \quad (2.35)$$

with some measure $\mathcal{D}U$ for the parallel transporters. This measure should take care of the redundancy arising from the properties

$$U(\mathcal{C} \circ \mathcal{C}') = U(\mathcal{C})U(\mathcal{C}') \quad \text{and} \quad U(-\mathcal{C}) = U(\mathcal{C})^{-1} \quad (2.36)$$

for two paths $\mathcal{C}, \mathcal{C}'$ and with $-\mathcal{C}$ the path \mathcal{C} traversed in the reversed direction. Schematically we could have $\mathcal{D}U = \prod_{\mathcal{C}^*} dU(\mathcal{C}^*)$, a product over some “independent” paths \mathcal{C}^* .

2.2.2 QCD on a lattice

The formulation of QCD on a discretized space-time serves two purposes. From a theoretical point of view, the finite lattice spacing introduces an ultraviolet regulator which is a necessary device to make the expressions finite in QFT and thus allow predictions for physical quantities. From a practical point of view, combined with restricting space-time to a finite volume, it leads to a finite number of degrees of freedom and therefore makes numerical calculations possible.

Let us then restrict the Euclidean space-time to a finite 4-dimensional hypercubic lattice

$$\Lambda \equiv \{a\mathbf{n} \in \mathbb{R}^4 \mid n_\mu = 0, \dots, N-1\}. \quad (2.37)$$

The extent in each direction is $L = Na$, and the lattice spacing a enforces a momentum cutoff of order $1/a$.

Naive discretized action

On the lattice, the definition of the measure $\mathcal{D}U$, which was troublesome in the continuum becomes straightforward. Indeed, any path is the concatenation of elementary straight lines of length a between neighboring sites of the lattice. Using the properties (2.36), this means that the parallel transporter of any path can be reconstructed from the *gauge links* (see fig. 2.1)

$$U_\mu(x) \equiv U(\mathcal{C}_{x, x+a\hat{\mu}}), \quad x \in \Lambda, \quad \mu = 1, \dots, 4. \quad (2.38)$$

Since these gauge links are independent and complete, we can use them as the gauge degrees of freedom and choose the measure

$$\mathcal{D}U = \prod_{x \in \Lambda} \prod_{\mu=1}^4 dU_\mu(x) \quad (2.39)$$

where $dU_\mu(x)$ is the Haar measure for $SU(3)$, which ensures that $\mathcal{D}U$ is gauge-invariant. The quark degrees of freedom are simply the value of the fields at each lattice site, with a measure

$$\prod_{x \in \Lambda} d\psi(x) d\bar{\psi}(x) \quad (2.40)$$

Note that this is now a well-defined product over a finite number of terms, contrary to the formal \prod_x that we used in the continuum.

We can then introduce a gauge-invariant action on the lattice for these degrees of freedom

$$S^\Lambda[\psi, \bar{\psi}, U] \equiv S_F^\Lambda[\psi, \bar{\psi}, U] + S_G^\Lambda[U] \quad (2.41)$$

using the naive fermion action

$$S_F^\Lambda[\psi, \bar{\psi}, U] = a^4 \sum_{x \in \Lambda} \sum_{f=1}^{N_f} \bar{\psi}^f(x) \left[\gamma_\mu \frac{U_\mu(x) \psi^f(x + a\hat{\mu}) - U_{-\mu}(x) \psi^f(x - a\hat{\mu})}{2a} + m^f \psi^f(x) \right]. \quad (2.42)$$

with the shorthand $U_{-\mu}(x) = U_\mu(x - a\hat{\mu})^{-1}$ and the *Wilson action*

$$S_G^\Lambda[U] = \frac{2}{g^2} \sum_{x \in \Lambda} \sum_{\mu < \nu} \text{Re Tr} [\mathbb{1} - U_{\mu\nu}(x)] \quad (2.43)$$

where we defined the *plaquette* (see fig. 2.1)

$$U_{\mu\nu}(x) = U_\mu(x) U_\nu(x + a\hat{\mu}) U_\mu(x + a\hat{\nu})^{-1} U_\nu(x)^{-1}, \quad x \in \Gamma, \quad \mu \neq \nu. \quad (2.44)$$

Equations (2.33) and (2.34) guarantee that the continuum action is recovered as the lattice spacing a approaches zero and the volume is taken to infinity

$$S[\psi, \bar{\psi}, A] = \lim_{a \rightarrow 0} \lim_{L \rightarrow \infty} S^\Lambda[\psi, \bar{\psi}, U]. \quad (2.45)$$

While irrelevant in the limit of an infinite lattice, periodic boundary conditions are usually taken in the spatial directions $\mu = 1, 2, 3$ to ensure translational invariance. In the temporal direction $\mu = 4$, the boundary conditions are taken as periodic for the gauge field but antiperiodic for the fermion fields, for technical reasons related to the reconstruction of the Minkowski theory.

Doubling problem and alternative actions

The action defined in (2.41) is only one example of all the lattice actions with the proper limit (2.45). For any such lattice action S^Λ , we can define a path integral similarly as (2.35)

$$\langle F[\hat{\psi}, \hat{\bar{\psi}}, \hat{U}] \rangle_\Lambda = \frac{1}{Z_\Lambda} \int \prod_{x \in \Lambda} \left\{ d\psi(x) d\bar{\psi}(x) \prod_{\mu=1}^4 dU_\mu(x) \right\} e^{-S^\Lambda[\psi, \bar{\psi}, U]} F[\psi, \bar{\psi}, U], \quad (2.46)$$

where Z_Λ is fixed by $\langle 1 \rangle_\Lambda = 1$. This integral is finite-dimensional and well-defined.

The left-hand side of (2.46) represents correlations functions for a QCD-like quantum field theory describing particles on the lattice. Although the lattice action approaches the QCD action as (2.45) there is no guarantee that all the correlation functions converge towards those of QCD, primarily because the lattice action does not exhibit the same symmetries as the one in the continuum.

As an important example, it can be shown that at any value of the lattice spacing, the naive fermion action (2.42) leads to a dispersion relation such that all energy levels have a degeneracy of 16 states¹. This is known as the *doubling problem* and means that the QFT induced by this lattice action describes 16 times more physical fermions than the continuum one. To circumvent this issue, Wilson proposed an alternative discretization of the fermion action by adding the following term to (2.42)

$$-a \sum_{x \in \Lambda} \sum_{f=1}^{N_f} \sum_{\mu=1}^4 \bar{\psi}^f(x) \frac{U_{\mu}(x)\psi^f(x+a\hat{\mu}) - 2\psi^f(x) + U_{-\mu}(x)\psi^f(x-a\hat{\mu})}{2a^2}. \quad (2.47)$$

It is gauge invariant and vanishes for $a \rightarrow 0$ so that the resulting action is still satisfying. Furthermore, it lifts the degeneracy of the states so that toward the continuum limit, only one state per flavor recovers the dispersion relation of a particle of mass m^f while the other 15 states acquire infinite masses. However, while solving the doubling problem, the new term explicitly breaks chiral symmetry so that some important features of QCD cannot be reproduced. The fermions described by such an action are called *Wilson fermions*.

Many other valid lattice actions have been proposed, for two main objectives. The first objective is to improve the convergence of the discretized action towards the continuum one. For example, the Wilson gauge action has a convergence rate of $O(a^2)$ while the action for Wilson fermions only converges as $O(a)$. The action for *clover fermions* is obtained by adding new terms to the action of the Wilson fermions so that the terms in $O(a)$ vanish and the overall action converges as $O(a^2)$. Another objective is to keep an aspect of chiral symmetry on the lattice but such considerations are beyond the scope of this thesis.

Continuum limit

With the rescaling $\psi^f \rightarrow \sqrt{am^f + 4a^{3/2}}\psi$ and a similar one for $\bar{\psi}^f$, the lattice fermion fields in the path integral (2.46) can be made dimensionless. This rescaling simply factors out a constant which is absorbed in Z_{Λ} . Then, the action for Wilson fermions can be compactly written as

$$S_F^{\Lambda}[\psi, \bar{\psi}, U] = \sum_{x \in \Lambda} \sum_{f=1}^{N_f} \left[\bar{\psi}^f(x)\psi^f(x) - \kappa^f \sum_{\pm} \sum_{\mu=1}^4 \bar{\psi}^f(x)(1 \mp \gamma_{\mu})U_{\pm\mu}(x)\psi^f(x \pm a\hat{\mu}) \right]. \quad (2.48)$$

where $\kappa^f = 1/(2am^f + 8)$ is called the *hopping parameter*. Since a does not appear explicitly in the gauge action (2.43) and $(x, x \pm a\hat{\mu})$ above are only indices for the integration variables $\psi, \bar{\psi}$, the whole path integral can be written independently of a , with dimensionless degrees of freedom and dimensionless parameters κ^f and $\beta = 6/g^2$. Now, if these are the only parameters of the lattice, how do we take the continuum limit?

On one side, the correlation functions of “real-world” QCD (and thus quantities to be compared with experiments) can be obtained up to corrections of order $O(a)$ (or better) by computing the path integral for a lattice² with a suitable choice of parameters $\kappa^f(a)$ and $\beta(a)$ as $a \rightarrow 0$. Here, a is just a dummy parameter and $\kappa^f(a)$ and $\beta(a)$ some functions to be determined.

¹ The dispersion relation for each flavor, obtained from the pole locations of the free fermion propagator, is given by $\sum_{\mu=1}^4 \sin(p_{\mu}a)^2 = (m^f a)^2$. It has 0 or 16 solutions for p_{μ} within the first Brillouin zone $(-\pi/a, \pi/a]$.

² Technically an infinite lattice but the limit $N \rightarrow \infty$ is trivial, if computationally expensive.

On the other side, if we compute the path integral for a (infinite) lattice and some parameters $X_\Lambda = (\{\kappa^f\}_{f=1}^{N_f}, \beta)$, we obtain correlation functions which correspond to those of a continuum QCD-like theory, let us call it \mathcal{T} , up to corrections $O(a_{\mathcal{T}}(X_\Lambda))$ and to those of another theory \mathcal{T}' up to corrections $O(a_{\mathcal{T}'}(X_\Lambda))$, etc. These two theories have the same content and symmetries as “real-world” QCD, let us call it \mathcal{T}_φ for physical, but lead to different values for observables, e.g. the hadron masses. To make predictions on real-world quantities, it is then necessary to choose the lattice parameters such that $a_{\mathcal{T}_\varphi}(X_\Lambda)$ approaches zero. This is called the continuum limit at the *physical point*. Note that with previous notations, $a = a_{\mathcal{T}_\varphi}(\{\kappa^f(a)\}_{f=1}^{N_f}, \beta(a))$. One can also explore the continuum limit away from the physical point, i.e. $a_{\mathcal{T}}(X_\Lambda) \rightarrow 0$ where \mathcal{T} is for example a theory for which the pion mass is heavier than the physical one. It can give valuable insight, is often less computationally demanding and may be related to \mathcal{T}_φ by e.g. chiral extrapolation.

These qualitative considerations can be made rigorous in the framework of the renormalization group. For this thesis, it will suffice to say that the continuum limit corresponds to $\beta \rightarrow \infty$ and that κ^f must be tuned to reach the physical point.

2.2.3 Computation

We have seen how the Euclidean correlation functions of QCD can be recovered in some limit from the path integral on the right-hand side of (2.46), a well-defined integral, with an appropriate choice of parameters κ^f and β . A detail that was ignored so far is that the quarks being fermions, their fields anticommute. This is implemented by requiring that the integration parameters $\psi(x)$ and $\bar{\psi}(x)$ for $x \in \Lambda$ be anticommuting numbers, called *Grassman variables*. Since such numbers cannot be treated by a computer, we first integrate over the quark degrees of freedom analytically in the path integral. To do so, note that the action for Wilson fermion (2.48) (and any other bilinear action) can be written as

$$S_F^\Lambda[\psi, \bar{\psi}, U] = \sum_{x, y \in \Lambda} \sum_{A, B} \bar{\psi}_A(x) D_{A, B}(x, y) \psi_B(y). \quad (2.49)$$

where D is a U -dependent matrix, called the *Dirac operator*, with position indices (x, y) as well as flavor, spin and color indices which are compactly represented as (A, B) . Then it can be shown that for a functional

$$F[\psi, \bar{\psi}, U] = F[U] \psi_{A_1}(x_1) \bar{\psi}_{B_1}(y_1) \cdots \psi_{A_n}(x_n) \bar{\psi}_{B_n}(y_n) \quad (2.50)$$

the path integral is given after integration of the quark fields by

$$\langle F[\hat{\psi}, \hat{\bar{\psi}}, \hat{U}] \rangle_\Lambda = (-1)^n \sum_{\sigma \in S_n} \text{sign}(\sigma) \frac{\int \mathfrak{D}U F[U] D_{A_1, B_{\sigma_1}}^{-1}(x_1, y_{\sigma_1}) \cdots D_{A_n, B_{\sigma_n}}^{-1}(x_n, y_{\sigma_n})}{\int \mathfrak{D}U} \quad (2.51)$$

with S_n the set of permutations of $\{1, \dots, n\}$ and the following measure for the integration on the gauge links

$$\mathfrak{D}U \equiv \mathcal{D}U e^{-S_G^\Lambda[U]} \det[D]. \quad (2.52)$$

Actually, any functional with a non-zero expectation value is a combination of functionals described by (2.50). It is then sufficient to compute numerically the kind of integrals which appears in the right-hand side of (2.51). Since such integrals are

typically over a huge number of dimensions ($32N^4$ for the lattice considered here), the method of choice is Monte-Carlo integration. The idea is to generate M *gauge configurations*, i.e. M sets U_i of gauge links for the whole lattice, such that their distribution approaches $\mathfrak{D}U$ as M grows. Then the integrals are evaluated as the limit

$$\frac{\int \mathfrak{D}U f(U)}{\int \mathfrak{D}U} = \lim_{M \rightarrow \infty} \frac{1}{M} \sum_{i=1}^M f(U_i). \quad (2.53)$$

Typically, the generation of the gauge configurations U_i is very computationally expensive. However, once they are generated and stored, one can compute integrals as above for any function f desired.

Note that the measure $\mathfrak{D}U$ is positive (as expected for a measure) and decays exponentially for large values of the gauge action. Such a behavior is crucial to the fast convergence of the limit (2.53) since the space of the gauge configurations which contribute significantly to the integral is much smaller than the total integration space. The method described previously, i.e. sampling gauge configurations according to the distribution $\mathfrak{D}U$ so that the ones with the largest contributions to the integral appear more often in the chain U_i , is called *importance sampling*. It is one of the most compelling advantages to make computations in Euclidean space. Indeed, for the path integral in Minkowski space, the contribution of all the gauge configurations are of similar importance towards the final result and must be taken into account, a task clearly impossible in an infinite space.

2.3 LATTICE SPECTROSCOPY

We have seen how the framework of lattice QCD allows to compute the Euclidean correlation functions of QCD using computer simulations. These correlation functions can be used to extract any relevant information of QCD in Euclidean space. However, to obtain predictions for the “real-world”, the Euclidean correlation functions must be analytically continued to Minkowski space using the Wick rotation introduced in subsection 2.1.1. As we will see, this analytical continuation cannot be performed from the results of numerical simulations but meaningful predictions can still be obtained. One important prediction allowed by lattice QCD is about the energy-levels of the theory, i.e. the spectrum of the Hamiltonian operator.

2.3.1 Euclidean correlators

We will call *correlators* the particular case of correlation functions where the functional can be separated as

$$F[\psi, \bar{\psi}, U] = O_1[\psi(\cdot, t_1), \bar{\psi}(\cdot, t_1), U(\cdot, t_1)] O_2[\psi(\cdot, t_2), \bar{\psi}(\cdot, t_2), U(\cdot, t_2)], \quad (2.54)$$

i.e. the product of two functionals O_1 and O_2 which only involve the fields at times t_1 and t_2 respectively, with $t_1 > t_2$. For $i = 1, 2$ define the following operator acting on the Hilbert space \mathcal{H}

$$\hat{O}_i(t) = O_i[\hat{\psi}(\cdot, t), \hat{\bar{\psi}}(\cdot, t), \hat{U}(\cdot, t)]. \quad (2.55)$$

In Minkowski space, the correlation function associated to a functional of the type (2.54) is

$$\langle 0|F[\hat{\psi}, \hat{\bar{\psi}}, \hat{U}]|0\rangle = \langle 0|\hat{O}_1(t_1)\hat{O}_2(t_2)|0\rangle = \langle 0|\hat{O}_1(0) e^{-i\hat{H}(t_1-t_2)}\hat{O}_2(0)|0\rangle \quad (2.56)$$

where \hat{H} is the Hamiltonian operator of QCD which has a discrete spectrum in finite volume. Let $|n\rangle$ and W_n ($n = 1, \dots$) be the eigenstates and associated eigenenergies of the Hamiltonian which couple with the states $\hat{O}_2(0)|0\rangle$ and $\hat{O}_1(0)^\dagger|0\rangle$. The energies W_n are assumed strictly increasing with n . Expanding on the complete set of eigenstates of the Hamiltonian, we get

$$\langle 0|\hat{O}_1(t_1)\hat{O}_2(t_2)|0\rangle = \sum_n \langle 0|\hat{O}_1(0)|n\rangle\langle n|\hat{O}_2(0)|0\rangle e^{-iW_n(t_1-t_2)}. \quad (2.57)$$

Both sides can be analytically continued to Euclidean times $\tau_k = it_k$ as

$$\langle \hat{O}_1(\tau_1)\hat{O}_2(\tau_2)\rangle = \sum_n \langle 0|\hat{O}_1(0)|n\rangle\langle n|\hat{O}_2(0)|0\rangle e^{-W_n(\tau_1-\tau_2)}. \quad (2.58)$$

We have thus related an Euclidean correlation function on the left-hand side, which can be computed in lattice QCD, to matrix elements and eigenenergies of the theory in Minkowski space. Note that the analytic continuation supposes an infinite extent in the temporal direction.

As we will see in the next subsection, it is possible to approximate the matrix elements and eigenenergies for the first few eigenstates n but it would require an infinite number of numerical calculations to extract all of them. While these first few eigenstates may be enough to obtain the Euclidean correlator due to the exponential suppression $e^{-W_n(\tau_1-\tau_2)}$, there is no such suppression in Minkowski space so that all the eigenstates may contribute significantly to the correlator. This is why the analytic continuation from numerical results back to correlation functions in Minkowski space is in general an ill-defined problem. However, gaining information for the lower part of the spectrum is already very useful as will be discussed in later chapters.

2.3.2 Spectrum extraction

In this subsection, we will implicitly consider that times noted t are Euclidean. The fundamental identity derived above for the Euclidean correlators is then

$$\langle \hat{O}_1(t)\hat{O}_2(0)\rangle = \sum_n \langle 0|\hat{O}_1(0)|n\rangle\langle n|\hat{O}_2(0)|0\rangle e^{-W_n t}. \quad (2.59)$$

\hat{O}_2 is usually called the *source operator* and \hat{O}_1 the *sink operator*.

Naive method

At large time separations t , the contribution from the *ground state* $|n = 1\rangle$ dominates the correlator

$$\langle \hat{O}_1(t)\hat{O}_2(0)\rangle = C e^{-W_1 t} [1 + O(e^{-(W_2-W_1)t})] \quad (2.60)$$

where $C \equiv \langle 0|\hat{O}_1(0)|n = 1\rangle\langle n = 1|\hat{O}_2(0)|0\rangle$. This means that one can extract the ground state energy W_1 and the coefficient C by fitting this correlator at large enough t . One can equally fit the correlator

$$\langle \hat{O}_1(t)\hat{O}_1(0)^\dagger\rangle = C' e^{-W_1 t} [1 + O(e^{-(W_2-W_1)t})] \quad (2.61)$$

where $C' \equiv |\langle 0|\hat{O}_1(0)|n = 1\rangle|^2$. Assuming that $C \neq C'$, we can cancel the contribution of the ground state as

$$C'\langle \hat{O}_1(t)\hat{O}_2(0)\rangle - C\langle \hat{O}_1(t)\hat{O}_1(0)^\dagger\rangle = C'' e^{-W_2 t} [1 + O(e^{-(W_3-W_2)t})] \quad (2.62)$$

for some constant C'' .

In conclusion, we can extract the energy W_1 from correlators (2.61) involving one operator and additionally the energy W_2 from correlators (2.62) involving two operators. It is easy to see that with correlators involving N_{op} operators we can extract the N_{op} first energies of the spectrum.

An issue with this method is that numerical simulations are performed for a space-time with a finite extent in the temporal direction L_t . Therefore, the method breaks down when two consecutive energies are too close in the sense that they do not satisfy $(W_{n+1} - W_n)L_t \gg 1$. In typical simulations, this may happen as soon as $n = 1$.

Variational method

The *variational method* is a smarter approach to the extraction of the first few eigenenergies W_n from Euclidean correlators. Assume that we have chosen a set of independent operators \hat{O}_i ($i = 1, \dots, N_{\text{op}}$). From numerical simulations, create a time-dependent *correlation matrix* $C(t)$ with coefficients

$$C_{ij}(t) = \langle \hat{O}_i(t) \hat{O}_j(0)^\dagger \rangle, \quad i, j = 1, \dots, N_{\text{op}}. \quad (2.63)$$

Instead of fitting each correlator separately as proposed before, we will use them all at the same time. For two times t and t_0 , solve the following generalized eigenvalue problem (GEVP)

$$C(t)v_n(t, t_0) = \lambda_n(t, t_0)C(t_0)v_n(t, t_0), \quad n = 1, \dots, N_{\text{op}}. \quad (2.64)$$

Lüscher and Wolff first showed [19] that the eigenvalues have the following asymptotic behavior

$$W_n^{\text{eff}}(t, t_0) \equiv -\partial_t \log \lambda_n(t, t_0) = W_n + O(e^{-\Delta W_n t}), \quad \Delta W_n = \min_{m \neq n} |W_m - W_n|, \quad (2.65)$$

This means that at fixed t_0 the eigenvalues decay exponentially in t with a rate which approaches the eigenenergies W_n at large t . Unfortunately, the method still breaks down if two consecutive energies are too close in the same sense as for the naive method³.

By considering the contribution of the energy eigenstates $|n\rangle$ for $n > N_{\text{op}}$ as perturbations, it was later shown [20] that for t_0 and t chosen such that $t < 2t_0$, the solutions have the stronger asymptotic behavior

$$W_n^{\text{eff}}(t, t_0) = W_n + O(e^{-(W_{N_{\text{op}}+1} - W_n)t}), \quad n = 1, \dots, N_{\text{op}}. \quad (2.66)$$

We see that one can reliably extract the eigenenergies n for which $(W_{N_{\text{op}}+1} - W_n)L_t \gg 1$, a condition typically satisfied at least for the first few eigenstates $n \ll N_{\text{op}}$. The variational method is therefore an efficient method to extract the spectrum from lattice simulations. It is the method used in most modern computations, with a number of operators N_{op} which can be very large for high-precision calculations.

³ Even then, the variational method is still more numerically stable than the naive method. Consider e.g. equation (2.62) when C and C' have some uncertainty and the ground state contribution is not exactly cancelled.

Two-particle channels

Free theories are trivial and physics really becomes interesting when interactions come into play. However, any physical process involving interactions is the result of an infinity of more or less important contributions and cannot be treated exactly. *Scattering theory* is a framework to study simplified interacting processes in a way which is amenable to calculations. It assumes an initial state in the “distant past” $t = -\infty$ consisting of a set of *free* objects (particles, waves, classical bodies) and a final state in the “distant future” $t = +\infty$ consisting of a possibly different set of free objects. At intermediate times, these objects can interact according to a predetermined theory.

Most of what we know about the microscopic world is based on the study of such scattering processes. Indeed, since a microscopic object cannot be observed directly, a standard method of observation is to *probe* this object by sending other objects with known properties to interact with it. The analysis of the change in the properties of the probing objects after interaction will provide insight on the scatterer. Alternatively, a theory such as the Standard Model can be (and has been extensively) tested by comparing its predictions for scattering processes to experimental data.

Scattering theory has a long history and while it may involve different mathematical formalisms in classical physics, quantum mechanics and quantum field theories, it is enlightening to consider their similarities and the evolution between them. We will therefore start this chapter by introducing these three mathematical formalisms, with a focus on two-body processes.

The following of the chapter is dedicated to the study of two-particle scattering processes in quantum field theory using lattice simulations. The Standard Model has encountered great success for its prediction of scattering processes using perturbative approaches. However, many processes such as nucleon-nucleon scattering must be treated in a non-perturbative approach, for which lattice simulations are the only known candidates. We will therefore present the finite size formula and the HAL QCD method which are currently the two main concepts to study two-body processes from lattice simulations of quantum field theory.

3.1 SCATTERING THEORY

3.1.1 Classical mechanics

In classical mechanics, the simplest scattering process is that of two bodies interacting through a central conservative force assumed to vanish at infinite distances. Let m_1 and m_2 be the masses of the scattering bodies and $V(r)$ be the potential associated with the interaction, r being the distance between the two bodies. As is well-known,

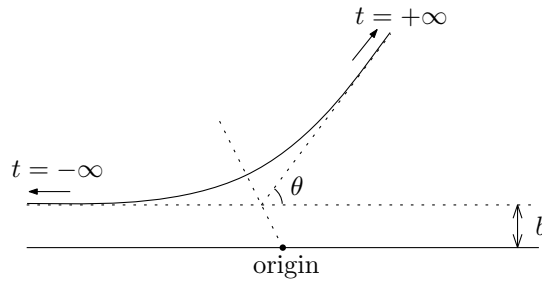


Figure 3.1: Impact parameter b and scattering angle θ in classical mechanics.

such a classical two-body problem can be reduced to the scattering of a body of mass $\mu = \frac{m_1 m_2}{m_1 + m_2}$, the reduced mass of the original system, off a stationary body at the origin with an interaction given by the same potential V .

At $t = -\infty$, the two bodies are infinitely distant and thus the non-stationary body moves freely along a straight line with a speed v_∞ . The distance b (see fig. 3.1) between this line and the origin, i.e. the shortest distance that the two bodies would reach in the absence of interaction, is called the *impact parameter*. Assuming they do not form a bound state, the two bodies at $t = +\infty$ are again infinitely distant and the non-stationary body moves freely with the same speed v_∞ (by energy conservation) along a straight line making an angle θ (see fig. 3.1) with the initial one in the plane containing the origin (movements in central potentials being planar). The angle θ is called the *scattering angle*. Note that it is also the angle between the incoming and outgoing directions of each body in the initial two-body problem.

By conservation of the total classical energy $E = \frac{1}{2}\mu v_\infty^2$, one can show that the scattering angle is related to the impact parameter by

$$\theta(b) = \pi - 2 \int_{r_{\min}}^{\infty} dr \frac{1}{\sqrt{1 - b^2/r^2 - V(r)/E}} \frac{b}{r^2} \quad (3.1)$$

where r_{\min} , the shortest distance between the two bodies in the presence of interaction, solves

$$1 - b^2/r_{\min}^2 - V(r_{\min})/E = 0. \quad (3.2)$$

In order to have a scattering angle in the range $[\theta, \theta + d\theta]$, corresponding to a solid angle $d\Omega = 2\pi \sin \theta d\theta$ by rotational symmetry, the moving particle must pass at $t = -\infty$ through an annulus of cross-sectional area $d\Sigma = 2\pi b(\theta) db(\theta)$. Here, the function $b(\theta)$ can be obtained by inverting (3.1). The *differential scattering cross-section* is then defined as

$$\sigma(\Omega) \equiv \frac{d\Sigma}{d\Omega} = \frac{b}{\sin \theta} \left| \frac{db}{d\theta} \right| \quad (3.3)$$

and the *total scattering cross-section* as its integral over all solid angles

$$\sigma_{\text{tot}} = \int d\Omega \sigma(\Omega). \quad (3.4)$$

The cross-section has the following interpretation. Imagine that the scattering process is repeated a large number of times, at the same energy but with a uniform distribution for the initial direction of the incident body in the plane perpendicular to the line $b = 0$. Then, the probability distribution for the solid angle Ω of the outgoing line at $t = +\infty$ is given by $\sigma(\Omega)/\sigma_{\text{tot}}$. Alternatively, if incident bodies come in a uniform beam parallel to the line $b = 0$ with intensity I , the number of outgoing bodies scattered

at a solid angle $d\Omega$ per unit of time will be $I\sigma(\Omega)d\Omega$. The latter interpretation shows how the differential scattering cross-section can be directly measured experimentally. It is actually the main quantity of interest in many scattering experiments because the initial state of incoming particles is not precisely known so that sending a large number in an approximately uniform beam can mitigate this uncertainty.

3.1.2 Quantum mechanics

Two-particle states

Before discussing the formulation of scattering theory in quantum mechanics we will first consider the structure of a general two-particle state. The state with a well-defined energy E of two particles at positions \mathbf{x} and \mathbf{y} in their center-of-mass frame is described by a wave function of the form $\Psi(\mathbf{x}, \mathbf{y}, t) = \psi(\mathbf{r})e^{-iEt}$ where $\mathbf{r} = \mathbf{x} - \mathbf{y}$. The wave function ψ is a solution of the time-independent Schrödinger equation

$$H\psi = E\psi. \quad (3.5)$$

We take the Hamilton operator to be

$$H = -\frac{1}{2\mu}\Delta + V(r), \quad r = |\mathbf{r}| \quad (3.6)$$

where Δ is the Laplacian with respect to \mathbf{r} and the potential is assumed to have a finite range R for simplicity, i.e. $V(r) = 0$ for $r > R$. For rapidly-decaying potentials, this is a good approximation. The wave function can be expanded on the spherical harmonics basis as

$$\psi(\mathbf{r}) = \sum_{l=0}^{\infty} \sum_{m=-l}^l Y_{lm}(\hat{\mathbf{r}})\psi_{lm}(r), \quad \mathbf{r} = r\hat{\mathbf{r}}^1 \quad (3.7)$$

where the *partial waves* $\psi_{lm}(r)$ are solutions of the radial Schrödinger equation

$$\left[\frac{d^2}{dr^2} + \frac{2}{r} \frac{d}{dr} - \frac{l(l+1)}{r^2} + k^2 - 2\mu V(r) \right] \psi_{lm}(r) = 0. \quad (3.8)$$

with $k^2 = 2\mu E$. This equation has only one solution $u_l(r; k)$ which is bounded near the origin and there exist some constants b_{lm} such that $\psi_{lm}(r) = b_{lm}u_l(r; k)$. Furthermore, in the region $r > R$ this equation reduces to the radial Helmholtz equation for which the two linearly independent solutions are known to be the spherical Bessel functions j_l and n_l . We deduce that there are constants $\alpha_l(k)$ and $\beta_l(k)$ such that

$$u_l(r; k) = \alpha_l(k)j_l(kr) + \beta_l(k)n_l(kr), \quad r > R. \quad (3.9)$$

The asymptotic behavior of $u_l(r)$ at large r is thus given by

$$u_l(r; k) \sim \frac{1}{kr} [\alpha_l(k) \sin(kr - l\frac{\pi}{2}) - \beta_l(k) \cos(kr - l\frac{\pi}{2})]. \quad (3.10)$$

Define the *scattering phase shifts* $\delta_l(k)$ by

$$e^{2i\delta_l(k)} = \frac{\alpha_l(k) - i\beta_l(k)}{\alpha_l(k) + i\beta_l(k)}. \quad (3.11)$$

¹ In general, we will use the notation $\mathbf{r} = r\hat{\mathbf{r}}$ where r is the norm of \mathbf{r} and $\hat{\mathbf{r}}$ its angular part.

which is well-defined since the right-hand side has modulus 1 for real $\alpha_l(k)$ and $\beta_l(k)$. The asymptotic behavior of the partial waves at large r are then

$$\psi_{lm}(r) \sim C_{lm} \frac{\sin(kr - l\frac{\pi}{2} + \delta_l(k))}{kr}. \quad (3.12)$$

where the constants $C_{lm} = b_{lm} \alpha_l(k) / \cos \delta_l(k)$ may be fixed by appropriate boundary conditions.

Scattering processes

Equation (3.12) shows that wave function for two particles interacting through a potential $V(r)$ is determined at large relative distances only by the scattering phase shifts $\delta_l(k)$. We will now discuss the consequences of this result for scattering experiments.

As we have seen in the classical case, a typical scattering experiment consists in directing a uniform beam of particles with momentum \mathbf{k} and mass μ towards a target and measuring the distribution of the outgoing flux as a function of the scattering angle. Assuming that there is no interaction between the incoming particles and that the scattering is *elastic*, i.e. the particle content is not modified by the interaction, we only need to consider the system made of one incoming particle and the target. The previous discussion showed that it may be represented by a wave function $\psi(\mathbf{r})$ with a large- r behavior satisfying (3.12) with $k = |\mathbf{k}|$. Taking \mathbf{k} in the direction of the z -axis, the rotational symmetry of the system enforces $C_{lm} = C_l \delta_{m0}$.

The incoming particle has definite momentum \mathbf{k} so that it can be represented by a plane wave

$$\psi_{\text{in}}(\mathbf{r}) \equiv e^{i\mathbf{k}\cdot\mathbf{r}} = \sum_{l=0}^{\infty} D_l j_l(kr) Y_{l0}(\hat{\mathbf{r}}) \quad (3.13)$$

with $D_l = i^l \sqrt{4\pi(2l+1)}$. At large r , the wave function ψ is thus the superposition of the incoming wave function ψ_{in} and a scattering wave function $\psi_{\text{sc}} \equiv \psi - \psi_{\text{in}}$ which has an asymptotic behavior

$$\psi_{\text{sc}}(\mathbf{r}) \sim \frac{e^{ikr}}{kr} \left[\sum_{l=0}^{\infty} \frac{C_l e^{i\delta_l(k)} - D_l}{2i^{1+l}} Y_{l0}(\hat{\mathbf{r}}) \right] - \frac{e^{-ikr}}{kr} \left[\sum_{l=0}^{\infty} \frac{C_l e^{-i\delta_l(k)} - D_l}{2i^{1-l}} Y_{l0}(\hat{\mathbf{r}}) \right]. \quad (3.14)$$

Since the scattering wave function must propagate from the origin outward, we require the second term in e^{-ikr} to vanish. This effectively fixes the constants C_l to $C_l = e^{i\delta_l(k)} D_l$, i.e. the asymptotic partial waves in the presence of interaction are obtained from the incoming (free) ones by a simple phase shift of $\delta_l(k)$. The total wave function then reads at large r as

$$\psi(\mathbf{r}) \sim e^{i\mathbf{k}\cdot\mathbf{r}} + f(\hat{\mathbf{r}}) \frac{e^{ikr}}{k} \quad (3.15)$$

with the scattering amplitude

$$f(\hat{\mathbf{r}}) = 2\pi^{1/2} \sum_{l=0}^{\infty} \sqrt{2l+1} e^{i\delta_l(k)} \sin \delta_l(k) Y_{l0}(\hat{\mathbf{r}}). \quad (3.16)$$

The non-oscillating part of the asymptotic flux is given by

$$\mathbf{j} \equiv \frac{-i}{2\mu} (\psi^* \nabla \psi - \psi \nabla \psi^*) \sim \frac{\mathbf{k}}{\mu} + \frac{k}{\mu} \frac{|f(\hat{\mathbf{r}})|^2}{r^2} \hat{\mathbf{r}} + O(r^{-3}). \quad (3.17)$$

This is the flux per unit area and the flux per unit solid angle is obtained as $r^2 \mathbf{j} \cdot \hat{\mathbf{r}}$. We deduce that the differential scattering cross-section, defined similarly as in the classical case as the ratio of the scattered flux in a certain solid angle to the total incoming flux is given by

$$\sigma(\hat{\mathbf{r}}) = |f(\hat{\mathbf{r}})|^2. \quad (3.18)$$

The total scattering cross-section is then directly found to be

$$\sigma_{\text{tot}} = \frac{4\pi}{k^2} \sum_{l=0}^{\infty} (2l+1) \sin^2 \delta_l(k). \quad (3.19)$$

Low-energy limit

We once again assume that the potential vanishes or becomes negligible beyond some radius R . Defining the logarithmic derivative of the solution u_l

$$\gamma(r; k) = \frac{1}{u_l(r; k)} \frac{d}{dr} u_l(r; k). \quad (3.20)$$

one can show from (3.9) and (3.11) that the following equality holds for any $r \geq R$,

$$\tan \delta_l(k) = \frac{k j_l'(kr) - \gamma(r; k) j_l(kr)}{k n_l'(kr) - \gamma(r; k) n_l(kr)}. \quad (3.21)$$

At low energies, in the sense that momenta k are such that $kR \ll 1$, one can plug the asymptotic behavior of the spherical Bessel functions in the above equality evaluated at $r = R^+$ to get

$$\tan \delta_l(k) \underset{k \rightarrow 0}{\sim} \frac{(l+1) - R\gamma(R^+; 0)}{l + R\gamma(R^+; 0)} \frac{(kR)^{2l+1}}{(2l+1)!!(2l-1)!!} \propto (kR)^{2l+1}. \quad (3.22)$$

This shows that at low energies, the phase shifts are exponentially suppressed in l . Therefore, it is often sufficient to only consider the scattering of the s-wave ($l = 0$). For the s-wave, the phase shift at low energies can be parameterized as

$$k \cot \delta_0(k) = -\frac{1}{a_0} + \frac{1}{2} r_0 k^2 + O(k^4) \quad (3.23)$$

where a_0 is called the *scattering length* and r_0 the *effective range* of the interaction. The scattering length can be interpreted geometrically by noting that for $r > R$ the $l = 0$ radial wave function for the scattering process discussed previously is

$$\psi_{00}(r) = \sqrt{4\pi} e^{i\delta_0(k)} \frac{\sin(kr + \delta_0(k))}{kr} \underset{k \rightarrow 0}{\sim} \sqrt{4\pi} \left(1 - \frac{a_0}{r}\right). \quad (3.24)$$

Therefore, in the region where $r > R$ and $kr \ll 1$, $r\psi_{00}(r)$ is simply a line and a_0 is the point at which it changes sign when extrapolated to any value of r . While it depends on the specifics of the potential, a negative scattering length $a_0 < 0$ is thus characteristic of a weakly attractive potential which do not support bound states while $a_0 > 0$ may result from a repulsive potential or an attractive potential supporting a shallow bound state. Furthermore, the scattering cross-section in the low-energy limit is simply obtained from the scattering length as

$$\sigma_{\text{tot}} \underset{k \rightarrow 0}{\sim} 4\pi a_0^2. \quad (3.25)$$

3.1.3 Quantum field theory

Many of the concepts of scattering theory in quantum mechanics have equivalent in quantum field theory. In this subsection, we will only treat the simpler case of a quantum field $\phi(x)$ describing a scalar particle of mass m , i.e. the same context as in section 2.1 so that we use consistent notations. We will treat the theory in Minkowski space to account for real-time processes.

LSZ formalism

To study scattering processes in quantum field theory, we need to define “in” and “out” states. These states represent a certain number of particles, propagating freely in a “distant” past or future. The first step is to define some new fields $\phi_{\text{in}}(x)$ and $\phi_{\text{out}}(x)$ through the Yang-Feldman equations

$$\sqrt{Z}\phi_{\text{in(out)}}(x) \equiv \phi(x) - \int d^4y \Delta_{\text{ret(adv)}}(x-y)j(y), \quad (3.26)$$

where $\Delta_{\text{ret(adv)}}(x-y)$ is the retarded (advanced) Green’s function for the Klein–Gordon operator $\partial^\mu\partial_\mu + m^2$ and the source is $j(y) = (\partial^\mu\partial_\mu + m^2)\phi(y)$. The in and out fields thus created are free scalar fields as can be seen from

$$(\partial^\mu\partial_\mu + m^2)\phi_{\text{in(out)}}(x) = 0. \quad (3.27)$$

They can therefore be expanded on plane waves

$$\phi_{\text{in(out)}}(x) = \int \widetilde{d\mathbf{k}} \left[e^{-ik \cdot x} a_{\text{in(out)}}(\mathbf{k}) + e^{ik \cdot x} a_{\text{in(out)}}^\dagger(\mathbf{k}) \right]_{k_0=\omega_{\mathbf{k}}}, \quad (3.28)$$

where the Lorentz-invariant measure is defined as

$$\widetilde{d\mathbf{k}} \equiv \frac{d^3\mathbf{k}}{(2\pi)^3 2\omega_{\mathbf{k}}}, \quad (3.29)$$

with $\omega_{\mathbf{k}} = \sqrt{m^2 + \mathbf{k}^2}$. The normalization constant \sqrt{Z} in (3.26) is chosen such that the creation and annihilation operators for the in field $a_{\text{in}}^{(\dagger)}$ satisfy the canonical commutation relations². These operators can be recovered from the fields using

$$a_{\text{in(out)}}(\mathbf{k}) = i \int d^3\mathbf{x} e^{ikx} \overleftrightarrow{\partial}_0 \phi_{\text{in(out)}}(x), \quad (3.30)$$

where the right-hand side is independent of x_0 and $f \overleftrightarrow{\partial}_0 g = f(\partial_0 g) - (\partial_0 f)g$.

The “in” and “out” states discussed previously are then simply defined using the creation operators of the in and out fields. For example, the incoming and outgoing states of n particles with momenta \mathbf{k}_i are

$$|\mathbf{k}_1, \dots, \mathbf{k}_n \text{ in(out)}\rangle = \prod_{i=1}^n a_{\text{in(out)}}^\dagger(\mathbf{k}_i)|0\rangle. \quad (3.31)$$

They are orthonormal when using the measure $\widetilde{d\mathbf{k}}$ for momentum integration.

Since $S_{\text{ret}}(x-y) = 0$ for $x_y < y_0$, it seems that the integral in (3.26) will vanish and $\phi(x)$ approach $\sqrt{Z}\phi_{\text{in}}(x)$ as $x_0 \rightarrow -\infty$, with a similar situation for the out field as

² The creation and annihilation operators for the out field will then also satisfy these relations.

$x_0 \rightarrow +\infty$. This is not exact but a rigorous statement of this idea is that for any two normalizable states $|\alpha\rangle, |\beta\rangle$ and any on-shell momentum k , the following limits hold

$$\lim_{x_0 \rightarrow -\infty(+\infty)} \int d^3\mathbf{x} \langle \alpha | e^{ik \cdot x} \overleftrightarrow{\partial}_0 \phi(x) | \beta \rangle = \sqrt{Z} \int d^3\mathbf{x} \langle \alpha | e^{ik \cdot x} \overleftrightarrow{\partial}_0 \phi_{\text{in(out)}}(x) | \beta \rangle. \quad (3.32)$$

Combining (3.30) and (3.32), we can compute any matrix element between in and out states from correlation functions of the field $\phi(x)$. In particular, one can obtain the LSZ reduction formula (named after Lehmann, Symanzik and Zimmermann) for scalar fields

$$\begin{aligned} \langle \mathbf{p}_1, \dots, \mathbf{p}_m \text{ out} | \mathbf{q}_1, \dots, \mathbf{q}_n \text{ in} \rangle &= \left(\frac{i}{\sqrt{Z}} \right)^{m+n} \int \prod_{i=1}^m [d^4x_i e^{-ip_i \cdot x_i} (\partial_{x_i}^2 + m^2)] \\ &\times \prod_{j=1}^n [d^4y_j e^{iq_j \cdot y_j} (\partial_{y_j}^2 + m^2)] \langle 0 | T \phi(x_1) \cdots \phi(x_m) \phi(y_1) \cdots \phi(y_n) | 0 \rangle. \end{aligned} \quad (3.33)$$

where $p_i = (\omega_{\mathbf{p}_i}, \mathbf{p}_i)$ and $\partial_{x_i}^2$ is the d'Alembert operator $\partial^\mu \partial_\mu$ acting on the coordinate x_i .

S-matrix

The S-matrix \mathcal{S} is defined as the operator which links the bases made by the “in” and the “out” states

$$\mathcal{S}_{\alpha\beta} \equiv \langle \beta \text{ out} | \alpha \text{ in} \rangle \quad \text{so that} \quad |\alpha \text{ in} \rangle = \sum_{\beta} \mathcal{S}_{\alpha\beta} |\beta \text{ out} \rangle \quad (3.34)$$

where α and β denote the details of the states, i.e. the number of particles and their momenta. The sum is over all possible states (discrete for the number of particles and continuous with measure $\widetilde{d\mathbf{k}}$ for the momenta). We make the conservation of total energy-momentum explicit by writing the matrix elements as

$$S_{\alpha\beta} = (2\pi)^4 \delta(W_{\text{in}} - W_{\text{out}}) \delta(\mathbf{P}_{\text{in}} - \mathbf{P}_{\text{out}}) S(\beta | \alpha) \quad (3.35)$$

where $W_{\text{in(out)}}$ and $\mathbf{P}_{\text{in(out)}}$ are the total energy and momentum of the incoming (outgoing) particles described by α (β).

To ensure conservation of probability, the S-matrix must be an unitary operator. Consider two incoming particles, the unitarity condition is then given by

$$\begin{aligned} (2\pi)^4 \delta(\tilde{p}' + \tilde{q}' - \tilde{p} - \tilde{q}) \sum_n \int \prod_{i=1}^n \widetilde{d\mathbf{k}_i} (2\pi)^4 \delta(\tilde{p} + \tilde{q} - \sum_{i=1}^n \tilde{k}_i) \\ S(\mathbf{k}_1, \dots, \mathbf{k}_n | \mathbf{p}', \mathbf{q}')^* S(\mathbf{k}_1, \dots, \mathbf{k}_n | \mathbf{p}, \mathbf{q}) = (2\pi)^6 2\omega_{\mathbf{p}} 2\omega_{\mathbf{q}} \delta(\mathbf{p} - \mathbf{p}') \delta(\mathbf{q} - \mathbf{q}') \end{aligned} \quad (3.36)$$

with the shorthand $\tilde{p} = (\omega_{\mathbf{p}}, \mathbf{p})$, etc. for on-shell 4-momenta. The sum is over all possible numbers n of outgoing particles and all momenta for these particles. If the energy is below the *inelastic threshold*, i.e. the lowest energy which can support more than two on-shell particles, only terms with $n = 2$ contribute to the sum. Furthermore, the condition in the center-of-mass frame is simplified to

$$\frac{\delta(\mathbf{p}' - \mathbf{p})}{32\pi} \int d\hat{\mathbf{k}} S(\mathbf{k}, -\mathbf{k} | \mathbf{p}', -\mathbf{p}')^* S(\mathbf{k}, -\mathbf{k} | \mathbf{p}, -\mathbf{p}) = (2\pi)^3 (2\omega_{\mathbf{p}})^2 \delta(\mathbf{p}' - \mathbf{p}) \quad (3.37)$$

where $\mathbf{k} = p\hat{\mathbf{k}}$. The Dirac delta function on the right-hand side can be expanded on the spherical harmonics as

$$\delta(\mathbf{p}' - \mathbf{p}) = \frac{\delta(p' - p)}{p^2} \sum_{l=0}^{\infty} \sum_{m=-l}^l Y_{lm}^*(\hat{\mathbf{p}}') Y_{lm}(\hat{\mathbf{p}}) \quad (3.38)$$

The two previous equations, combined with the spherical symmetry of the interaction, lead to the following expansion of the S-matrix elements in the center-of-mass frame under the inelastic threshold

$$S(\mathbf{p}', -\mathbf{p}' | \mathbf{p}, -\mathbf{p}) = \frac{16\pi^2 W}{p} \sum_{l=0}^{\infty} \sum_{m=-l}^l e^{2i\delta_l(p)} Y_{lm}^*(\hat{\mathbf{p}}') Y_{lm}(\hat{\mathbf{p}}) \quad (3.39)$$

where $p' = p$ and $W = 2\omega_{\mathbf{p}}$ is the total energy. The norms of the coefficients in the expansion are fixed by unitarity as we have seen but their phases depend on the specifics of the interaction and are conventionally chosen as $2\delta_l(p)$, which effectively defines the scattering phase shifts in scalar quantum field theory.

An important remark is that we assumed the two incoming particles to be distinguishable, which requires some internal degree of freedom such as isospin in the current context. If the particles are not distinguishable, the right-hand side of (3.36) has four terms and the S-matrix elements get a multiplicative factor of 2.

Cross-section

To separate the effect of the interaction from the free propagation, it is useful to introduce the T-matrix defined by $S = \mathbf{1} + iT$. With the same context and notations as for equation (3.39), we get for the T-matrix elements

$$T(\mathbf{p}, -\mathbf{p} | \mathbf{p}_z, -\mathbf{p}_z) = \frac{16\pi^{3/2} W}{p} \sum_{l=0}^{\infty} \sqrt{2l+1} e^{i\delta_l(p)} \sin \delta_l(p) Y_{l0}(\hat{\mathbf{p}}) \quad (3.40)$$

where $|\mathbf{p}| = |\mathbf{p}_z| = p$, \mathbf{p}_z is along the z -axis and the remark about distinguishability of the particles still applies. By rotations and Lorentz boosts, this expression can be generalized to any frame and incoming momenta.

Note the similarity of (3.40) with the expression (3.16) of the scattering amplitude $f(\hat{\mathbf{r}})$ in quantum mechanics (QM). It is then possible to define the cross-section in quantum field theory with similar arguments as we have done in QM. For the purpose of this thesis, it suffices to say that the interaction-dependent part of the differential cross section is given by the squared modulus of the T-matrix elements (cf. (3.18) for the analogous expression in the QM). In the context of two-particle elastic scattering, we have shown that it is once again completely determined by the knowledge of the scattering phase shifts $\delta_l(p)$.

3.2 FINITE-SIZE METHOD

We have reviewed the mathematical framework to describe scattering processes from classical mechanics to quantum field theory. In the case of the elastic scattering of two particles, two incoming particles propagate freely in the distant past, interact at intermediate times and propagate freely again in the distant future. The discrepancy between the incoming and outgoing states can be completely characterized by the scattering phase shifts. The phase shifts can be measured experimentally and linked to

the theoretical description of the interaction (the potential for classical and quantum mechanics, the correlation functions for quantum field theory via the LSZ reduction formula). One can thus test a theory or make useful predictions for real-world events.

In the context of quantum field theory, we have seen in chapter 2 that the Euclidean correlation functions can be computed using lattice techniques. However, the explicit expression of the S-matrix provided by the LSZ reduction formula involves correlation functions in Minkowski space. Since the analytic continuation to Minkowski space of the correlation functions computed on the lattice is ill-defined, we need another way to extract the S-matrix.

We know from section 2.3 that the energy spectrum can be extracted from lattice inputs. Lattice calculations are performed for a finite volume so that the spectrum is discrete and varies with the volume. A remarkable result is that the two-particle energy spectrum of a theory in finite volume is directly related to the scattering phase shifts of this theory in infinite volume at the corresponding energies. The idea is that the boundary conditions restrict the spectrum in finite volume in a way which can be worked out analytically with an explicit dependence on the scattering phase shifts. This relation was first derived by Martin Lüscher and is since known as the *finite-size formula*, Lüscher’s formula or the Lellouch-Lüscher formula. It is valid if the lattice extent is larger than twice the effective range of the interaction.

The formula was first proven by Lüscher for a system of two scalar particles of identical mass m with zero total momentum in a finite box with periodic boundary conditions. Since then, it has been expanded to “moving” frames [21] (systems with non-zero total momentum), asymmetric lattices [22], twisted boundary conditions [23], particles with arbitrary spins [24], arbitrary number of coupled two-particle channels [25], systems with more than two particles [26], etc.

Given the finite-size formula, the strategy to study two-particle channels on the lattice is the following. Using the variational method described in section 2.3.2, one can extract the lower part of the energy spectrum from lattice simulations. This spectrum corresponds to the spectrum of the theory in a finite box up to corrections due to the non-zero lattice spacing. After taking the continuum limit at fixed volume, one uses the finite-size formula to relate the obtained spectrum to the scattering phase shifts of the theory in infinite-volume at these energies. This approach will be referred to as the *finite-volume method*. To obtain the phase shifts at different energies, one can then repeat the process with a different volume or a different total momentum.

In this section, we will follow Lüscher’s original derivation [8, 9, 27] of the finite-size formula. The first part is to prove the formula for a quantum mechanical system where the wave function satisfies the Schrödinger equation. The second part is to show that an effective Schrödinger equation can be derived in quantum field theory so that the result is still valid.

3.2.1 Two-particle states on a torus

We have discussed at the beginning of subsection 3.1.2 the structure of the wave function $\psi(\mathbf{r})$ describing a quantum mechanical system of two scalar particles of mass m in infinite volume in the center-of-mass frame. We keep the same notations and, as previously, we assume that the interaction between the particles derives from a spherically symmetric potential $V(r)$ with finite extent R , i.e. $V(r) = 0$ for $r > R$.

Boundary conditions

In infinite volume, we have found that the partial waves $\psi_{lm}(r)$ defined by (3.7) are solutions of the radial Schrödinger equation (3.8). In the region $r > R$, the potential vanishes and the partial waves are linear combinations of the spherical Bessel functions:

$$\psi_{lm}(r) = b_{lm} [\alpha_l(k)j_l(kr) + \beta_l(k)n_l(kr)], \quad (3.41)$$

for some constants b_{lm} and where the energy-dependent functions $\alpha_l(k)$ and $\beta_l(k)$ are related to the phase shifts by (3.11). Remember that k is related to the energy E by $k^2 = 2\mu E$.

Now, consider the same system in a finite cubic box of size $L \times L \times L$ with periodic boundary conditions. The wave function is periodic, $\psi(\mathbf{r}) = \psi(\mathbf{r} + \mathbf{n}L)$ for any $\mathbf{n} \in \mathbb{Z}^3$, and the interaction is described by the periodic potential

$$V_L(\mathbf{r}) = \sum_{\mathbf{n} \in \mathbb{Z}^3} V(|\mathbf{r} + \mathbf{n}L|). \quad (3.42)$$

The problem is greatly simplified if $R < L/2$, which we will assume from now on. Indeed, for $r < L/2$ the potential is simply $V_L(\mathbf{r}) = V(r)$ so that the partial waves $\psi_{lm}(r)$ satisfy the same radial Schrödinger equation as in the infinite volume. Therefore, the relation (3.41) still holds in the region $R < r < L/2$ for some constants b_{lm} possibly different from that of the infinite-volume partial waves. For $R < L/2$, the finite-volume wave functions are therefore directly related to the scattering phase shifts.

We will now see how the periodic boundary conditions constrain the solutions of the Schrödinger equation and thus the energy spectrum. The potential $V_L(\mathbf{r})$ vanishes if $|\mathbf{r} + \mathbf{n}L| > R$ for any $\mathbf{n} \in \mathbb{Z}$. In this *exterior region*, the wave function satisfy the Helmholtz equation

$$(\Delta + k^2)\psi(\mathbf{r}) = 0. \quad (3.43)$$

Ref. [9] studied in detail the periodic solutions to this equation. By Fourier transform, the momenta for periodic solutions take value in the lattice

$$\Lambda = \left\{ \frac{2\pi}{L} \mathbf{n} \in \mathbb{R}^3 \mid \mathbf{n} \in \mathbb{Z}^3 \right\}. \quad (3.44)$$

A technical issue arises if an energy in finite volume is such that the associated k is exactly the norm of some element of Λ . These energies must be treated separately and we refer to ref. [9] for details. However, this case should be anecdotal in practice because Λ is discrete so in the following we will assume that k is “regular”, meaning that it is not the norm of any element of Λ . It is then straightforward to see that the function

$$G(\mathbf{r}; k^2) = \frac{1}{L^3} \sum_{\mathbf{p} \in \Lambda} \frac{e^{i\mathbf{p}\cdot\mathbf{r}}}{\mathbf{p}^2 - k^2} \quad (3.45)$$

is well-defined and is a periodic solution of the Helmholtz equation. Further solutions can be defined by differentiation. A convenient choice is

$$G_{lm}(\mathbf{r}; k^2) = \mathcal{Y}_{lm}(\nabla)G(\mathbf{r}; k^2) \quad (3.46)$$

with the harmonic polynomials defined by

$$\mathcal{Y}_{lm}(\mathbf{r}) = r^l Y_{lm}(\hat{\mathbf{r}}). \quad (3.47)$$

It can be shown that the functions $G_{lm}(\mathbf{r}; k^2)$ are linearly independent by looking at their behavior around $r = 0$. Furthermore, on the set of periodic solutions of the Helmholtz equation of order ν , i.e. the solutions ψ such that $r^{\nu+1}\psi(\mathbf{r}) = O(1)$ near the origin $r = 0$, the functions $G_{lm}(\mathbf{r}; k^2)$ with $l \leq \nu$ are complete and therefore form a basis.

The trick is then to put an angular momentum cutoff ν on the interaction, i.e. consider the system where the interaction is described by an operator \hat{V}_ν such that

$$\hat{V}_\nu \psi(\mathbf{r}) = V(r) \sum_{l=0}^{\nu} \sum_{m=-l}^l Y_{lm}(\hat{\mathbf{r}}) \psi_{lm}(r). \quad (3.48)$$

Obviously the original system is recovered as $\nu \rightarrow \infty$. At finite ν however, the wave functions of the Hamiltonian eigenstates are guaranteed to be of order order ν and therefore can be expanded in the exterior region as

$$\psi(\mathbf{r}) = \sum_{l=0}^{\nu} \sum_{m=-l}^l v_{lm} G_{lm}(\mathbf{r}; k^2) \quad (3.49)$$

for some coefficients v_{lm} . To write this in terms of partial waves, we need the spherical harmonics expansion of the functions $G_{lm}(\mathbf{r}; k^2)$. It is given for $r < L/2$ by

$$G_{lm}(\mathbf{r}; k^2) = \frac{(-1)^l}{4\pi} k^{l+1} \left\{ Y_{lm}(\mathbf{r}) n_l(kr) + \sum_{l'=0}^{\infty} \sum_{m'=-l'}^{l'} \mathcal{M}_{lm, l'm'} Y_{l'm'}(\mathbf{r}) j_{l'}(kr) \right\}. \quad (3.50)$$

An explicit expression for the elements of the matrix \mathcal{M} is given in equation (3.34) of ref. [9]. We then find for $l \leq \nu$ and $R < r < L/2$ that the partial waves are given by

$$\psi_{lm}(r) = \left[v_{lm} \frac{(-1)^l}{4\pi} k^{l+1} \right] n_l(kr) + \left[\sum_{l'=0}^{\nu} \sum_{m'=-l'}^{l'} v_{l'm'} \frac{(-1)^{l'}}{4\pi} k^{l'+1} \mathcal{M}_{l'm', lm} \right] j_l(kr). \quad (3.51)$$

On the other hand, the partials waves $\psi_{lm}(r)$ for $l \leq \nu$ still satisfy the same radial Schrödinger equation after the introduction of the angular momentum cutoff. Therefore, the expression (3.41) in terms of the phase shifts still holds for $l \leq \nu$ and $R < r < L/2$.

Quantization condition

The previous discussion provides some understanding of the structure of the wave functions of two particles in finite volume. If the interaction range R is smaller than $L/2$ there is a spherically symmetric region $R < r < L/2$ where the wave function describes a free propagation. Equation (3.41) shows that the resulting wave function is completely determined by (i) a set of constants depending on the boundary conditions and (ii) the scattering phase shifts. In both finite and infinite volume, the boundary condition at $r = R^+$ encodes the effect of the interaction in the interior region $r < R$. In finite volume however, the periodic boundary conditions enforce an additional constraint given by (3.51). While the two-particle spectrum in infinite volume is continuous, the two constraints in finite volume are only compatible for a certain set of values of k . This implies that the finite-volume spectrum is discrete but also that it is directly related to the scattering phase shifts.

Consider \mathcal{H}_ν the Hilbert space of complex vectors v with components v_{lm} where $l = 0, \dots, \nu$ and $m = -l, \dots, l$. These vectors will represent the finite number of degrees

l	P	A_1^P	A_2^P	E^P	T_1^P	T_2^P
0	+	1	0	0	0	0
1	-	0	0	0	1	0
2	+	0	0	1	0	1
3	-	0	1	0	1	1
4	+	1	0	1	1	1
5	-	0	0	1	2	1
6	+	1	1	1	1	2

Table 3.1: Multiplicity $N(\Gamma, l)$ of the irreducible representation $\Gamma = A_1^+, \dots$ of the cubic group in the decomposition of the representation ρ_l for the first few angular momenta l .

of freedom of the wave function ψ in the exterior region in the presence of the cutoff ν . Define the linear operators A , B and M acting on \mathcal{H}_ν by

$$[Av]_{lm} = \alpha_l(k)v_{lm}, \quad [Bv]_{lm} = \beta_l(k)v_{lm}, \quad [Mv]_{lm} = \sum_{l'=0}^{\nu} \sum_{m'=-l'}^{l'} \mathcal{M}_{lm, l'm'} v_{l'm'}. \quad (3.52)$$

Then, the two constraints (3.41) and (3.51) can be simply written in \mathcal{H}_ν as

$$\det[A - BM] = 0. \quad (3.53)$$

Using the definition (3.11), we can make the phase shifts dependence explicit with

$$\det[e^{2i\delta} - U] = 0, \quad U = (M + i)/(M - i), \quad (3.54)$$

where $e^{2i\delta}$ is diagonal with elements $e^{2i\delta_l(k)}$ and matrix U can be shown to be well-defined.

The long-awaited *finite-size formula* is given by (3.54) as the momentum cutoff ν is driven to infinity. It characterizes the energies which are possible in finite volume thanks to the compatibility of the two boundary conditions discussed previously. Note that it involves the determinant of an infinite matrix as $\nu \rightarrow \infty$. However, the scattering phase shifts can often be neglected above some value of the angular momentum so that keeping ν finite leads to a good approximation. Furthermore, we can use the symmetries of the finite-volume system to simplify this formula.

Cubic symmetry

In infinite volume, the two-particle system is spherically symmetric, meaning that it is invariant under the action of all the rotations R in $SO(3)$. In a finite cubic box, the system is only invariant under a finite set of 24 rotations forming the octahedral symmetry group \mathcal{O} . Combining rotations with reflections, the finite-size system is invariant under the achiral octahedral symmetry group \mathcal{O}_h , or *cubic group*, which contains 48 transformations. The group \mathcal{O} has 5 irreducible representations A_1 , A_2 , E , T_1 and T_2 with respective dimensions 1, 1, 2, 3 and 3. The cubic group \mathcal{O}_h has twice as many, obtained from those of \mathcal{O} using the tensor product with the two irreducible representations of the parity operator and therefore denoted as A_1^+ , A_1^- , etc.

Under the action of an element R of $O(3)$, the spherical harmonics transform as

$$Y_{lm}(R\hat{\mathbf{r}}) = \sum_{m'=-l}^l D_{mm'}^{(l)}(R)Y_{lm'}(\mathbf{r}), \quad (3.55)$$

where $D^{(l)}(R)$ are the Wigner D-matrices. For any $R \in O(3)$, we can define the operators $D(R)$ and $D_l(R)$ in \mathcal{H}_ν with elements

$$[D(R)]_{lm,l'm'} = \delta_{ll'} D_{mm'}^{(l)}(R), \quad [D_l(R)]_{l'm',l''m''} = \delta_{ll'} \delta_{l''l'} D_{m'm''}^{(l)}(R) \quad (3.56)$$

Using (3.55), it is easy to see that $\rho : R \in \mathcal{O}_h \mapsto D(R)$ and $\rho_l : R \in \mathcal{O}_h \mapsto D_l(R)$ form representations of \mathcal{O}_h on \mathcal{H}_ν . Furthermore, these representations have the following decompositions

$$\rho = \bigoplus_{l=0}^{\nu} \rho_l, \quad \rho_l = \bigoplus_{\Gamma} N(\Gamma, l) \Gamma, \quad (3.57)$$

where the second direct sum runs over the irreducible representations Γ (of respective dimensions d_Γ) of the cubic group $\Gamma = A_1^+, \dots$ and $N(\Gamma, l)$ denotes the multiplicity of Γ in ρ_l . Table 3.1 summarizes the values of these multiplicities for the first few angular momenta. This decomposition of ρ ensures the existence of an orthonormal basis

$$|\Gamma, \alpha; l, n\rangle, \quad \Gamma \in \{A_1^+, \dots\}, \alpha \in \{1, \dots, d_\Gamma\}, l \in \{0, \dots, \nu\}, n \in \{1, \dots, N(\Gamma, l)\}, \quad (3.58)$$

which transforms under the action of the cubic group as (Γ, α) .

It can be shown using the explicit expression of the elements $\mathcal{M}_{lm,l'm'}$ that the operator M in \mathcal{H}_ν commutes with all the matrices $D(R)$ for R in the cubic group \mathcal{O}_h . The application of Schur's lemma then implies that the operator M is block-diagonal in the basis $|\Gamma, \alpha; l, n\rangle$ with identical blocks for each occurrence of a representation Γ , i.e.

$$\langle \Gamma, \alpha; l, n | M | \Gamma', \alpha'; l', n' \rangle = \delta_{\Gamma\Gamma'} \delta_{\alpha\alpha'} \mathcal{M}(\Gamma)_{ln,l'n'}. \quad (3.59)$$

The elements of the matrices $\mathcal{M}(\Gamma)$ are given in appendix E of ref. [9] for $l, l' \leq 4$.

Consider $\mathcal{H}_\nu^{\Gamma\alpha}$ the subspace of \mathcal{H}_ν spanned by $|\Gamma, \alpha; l, n\rangle$ at fixed (Γ, α) . We can define the operators $M(\Gamma)$ and $e^{2i\delta}$ acting on $\mathcal{H}_\nu^{\Gamma\alpha}$ by

$$[e^{2i\delta} v]_{ln} = e^{2i\delta_l(k)} v_{ln}, \quad [M(\Gamma)v]_{ln} = \sum_{l'=0}^{\nu} \sum_{n'=1}^{N(\Gamma,l')} \mathcal{M}(\Gamma)_{ln,l'n'} v_{l'n'}, \quad (3.60)$$

for any v in $\mathcal{H}_\nu^{\Gamma\alpha}$.

In the basis $|\Gamma, \alpha; l, n\rangle$, we have seen that the operator M is block-diagonal. Therefore, the determinant in (3.54) becomes a product of determinants and for it to be zero, there must be at least one irreducible representation Γ such that

$$\det[e^{2i\delta} - M(\Gamma)] = 0, \quad U(\Gamma) = (M(\Gamma) + i)/(M(\Gamma) - i). \quad (3.61)$$

The discussion in this subsection implies that the finite-size spectrum can be separated in 10 sets of eigenenergies, one for each irreducible representation Γ of the cubic group. In lattice simulations, it is advantageous to use operators which only couple with eigenstates in a certain channel (Γ, α) . In this case, all the eigenenergies satisfy the condition (3.61) for this Γ . As an example, consider $\Gamma = A_1^+$. The original condition (3.54) involves the scattering phase shifts for any angular momentum $l \geq 0$ while the reduced condition (3.61) only involves those for angular momenta $l = 0, l = 4$, etc. (see table 3.1). Neglecting the phase shifts for $l \geq 4$ (which is often a very good approximation), the reduced condition simply reads

$$\cot \delta_0(k) = \frac{1}{\pi^{3/2} q} \mathcal{Z}_{00}(1; q^2), \quad q = \frac{kL}{2\pi} \quad (3.62)$$

because the determinant is that of a 1×1 matrix. The zeta function appearing above is defined for $\text{Re } s > 3/2$ by

$$\mathcal{Z}_{00}(s; q^2) = \frac{1}{\sqrt{4\pi}} \sum_{\mathbf{n} \in \mathbb{Z}^3} \frac{1}{(\mathbf{n}^2 - q^2)^s} \quad (3.63)$$

and by analytic continuation otherwise.

3.2.2 Potential in QFT

Following ref. [8], we will now present an argument proving that the quantization conditions derived previously still hold in quantum field theory, up to corrections exponentially small in the size of the box. Once again, we consider the quantum field theory of a field $\phi(x)$ describing a scalar particle of mass m .

Instead of wave functions as in quantum mechanics, the basic objects in QFT will be the connected Euclidean correlation functions³ $\langle \phi(x_1) \cdots \phi(x_n) \rangle_C$ defined in (2.12). The full Euclidean propagator is defined as

$$G(p) = \int d^4x e^{-ip \cdot x} \langle \phi(x) \phi(0) \rangle_C \quad (3.64)$$

and we assume that the field ϕ is normalized so that the propagator has a pole with unit residue on the mass shell

$$G(p)^{-1} = m^2 + p^2 - \Sigma(p), \quad \Sigma(p) \Big|_{p^2 = -m^2} = \frac{\partial}{\partial p^\mu} \Sigma(p) \Big|_{p^2 = -m^2} = 0. \quad (3.65)$$

The full-propagator-amputated connected correlation function $G(p_1, \dots, p_n)$ is defined by

$$\begin{aligned} \langle \phi(x_1) \cdots \phi(x_n) \rangle_C &= \int \frac{d^4p_1}{(2\pi)^4} \cdots \frac{d^4p_n}{(2\pi)^4} e^{i(p_1 \cdot x_1 + \cdots + p_n \cdot x_n)} \\ &\quad \cdot (2\pi)^4 \delta(p_1 + \cdots + p_n) G(p_1) \cdots G(p_n) G(p_1, \dots, p_n). \end{aligned} \quad (3.66)$$

As seen in section 2.1.1, the correlation functions in Minkowski space can be recovered from the Euclidean ones by a Wick rotation. Combining this with the LSZ reduction formula (3.33), we obtain an expression for the two-particle T-matrix element introduced in section 3.1.3 as

$$T(\mathbf{p}', \mathbf{q}' | \mathbf{p}, \mathbf{q}) = \lim_{\epsilon \rightarrow 0^+} G(p', q', -p, -q), \quad (3.67)$$

with the Euclidean 4-vectors $p = (\mathbf{p}, i\omega_{\mathbf{p}} - \epsilon)$, $p' = (\mathbf{p}', i\omega_{\mathbf{p}'} - \epsilon)$, etc.

Connected 4-point function

We are interested in the properties of the connected 4-point function $G(p_1, p_2, p_3, p_4)$ in the center-of-mass frame which is related to the scattering phase shifts through the T-matrix by (3.67) and (3.40). To this purpose, we introduce the following usual notations for two-particle channels

$$\begin{aligned} p_1 &= \frac{1}{2}P + p', & p_2 &= \frac{1}{2}P - p', \\ p_3 &= -(\frac{1}{2}P + p), & p_4 &= -(\frac{1}{2}P - p), \end{aligned} \quad (3.68)$$

³ From now on, we omit the hat on the field operator $\phi(x)$ and other operators since there is no confusion with the classical fields introduced for the path integral.

where we enforced the conservation of total momentum. In the center-of-mass frame, we note the Euclidean total momentum as $P = (\mathbf{0}, iW)$, which corresponds to a total energy of W after performing the Wick rotation. Assuming that there are neither bound states nor additional stable particles, the inelastic threshold is at $W_{\text{th}} = 4m$ where 4 on-shell particles can be created. We will consider the structure of the 4-point function for energies in the strip $0 \leq \text{Re } W < 4m$, or *elastic energy region*.

An important tool for the study of two-particle states is the *Bethe-Salpeter kernel* $BS(p_1, p_2, p_3, p_4)$. It is defined as the sum of all the Feynman diagrams contributing to $G(p_1, p_2, p_3, p_4)$ which are two-particle irreducible in the (p_1, p_2) -channel. With the shorthands

$$K(p', p) = BS(p_1, p_2, p_3, p_4), \quad (3.69)$$

$$G_4(p', p) = G(p_1, p_2, p_3, p_4), \quad (3.70)$$

$$G_2(k) = G(\frac{1}{2}P + k)G(\frac{1}{2}P - k), \quad (3.71)$$

the 4-point function G_4 and the Bethe-Salpeter (BS) kernel K are related through

$$G_4(p', p) = K(p', p) + \frac{1}{2} \int \frac{d^4 k}{(2\pi)^4} K(p', k) G_2(k) G_4(k, p). \quad (3.72)$$

In ref. [8], Lüscher studied in detail the regularity of the propagator G_2 and the BS kernel K in the elastic energy region. He proved that the kernel $K(p', p)$ is analytic in the domain

$$|\text{Re } W| < 4m, \quad |\text{Im } p'_4| < m, \quad |\text{Im } p_4| < m, \quad (3.73)$$

and that the singularities of the propagator G_2 are such that for any function $f(p_4)$ analytic in the strip $|\text{Im } p_4| < m$, the integral

$$I_{\mathbf{k}}(W) = \int \frac{dk_4}{2\pi} f(k_4) G_2(k), \quad (3.74)$$

where $k = (\mathbf{k}, k_4)$, extends to an analytic function of W in the region $0 \leq \text{Re } W < 4m$ except, if $\omega_{\mathbf{k}} < 2m$, at $W = 2\omega_{\mathbf{k}}$ where it has a simple pole with residue $-f(0)/(2\omega_{\mathbf{k}})^2$. This results motivated the definition of a new kernel \hat{K} as

$$\hat{K}(p', p) = K(p', p) + \frac{1}{2} \int \frac{d^4 k}{(2\pi)^4} K(p', k) \left[G_2(k) - \frac{2\pi\delta(k_4)h(\mathbf{k})}{(2\omega_{\mathbf{k}})^2(2\omega_{\mathbf{k}} - W)} \right] \hat{K}(k, p), \quad (3.75)$$

which can be shown to be analytic in the elastic energy region if h is any function such that $h(\mathbf{k}) = 1$ at $W = 2\omega_{\mathbf{k}} < 4m$. This regularity is obtained because the singularities of G_2 are cancelled in the integral.

In terms of the new kernel \hat{K} , the relation (3.72) reads

$$G_4(p', p) = \hat{K}(p', p) + \frac{1}{2} \int_{k_4=0} \frac{d^3 \mathbf{k}}{(2\pi)^3} \hat{K}(p', k) \frac{h(\mathbf{k})}{(2\omega_{\mathbf{k}})^2(2\omega_{\mathbf{k}} - W)} G_4(k, p). \quad (3.76)$$

In summary, the integral over k_4 is performed and the regular part of G_2 is incorporated into \hat{K} while its singular part is made explicit.

Effective Schrödinger equation

We now provide a completely 3-dimensional formulation of (3.76). For any vector \mathbf{k} with $\omega_{\mathbf{k}} < 2m$, define the “wave function”

$$\psi_{\mathbf{k}}(\mathbf{r}) = (e^{i\mathbf{k}\cdot\mathbf{r}} + e^{-i\mathbf{k}\cdot\mathbf{r}}) + \lim_{\epsilon \rightarrow 0^+} \int \frac{d^3 \mathbf{p}}{(2\pi)^3} \frac{m e^{i\mathbf{p}\cdot\mathbf{r}}}{\mathbf{p}^2 - \mathbf{k}^2 - i\epsilon} \rho(\mathbf{p}) G_4(p, k) \rho(\mathbf{k}) \Big|_{\substack{p_4=k_4=0 \\ W=2\omega_{\mathbf{k}}+i\epsilon}} \quad (3.77)$$

using the normalizing function

$$\rho(\mathbf{p}) = \frac{1}{4\omega_{\mathbf{p}}} \sqrt{\frac{h(\mathbf{p})(2\omega_{\mathbf{p}} + W)}{m}}. \quad (3.78)$$

Similarly, define the “potential”

$$U_E(\mathbf{r}', \mathbf{r}) = - \lim_{\epsilon \rightarrow 0^+} \int \frac{d^3 \mathbf{p}'}{(2\pi)^3} \frac{d^3 \mathbf{p}}{(2\pi)^3} e^{i(\mathbf{p}' \cdot \mathbf{r}' - \mathbf{p} \cdot \mathbf{r})} \rho(\mathbf{p}') \hat{K}(p', p) \rho(\mathbf{p}) \Big|_{\substack{p'_4 = p_4 = 0 \\ W = 2\omega_{\mathbf{k}} + i\epsilon}}. \quad (3.79)$$

with a subscript $E = \mathbf{k}^2/m$ denoting explicitly the \mathbf{k}^2 -dependence.

After some algebra, one finds that (3.76) implies

$$-\frac{1}{2\mu} \Delta \psi_{\mathbf{k}}(\mathbf{r}) + \frac{1}{2} \int d^3 \mathbf{r}' U_E(\mathbf{r}, \mathbf{r}') \psi_{\mathbf{k}}(\mathbf{r}') = E \psi_{\mathbf{k}}(\mathbf{r}) \quad (3.80)$$

with $\mu = m/2$.

We have recovered from QFT the Schrödinger equation for the scattering of two indistinguishable particles in the center-of-mass frame with incoming relative momentum \mathbf{k} and total energy E . Furthermore, using the relation (3.67) between the T-matrix elements and the 4-point function as well as the expansion (3.40) of the T-matrix elements in terms of the scattering phase shifts, one can show that the “wave function” $\psi_{\mathbf{k}}(\mathbf{r})$ has the same asymptotic behavior as the wave function in quantum mechanics⁴

The “potential” U_E is *energy-dependent* but this does not matter since the relation with the phase shifts is valid at fixed energy. With the choice of $h(\mathbf{p}) = \exp[(mE - \mathbf{p}^2)/m^2]$, it is analytic in E in the range $-m < E < 3m$, rotationally invariant, smooth in \mathbf{r} and \mathbf{r}' and decays exponentially in all directions.

Finite volume

We now consider the same quantum field theory in a finite box of size $L \times L \times L$ with periodic boundary conditions. In this case, the momenta only take values on the lattice Λ , see (3.44). The Bethe-Salpeter kernel is thus modified since all the loop integral appearing in the two-particle irreducible Feynman diagrams become sums over Λ . Let K_L be the finite-volume equivalent of K in finite-volume. Lüscher showed using graph-theoretical techniques [8] that $K - K_L$ decays exponentially in L .

A useful result to relate the finite-volume quantities to the infinite-volume ones is that

$$\frac{1}{L^3} \sum_{\mathbf{p} \in \Lambda} f(\mathbf{p}) = \int \frac{d^3 \mathbf{p}}{(2\pi)^3} f(\mathbf{p}) + O(L^{-N}) \quad (3.81)$$

for any continuous and integrable function f which has integrable derivatives up to the N -th order ($N \geq 1$). With this relation, one can exchange all sums for integrals when the integrand is regular and prove that the effective Schrödinger equation (3.80) still holds in finite volume up to corrections decaying faster than any power of L^{-1} . A more detailed analysis, cf. section 4.3, shows that the corrections actually decay exponentially in L .

The last difference with the quantum mechanical case is that the potential U_E does not have a finite range, even less one which is smaller than L . A work-around is to

⁴ The argument is similar to the one for the Bethe-Salpeter wave function which will be discussed in detail in section 3.3.1.

multiply $U_E(\mathbf{r}, \mathbf{r}')$ by a smooth radial function which is equal to 1 for r and r' smaller than say $.3L$ and equal to 0 for r and r' larger than $.4L$. The resulting “potential” has the same regularity as U_E and but it also has a finite range $R = .4L < L/2$. Furthermore, since U_E decays exponentially in all directions, we can replace U_E by the finite-ranged potential in the Schrödinger equation and only cause corrections decaying exponentially in L .

From the above arguments, we deduce that the quantization conditions derived for the quantum mechanical system are still valid in quantum field theory up to corrections vanishing exponentially with L .

3.3 HAL QCD METHOD

The finite-size method relies on the ability to extract numerically the lower part of the spectrum of the theory in finite volume. In practice, the key equation is therefore (2.58), which allows to obtain from lattice simulations the energies W_n of the finite-size Hamiltonian eigenstates $|n\rangle$ as well as matrix elements of the type $\langle 0|O(0)|n\rangle$ where $O(0)$ is an operator involving the field operators of the theory at time $t = 0$.

In contrast with the finite-size method, the HAL QCD method [10–12] proposes to extract the scattering phase shifts in infinite volume not from the finite-size energy spectrum but from some specific matrix elements. Since its inception, it has been applied to the study of many two-hadron channels (see e.g. [28] for a review) by the HAL QCD (Hadron to Atomic nuclei from Lattice QCD) collaboration.

3.3.1 Bethe-Salpeter wave function

As previously, we will introduce the method with the example of a quantum field theory of a field $\phi(x)$ describing a scalar particle of mass m , normalized in the same way as for the previous section. Furthermore, we assume for simplicity the absence of bound states and resonances.

In the center-of-mass frame, the eigenstates of the Hamiltonian with energies $2m \leq W < 4m$ all describe two-particle scattering states. In infinite volume, the eigenspace corresponding to an energy W in this region is therefore spanned by the states $|\mathbf{k}, -\mathbf{k} \text{ in}\rangle$ with $W = 2\omega_{\mathbf{k}}$, which we introduced in (3.31). The two incoming particles will be assumed distinguishable but it is straightforward to extend the results to indistinguishable particles. In the case of scalar particles, this requires the existence of internal degree of freedoms which will be kept implicit.

The Bethe-Salpeter (BS) wave function in infinite volume is defined as

$$\psi_{\mathbf{k}}(\mathbf{r}) = \langle 0|\phi(0, \frac{\mathbf{r}}{2})\phi(0, -\frac{\mathbf{r}}{2})|\mathbf{k}, -\mathbf{k} \text{ in}\rangle, \quad (3.82)$$

where $\phi(0, \mathbf{r})$ is the field operator taken at position \mathbf{r} and Minkowski time 0.

Asymptotic behavior

We show in this section how the asymptotic behavior of the BS wave function in infinite volume can be used to extract the scattering phase shifts [12, 29, 30]. All considerations in this subsection are made in Minkowski space.

Using the techniques that led to the LSZ reduction formula (3.33), in particular the explicit expression of the “in” states, we arrive to the following expression of the

BS wave functions⁵

$$\psi_{\mathbf{k}}(\mathbf{r}) = - \int d^4x d^4y e^{i(\omega_{\mathbf{k}}x_0 - \mathbf{k}\cdot\mathbf{x})} e^{i(\omega_{\mathbf{k}}y_0 + \mathbf{k}\cdot\mathbf{y})} (\partial_x^2 + m^2)(\partial_y^2 + m^2) \langle 0|T\phi(0, \frac{\mathbf{r}}{2})\phi(0, -\frac{\mathbf{r}}{2})\phi(x)\phi(y)|0\rangle. \quad (3.83)$$

Define the proper vertex Γ as the connected time-ordered correlation function in momentum-space amputated by the free propagator⁶

$$\langle 0|T\phi(x_1)\cdots\phi(x_n)|0\rangle_C = i^n \int \frac{d^4p_1}{(2\pi)^4} \cdots \frac{d^4p_n}{(2\pi)^4} e^{i(p_1\cdot x_1 + \cdots + p_n\cdot x_n)} \cdot (2\pi)^4 \delta(p_1 + \cdots + p_n) \frac{\Gamma(p_1, \dots, p_n)}{(p_1^2 - m^2 + i\epsilon) \cdots (p_n^2 - m^2 + i\epsilon)}. \quad (3.84)$$

The proper vertex with 4 external particles is related to the T-matrix element by

$$\Gamma(p_1, p_2, -p_3, -p_4) = iT(\mathbf{p}_1, \mathbf{p}_2|\mathbf{p}_3, \mathbf{p}_4), \quad (3.85)$$

in the elastic energy region if all p_i are on-shell. Furthermore, we introduce the shorthand $\Gamma_4(p', p) = \Gamma(p_1, p_2, p_3, p_4)$, keeping the total momentum P implicit and using the notations (3.68), more convenient for two-particle channels.

With its explicit expression derived previously, the BS wave function can be related to the proper vertex by

$$\psi_{\mathbf{k}}(\mathbf{r}) = e^{i\mathbf{k}\cdot\mathbf{r}} - \int \frac{d^4p}{(2\pi)^4} e^{ip\cdot\mathbf{r}} \frac{\Gamma_4(p, \tilde{\mathbf{k}})}{((\frac{1}{2}P + p)^2 - m^2 + i\epsilon)((\frac{1}{2}P - p)^2 - m^2 + i\epsilon)} \quad (3.86)$$

where the total momentum is $P = (2\omega_{\mathbf{k}}, \mathbf{0})$ and $\tilde{\mathbf{k}} = (0, \mathbf{k})$.

We use the residue theorem to integrate out p_0 in (3.86) with a contour encircling the upper complex plane and get

$$\psi_{\mathbf{k}}(\mathbf{r}) = e^{i\mathbf{k}\cdot\mathbf{r}} - i \int \frac{d^3\mathbf{p}}{(2\pi)^3} e^{ip\cdot\mathbf{r}} \frac{\omega_{\mathbf{p}} + \omega_{\mathbf{k}}}{8\omega_{\mathbf{p}}\omega_{\mathbf{k}}} \frac{\Gamma_4(\tilde{p}, \tilde{\mathbf{k}})}{\mathbf{p}^2 - \mathbf{k}^2 - i\epsilon} + I(\mathbf{r}), \quad (3.87)$$

where $\tilde{p} = (\omega_{\mathbf{k}} - \omega_{\mathbf{p}}, \mathbf{p})$. Only the residue corresponding to the two-particle pole of the propagator is worked out explicitly. The other poles, due to inelastic channels, do not contribute to the asymptotic behaviour of the BS wave function in the elastic energy region and are aggregated in a function $I(\mathbf{r})$ which is expected to vanish rapidly at large r .

Introduce the following radial functions

$$f_{lm}(p) = i^{l-1} \frac{\omega_{\mathbf{p}} + \omega_{\mathbf{k}}}{8\omega_{\mathbf{p}}\omega_{\mathbf{k}}} \int d\hat{\mathbf{p}} Y_{lm}^*(\hat{\mathbf{p}}) \Gamma_4(\tilde{p}, \tilde{\mathbf{k}}). \quad (3.88)$$

Then, the BS wave function can be expanded on the spherical harmonics with partial waves given by

$$[\psi_{\mathbf{k}}]_{lm}(r) = 4\pi i^l j_l(kr) Y_{lm}^*(\hat{\mathbf{k}}) + \int_0^\infty \frac{p^2 dp}{2\pi^2} \frac{j_l(pr) f_{lm}(p)}{p^2 - k^2 - i\epsilon} + I_{lm}(r). \quad (3.89)$$

⁵ With $Z = 1$ due to the normalization of ϕ .

⁶ In comparison, $G(p_1, p_2, p_3, p_4)$ was defined in section 3.2 as the connected part of the *Euclidean* 4-point correlation function in momentum-space amputated by the *full* propagator.

where $k^2 = \mathbf{k}^2$.

Assume that due to the limited range of the interaction, the proper vertex is such that $\int_0^\infty f_{lm}(p)p^{-l}j_0(pr)p^2dp$ decays exponentially with r . The second term in the right-hand side of the previous equation can then be evaluated to⁷

$$\int_0^\infty \frac{p^2 dp}{2\pi^2} \frac{j_l(pr)f_{lm}(p)}{p^2 - k^2 - i\epsilon} = i \frac{k}{4\pi} f_{lm}(k)[j_l(kr) + in_l(kr)] \quad (3.90)$$

up to corrections vanishing exponentially in r , which will be incorporated in $I_{lm}(r)$. We recover a term $f_{lm}(k)$ involving $\Gamma_4(\tilde{p}, \tilde{k})$ taken at $\mathbf{p}^2 = k^2$, i.e. for the momenta of the 4 particles taken on-shell. With the relation (3.85), one may then relate $f_{lm}(k)$ to the T-matrix and thus to the phase shifts.

Combining the different parts of the plane waves, we finally obtain an asymptotic behavior at large r in terms of the scattering phase shifts,

$$[\psi_{\mathbf{k}}]_{lm}(r) \sim C_{lm} \frac{\sin(kr - l\frac{\pi}{2} + \delta_l(k))}{kr}, \quad (3.91)$$

where $C_{lm} = 4\pi i^l e^{i\delta_l(k)} Y_{lm}^*(\hat{\mathbf{k}})$. This expression is actually identical to the one for the quantum mechanical wave function of two particles (3.12).

Composite particles

The elementary fields of QCD are the quark, antiquark and gluon fields. Due to confinement, single quarks cannot form asymptotic states so that all stable particles are composite.

In section (3.1.3), we have shown how the Yang-Feldman equations can be used to define a field $\phi_{\text{in}}(x)$ which creates asymptotic states in the case of a theory with one elementary field $\phi(x)$. It was shown by Nishijima, Zimmermann and Haag (see [31] for a review) that the same equations can be used to define a field $O_{\text{in}}(x)$, which create asymptotic composite particles, from an *interpolator* $O(x)$. An interpolator $O(x)$ is a polynomial of the elementary fields and possibly their derivatives, all taken at the same space-time point x . For example, interpolators of the pion π^+ may be

$$\begin{aligned} O_1^\pi(x) &= \bar{u}(x)\gamma_5 d(x), \\ O_2^\pi(x) &= \bar{u}(x)\gamma_5 \gamma_t d(x), \\ O_3^\pi(x) &= \bar{u}(x)\overleftarrow{\nabla}\gamma_5 \overrightarrow{\nabla} d(x), \text{ etc.} \end{aligned} \quad (3.92)$$

All the results thus far may therefore be generalized to composite particles replacing $\phi(x)$ by appropriate interpolators $O(x)$. Naturally, the definition of the BS wave function becomes dependent on the choice of such interpolators.

Computation

In this section, we will discuss as the BS wave functions, defined in infinite volume, are related to finite-volume objects which can be computed with lattice simulations.

Consider the BS wave function of two incoming particles 1 and 2 and two outgoing particles 3 and 4. Let O_3 and O_4 be a choice of interpolators for the particles 3 and 4. Denoting $|1(\mathbf{k}), 2(-\mathbf{k}) \text{ in}\rangle$ the incoming state in the center-of-mass frame where

⁷ The argument will be made more rigorous in section 4.3.

particle 1 has initial momentum \mathbf{k} and particle 2 has initial momentum $-\mathbf{k}$, the BS wave function reads

$$\psi_{\mathbf{k}}(\mathbf{r}) = \langle 0 | O_3(0, \frac{\mathbf{r}}{2}) O_4(0, -\frac{\mathbf{r}}{2}) | 1(\mathbf{k}), 2(-\mathbf{k}) \text{ in} \rangle. \quad (3.93)$$

In infinite volume, the projection operator on the physical states of energy W under the inelastic threshold may be defined as

$$P_W = \int \frac{d^3\mathbf{p}}{(2\pi)^3 W_{\mathbf{p}}} 2\pi \delta(W_{\mathbf{p}} - W) | 1(\mathbf{p}), 2(-\mathbf{p}) \text{ in} \rangle \langle 1(\mathbf{p}), 2(-\mathbf{p}) \text{ in} | \quad (3.94)$$

where $W_{\mathbf{p}}$ is the total energy⁸ of two asymptotic particles 1 and 2 with relative momentum \mathbf{p} .

Let $O_{\text{src}}(0)$ be an operator made of the elementary fields and their derivatives at time $t = 0$ such that $P_W O_{\text{src}}(0) | 0 \rangle \neq 0$. Note that there are no requirement of locality on $O_{\text{src}}(0)$ contrary to the interpolators O_3 and O_4 . Define the wave function

$$\psi_W(\mathbf{r}) = \langle 0 | O_3(0, \frac{\mathbf{r}}{2}) O_4(0, -\frac{\mathbf{r}}{2}) P_W O_{\text{src}}(0) | 0 \rangle. \quad (3.95)$$

It follows from the previous definitions that

$$\psi_W(\mathbf{r}) = \int d\hat{\mathbf{k}} \eta(\hat{\mathbf{k}}) \psi_{\mathbf{k}}(\mathbf{r}) \quad (3.96)$$

where $\mathbf{k} = k\hat{\mathbf{k}}$ and $W = W_{\mathbf{k}}$. Here, $\eta(\hat{\mathbf{k}})$ is a function of the angular part of \mathbf{k} which depends on the choice of $O_{\text{src}}(0)$. In summary, ψ_W is a linear combination of the BS wave functions $\psi_{\mathbf{k}}$ with the norm of \mathbf{k} fixed by $W = W_{\mathbf{k}}$. It is easy to see that ψ_W retains the asymptotic behavior (3.91) in terms of the phase shift $\delta_l(k)$.

In finite volume, the energy eigenstates cannot be labelled with an asymptotic momentum. For a cubic box of extent L , we will note the energy eigenstates $|n, m, L\rangle$ with associated energies W_n . The label m denotes the degeneracy of the energy⁹. The projection on the energy $W = W_n$ is therefore

$$P_n^L = \sum_m |n, m, L\rangle \langle n, m, L|. \quad (3.97)$$

and one can define the following finite-volume functions

$$\psi_{L,n}(\mathbf{r}) = \langle 0 | O_3(0, \frac{\mathbf{r}}{2}) O_4(0, -\frac{\mathbf{r}}{2}) P_n^L O_{\text{src}}(0) | 0 \rangle. \quad (3.98)$$

For an energy W below the inelastic threshold, define L_i ($i = 1, \dots$) the increasing sequence of lattice sizes for which the spectrum contains W , as well as n_i the index of W in this spectrum. One can expect that the following limit holds

$$\psi_W(\mathbf{r}) = C_W \lim_{i \rightarrow \infty} \psi_{L_i, n_i}(\mathbf{r}), \quad (3.99)$$

for a constant C_W independent of \mathbf{r} .

The last object to introduce is the following Euclidean correlator in finite volume

$$\Psi_L(\mathbf{r}, \tau) = \langle O_3(\frac{\mathbf{r}}{2}, \tau) O_4(-\frac{\mathbf{r}}{2}, \tau) O_{\text{src}}(0) \rangle, \quad (3.100)$$

⁸ $W_{\mathbf{p}} = \sqrt{\mathbf{p}^2 + m_1} + \sqrt{\mathbf{p}^2 + m_2}$ if m_1 and m_2 are the masses of the particles 1 and 2.

⁹ We will see in section 4.3 an explicit description of the energy eigenspaces in finite volume.

where τ denotes the time in Euclidean space. As we have seen in section 2.3, Euclidean correlators can be expanded on the eigenstates $|n\rangle$ of the finite-volume Hamiltonian. In the case of the correlator above, it gives precisely

$$\Psi_L(\mathbf{r}, \tau) = \sum_n e^{-W_n \tau} \psi_{L,n}(\mathbf{r}). \quad (3.101)$$

In summary, the correlators $\Psi_L(\mathbf{r}, \tau)$ can be evaluated using lattice simulations. With e.g. the variational method, one can use the τ -dependence of these correlators to extract the matrix elements $\psi_{L,n}(\mathbf{r})$. In the infinite-volume limit $L \rightarrow \infty$, these matrix elements converge towards the functions $\psi_W(\mathbf{r})$. These functions are directly related to the BS wave functions and in particular have the same asymptotic behavior in terms of the scattering phase shifts. The combination of this steps gives a strategy to compute the scattering phase shifts from lattice simulations.

3.3.2 Energy-independent potential

For some energy $W < W_{\text{th}}$ below the inelastic threshold, let k be such that $W = W_k$. Due to the asymptotic behavior of ψ_W , the function $(\Delta + k^2)\psi_W(\mathbf{r})$ decays rapidly at large r . Let R be the smallest radius such that $(\Delta + k^2)\psi_W(\mathbf{r})$ is negligible¹⁰ for any $r > R$ and $W < W_{\text{th}}$. This R can be thought of as the effective range of the interaction below the inelastic threshold.

Let W_n for $n = 1, \dots$ be the eigenenergies in finite volume, with k_n such that $W_n = W_{k_n}$ and $W_{n_{\text{th}}}$ the lowest eigenenergy above the inelastic threshold. The mixing of the functions $\psi_{L,n}$ under the inelastic threshold can be summarized in the norm matrix \mathcal{N}^L with elements

$$\mathcal{N}_{n,n'}^L = \int d^3\mathbf{r} \psi_{L,n}^*(\mathbf{r}) \psi_{L,n'}(\mathbf{r}), \quad (3.102)$$

for $n, n' < n_{\text{th}}$.

The HAL QCD potential in finite volume is defined as

$$U_{\text{HAL}}^L(\mathbf{r}, \mathbf{r}') = \frac{1}{2\mu} \sum_{n,n' < n_{\text{th}}} [(\Delta + k_n^2)\psi_{L,n}(\mathbf{r})][\mathcal{N}^L]_{n,n'}^{-1} \psi_{L,n'}^*(\mathbf{r}'). \quad (3.103)$$

With the previous argument, we can say that $U_{\text{HAL}}^L(\mathbf{r}, \mathbf{r}') \simeq 0$ for $R < r \ll L$ but it is difficult to extract more properties of this non-local potential.

From the definition of the potential, it is clear that the following Schrödinger equation holds for any elastic eigenstate $n < n_{\text{th}}$

$$(\Delta + k_n^2)\psi_{L,n}(\mathbf{r}) = 2\mu \int d^3\mathbf{r}' U_{\text{HAL}}^L(\mathbf{r}, \mathbf{r}') \psi_{L,n}(\mathbf{r}'). \quad (3.104)$$

Actually, with the proper definition of U_{HAL}^L , the functions $\psi_{L,n}$ can be shown to satisfy any number of equation. The choice of the Schrödinger equation is of course chosen for physical reasons in the hope that the potential U_{HAL}^L thus created would be well-behaved.

¹⁰ Of course, this is subject to interpretation but the tail of this function is often exponential in QCD so one may chose R to be around two or three decay lengths.

Infinite volume

The potential U_{HAL}^L is well-defined in finite volume since there are a finite number of eigenstates under the inelastic threshold and the functions $\psi_{L,n}$ are defined on the compact space $[-\frac{L}{2}, \frac{L}{2}]^3$. In the infinite-volume limit, this is no longer the case, which could introduce mathematical difficulties. For this reason, we will take the infinite-volume limit as a formal one, which may or may not be well-defined in the theory of distributions.

In the infinite-volume limit, the Schrödinger equation (3.104) implies that the functions ψ_W satisfy

$$(\Delta + k^2)\psi_W(\mathbf{r}) = 2\mu \int d^3\mathbf{r}' U_{\text{HAL}}(\mathbf{r}, \mathbf{r}')\psi_W(\mathbf{r}'), \quad (3.105)$$

for any energy $W < W_{\text{th}}$, with the potential

$$U_{\text{HAL}}(\mathbf{r}, \mathbf{r}') = \lim_{L \rightarrow \infty} U_{\text{HAL}}^L(\mathbf{r}, \mathbf{r}'). \quad (3.106)$$

The strategy of the HAL QCD method is to first approximate the potential U_{HAL}^L , and thus U_{HAL} , from lattice input. With this potential, the Schrödinger equation (3.105) is solved in infinite-volume at all elastic energies $W < W_{\text{th}}$. This provides an approximation of the functions $\psi_W(\mathbf{r})$ and therefore of the scattering phase shifts.

Note that (3.105) is formally equivalent to (3.80), encountered in the derivation of the finite-size method, once we take $E = k^2/2\mu$. Both U_{HAL} and U_E are non-local but U_{HAL} has the particularity that it is not energy-dependent. However, the properties of U_E are known because it is related to the Bethe-Salpeter kernel. An attempt to relate the potential U_{HAL} to the BS kernel will lead to the kernel approximation method proposed in section 4.3 for this thesis.

Velocity expansion

We now discuss how U_{HAL} can be approximated from lattice input. As seen before, it is possible to extract using the variational method a finite number of functions $\psi_{L,n}$ using the correlators Ψ_L . The approximation then relies on the assumption that the potential U_{HAL} is only moderately non-local and satisfies some symmetries.

Take the partial Fourier transform of U_{HAL} as

$$V(\mathbf{r}, \mathbf{p}) = \int d^3\mathbf{r}' U_{\text{HAL}}(\mathbf{r}, \mathbf{r}') e^{i\mathbf{p} \cdot (\mathbf{r} - \mathbf{r}')}, \quad (3.107)$$

and assume that the following power series converges for an \mathbf{p} in \mathbb{R}^3

$$V(\mathbf{r}, \mathbf{p}) = \sum_{\mathbf{n} \in \mathbb{N}^3} V_{\mathbf{n}}(\mathbf{r}) (i\mathbf{p})^{\mathbf{n}}, \quad (3.108)$$

where $\mathbf{p}^{\mathbf{n}} = p_1^{n_1} p_2^{n_2} p_3^{n_3}$. This series is called the *velocity expansion* of U_{HAL} . The assumption of moderate non-locality is that the velocity expansion converges quickly in $|\mathbf{n}|$ so that it can be truncated.

If the potential U_{HAL} is further assumed to have some symmetries, the non-zero terms in the velocity expansion can be restricted. For example, Okubo and Marshak showed [32] that under some assumptions¹¹, the velocity expansion for the nucleon-nucleon interaction reads

$$V(\mathbf{r}, \mathbf{p}) = V_0(r) + V_\sigma(r) \boldsymbol{\sigma}_1 \cdot \boldsymbol{\sigma}_2 + V_T(r) S_{12} + V_{LS}(r) \mathbf{L} \cdot \mathbf{S} + \mathcal{O}(\mathbf{p}^2), \quad (3.109)$$

¹¹ Namely hermiticity, translational invariance in space and time, Galilei invariance, rotational invariance, parity and time-reversal invariance, fermi statistics and isospin invariance.

where $\boldsymbol{\sigma}_{1,2}$ are the spin Pauli matrices, $\mathbf{S} = (\boldsymbol{\sigma}_1 + \boldsymbol{\sigma}_2)/2$ and $\mathbf{L} = \mathbf{r} \times \mathbf{p}$.

In summary, the assumed symmetries of the potential induce a form

$$V(\mathbf{r}, \mathbf{p}) = \sum_{a=1}^{\infty} V_a(\mathbf{r}) \sum_{\mathbf{n} \in \mathbb{N}^3} M_{a,n} (i\mathbf{p})^{\mathbf{n}}, \quad (3.110)$$

with some known matrices M having a finite number of non-zero elements (e.g. $M_{0,\mathbf{n}} = \delta_{\mathbf{0},\mathbf{n}}$ for a local term). Then, the assumption of moderate non-locality means that the sum over a can be truncated. With such a form, equation (3.104) reads

$$(\Delta + k_n^2) \psi_{L,n}(\mathbf{r}) \simeq 2\mu \sum_{a=1}^A V_a(\mathbf{r}) \sum_{\mathbf{n} \in \mathbb{N}^3} M_{a,n} \nabla^{\mathbf{n}} \psi_{L,n}(\mathbf{r}). \quad (3.111)$$

for large A and L . It is easy to see that this equation can be inverted at each \mathbf{r} to obtain $V_a(\mathbf{r})$ if A linearly-independent functions $\psi_{L,n}(\mathbf{r})$ have been computed. The HAL QCD potential U_{HAL} has thus been approximated and can be used as described previously.

Time-dependent method

In practice, it is often very costly or even impossible with current computational limitations to extract one or several functions $\psi_{L,n}(\mathbf{r})$ with good accuracy from lattice simulations. This is especially the case when the spectrum W_n is rather dense around the ground state and the variational method breaks down. We will now show a way to mitigate this problem [33]. For simplicity, we assume that the particles 1 and 2 have the same mass m , although the argument can be generalized to channels where this is not the case [34].

On the lattice, compute the following correlators for one or several linearly-independent source operators $O_{\text{src}}^i(0)$ ($i = 1, \dots, N_{\text{src}}$)

$$R_L^i(\mathbf{r}, \tau) \equiv e^{2m\tau} \langle O_3(\frac{\mathbf{r}}{2}, \tau) O_4(-\frac{\mathbf{r}}{2}, \tau) O_{\text{src}}^i(0) \rangle = \sum_{\mathbf{n}} e^{-(W_n - 2m)\tau} \psi_{L,n}^i(\mathbf{r}). \quad (3.112)$$

Compared to Ψ_L defined in (3.100), we added an overall factor $e^{2m\tau}$ and an index i labelling the source operator used for the computation.

Using the identity $\frac{k^2}{m} = (W - 2m) + \frac{(W - 2m)^2}{4m}$ where $W = W_k = 2\sqrt{k^2 + m^2}$, it is possible to show that the previously defined correlators satisfy

$$\left(\frac{1}{4m} \frac{\partial^2}{\partial \tau^2} - \frac{\partial}{\partial \tau} + \frac{\Delta}{m} \right) R_L^i(\mathbf{r}, \tau) \simeq \sum_{a=1}^A V_a(\mathbf{r}) \sum_{\mathbf{n} \in \mathbb{N}^3} M_{a,n} \nabla^{\mathbf{n}} R_L^i(\mathbf{r}, \tau) + \mathcal{O}(e^{-(W_{\text{th}} - 2m)\tau}). \quad (3.113)$$

for $i = 1, \dots, N_{\text{src}}$. The second part on the right-hand side is the contribution of the states above the inelastic threshold and may be neglected in practice at τ reasonably large. It is clear that similarly as (3.111), one can invert the previous equation to obtain $V_a(\mathbf{r})$ if correlators R_L^i for $N_{\text{src}} \geq A$ linearly-independent source operators have been computed.

The improved method described here takes advantage of the known time-dependence of the correlator. It is very useful since it does not require to separate the contribution of each eigenstate. However, it relies heavily on the assumption that the truncated velocity expansion (3.110) is valid.

Towards better methods

4.1 HAL QCD METHOD ABOVE THE INELASTIC THRESHOLD

The HAL QCD method relies on the asymptotic behavior of the two-particle Bethe-Salpeter wave functions below the inelastic threshold. Therefore, it breaks down when inelastic channels make important contributions to the lattice correlators and cannot be neglected. In this section, we show how to treat this problem and extend the definition of the HAL QCD potential to energies above the inelastic threshold. We will consider two cases of inelastic channels in particular. The first one is the case where outgoing particles are created by the interaction, schematically $A + B \rightarrow A + B + C + \dots$. The second one represents coupled two-particle channels, i.e. $A + B \rightarrow C + D$ where the channel (C, D) opens at a higher energy than (A, B) .

4.1.1 Multi-particle channels

To make the presentation more concrete, we will treat the nucleon-nucleon (NN) scattering in the center-of-mass frame. The (first) inelastic threshold is $W_{\text{th}}^1 = 2m_N + m_\pi$ which corresponds to the opening of the channel $NN \rightarrow NN + \pi$. Here m_N is the mass of the nucleon and m_π that of the pion. Other threshold energies are naturally defined as $W_{\text{th}}^n = 2m_N + n \times m_\pi$, corresponding to the creation of n pions. Note that the production of particles other than the pion such $N\bar{N}$ or $K\bar{K}$ can be treated similarly and we restrict the argument to $NN \rightarrow NN + n\pi$ for notational simplicity.

For an energy W in the interval $\Delta_n = [W_{\text{th}}^n, W_{\text{th}}^{n+1}]$ ($n = 0, 1, \dots$), we can define the asymptotic states $|NN + i\pi, W, c_i \text{ in}\rangle$ corresponding to two nucleons and $i \leq n$ pions. The momenta, helicities and other quantum numbers of the particles are collectively represented as c_i . c_i contains in particular the momenta $\mathbf{p}_1, \mathbf{p}_2$ of the nuclei and \mathbf{k}_l ($l = 1, \dots, i$) of the pions which are such that $\mathbf{p}_1 + \mathbf{p}_2 + \sum_{l=1}^i \mathbf{k}_l = \mathbf{0}$ and

$$W = \sqrt{m_N^2 + \mathbf{p}_1^2} + \sqrt{m_N^2 + \mathbf{p}_2^2} + \sum_{l=1}^i \sqrt{m_\pi^2 + \mathbf{k}_l^2}. \quad (4.1)$$

The set of configurations c_i compatible with W in the sense described above is noted \mathcal{C}_W^i . The kinetic energy for c_i is defined as

$$E_{W, c_i}^i = \frac{\mathbf{p}_1^2}{2m_N} + \frac{\mathbf{p}_2^2}{2m_N} + \sum_{l=1}^i \frac{\mathbf{k}_l^2}{2m_\pi}. \quad (4.2)$$

Define the Bethe-Salpeter wave functions ψ_{W,c_i}^{ki} for $NN + i\pi \rightarrow NN + k\pi$ as

$$Z_N Z_\pi^{k/2} \psi_{W,c_i}^{ki}([\mathbf{r}]_k) = \langle 0 | N(0, \mathbf{0}) N(0, \mathbf{r}_0) \prod_{l=1}^k \pi(0, \mathbf{r}_l) \rangle | NN + i\pi, W, c_i \text{ in} \rangle, \quad (4.3)$$

where $i \leq n$ but $k = 0, 1, \dots$ since the k pions are virtual. Z_N and Z_π are the renormalization constants for the nucleon and pion field defined as in section 3.1.3. N and π are some interpolators for the nucleon and pion. The relative distances of the particles to the first nucleon are given by $[\mathbf{r}]_k = \mathbf{r}_0, \dots, \mathbf{r}_l$. The spinor and flavor degrees of freedom are kept implicit.

Multi-particle potential

We will now build a potential which leads to a Schrödinger-like equation similar to (3.105) for energies W up to $W_{\text{th}}^{n_{\text{max}}+1}$ ($n_{\text{max}} \geq 0$).

For an energy $W \in \Delta_n$ ($n \leq n_{\text{max}}$) and compatible configurations $c_i \in \mathcal{C}_W^i$ ($i \leq n$), define the vector of wave functions

$$|\psi_{W,c_i}^i\rangle_{BS} = \left(\psi_{W,c_i}^{0i}, \psi_{W,c_i}^{1i}, \dots, \psi_{W,c_i}^{n_{\text{max}}i} \right)^T. \quad (4.4)$$

It includes the wave functions corresponding (in addition to the nuclei) to i incoming pions and any number of virtual intermediate pions up to n_{max} . We use the bra and ket formalism for easier notations. Note however that these $(n_{\text{max}} + 1)$ -dimensional vectors are not in the Hilbert space of the physical states (which contains for example the vacuum $|0\rangle$) but in a product of function spaces. We add a subscript BS to make this difference explicit.

For notational simplicity, we define $\Omega_{n_{\text{max}}}$ the set of all possible incoming states below $W_{\text{th}}^{n_{\text{max}}+1}$

$$\Omega_{n_{\text{max}}} = \left\{ W, i, c_i \mid n \leq n_{\text{max}}, W \in \Delta_n, i \leq n, c_i \in \mathcal{C}_W^i \right\}. \quad (4.5)$$

Remember that W is the total energy, n the maximal number of outgoing pions, i the number of incoming pions and c_i contains the incoming momenta, etc.

For two incoming states (W, i, c_i) and (W', j, c'_j) in $\Omega_{n_{\text{max}}}$, define the elements of the norm matrix \mathcal{N} as

$$\mathcal{N}_{Wc_i, W'c'_j} = {}_{BS} \langle \psi_{W,c_i}^i | \psi_{W',c'_j}^j \rangle_{BS} = \sum_{k=0}^{n_{\text{max}}} \int d[\mathbf{r}]_k \left\{ \psi_{W,c_i}^{ki}([\mathbf{r}_k]) \right\}^* \psi_{W',c'_j}^{kj}([\mathbf{r}_k]), \quad (4.6)$$

where the last part effectively defines the inner product on the space of vectors $|\psi_{W,c_i}^i\rangle_{BS}$. While the BS wave functions may be linearly dependent, it is highly unlikely that the $(n_{\text{max}} + 1)$ -dimensional vectors of BS wave functions are linearly independent. Therefore, we expect the norm matrix to have an inverse \mathcal{N}^{-1} .

The inverse of the norm matrix can be used to construct a dual basis to the vectors $|\psi_{W,c_i}^i\rangle_{BS}$ as

$$|\bar{\psi}_{W,c_i}^i\rangle_{BS} = \sum_{W', j, c'_j \in \Omega_{n_{\text{max}}}} \left\{ \mathcal{N}_{Wc_i, W'c'_j}^{-1} \right\}^* |\psi_{W',c'_j}^j\rangle_{BS}, \quad (4.7)$$

which is such that

$${}_{BS} \langle \bar{\psi}_{W,c_i}^i | \psi_{W',c'_j}^j \rangle_{BS} = \delta_{W,W'} \delta_{i,j} \delta_{c_i, c'_j}. \quad (4.8)$$

Define the $(n_{\max} + 1) \times (n_{\max} + 1)$ diagonal matrices E_{W,c_i} and H_0 with elements

$$[E_W]_{kk} = E_W^k \equiv (W^2 - (W_{\text{th}}^k)^2)/2W_{\text{th}}^k, \quad (4.9)$$

and

$$[H_0]_{kk} = H_0^k \equiv -\frac{\nabla_{\mathbf{r}_0}^2}{2m_N} - \sum_{l=1}^k \frac{\nabla_{\mathbf{r}_l}^2}{2m_\pi}. \quad (4.10)$$

Note that $E_{W,c_0}^0 = E_W^0$ independently of c_0 but in general $E_{W,c_k}^k \neq E_W^k$ for $k > 1$.

The potential operator is then defined in the following way

$$U = \sum_{W,i,c_i \in \Omega_{n_{\max}}} (E_W - H_0) |\psi_{W,c_i}^i\rangle_{BS} {}_{BS}\langle \bar{\psi}_{W,c_i}^i|, \quad (4.11)$$

The operator U is therefore an $(n_{\max} + 1) \times (n_{\max} + 1)$ matrix of non-local potentials $U_{kl}([\mathbf{r}]_k, [\mathbf{r}']_l)$.

Observe that for any two incoming states (W, i, c_i) and (W', j, c'_j) in $\Omega_{n_{\max}}$,

$${}_{BS}\langle \psi_{W,c_i}^i | (U - U^\dagger) | \psi_{W',c'_j}^j \rangle_{BS} = {}_{BS}\langle \psi_{W,c_i}^i | (E_{W'} - E_W) | \psi_{W',c'_j}^j \rangle_{BS}. \quad (4.12)$$

Therefore, the operator U is Hermitian on the space spanned by $|\psi_{W,c_i}^i\rangle_{BS}$ for (W, i, c_i) in $\Omega_{n_{\max}}$, at *fixed energy* W . This is the space which is relevant for physical processes. However, the potential U is not Hermitian on the full Hilbert space.

With such definitions, it is easy to see that we recover a set of coupled Schrödinger equations which reads

$$(E_W^k - H_0^k) \psi_{W,c_i}^{ki}([\mathbf{r}]_k) = \sum_{l=0}^{n_{\max}} \int d[\mathbf{r}']_l U_{kl}([\mathbf{r}]_k, [\mathbf{r}']_l) \psi_{W,c_i}^{li}([\mathbf{r}']_l) \quad (4.13)$$

for any $(W, i, c_i) \in \Omega_{n_{\max}}$ and $k \leq n_{\max}$.

Having reached our goal, we end with some mathematical remarks. All of the above is well-defined if $\Omega_{n_{\max}}$ is a finite set (and the notations we used implied this). Of course, this is not the case so that one may define the potential operator in finite volume and take the infinite-volume limit as was done in section 3.3.2. The same remarks apply here and the result may be taken at least formally.

Non-relativistic approximation

For channels with two outgoing particles, we have seen in section 3.3.1 (in the case of scalars but it can be extended to spin 1/2 particles [12]) that the asymptotic behavior of the BS wave functions can be used to recover the scattering phase shifts. The BS wave functions corresponding to the previous section are ψ_{W,c_0}^{00} , i.e. with zero incoming or outgoing pions, but this result can be extended to ψ_{W,c_i}^{0i} with any i . Furthermore, this asymptotic behavior implies that the wave functions are solutions of the Helmholtz equation at large distances. One can then show that the non-local potential $U_{0l}([\mathbf{r}]_0, [\mathbf{r}']_l)$ for any $l \leq n_{\max}$ vanishes at large $|\mathbf{r}_0|$.

The study of the BS wave functions with more than two outgoing particles is more complex and was performed in [35] in the case of an arbitrary number of outgoing scalar particles with identical masses. It was shown that in the *non-relativistic approximation*, the BS wave function has a similar asymptotic behavior as in the two-particle case, governed by some generalized scattering phase shifts which can be related to the T-matrix and therefore are physical observables.

The non-relativistic approximation is to be understood as the regime where all incoming and outgoing particles have momenta which are small compared to their masses. For the system presented in this section, the BS wave function ψ_{W,c_i}^{ki} (with k outgoing particles) contains contributions from possibly any set of outgoing momenta compatible with W according to (4.1) (while the incoming momenta are fixed by c_i). In general, the only way to be sure that all these contributions are in the non-relativistic approximation is if $W - W_{\text{th}}^k \ll m_\pi$. Note that if $W - W_{\text{th}}^k < 0$, the energy is not sufficient to create k outgoing pions so that ψ_{W,c_i}^{ki} vanishes rapidly at large distances.

To sum up, we can restrict the incoming states considered up to now to the set

$$\Omega_{n_{\text{max}}}^{\text{NR}} = \left\{ (W, i, c_i) \in \Omega_{n_{\text{max}}} \mid (W - W_{\text{th}}^i \ll m_\pi, c_i \text{ is non-relativistic}) \text{ if } i \geq 1 \right\}. \quad (4.14)$$

where a non-relativistic c_i means a set of non-relativistic incoming momenta. There are no restrictions on the states with 2 incoming particles.

For any state $(W, i, c_i) \in \Omega_{n_{\text{max}}}^{\text{NR}}$, we get from the above argument a $3(i+1)$ -dimensional Helmholtz equation

$$(E_W^i - H_0^i) \psi_{W,c_i}^{ii}([\mathbf{r}]_i) \sim 0 \quad (4.15)$$

at large distances (i.e. large $\min_{i \neq j} |\mathbf{r}_i - \mathbf{r}_j|$ and large $\min_i |\mathbf{r}_i|$) and we can extract a generalized phase shift from the asymptotic behavior of $\psi_{W,c_i}^{ii}([\mathbf{r}]_i)$. Unfortunately, we cannot say the same for ψ_{W,c_i}^{ki} with $k > i$ and an energy W large enough to create k pions. Indeed, the condition $W - W_{\text{th}}^k \ll m_\pi$ is not satisfied so that ψ_{W,c_i}^{ki} can contain contributions from states with non-relativistic outgoing pions. We deduce that $U_{kl}([\mathbf{r}]_k, [\mathbf{r}']_l)$ with $k > 0$ does not in general decay rapidly at large separations $[\mathbf{r}]_k$. This observation may question the validity of the truncation of a possibly generalized velocity expansion. However, note that it is possible that if the interaction is weak enough, relativistic outgoing configurations may have small contributions to BS wave functions with non-relativistic incoming configurations.

Computation

The computation method for the generalized potential described previously goes along the same line as for the usual HAL QCD potential described in section 3.3.2. From lattice simulations at large sizes L , compute Euclidean correlators

$$R_L^k([\mathbf{r}]_k, \tau) \equiv e^{W_{\text{th}}^k \tau} \langle N(\mathbf{0}, \tau) N(\mathbf{r}_0, \tau) \prod_{l=1}^k \pi(\mathbf{r}_l, \tau) O_{\text{src}}(0) \rangle \quad (4.16)$$

for some source operator $O_{\text{src}}(0)$ which couples to the NN states.

Using that $E_W^k \simeq (W - W_{\text{th}}^k) + \frac{(W - W_{\text{th}}^k)^2}{4m_N}$ is exact at $k = 0$ and a very good approximation if $k > 0$ and $W - W_{\text{th}}^k \ll m_\pi$, we can show that for any $k \leq n_{\text{max}}$ we have the following time-dependent Schrödinger-like equation

$$\left(\frac{1}{4m} \frac{\partial^2}{\partial \tau^2} - \frac{\partial}{\partial \tau} - H_0^k \right) R_L^k([\mathbf{r}]_k, \tau) = \sum_{l=0}^{n_{\text{max}}} \int d[\mathbf{r}']_l U_{kl}([\mathbf{r}]_k, [\mathbf{r}']_l) R_L^k([\mathbf{r}']_l, \tau), \quad (4.17)$$

up to corrections in $\mathcal{O}(e^{-(W_{\text{th}}^{n_{\text{max}}+1} - W_{\text{th}}^k)\tau})$. For low k these corrections decay very quickly. The key to obtain the above equation is that the Schrödinger equation (4.13)

is the same for any number of incoming particles i and any momentum configuration c_i . Therefore, it is still valid when taking linear combinations.

Now, assume that each potential U_{kl} can be approximated by a finite number of terms as (3.111), involving a finite number N_{unk} of unknown functions V_{kl}^a . It suffices to compute correlators R_L^k for as many linearly independent sources as there are unknown functions and then invert the resulting set of equations (4.17) to obtain the functions V_{kl}^a and thus an approximation of the full potential matrix U .

Once the potential matrix U is approximated, the coupled equations (4.13) can be solved at any energy W . As discussed previously, the asymptotic behavior of the solutions is determined by some generalized scattering phase shifts which can be related to experimental observables. This method therefore allows to extract possibly useful predictions above the NN interaction about the pion production threshold, or any other similar system.

A final remark is that the correlator R_L^k receives contributions from states with relativistic incoming momenta. This leads to two conclusions. If one can extract the actual BS wave functions from the correlators, using e.g. the variational method or ground state saturation, the incoming state could be identified and the contribution of the relativistic incoming momenta excluded. Then, the previous discussion holds with a restriction of the incoming states to $\Omega_{n_{\text{max}}}^{\text{NR}}$. However, if such a separation of the incoming states is not possible, the time-dependent method relying on (4.17) is the only practical choice. Then, all the states in $\Omega_{n_{\text{max}}}$, not only the non-relativistic ones, need to be incorporated in the potential U as was described in (4.11). This could lead to an even more non-local potential and jeopardize the convergence of the velocity expansion.

Alternative definition

In nuclear physics for example, many potentials have been used to reproduce the experimental scattering phase shifts. These different potentials usually lead to different wave functions, albeit with similar asymptotic behavior. In the HAL QCD method, the wave functions are fixed by the choice of the interpolators but the potential is still not unique. Several alternative definitions of the potential are described in the appendix of Ref. [3]. We will discuss here one of these definitions with interesting properties.

Instead of treating all incoming states up to an energy threshold $W_{\text{th}}^{n_{\text{max}}+1}$, we will look at each energy range Δ_n (consisting of the energie between two successive thresholds) separately and define the potential recursively. We thus define the set of incoming states indices compatible with energies in Δ_n ($n \geq 0$) as

$$\tilde{\Omega}_n = \left\{ W, i, c_i \mid W \in \Delta_n, i \leq n, c_i \in \mathcal{C}_W^i \right\}. \quad (4.18)$$

For any $n \geq 0$, define the norm matrix \mathcal{N}^n by its elements

$$\mathcal{N}_{W c_i, W' c'_j}^n = \int d[\mathbf{r}]_n \left\{ \psi_{W c_i}^{ni}([\mathbf{r}]_n) \right\}^* \psi_{W' c'_j}^{nj}([\mathbf{r}]_n), \quad (4.19)$$

for (W, i, c_i) and (W', j, c'_j) in $\tilde{\Omega}_n$. The requirement of the invertibility of this norm matrix \mathcal{N}^n is stronger than the equivalent requirement for \mathcal{N} but remains reasonable. The inverse of the norm matrix can then be used to construct a set of functions

$$\bar{\psi}_{W c_i}^{ni} = \sum_{W', j, c'_j \in \tilde{\Omega}_n} \left\{ [\mathcal{N}^n]_{W c_i, W' c'_j}^{-1} \right\}^* \psi_{W' c'_j}^{nj} \quad (4.20)$$

dual to the BS wave functions in the sense that

$$\int d[\mathbf{r}]_n \left\{ \bar{\psi}_{W,c_i}^{ni}([\mathbf{r}_n]) \right\}^* \psi_{W',c'_j}^{nj}([\mathbf{r}_n]) = \delta_{W,W'} \delta_{i,j} \delta_{c_i,c'_j}. \quad (4.21)$$

Note that these are functions as opposed to the vectors of functions used in the first construction of the potential.

The starting point for a recursive construction of the potential is

$$\tilde{U}_{00}([\mathbf{r}]_0, [\mathbf{r}']_0) = \sum_{W,c_0 \in \tilde{\Omega}_0} (E_W^0 - H_0^0) \psi_{W,c_0}^{00}([\mathbf{r}]_0) \left\{ \bar{\psi}_{W,c_0}^{00}([\mathbf{r}']_0) \right\}^*. \quad (4.22)$$

Note that it is exactly equivalent to the potential described in section (3.3.2). This construction is therefore an actual *extension* of the HAL QCD potential above the first inelastic threshold.

Now, suppose that the potential \tilde{U}_{kl} is defined for $k, l < n$. For $k < n$, define the off-diagonal element

$$\tilde{U}_{kn}([\mathbf{r}]_k, [\mathbf{r}']_n) = \sum_{W,i,c_i \in \tilde{\Omega}_n} \left[(E_W^k - H_0^k) \psi_{W,c_i}^{ki}([\mathbf{r}]_k) - K_{W,c_i}^{n,ki}([\mathbf{r}]_k) \right] \left\{ \bar{\psi}_{W,c_i}^{ni}([\mathbf{r}']_n) \right\}^*. \quad (4.23)$$

where the function

$$K_{W,c_i}^{n,ki}([\mathbf{r}]_k) = \sum_{l=0}^{n-1} \int d[\mathbf{r}']_l \tilde{U}_{kl}([\mathbf{r}]_k, [\mathbf{r}']_l) \psi_{W,c_i}^{li}([\mathbf{r}']_l) \quad (4.24)$$

only involves the parts of the potential which were previously defined. The rest of the off-diagonal elements are then fixed for Hermiticity to $\tilde{U}_{nk} = (\tilde{U}_{kn})^\dagger$ for $k < n$. Once all the off-diagonal elements are defined, we can take $k = n$ in both (4.23) and (4.24) to define the last diagonal element \tilde{U}_{nn} . By recurrence over n , the potential is then defined up to any inelastic threshold.

The potential thus constructed leads to the following coupled Schrödinger equations for the BS wave functions at an energy $W \in \Delta_n$

$$(E_W^k - H_0^k) \psi_{W,c_i}^{ki}([\mathbf{r}]_k) = \sum_{l=0}^n \int d[\mathbf{r}']_l \tilde{U}_{kl}([\mathbf{r}]_k, [\mathbf{r}']_l) \psi_{W,c_i}^{li}([\mathbf{r}']_l). \quad (4.25)$$

Apart from the potential, the main difference with the previous equation (4.13) is that the BS wave functions with $k > n$ outgoing pions (which have no observable asymptotic behavior) are not included.

This alternative construction of the potential has several advantages over the first that we considered. It does not necessitate an a priori cutoff n_{\max} . Except possibly for the diagonal elements, the potential is Hermitian (not just on a subspace as previously). The non-physical channels with $k > n$ for an energy $W \in \Delta_n$ are not included.

Another advantage is that each potential \tilde{U}_{kl} only includes the information of the BS wave functions in the energy range Δ_n where $n = \max(k, l)$. This should lead to potentials which are “better-behaved” than those of the first construction (4.11). For example, consider the potentials for two outgoing particles \tilde{U}_{2n} . It would be sensible that the two-particle interaction below the first inelastic threshold is representative of the two-particle interaction above it, where additional terms from n -particle interaction would account mostly for the change of physics. In this case, \tilde{U}_{2n} would essentially decay with n and the full matrix \tilde{U} have its principal elements around the diagonal.

The main inconvenient of this construction compared to the first one is that it is not compatible with the time-dependent method. This is due to the fact that the BS wave functions satisfy a different set of Schrödinger equations depending on the initial energy. Whether this inconvenient is surmountable in practice (using e.g. the variational method) will depend greatly on the system of interest. Note that the remarks about the non-relativistic approximation apply as before.

4.1.2 Coupled two-particle channels

The difficulties faced by the two constructions discussed in the previous subsection, notably the separation of relativistic and non-relativistic contributions, show how challenging a correct and practically useful treatment of the multi-particle channels via potential approaches can be. In this subsection, we discuss a case where the extension of the potential approach above the inelastic threshold is significantly simpler, namely coupled *two-particle* channels. A first attempt to this extension was made before this work in [36].

An example of coupled two-particle channels is given in QCD by the channel with strangeness $S = -2$ and isospin $I = 0$ where the $\Lambda\Lambda$, $N\Xi$ and $\Sigma\Sigma$ channels coexist above energies $W = 2m_\Sigma$.

In general, we consider the processes $A_i + B_i \rightarrow A_j + B_j$ where $i, j = 0, \dots, n_{\max}$. The masses of A_i and B_i are denoted m_{A_i} and m_{B_i} . At an energy W in the center-of-mass frame, the incoming relative momentum \mathbf{p}_i satisfies

$$W = \sqrt{m_{A_i}^2 + \mathbf{p}_i^2} + \sqrt{m_{B_i}^2 + \mathbf{p}_i^2}. \quad (4.26)$$

The kinetic energy and the free Hamiltonian operator are given by

$$E_W^i \equiv \frac{(W^2 - m_{A_i}^2 - m_{B_i}^2)^2 - 4m_{A_i}^2 m_{B_i}^2}{8\mu_i W^2} = \frac{\mathbf{p}_i^2}{2\mu_i}, \quad H_0^i \equiv -\frac{\Delta}{2\mu_i}, \quad (4.27)$$

where μ_i is the reduced mass of the channel $A_i B_i$. We assume that the channels are ordered by their threshold energy $W_{\text{th}}^i \equiv m_{A_i} + m_{B_i}$, i.e. $W_{\text{th}}^i < W_{\text{th}}^j$ if $i < j$.

The incoming states are denoted $|A_i B_i, W, c_i \text{ in}\rangle$ where c_i contains the direction of the relative momentum and the helicities if the particles have non-zero spin. For an energy $W \in \Delta_n$ ($n \leq n_{\max}$), define the Bethe-Salpeter wave functions ψ_{W, c_i}^{ki} as

$$\sqrt{Z_{A_i} Z_{B_i}} \psi_{W, c_i}^{ki}(\mathbf{r}) = \langle 0 | A_k(0, \mathbf{0}) B_k(0, \mathbf{r}) | A_i B_i, W, c_i \text{ in}\rangle, \quad (4.28)$$

where $0 \leq i \leq n$, $0 \leq k \leq n_{\max}$. A_k and B_k are interpolators for the corresponding particles. The renormalization factors Z_{A_i} and Z_{B_i} are defined as usual.

We construct the potential as in the first part of the previous subsection. Following (4.4), we define $(n_{\max} + 1)$ -dimensional vectors $|\psi_{W, c_i}^i\rangle_{BS}$. Using the inverse of a norm matrix, we obtain a dual set of vectors $|\bar{\psi}_{W, c_i}^i\rangle_{BS}$. The potential matrix U is then defined as in (4.11) but with the diagonal elements of the matrices E_W and H_0 given by (4.27). This leads to the following coupled Schrödinger equation

$$(E_W^k - H_0^k) \psi_{W, c_i}^{ki}(\mathbf{r}) = \sum_{l=0}^{n_{\max}} \int d\mathbf{r}' U_{kl}(\mathbf{r}, \mathbf{r}') \psi_{W, c_i}^{li}(\mathbf{r}') \quad (4.29)$$

for any $(W, i, c_i) \in \Omega_{n_{\max}}$ and $k \leq n_{\max}$.

Since all the BS wave functions have two outgoing particles, they satisfy the Helmholtz equation at large separations \mathbf{r} . This implies that the potentials $U_{kl}(\mathbf{r}, \mathbf{r}')$ all

decay rapidly in \mathbf{r} , which may lead to a rapidly convergent velocity expansion. Furthermore, all BS wave functions have asymptotic behaviors governed by experimentally observable phase shifts. Note that there is no need of a relativistic approximation for these two results, as opposed to the case of channels with more than two outgoing particles.

Finally, the time-dependent method can be used to extract the potential from lattice simulations, *without* the annoying caveat that the contribution of relativistic states must somehow be separated. In the simple case of equal-mass particles in each channel, i.e. $m_{A_i} = m_{B_i}$ for $i \leq n_{\max}$, the method is very similar to the non-coupled channels, see section 3.3.2, so we will not repeat it here. The general case with possibly unequal masses is difficult but amenable [34].

4.2 EFFECTIVE POTENTIAL METHOD

The finite-size method relies in practice on the ability to extract the spectrum in finite volume from lattice simulations via the variational method. This is done by choosing a set of linearly-independent field operators, called the variational basis, and untangling the mixing between the states they create and the energy eigenstates. Many considerations factor in the choice of the variational basis. The number of fields should be sufficiently large that contributions from high-energy eigenstates can be well separated from those of low-energy states. However, the statistical noise in the correlators increases with the number of fields and the fields should not overlap too much with each other that statistical noise render them effectively linearly dependent. Furthermore, increasing the number of fields may also increase the contributions from unwanted high-energy eigenstates. Therefore, an optimal but in practice difficult choice would be a set of fields such that their associated operators create states as close as possible to the low-energy eigenstates.

Although the variational method can be applied to any system, we particularly focus in this section on systems of two particles, for simplicity assumed to have equal mass m . In this context, the difficulties discussed above in the choice of a variational basis are magnified as the spatial extent L of the lattice increases. Indeed, apart from a few possible bound states, the low-energy eigenstates correspond to scattering two-particle states with energies close to their free value of $2\sqrt{m^2 + (2\pi n/L)^2}$ where n is the norm of a 3-vector with integer coordinates. For large L , the energy difference between consecutive energy eigenstates is thus of the order of $(2\pi/L)^2/m$. In this case of a dense energy spectrum, even with a good choice of a variational basis, statistical errors usually render difficult the application of the variational method.

In response to these concerns, we will present in this section an alternative approach to extract the lower energy spectrum of lattice field theories in two-particle channels. The basic idea is to construct an effective Hamiltonian operator which coincides with the actual Hamiltonian of the system on a certain subspace of the physical states' Hilbert space. After a large (Euclidean) temporal shift of the fields, this subspace contains the low-energy eigenstates, making it possible to extract their energies from the eigenvalues of the effective Hamiltonian. This approach can be implemented in various ways and we will discuss in detail a particular one in which the effective Hamiltonian is chosen by analogy with non-relativistic physics were the interaction is given through a potential. We will call this approach the *effective potential method*.

The effective potential method introduced in this section is in some sense a generalization of the finite-size method which draws inspiration from the fundamental ideas

of the HAL QCD method. Therefore, it can be thought as a new, intermediate method which intends to combine their strong points while mitigating their shortcomings.

4.2.1 Effective Hamiltonian

Correlation matrices

For a given quantum field theory, we will call an equal-time operator a polynomial of the elementary fields and their derivatives, all taken in the same time slice. Choose two sets of equal-time operators: $O_i(t)$ for $i = 1, \dots, N_{\text{snk}}$ called the *sink operators* and $S_j(t)$ for $j = 1, \dots, N_{\text{src}}$ called the *source operators*. Define the $N_{\text{snk}} \times N_{\text{src}}$ time-dependent correlation matrix $C(t)$ with elements

$$C_{ij}(t) \equiv \langle O_i(t) S_j(0) \rangle, \quad (4.30)$$

The brackets $\langle \cdot \rangle$ denote as usual the Euclidean correlation functions, here in a finite box of size $L \times L \times L$.

As discussed in section 2.3.1, the Euclidean correlators can be expanded on the energy eigenstates $|n\rangle$ ($n \geq 1$) with energy W_n , giving the following expression of the correlation matrix elements

$$C_{ij}(t) = \sum_{n=1}^{\infty} P_{in} Q_{nj} e^{-W_n t}, \quad (4.31)$$

where the half-infinite matrices P and Q are defined by their elements

$$P_{in} = \langle 0 | O_i(0) | n \rangle, \quad Q_{nj} = \langle n | S_j(0) | 0 \rangle, \quad i \leq N_{\text{snk}}, \quad j \leq N_{\text{src}}, \quad n \geq 1. \quad (4.32)$$

The brackets $\langle 0 | \cdot | 0 \rangle$ denote as usual the finite-volume matrix elements in Minkowski space.

The matrices P and Q represent the mixing between the states created by the source and sink operators and the energy eigenstates. We also introduce the finite matrices $P^{(0)}$ and $Q^{(0)}$ which are obtained from the matrices P and Q respectively by only considering the energy eigenstates with indices $n = 1, \dots, \min(N_{\text{src}}, N_{\text{snk}})$.

We will consider three cases for the choice of sink and source operators

- A) the sink and source operators are conjugate, i.e. $N_{\text{snk}} = N_{\text{src}}$ and $O_i = S_i^\dagger$ for all $i \leq N_{\text{src}}$, and the square mixing matrix $P^{(0)} = [Q^{(0)}]^\dagger$ is invertible,
- B) there are as many sink and source operators, i.e. $N_{\text{snk}} = N_{\text{src}}$, and the square mixing matrices $P^{(0)}$ and $Q^{(0)}$ are both invertible,
- C) there are at least as many sink than source operators, i.e. $N_{\text{snk}} \geq N_{\text{src}}$, the square mixing matrix $Q^{(0)}$ is invertible and the rectangular mixing matrix $P^{(0)}$ has full column rank.

The condition on the rank of the mixing matrices ensures that the states created by the operators are linearly independent as well as their projections on the first N_{src} eigenstates. It also ensures that the correlation matrices $C(t)$ have full column rank for large enough times t .

Note that case A is included in case B and case B is included in case C. Furthermore, case A is exactly equivalent to what we described in section 2.3.2 and can be considered the “standard” setting.

We remind that the basis of the variational method is to solve the generalized eigenvalue problem (GEVP)

$$C(t)v_n(t, t_0) = \lambda_n(t, t_0)C(t_0)v_n(t, t_0) \quad (4.33)$$

for two time coordinates t and t_0 . While the GEVP may be defined for non-square matrices, there is no general algorithm to solve such problems and there may be no solutions at all. Therefore, in the context of the variational method, we can only consider the cases A and B corresponding to an equal number of sink and source operators, $N_{\text{snk}} = N_{\text{src}}$.

We have seen in section 2.3.2 that for t_0 and t chosen such that $t < 2t_0$, the solutions have the asymptotic behavior

$$W_n^{\text{eff}}(t, t_0) \equiv -\partial_t \log \lambda_n(t, t_0) = W_n + O(e^{-(W_{N_{\text{src}}+1}-W_n)t}), \quad n = 1, \dots, N_{\text{src}}. \quad (4.34)$$

The proof of this result, shown in [20], was done in case A where the correlation matrices are Hermitian but can easily be expanded to case B.

A practical way to have $t < 2t_0$ is to keep $t - t_0$ fixed and increase t_0 . Considering the limit of $t - t_0$ approaching zero, we can then introduce an alternative generalized eigenvalue problem

$$[-\partial_t C](t)v_n(t) = \lambda_n(t)C(t)v_n(t), \quad (4.35)$$

and it is straightforward that its solutions are

$$v_n(t) = v_n(t, t), \quad \lambda_n(t) = W_n^{\text{eff}}(t, t). \quad (4.36)$$

Generalized variational method

Our goal is to extend the variational method to case C, which includes the possibility of non-square correlation matrices with $N_{\text{snk}} > N_{\text{src}}$. The main incentive to do so is that the practical situation often arises where the computational cost of the evaluation of the correlation matrices is mostly driven by the number of source operators; for example, by the computation of source-to-all propagators in lattice QCD. In this situation, the number of sink operators can be increased at little additional cost. As each sink operator probes the eigenstates differently, it is advantageous to be able to use all this information instead of being restricted to $N_{\text{snk}} = N_{\text{src}}$.

As mentioned previously, the generalized eigenvalue problems defined by eq. (4.33) and (4.35) are still well-defined for non-square matrices although they have no exact solutions in general, due to statistical errors and contamination from eigenstates $|n\rangle$ with $n > N_{\text{src}}$. We will discuss here an approach to treat such overdetermined problems.

Assume that there is a “scheme” to construct $N_{\text{snk}} \times N_{\text{snk}}$ t -dependent matrices $H(t)$ satisfying,

$$H(t)C(t) = [-\partial_t C](t). \quad (4.37)$$

This can be abstracted as $H(t) \equiv f(C(t), \partial_t C(t))$ where f is a function, the “scheme”, satisfying $f(A, B)A + B = 0$ for any matrices A and B in the relevant vector space. We further require that $H(t)$ converges at large t .

From the above equation, the matrix $H(t)$ may be interpreted as an *effective Hamiltonian operator*, which coincides with the actual Hamiltonian \hat{H} at least on $\mathcal{V}(t)$, the column space of the correlation matrix $C(t)$.

Let $\lambda_i(t)$ ($i \leq N_{\text{snk}}$) be the eigenvalues of $H(t)$ in ascending order. It is shown in detail in appendix A.1 that N_{src} of these eigenvalues have the asymptotic behavior

$$\lambda_{i_n}(t) = W_n + O(e^{-(W_{N_{\text{src}}+1}-W_n)t}), \quad n = 1, \dots, N_{\text{src}}, \quad (4.38)$$

where the index $i_n \leq N_{\text{snk}}$ identifies the eigenvalue related to the eigenenergy W_n . This provides a way to extract the N_{src} first eigenenergies from the spectrum of $H(t)$, with the same asymptotic corrections as the solutions of the GEVP (4.35).

Since $H(t)$ has in total $N_{\text{snk}} \geq N_{\text{src}}$ eigenvalues, one needs a way to identify which eigenvalues satisfy the previous equation. It is found in the same appendix that at large t , a sufficient but not necessary condition for an eigenvalue λ of $H(t)$ to approximate an eigenenergy in the way of eq. (4.38) is that an associated eigenvector v satisfies

$$\frac{\|P_t H(t)(1 - P_t)v\|}{\|\lambda P_t v\|} \ll 1, \quad (4.39)$$

where P_t is the orthogonal projector on $\mathcal{V}(t)$.

The relation (4.38) can be understood as follows. Define

$$\mathcal{V}_{\text{src}}(t) = \text{span}_{j \leq N_{\text{src}}} \left\{ T e^{-\hat{H}t} S_j(0)|0\rangle \right\}, \quad \mathcal{V}_{\text{snk}} = \text{span}_{i \leq N_{\text{snk}}} \left\{ O_i^\dagger(0)|0\rangle \right\}, \quad (4.40)$$

the linear span of the states created by the source and sink operators, where T is again the time ordering operator. Then, $\mathcal{V}(t)$ can be identified with the projection of $\mathcal{V}_{\text{src}}(t)$ on \mathcal{V}_{snk} . At large t , the space $\mathcal{V}_{\text{src}}(t)$ ‘‘approaches’’

$$\mathcal{V}_{\text{eig}} = \text{span}_{n \leq N_{\text{src}}} \{|n\rangle\}, \quad (4.41)$$

the linear span of the first N_{src} Hamiltonian eigenstates since the contributions from higher eigenstates become negligible. In this limit, the effective Hamiltonian operator $H(t)$ coincides with the actual Hamiltonian on the low-energy eigenstates, i.e. these eigenstates become also eigenvectors of the effective Hamiltonian and their associated eigenvalues are the eigenenergies.

If there are as many source as sink operators, $N_{\text{src}} = N_{\text{snk}}$, there exists a unique matrix $H(t)$ which satisfies eq. (4.37) and this approach is equivalent to solving the generalized eigenvalue problem similar to (4.35) but for left eigenvectors. In this sense, the present approach can be seen as a generalization of the variational method. A more direct generalization, taking the ‘‘standard’’ GEVP (4.33) as the starting point, would be the consideration of matrices $T(t, t_0)$ such that

$$T(t, t_0) C(t_0) = C(t). \quad (4.42)$$

The matrix $T(t, t_0)$ could then be identified as an effective time-translation operator, or transfer matrix. Both approaches are equivalent but it is easier to choose a ‘‘scheme’’ for $H(t)$ than $T(t, t_0)$ as we will see later.

In the case of $N_{\text{snk}} > N_{\text{src}}$, the projection $P_t v$ of an eigenvector v of $H(t)$ on $\mathcal{V}(t)$ can be associated with an approximate solution of the GEVP (4.35) and the left-hand side of (4.39) is an upper bound on the error of this approximation. Furthermore, there are many matrices $H(t)$ satisfying eq. (4.37) as guaranteed by the condition on the rank of $C(t)$. Different constructions of $H(t)$ may provide approximations of the energies W_n with the same asymptotic behavior but converging more or less rapidly for practically accessible times t . The choice of a particular construction is therefore an important step and may rely on a physical interpretation of the problem, so that any insight into the specific system can be put to profit.

4.2.2 Effective potential

Consider the limit of low-energy two-particle states, i.e. states with energies such that $W_n \simeq 2m + E_n$, defining $W_n = 2\sqrt{m^2 + k_n^2}$ and $E_n = k_n^2/m$. In this section, we will propose a particular construction of $H(t)$ based on insights from this limit. At these energies, the system behaves similarly as its non-relativistic limit. Since the Hamiltonian of non-relativistic systems is better understood in terms of two-particle wave functions, we will introduce a specific choice of sink fields.

Choice of implementation

Define Λ_s the set of spatial sites of the lattice used for calculations and N_s the number of sites in each spatial direction. Let \mathbf{r}_i for $i = 1, \dots, N_s^3$ be an enumeration of Λ_s . Lattice wave functions are then a particular case of the correlation matrices introduced before with the sink operators chosen as

$$O_i(t) = \sum_{\mathbf{x} \in \Lambda_s} \phi_1(\mathbf{x} + \mathbf{r}_i, t) \phi_2(\mathbf{x}, t), \quad (4.43)$$

where ϕ_1 and ϕ_2 are local interpolators for the two outgoing particles. Each sink operator corresponds to the interpolators taken at a distance \mathbf{r}_i and projected on the center-of-mass frame. Therefore, the number of sink operators is $N_{\text{snk}} = N_s^3$.

By analogy with the non-relativistic limit of the system, we take $H(t)$ in the form

$$H(t) = 2m\mathbb{1} - \frac{1}{m}\Delta + U(t), \quad (4.44)$$

where Δ is a matrix acting on the sink operators indices with elements as the Laplacian acts on the associated vectors \mathbf{r}_i , i.e. with elements given by

$$\Delta_{ij} = \sum_{\mu=1}^3 \left[\delta_{\mathbf{r}_i + \boldsymbol{\mu}, \mathbf{r}_j} - 2\delta_{\mathbf{r}_i, \mathbf{r}_j} + \delta_{\mathbf{r}_i - \boldsymbol{\mu}, \mathbf{r}_j} \right], \quad i, j = 1, \dots, N_{\text{snk}}, \quad (4.45)$$

in lattice units with $\boldsymbol{\mu}$ the elementary lattice vector in the spatial direction μ . In the non-relativistic limit considered here, and only then, it is clear that the matrix $U(t)$ may be interpreted as an *effective potential*.

A choice of construction for $H(t)$ is equivalent to a choice of construction for $U(t)$ satisfying

$$U(t)C(t) = [(-\partial_t - 2m\mathbb{1} + \frac{1}{m}\Delta)C](t). \quad (4.46)$$

The number of degrees of freedom for $U(t)$ is $(N_{\text{snk}})^2$ and the above conditions fixes $N_{\text{src}}N_{\text{snk}}$ of them. In practical situations $N_{\text{src}} \ll N_s^3 = N_{\text{snk}}$, which leaves a very large freedom in the choice of $U(t)$.

We will choose a particular construction of $U(t)$ by mimicking the truncation of the velocity expansion of non-local potentials in non-relativistic quantum mechanics. We therefore impose the following constraints to fix the remaining degrees of freedom

Cubic symmetry In appendix A.2, we describe in detail the structure of the matrices acting on lattice wave functions, like $U(t)$, which transform covariantly under the action of the cubic group. As expected, it is found that the actual number of degrees of freedom left after this constraint is around 48 times less than that of general matrices. Furthermore, there is a basis such that these matrices are block-diagonal with one block for each irreducible representation of the cubic group. Therefore, if as is usually the case in practice the source operators transform

according to a particular irreducible representation, only one block is relevant to satisfy (4.46) and the remaining degrees of freedom can be removed. For example, restricting the source operators to the representation A_1^+ and enforcing the cubic symmetry for $U(t)$ divides the number of degrees of freedom by 384.

Minimal non-locality The last redundant degrees of freedom can be removed by keeping only hopping terms in $U(t)$ between sites with minimal separation and setting the others to zero. We detail in appendix A.3 an implementation of this idea. The locations of the non-zero elements of $U(t)$ are completely fixed by this requirement and their value is obtained by a (sparse) matrix inversion. In practice, high condition numbers make this inversion numerically impossible. By relaxing the non-locality constraint to accept no more minimal but “moderate” non-locality, i.e. any hopping between sites within a distance smaller than a cutoff R_{\max} , this method becomes numerically tractable. Furthermore, the dependence of $U(t)$ in the cutoff R_{\max} gives an estimate of the systematic uncertainties induced by this method.

Hermiticity Adding a Hermiticity constraint to $U(t)$ is only a slight modification of the construction achieved thus far, see appendix A.3. Unfortunately, the modified construction is found to be very numerically unstable and therefore unusable in practice. An alternative construction satisfying the three constraints and numerically stable might be discovered in the future but for the moment we cannot enforce Hermiticity. Note that Hermiticity is not required for the method to work.

The strategy of the *effective potential method* for the study of two-particle channels is then the following. After choosing a set of sources and interpolators, compute the lattice wave functions $C(t)$ from numerical simulations. Invert (4.46) to obtain $U(t)$ using the scheme discussed above. Compute the eigenvalues and eigenvectors of $H(t)$ which is related to $U(t)$ by (4.44). Among these, identify the ones satisfying the condition (4.39). Extract the lower part of the finite-size spectrum from these eigenvalues as (4.38). Relate the finite-size spectrum to the scattering phase shifts using the finite-size formula.

Note that while the choice of implementation described in this subsection was *motivated* by the consideration of a certain limit of the system, and thus is expected to give better results (i.e. a faster convergence rate) close to this limit, it can be used for any energy range.

Alternative implementation

We can take one step further the analogy with the non-relativistic limit by introducing a slightly modified approach, inspired by the time-dependent HAL QCD method. Rescale the correlation matrices as $C'(t) = e^{2mt}C(t)$ and consider the alternative generalized eigenvalue problem

$$[(-\partial_t + \frac{1}{4m}\partial_t^2)C'](t)v'_n(t) = \lambda'_n(t)C'(t)v'_n(t). \quad (4.47)$$

It is straightforward to relate its solutions to those of the GEVP (4.35) and get

$$v'_n(t) = v_n(t), \quad \lambda'_n(t) = \lambda_n(t) - 2m + \frac{(\lambda_n(t) - 2m)^2}{4m} = E_n + O(e^{-(W_{\text{Nsrc}+1} - W_n)t}), \quad (4.48)$$

so that the eigenvalues allow to extract directly E_n instead of W_n as previously, with the same asymptotic corrections.

The whole discussion thus far can be adapted to take (4.47) as a basis. Consider matrices $H'(t)$ such that

$$H'(t) C'(t) = [(-\partial_t + \frac{1}{4m} \partial_t^2) C'](t), \quad H'(t) = -\frac{1}{m} \Delta + U'(t). \quad (4.49)$$

Then, the spectrum of $H'(t)$ will asymptotically contain E_n for the N_{src} lowest eigenstates n . The eigenenergies W_n can be recovered directly from E_n . The construction of $U'(t)$ is chosen similarly to $U(t)$ but with the constraint

$$U'(t) C'(t) = [(-\partial_t + \frac{1}{4m} \partial_t^2 + \frac{1}{m} \Delta) C'](t). \quad (4.50)$$

instead of (4.46).

This modified approach has the following advantage. As demonstrated in section 3.3.2 for the HAL QCD method, the right-hand side of (4.50) vanishes on the rows i corresponding to large $|\mathbf{r}_i|$ (compared to the typical interaction range) if t is large enough that the inelastic channels can be neglected. Therefore, a large part of the effective potential $U'(t)$ can be set to zero which simplifies the computations and reduces the statistical errors. In the case of $U(t)$ discussed before, this simplification only happens in the non-relativistic limit where $W_n \simeq 2m + E_n$.

4.2.3 Qualitative comparison with other methods

The effective potential method is primarily a way to extract the finite-size spectrum of two-particle channels. It is therefore to be compared directly with the variational method. Combined with the finite-size formula, it enables to extract the scattering phase shifts. However, the equations defining the method are very similar to the ones in the HAL QCD method. This is why it can be thought as minimalist version of the HAL QCD method, omitting any relation of the effective potential $U(t)$ with a possible analogous object in infinite-volume. The derivation is purely restricted to finite-volume and does not make any assumptions.

By considering lattice wave functions, or more generally non-square correlation matrices, the effective potential method allows to use more information from the system than the variational method at little additional cost. Furthermore, one can use information on the type of Hamiltonian of the system to possibly speed up convergence towards the eigenenergies while the GEVP in the variational is more of a black box. Compared to the HAL QCD method, it does not make assumptions on the convergence of the velocity expansion of some potential or the fast decay of the inelastic channels and it makes proper use of the cubic symmetry in finite volume. We stress that one can gain confidence in the correctness of the results by the appearance of a plateau of the eigenvalues and the validity of (4.39). If these conditions are not met for some eigenvalues, no definitive conclusion may be drawn for the corresponding eigenenergies.

4.3 KERNEL APPROXIMATION METHOD

The HAL QCD method and the finite-size method are quite different in their execution but are similar in their derivation. In the HAL QCD method, the scattering phase shifts are related to the asymptotic behavior of Bethe-Salpeter wave functions (BS) in quantum field theory under the inelastic threshold. A kernel equivalent to the BS wave functions through the Schrödinger equation is then defined and the goal is to

approximate it by lattice input, assuming some analytic form. In the finite-size method, a relation is found between the spectrum in finite volume and the scattering phase shifts. This relation is obtained by the study of the finite-volume wave functions in quantum mechanics outside the interaction region, then extended to quantum field theories by finding some equivalent objects. Avoiding the analogy with quantum mechanics, derivations of the finite-size formula based on wave functions have also been given in purely field-theoretical frameworks [29, 30, 37]. In any case, the derivation stems from the study of an ad hoc definition of “wave functions” in quantum field theory.

The difference is that the wave functions play a center role in the HAL QCD method while they are merely a mathematical device in the derivation of the finite-size formula. Indeed, other derivations [24, 38] have been given based on the study of the poles of the finite-volume 4-point function. These derivations of the finite-size formula are simpler and have lead to painless generalizations.

Compared to modern derivations of the finite-size formula, the HAL QCD method lacks in two main ways. It does not consider the effect of the finite volume and the cubic symmetry on the BS wave functions. It is based on a potential of which the properties are basically unknown but are critically important to the applicability of the method. This section presents the result of an extensive study of wave function-like correlators in finite volume. It has lead to the development of a new method to extract the scattering phase shifts from lattice simulations, called the kernel approximation method. This method is similar to the HAL QCD method in several aspects but does not suffer the previously mentioned drawbacks.

As previously, we consider quantum field theories of a real scalar field which describes the physics of a self-interacting particle of mass m . We keep notations from section 3.2.2 but assume in addition that the particle has an internal degree of freedom (such as isospin) so that two incoming particles can be considered distinguishable.

4.3.1 The 4-point function

Infinite volume

We start our investigation by proving several results in infinite volume which will be useful when considering the finite-volume system.

In the case of two distinguishable particles, the integral relation (3.72) between the full connected 4-point function G_4 and the Bethe-Salpeter kernel K reads

$$G_4(p', p) = K(p', p) + \int \frac{d^4k}{(2\pi)^4} K(p', k) G_2(k) G_4(k, p). \quad (4.51)$$

We wish to derive a three-dimensional formalism in which the relative energies disappear. This is a standard procedure in the study of the Bethe-Salpeter kernel and several choices of formalisms have been used in the past. The idea is to extract the pole of the full two-particle propagator $G_2(k)$ in the elastic region, which can be made similar to that of the non-relativistic resolvent $R(\mathbf{k})$ defined by

$$R(\mathbf{k}) = \frac{1}{\mathbf{k}^2/m - \mathcal{E}(W)}, \quad \mathcal{E}(W) = \frac{W^2 - 4m^2}{4m}. \quad (4.52)$$

The following lemma describes the structure of the pole and generalizes Lemma 3.3. by Lüscher in ref. [8].

Lemma 4.1. For any function $f(k)$ of $k = (\mathbf{k}, k_4)$ and W analytic in the domain

$$0 \leq m' \leq m, \quad 0 \leq \operatorname{Re} W < 2(m + m'), \quad |\operatorname{Im} k_4| < \frac{m+m'}{2}, \quad |\operatorname{Im} \mathbf{k}| \leq \frac{m-m'}{2}, \quad (4.53)$$

the function

$$I(\mathbf{k}) = \int \frac{dk_4}{2\pi} G_2(k) f(k) - \frac{1}{2mW} R(\mathbf{k}) f(k)|_{k_4=0} \quad (4.54)$$

is analytically continuable in the domain (4.53) restricted by $k_4 = 0$.

Proof. The idea of the proof is the same as for Lemma 3.3. in ref. [8]. Lüscher assumes analyticity of f for any $|\operatorname{Im} k_4| < m$ so that he can deform the k_4 integration contour (to get an explicit singularity similar to that of $R(\mathbf{k})$) by any imaginary shift $m^* < m$ then take the limit $m^* \rightarrow m$. This leads to an analytic domain containing $0 \leq \operatorname{Re} W < 4m$. For a more general result, we keep track of the maximal region of analyticity of $I(\mathbf{k})$ if we only assume that $f(k)$ is analytic in $|\operatorname{Im} k_4| < \frac{m+m'}{2}$ with $m' \leq m$ (which restricts the possible deformations of the integration contour). Lüscher's result is obtained by setting $m' = m$. \square

Motivated by Ref. [39], we do not choose a particular formalism to integrate over the relative energy but keep the discussion general by introducing the concept of 3-projection.

Definition 4.1. A generalized function $\mathcal{P}(k)$ of the energy W and the Euclidean 4-vector k is called a 3-projection if for any function $f(k)$ of $k = (\mathbf{k}, k_4)$ and W analytic in the domain (4.53), the integral

$$J(\mathbf{k}) = \int \frac{dk_4}{2\pi} \mathcal{P}(k) f(k), \quad (4.55)$$

is analytically continuable in the domain (4.53) restricted by $k_4 = 0$ and we have $J(\mathbf{k}) = f(k)|_{k_4=0}$ at $W = 2\omega_{\mathbf{k}}$ if $\omega_{\mathbf{k}} < 2m$.

This choice of definition is such that for any 3-projections \mathcal{P}_L and \mathcal{P}_R , the 2-particle kernels

$$G_2(k', k) = (2\pi)^4 \delta(k' - k) G_2(k) \quad \text{and} \quad \hat{G}_2(k', k) = (2\pi)^3 \delta(\mathbf{k}' - \mathbf{k}) \mathcal{P}_R(k') \frac{R(\mathbf{k})}{2mW} \mathcal{P}_L(k) \quad (4.56)$$

have the same singularities in the elastic energy region, as can be seen from lemma 4.1.

The 3-projections are used to “project” kernels in 4-vector space to kernels in 3-vector space. For any choice of 3-projections \mathcal{P}_L and \mathcal{P}_R , define the operator $\tilde{\mathcal{P}}$ such that

$$[\tilde{\mathcal{P}} \cdot F](\mathbf{k}', \mathbf{k}) = \frac{1}{2mW} \int \frac{dk'_4}{2\pi} \frac{dk_4}{2\pi} \mathcal{P}_L(k') F(k', k) \mathcal{P}_R(k), \quad (4.57)$$

where $k' = (\mathbf{k}', k'_4)$ and $k = (\mathbf{k}, k_4)$.

In order to find an equation for the “projection” of the 4-point function $\tilde{G}_4 = \tilde{\mathcal{P}} \cdot G_4$, define a modified Bethe-Salpeter kernel \hat{K} by

$$\hat{K}(p', p) = K(p', p) + \int \frac{d^4 k'}{(2\pi)^4} \frac{d^4 k}{(2\pi)^4} K(p', k') \left[G_2(k', k) - \hat{G}_2(k', k) \right] \hat{K}(k, p), \quad (4.58)$$

and its “projection” $\tilde{U} = -\tilde{\mathcal{P}}_W \cdot \hat{K}$. The analyticity of the resulting kernel is guaranteed by the following theorem. In addition to the analyticity in the energy W discussed by Lüscher, we also prove analyticity in the 3-momenta, which will prove useful later.

Theorem 4.1. *The kernel $\tilde{U}(\mathbf{p}', \mathbf{p})$ is analytically continuable in the domain*

$$0 \leq m' \leq m, \quad 0 \leq \text{Re } W < 2(m + m'), \quad |\text{Im } \mathbf{p}'| \leq \frac{m-m'}{2}, \quad |\text{Im } \mathbf{p}| \leq \frac{m-m'}{2}. \quad (4.59)$$

Proof. In the proof of Theorem 3.1 by Lüscher in ref. [8], it was shown that the Bethe-Salpeter kernel $K(p', p)$ is analytically continuable for any momenta satisfying

$$|\frac{1}{4}\text{Im } P + s'\text{Im } p'| + |\frac{1}{4}\text{Im } P + s\text{Im } p| + |s'\text{Im } p' + s\text{Im } p| < 2m, \quad (4.60)$$

where $P = (\mathbf{0}, iW)$ is the total Euclidean momentum and s, s' are any of ± 1 . It is not difficult to show that this includes the domain

$$(4.59) \quad \text{and} \quad |\text{Im } p'_0| < \frac{m+m'}{2}, \quad |\text{Im } p_0| < \frac{m+m'}{2}. \quad (4.61)$$

Now, we can use Lemma 4.1 to show that

$$\begin{aligned} & \int \frac{d^4 k'}{(2\pi)^4} \frac{d^4 k}{(2\pi)^4} K(p', k') [G_2(k', k) - \hat{G}_2(k', k)] K(k, p) = \\ & \frac{1}{2mW} \int \frac{d\mathbf{k}}{(2\pi)^3} R(\mathbf{k}) \{K(p', k)K(k, p)|_{k_4=0} - J_R(p', \mathbf{k})J_L(\mathbf{k}, p)\} + I(p', p) \end{aligned} \quad (4.62)$$

where $I(p', p)$ is analytic in the domain (4.61) and e.g. $J_R(p', \mathbf{k}) = \int \frac{dk_4}{2\pi} K(p', k) \mathcal{P}_R(k)$. In the integral on the right-hand side, $R(\mathbf{k})$ has a simple pole for \mathbf{k} such that $W = 2\omega_{\mathbf{k}}$. However, the definition of a 3-projection implies that

$$J_R(p', \mathbf{k}) = K(p', k)|_{k_4=0} \quad \text{and} \quad J_L(\mathbf{k}, p) = K(k, p)|_{k_4=0} \quad (4.63)$$

at $W = 2\omega_{\mathbf{k}} < 4m$. We deduce that the integral on the left-hand side of (4.62) and by recurrence $\hat{K}(p', p)$ are analytically continuable in the domain (4.61). The properties of 3-projections finally ensure the claimed result for the analytic domain of \tilde{U} . \square

From now on, we assume that the 3-projections $\mathcal{P}_L(k)$ and $\mathcal{P}_R(k)$ have been chosen and that they decay sufficiently fast at large \mathbf{k} that the integrals over 3-momenta in the definition of \hat{K} are well-defined. In ref. [8, 9], Lüscher's derivation can be understood within the following choice of 3-projections

$$\mathcal{P}_L(k) = \mathcal{P}_R(k) = 2\pi\delta(k_4) e^{\frac{m\mathcal{E}(W) - k^2}{2m^2}}. \quad (4.64)$$

After some algebra, we obtain a fully three-dimensional formulation of the integral equation (4.51) as

$$-\tilde{G}_4(\mathbf{p}', \mathbf{p}) = \tilde{U}(\mathbf{p}', \mathbf{p}) + \int \frac{d^3 \mathbf{k}}{(2\pi)^3} \tilde{U}(\mathbf{p}', \mathbf{k}) R(\mathbf{k}) \tilde{G}_4(\mathbf{k}, \mathbf{p}). \quad (4.65)$$

The definition of a 3-projection ensures that when the two incoming and two outgoing particles are set on the mass-shell, the “projected” observables do not depend on the choice of the 3-projection. In particular, the scattering amplitude T is obtained from the 4-point function G_4 when setting the four particles on-shell, see (3.67). For any 3-projections, the following relation holds

$$T(\mathbf{p}', -\mathbf{p}' | \mathbf{p}, -\mathbf{p}) = \lim_{\epsilon \rightarrow 0^+} 2mW \tilde{G}_4(\mathbf{p}', \mathbf{p}) \quad (4.66)$$

for $W = 2\omega_{\mathbf{p}} + i\epsilon$, $\omega_{\mathbf{p}'} = \omega_{\mathbf{p}} < 2m$ and the scattering amplitude is characterized in terms of scattering phase shifts as

$$T(\mathbf{p}', -\mathbf{p}' | \mathbf{p}, -\mathbf{p}) = 8\pi^2 W \sum_{l=0}^{\infty} \sum_{m=-l}^l \frac{e^{2i\delta_l(p)} - 1}{2ip} Y_{lm}(\mathbf{p}') Y_{lm}^*(\mathbf{p}). \quad (4.67)$$

With this three-dimensional formulation we can define “wave functions” in momentum space from the 4-point function as follows. At any energy $W = 2\omega_q + i\epsilon$ with $\omega_q < 2m$, define the generalized function

$$\hat{\psi}_\infty^{\mathbf{q}}(\mathbf{p}) = (2\pi)^3 \delta(\mathbf{p} - \mathbf{q}) + R(\mathbf{p}) \tilde{G}_4(\mathbf{p}, \mathbf{q}), \quad (4.68)$$

where $\mathbf{p} \in \mathbb{R}^3$ and \mathbf{q} is an on-shell momentum, i.e. $|\mathbf{q}| = q$. Due to the rotational symmetry of the system, we only need to consider $\hat{\psi}_\infty(\mathbf{p}) = \hat{\psi}_\infty^{\mathbf{q}_z}(\mathbf{p})$ where \mathbf{q}_z is the momentum in the z direction with norm q and all the other functions can be recovered using rotations.

A direct consequence of the integral equation (4.65) is that $\hat{\psi}_\infty$ satisfies

$$-R(\mathbf{p})^{-1} \hat{\psi}_\infty(\mathbf{p}) = \int \frac{d^3 \mathbf{p}'}{(2\pi)^3} \tilde{U}(\mathbf{p}, \mathbf{p}') \hat{\psi}_\infty(\mathbf{p}'), \quad (4.69)$$

which is nothing but the Schrödinger equation in momentum space for the “potential” \tilde{U} . With ψ_∞ and U the inverse Fourier transforms of $\hat{\psi}_\infty$ and \tilde{U} , we get in position space

$$\frac{1}{m}(\Delta + q^2) \psi_\infty(\mathbf{r}) = \int d^3 \mathbf{r}' U(\mathbf{r}, \mathbf{r}') \psi_\infty(\mathbf{r}'), \quad (4.70)$$

where Δ is the Laplace operator and $\mathbf{r}, \mathbf{r}' \in \mathbb{R}^3$. The exponential decay of U is guaranteed by the following proposition.

Proposition 4.1. *For any $W_{\max} \in [0, 4m[$, define the range $\rho = \frac{1}{m - W_{\max}/4}$. Then, in the energy region $0 \leq \text{Re } W < W_{\max}$, the large-distance behavior of U is given by*

$$U(\mathbf{r}, \mathbf{r}') = O(e^{-\frac{r+r'}{\rho}}), \quad (4.71)$$

for positions $\mathbf{r}, \mathbf{r}' \in \mathbb{R}^3$ with norms r, r' .

Proof. Using Theorem 4.1, in the energy region $0 \leq \text{Re } W < W_{\max}$ the kernel $\tilde{U}(\mathbf{p}', \mathbf{p})$ can be analytically continued in the complex momentum region $|\text{Im } \mathbf{p}'| \leq \rho^{-1}$ and $|\text{Im } \mathbf{p}| \leq \rho^{-1}$. The assumed fast decay of the 3-projections also ensure that the kernel vanishes at infinity in this momentum region. We can therefore use a contour integral to show that

$$U(\mathbf{r}, \mathbf{r}') = e^{-\frac{r+r'}{\rho}} \int \frac{d\mathbf{p}'}{(2\pi)^3} \frac{d\mathbf{p}}{(2\pi)^3} e^{i\mathbf{p} \cdot \mathbf{r}} \tilde{U}(\mathbf{p} + i\frac{\mathbf{r}}{r\rho}, \mathbf{p}' - i\frac{\mathbf{r}'}{r'\rho}) e^{-i\mathbf{p}' \cdot \mathbf{r}'}. \quad (4.72)$$

The fast decay can again be used to show that the integral on the right-hand side is bounded. \square

Note that for energies approaching the inelastic threshold $4m$, the “effective range” ρ diverges. This does not mean that U cannot decay rapidly in this region but the effect of the inelastic threshold is highly non-trivial so no general argument may be given without further assumptions or techniques.

For any distance $R > 0$, define the compactly supported kernel

$$U_R(\mathbf{r}, \mathbf{r}') = \begin{cases} U(\mathbf{r}, \mathbf{r}') & \text{if } |\mathbf{r}| + |\mathbf{r}'| \leq 0.9R, \\ 0 & \text{if } |\mathbf{r}| + |\mathbf{r}'| \geq R, \end{cases} \quad (4.73)$$

with a smooth and spherically symmetric connection between the two regions. Proposition 4.1 ensures that in the region $0 \leq \text{Re } W < W_{\max}$, the Schrödinger equation (4.70) still holds if we replace U by U_R , up to corrections of order $O(e^{-0.9R/\rho})$ (with ρ defined as in the Proposition). Compactly supported functions can be treated using the following Proposition proved in appendix B.1.

Proposition 4.2. *Let h be a smooth function defined on \mathbb{R}^3 with compact support on $B(0, R)^1$. Then, its Fourier transform can be expanded as*

$$\hat{h}(\mathbf{p}) = \sum_{l=0}^{\infty} \sum_{m=-l}^l p^l f_{lm}(p) Y_{lm}(\hat{\mathbf{p}}), \quad (4.74)$$

for any \mathbf{p} in \mathbb{R}^3 , where $\mathbf{p} = p\hat{\mathbf{p}}$ and f_{lm} are even entire functions of exponential type R .

The function $h_R(\mathbf{r}) = \int d^3\mathbf{r}' U_R(\mathbf{r}, \mathbf{r}') \psi_{\infty}(\mathbf{r}')$ satisfies the condition of the Proposition above. Moving back to momentum space, it implies that there exist even entire functions f_{lm}^R of exponential type R such that

$$R(\mathbf{p})^{-1} \hat{\psi}_{\infty}(\mathbf{p}) = \sum_{l=0}^{\infty} \sum_{m=-l}^l p^l f_{lm}^R(p) Y_{lm}(\hat{\mathbf{p}}) + O(e^{-0.9R/\rho}). \quad (4.75)$$

Provided the properties of the functions f_{lm}^R , we can use the result (6a) of ref. [40] to obtain for any $r > R$ and angular momentum (l, m)

$$\int dp p^2 j_l(pr) \frac{p^l f_{lm}^R(p)}{p^2 - q^2 - i\epsilon} = \frac{i\pi}{2} q^{l+1} h_l^{(+)}(qr) f_{lm}^R(q), \quad (4.76)$$

where $h_l^{(+)}(qr) = j_l(qr) + in_l(qr)$. These integrals can be used to take the inverse Fourier transform of $\hat{\psi}_{\infty}(\mathbf{p})$ in (4.75) and obtain the expression²

$$\psi_{\infty}(\mathbf{r}) = e^{iqz \cdot \mathbf{r}} + \frac{m}{4\pi} \sum_{l=0}^{\infty} \sum_{m=-l}^l (iq)^{l+1} h_l^{(+)}(qr) f_{lm}^R(q) Y_{lm}(\hat{\mathbf{r}}) + O(e^{-0.9R/\rho}). \quad (4.77)$$

at any position $\mathbf{r} \in \mathbb{R}^3$ with norm $r > R$. Finally, the expression of the $f_{lm}^R(q)$ can be obtained by comparing (4.75) and the definition of $\hat{\psi}_{\infty}$. We get

$$q^l f_{lm}^R(q) = \frac{16\pi^2}{m} \frac{e^{2i\delta_l(q)} - 1}{2iq} Y_{lm}^*(\mathbf{e}_z) + O(e^{-0.9R/\rho}). \quad (4.78)$$

In summary, for any $R > 0$ and any position \mathbf{r} with $r = |\mathbf{r}| > R$, the infinite volume “wave function” ψ_{∞} at the energy $W = 2\omega_q + i\epsilon$ has the expression

$$\psi_{\infty}(\mathbf{r}) = \sum_{l=0}^{\infty} \sum_{m=-l}^l \alpha_{lm} [j_l(qr) - \tan \delta_l(q) n_l(qr)] Y_{lm}(\hat{\mathbf{r}}) + O(e^{-0.9R/\rho}), \quad (4.79)$$

where $\alpha_{lm} = 2\pi i^l (e^{2i\delta_l(q)} + 1) Y_{lm}^*(\mathbf{e}_z)$. In other words, it has the same expression as the quantum-mechanical wave function of two-particles outside of the (finite) interaction region, up to corrections decaying exponentially. Note that this result is general to any 3-projections satisfying the assumptions discussed up to now.

Finite volume

In a finite box of size $L \times L \times L$, the propagator $G_L(p_1)$ and amputated correlation functions $G_L(p_1, \dots, p_n)$ can be defined similarly as their infinite-volume counterparts as sums of Feynman diagrams. In both cases the contributing diagrams are the same

¹ The open ball of radius R centered at the origin.

² We have $\hat{\psi}_{\infty}(\mathbf{p}) = (2\pi)^3 \delta(\mathbf{p} - \mathbf{q}_z) + R(\mathbf{p}) [R(\mathbf{p})^{-1} \hat{\psi}_{\infty}(\mathbf{p})]$ due to the rules for the product of generalized functions.

but their values in finite-volume is obtained by replacing momentum integrals by sums over the lattice

$$\Lambda = \left\{ \frac{2\pi}{L} \mathbf{n} \mid \mathbf{n} \in \mathbb{Z}^3 \right\}. \quad (4.80)$$

The following proposition is useful to treat sums over Λ .

Proposition 4.3. *If the integrable function $f(\mathbf{k})$ of $\mathbf{k} \in \mathbb{R}^3$ can be continued analytically in the domain $|\operatorname{Im} \mathbf{k}| \leq \eta$ to a function vanishing at infinity, we have*

$$\frac{1}{L^3} \sum_{\mathbf{k} \in \Lambda} f(\mathbf{k}) = \int \frac{d\mathbf{k}}{(2\pi)^3} f(\mathbf{k}) + O(e^{-\eta L}). \quad (4.81)$$

Proof. Poisson's summation formula reads

$$\frac{1}{L^3} \sum_{\mathbf{k} \in \Lambda} f(\mathbf{k}) = \sum_{\mathbf{n} \in \mathbb{Z}^3} \int \frac{d\mathbf{k}}{(2\pi)^3} f(\mathbf{k}) e^{iL\mathbf{n} \cdot \mathbf{k}}. \quad (4.82)$$

For \mathbf{n} with $n = |\mathbf{n}| > 0$, we can use a contour integral to get

$$\int \frac{d\mathbf{k}}{(2\pi)^3} f(\mathbf{k}) e^{iL\mathbf{n} \cdot \mathbf{k}} = e^{-n\eta L} \int \frac{d\mathbf{k}}{(2\pi)^3} f(\mathbf{k} + i\eta \frac{\mathbf{n}}{n}) e^{iL\mathbf{n} \cdot \mathbf{k}} = O(e^{-n\eta L}). \quad (4.83)$$

The result follows. \square

Lüscher proved in [27] that the finite-volume propagator is equal to the infinite-volume propagator up to corrections exponentially small in the volume, namely

$$G_L(p) = G(p) + O(e^{-\frac{\sqrt{3}}{2}mL}). \quad (4.84)$$

Let K_L be the Bethe-Salpeter kernel in finite volume and U_L defined from K as U was defined from K (replacing the integral in (4.58) by a sum). Using the same graph-theoretical techniques developed in [27], it can be shown that $K_L - K$ decays exponentially with the volume. Combined with Proposition 4.3 and the analyticity domain of K described in the proof of Theorem 4.1, it is straightforward that $U_L - U$ also decays exponentially with the volume.

In the following we will not write explicitly any term decaying exponentially with the volume so that we have $G = G_L$ and $U = U_L$. Defining \tilde{G}_{4L} the finite-size counterpart of \tilde{G}_4 , we get

$$-\tilde{G}_{4L}(\mathbf{p}', \mathbf{p}) = \tilde{U}(\mathbf{p}', \mathbf{p}) + \frac{1}{L^3} \sum_{\mathbf{k} \in \Lambda} \tilde{U}(\mathbf{p}', \mathbf{k}) R(\mathbf{k}) \tilde{G}_{4L}(\mathbf{k}, \mathbf{p}). \quad (4.85)$$

Define infinite matrices with elements

$$[\mathcal{R}]_{\mathbf{p}', \mathbf{p}} = \delta_{\mathbf{p}', \mathbf{p}} L^{-3} R(\mathbf{p}), \quad [\tilde{\mathcal{U}}]_{\mathbf{p}', \mathbf{p}} = \tilde{U}(\mathbf{p}', \mathbf{p}), \quad [\tilde{\mathcal{G}}_{4L}]_{\mathbf{p}', \mathbf{p}} = \tilde{G}_{4L}(\mathbf{p}', \mathbf{p}), \quad (4.86)$$

where $\mathbf{p}', \mathbf{p} \in \Lambda$. Then (4.85) can be compactly written as

$$-\tilde{\mathcal{G}}_{4L} = \tilde{\mathcal{U}} + \tilde{\mathcal{U}} \mathcal{R} \tilde{\mathcal{G}}_{4L}. \quad (4.87)$$

In the rest of this subsection we take the energy as $W = 2\omega_q + i\epsilon$ with $0 \leq q^2 < 3m^2$ and ϵ infinitesimal. Furthermore we only consider energies such that q is not the norm of any momentum in Λ . Other energies can be considered “accidental” and may be treated separately.

For a kernel $F(\mathbf{p}', \mathbf{p})$ defined on any real momenta $\mathbf{p}', \mathbf{p} \in \mathbb{R}^3$, introduce the following four infinite matrices with elements

$$\begin{aligned} [\mathcal{F}]_{\mathbf{p}', \mathbf{p}} &= F(\mathbf{p}', \mathbf{p}), \\ [\mathcal{F}^\bullet]_{\mathbf{p}', lm} &= \int d\hat{\mathbf{q}} F(\mathbf{p}', \mathbf{q}) Y_{lm}(\hat{\mathbf{q}}), \\ [\mathcal{F}^\bullet]_{l'm', \mathbf{p}} &= \int d\hat{\mathbf{q}}' Y_{l'm'}^*(\hat{\mathbf{q}}') F(\mathbf{q}', \mathbf{p}), \\ [\mathcal{F}^{\bullet\bullet}]_{l'm', lm} &= \int d\hat{\mathbf{q}}' d\hat{\mathbf{q}} Y_{l'm'}^*(\hat{\mathbf{q}}') F(\mathbf{q}', \mathbf{q}) Y_{lm}(\hat{\mathbf{q}}), \end{aligned} \quad (4.88)$$

where $\mathbf{p}', \mathbf{p} \in \Lambda$, $|\mathbf{q}'| = |\mathbf{q}| = q$ and $l \geq 0, |m| \leq l$. The matrix \mathcal{F} contains the values of the kernel F when both arguments are momenta in Λ . The matrix \mathcal{F}^\bullet is composed of its values with a momentum in Λ as first argument and momenta on the mass shell as second argument, projected on a specific angular momentum (l, m) . The other two matrices are interpreted similarly. Note that the right-multiplication by \mathcal{F}^\bullet consists of a sum over the momenta in Λ while the left-multiplication by the same matrix consists of a sum over all angular momenta (l, m) .

With the notations (4.88) we are ready to establish the relation between the finite-volume \tilde{G}_{4L} and the infinite-volume \tilde{G}_4 . The following relation is shown in appendix B.2 to be valid up to corrections decaying exponentially with the volume³

$$\tilde{G}_{4L} = \tilde{G}_4 + \tilde{G}_4^\bullet \frac{1}{1 + \mathcal{M}^{\bullet\bullet} \tilde{G}_4^\bullet} \mathcal{M}^{\bullet\bullet} \tilde{G}_4^\bullet. \quad (4.89)$$

The matrix $\mathcal{M}^{\bullet\bullet}$ is in angular momentum space, like \tilde{G}_4^\bullet and the expression of its elements $[\mathcal{M}^{\bullet\bullet}]_{l_1 m_1, l_2 m_2}$ is given in (B.20).

The finite-volume 4-point function $\tilde{G}_{4L}(\mathbf{p}', \mathbf{p})$ is only defined for momenta \mathbf{p}', \mathbf{p} in Λ so that we cannot take it half or fully on-shell to define \tilde{G}_{4L}^\bullet , etc. It is however possible to do so with the infinite-volume 4-point function $\tilde{G}_4(\mathbf{p}', \mathbf{p})$ since it is defined for any real momenta \mathbf{p}', \mathbf{p} . Equation (4.89) is then a non-trivial but simple way to relate finite-volume physics to infinite-volume, asymptotic physics.

4.3.2 Finite-volume spectrum

Euclidean correlators

Consider general two-particle operators with mean Euclidean time t ,

$$\mathcal{O}^i(t) \equiv \int \frac{d^4 P}{(2\pi)^4} \frac{d^4 p}{(2\pi)^4} A_i(\mathbf{P}, p) e^{iP_4 t} \int d^4 x d^4 y e^{-i[P \cdot \frac{x+y}{2} + p \cdot (x-y)]} \phi(x) \phi(y), \quad (4.90)$$

where the index i denotes a specific choice of operator. As previously, we will only treat the system in the center-of-mass frame so that we set $A_i(\mathbf{P}, p) = (2\pi)^3 \delta(\mathbf{P}) A_i(p)$. The equivalent operators in finite volume are

$$\mathcal{O}_L^i(t) \equiv \frac{1}{L^3} \sum_{\mathbf{p} \in \Lambda} \int \frac{dP_4}{2\pi} \frac{dp_4}{2\pi} A_i(p) e^{iP_4 t} \int_{\text{FV}} d^4 x d^4 y e^{-i[P \cdot \frac{x+y}{2} + p \cdot (x-y)]} \phi(x) \phi(y), \quad (4.91)$$

where $P = (\mathbf{0}, P_4)$ and the integration over \mathbf{x} and \mathbf{y} is in the finite volume $[-\frac{L}{2}, \frac{L}{2}]^3$.

Let $|n\rangle$ and W_n for $n \geq 1$ be the eigenstates and eigenvalues of the finite-volume Hamiltonian operator. As is well-known, the Euclidean correlators are decomposed as

$$\mathcal{O}_L^{ij}(t) \equiv \langle \mathcal{O}_L^i(t) \mathcal{O}_L^j(0)^\dagger \rangle = \sum_{n \geq 1} \langle 0 | \mathcal{O}_L^i(0) | n \rangle \langle n | \mathcal{O}_L^j(0)^\dagger | 0 \rangle e^{-W_n t}. \quad (4.92)$$

³ The notation $\frac{1}{A}$ is a shorthand for A^{-1} but $\frac{A}{B}$ has no meaning for two matrices A and B .

We can also analyze the correlators using the explicit expression of the operators. This leads to⁴

$$C_L^{ij}(t) = \frac{1}{L^6} \sum_{\mathbf{p}', \mathbf{p} \in \Lambda} \int \frac{dP_4}{2\pi} \frac{dp'_4}{2\pi} \frac{dp_4}{2\pi} A_i(\mathbf{p}') e^{iP_4 t} A_j^\dagger(\mathbf{p}) \times \left[2\pi \delta(p'_4 - p_4) L^3 \delta_{\mathbf{p}', \mathbf{p}} + G2(\mathbf{p}') G_{4L}(\mathbf{p}', \mathbf{p}) \right] G2(\mathbf{p}). \quad (4.93)$$

Introduce the functions \mathcal{P}_L and \mathcal{P}_R defined by

$$\mathcal{P}_L(\mathbf{p}) = \left[\frac{\bar{A}_i(\mathbf{p})}{\sqrt{2mW}} \right]^{-1} A_i(\mathbf{p}) R(\mathbf{p})^{-1} G2(\mathbf{p}), \quad \mathcal{P}_R(\mathbf{p}) = \left[\frac{\bar{A}_j^\dagger(\mathbf{p})}{\sqrt{2mW}} \right]^{-1} A_j^\dagger(\mathbf{p}) R(\mathbf{p})^{-1} G2(\mathbf{p}), \quad (4.94)$$

where the operator- and energy-dependent function \bar{A}_i is⁵

$$\bar{A}_i(\mathbf{p}) = \frac{A_i(\mathbf{p})|_{p_4=0}}{\sqrt{2mW}} e^{-\eta \frac{m\mathcal{E}(W) - \mathbf{p}^2}{2m^2}}. \quad (4.95)$$

with the usual notation $P_4 = iW$ and some $\eta > 0$.

Using Lemma 4.1, we can show that \mathcal{P}_L and \mathcal{P}_R are 3-projections if $A_i(\mathbf{p})$ and $A_j(\mathbf{p})$ can be analytically continued in the region $|\text{Im } p_4| < m$, $|\text{Im } \mathbf{p}| \leq \frac{m}{2}$ and they either

i) do not depend on p_4 , in which case the 3-projections $\mathcal{P}_{L,R}(\mathbf{p})$ are given by

$$\mathcal{P}_L(\mathbf{p}) = \mathcal{P}_R(\mathbf{p}) = 2mW e^{\eta \frac{m\mathcal{E}(W) - \mathbf{p}^2}{2m^2}} R(\mathbf{p})^{-1} G2(\mathbf{p}), \quad (4.96)$$

i.e. they do not depend on the choice $A_{i,j}$ of operators at all. This corresponds to operators for two particles taken at the same Euclidean time (“equal-time” operators).

ii) depend on p_4 and do not vanish⁶ on the line $p_4 = 0$.

We will assume these conditions realized in the following.

The correlator $C_L^{ij}(t)$ is then the sum of two terms, one for the connected and one for the disconnected part. We can simplify the disconnected part by noting that

$$\int \frac{dP_4}{2\pi} e^{-iP_4 t} \left[\int \frac{dp_4}{2\pi} A_i(\mathbf{p}) G2(\mathbf{p}) A_j^\dagger(\mathbf{p}) - \bar{A}_i(\mathbf{p}) R(\mathbf{p}) \bar{A}_j^\dagger(\mathbf{p}) \right] = O(e^{-4\bar{m}t}), \quad (4.97)$$

for any $\bar{m} < m$ and \mathbf{p} in Λ . Due to Lemma 4.1 and the assumed properties of A_i , the integrand on the left-hand side is analytic for $0 \leq \text{Im } P_4 \leq 4m$ so that we can push the integration line to $\text{Im } P_4 = 4\bar{m}$.

The disconnected part is easily shown to involve the “projected” 4-point function \tilde{G}_{4L} defined by (4.57) using the 3-projections introduced in (4.94). Combining the two parts, we finally arrive to the simple expression

$$C_L^{ij}(t) = \int \frac{dP_4}{2\pi} e^{iP_4 t} \text{Tr} \left[\bar{A}_i (1 + \mathcal{R} \tilde{G}_{4L}) \mathcal{R} \bar{A}_j^\dagger \right] + O(e^{-4\bar{m}t}), \quad (4.98)$$

⁴ The functions A_i may have indices for internal degrees of freedom, which is why we use the Hermitian conjugation \dagger .

⁵ The exponential ensures the convergence of integrals like (4.58).

⁶ If they vanish, we can formally add a constant to $A_{i,j}$ and drive it towards zero at the end of the derivation.

with the matrices $\bar{\mathcal{A}}_i$ defined by

$$[\bar{\mathcal{A}}_i]_{\mathbf{p}', \mathbf{p}} = \delta_{\mathbf{p}', \mathbf{p}} \bar{\mathcal{A}}_i(\mathbf{p}), \quad (4.99)$$

for \mathbf{p}' and \mathbf{p} two momenta in Λ .

By identification of equations (4.92) and (4.98), we can deduce that the poles of the matrix $(1 + \mathcal{R}\tilde{\mathcal{G}}_{4L})\mathcal{R}$ in the domain $0 \leq \text{Im } P_4 < 4\bar{m}$ are associated to the eigenenergies by $P_4 = iW_n$. Furthermore, if $\tilde{\mathcal{X}}_n$ is the residue of this matrix at the pole $W = W_n < 4\bar{m}$, we have⁷

$$\text{Tr } \bar{\mathcal{A}}_i \tilde{\mathcal{X}}_n \bar{\mathcal{A}}_j^\dagger = \langle 0 | \mathcal{O}_L^i(0) | n \rangle \langle n | \mathcal{O}_L^j(0)^\dagger | 0 \rangle. \quad (4.100)$$

As discussed previously, for equal-time operators the 3-projections do not depend on the particular choice of operators and the residue is easily found from the above equation to be

$$[\tilde{\mathcal{X}}_n]_{\mathbf{p}', \mathbf{p}} = 2mW_n \left[e^{\eta \frac{m\varepsilon(W_n) - \mathbf{p}'^2}{2m^2}} \hat{\psi}_n(\mathbf{p}') \right] \left[e^{\eta \frac{m\varepsilon(W_n) - \mathbf{p}^2}{2m^2}} \hat{\psi}_n(\mathbf{p}) \right]^\dagger, \quad (4.101)$$

for \mathbf{p}', \mathbf{p} two momenta in Λ and the definition

$$\hat{\psi}_n(\mathbf{p}) = \frac{1}{L^3} \int_{\text{FV}} d^3 \mathbf{x} d^3 \mathbf{y} e^{-i\mathbf{p} \cdot (\mathbf{x} - \mathbf{y})} \langle 0 | \phi(\mathbf{x}) \phi(\mathbf{y}) | n \rangle, \quad (4.102)$$

where $x = (\mathbf{x}, 0)$, $y = (\mathbf{y}, 0)$.

Quantization condition

We have seen that the finite-size spectrum for two-particle states in the elastic energy region is given by the poles of the matrix $(1 + \mathcal{R}\tilde{\mathcal{G}}_{4L})\mathcal{R}$. This requires the use of 3-projections satisfying certain conditions discussed previously but we will focus on the simple and practically useful choice of (4.96) which is relevant to the study of equal-time operators. Using (4.87) we directly have the following matrix relations

$$\tilde{\mathcal{G}}_{4L} = -\tilde{\mathcal{U}} \frac{1}{1 + \mathcal{R}\tilde{\mathcal{U}}}, \quad (1 + \mathcal{R}\tilde{\mathcal{G}}_{4L})\mathcal{R} = \frac{1}{1 + \mathcal{R}\tilde{\mathcal{U}}}\mathcal{R}. \quad (4.103)$$

In the absence of interaction the Bethe-Salpeter vanishes, which leads to $\tilde{\mathcal{U}} = \tilde{\mathcal{G}}_{4L} = 0$. Then, the poles of $(1 + \mathcal{R}\tilde{\mathcal{G}}_{4L})\mathcal{R}$ are simply the poles of \mathcal{R} , which are $W = 2\omega_{\mathbf{k}}$ for \mathbf{k} in Λ . In the presence of interaction, some eigenenergies may “accidentally” be of this form but we focus on those which are not. Since $\tilde{\mathcal{U}}$ has no singularity in the elastic energy region, see Theorem 4.1, we conclude that the eigenenergies of interest are poles of the matrix $\tilde{\mathcal{G}}_{4L}$ and can be characterized by

$$\det(1 + \mathcal{R}\tilde{\mathcal{U}}) = 0, \quad (4.104)$$

where the determinant is over the momenta in Λ . This is the determinant of an infinite matrix but we can use the symmetries of the system to reduce it to the well-defined determinant of finite matrices.

The matrices considered so far in finite-volume such as $\tilde{\mathcal{U}}$ can be seen as operators in \mathbb{C}^Λ , the infinite-dimensional vector space of functions mapping Λ to \mathbb{C} . Their matrix representation corresponds to the basis given by the functions⁸

$$|\underline{\mathbf{p}}\rangle : \mathbf{p}' \in \Lambda \mapsto \delta_{\mathbf{p}, \mathbf{p}'} \quad (4.105)$$

⁷ Assuming that the eigenenergy W_n is not degenerate.

⁸ We use underlined bras and kets to distinguish these vectors from the physical states.

λ	A_1^+	A_2^+	E^+	T_1^+	T_2^+	A_1^-	A_2^-	E^-	T_1^-	T_2^-
$(0, 0, 0)$	1									
$(0, 0, a)$	1		1						1	
$(0, a, a)$	1		1		1				1	1
(a, a, a)	1				1		1		1	
$(0, a, b)$	1	1	2	1	1				2	2
(a, b, b)	1		1	1	2		1	1	2	1
(a, b, c)	1	1	2	3	3	1	1	2	3	3

Table 4.1: Number of occurrences $N(\Gamma, p\lambda)$ of the irreducible representation Γ of the cubic group in the decomposition of the representation \mathfrak{R}_p^λ depending on the shape of the elements of Λ_p^λ . Any set Λ_p^λ contains exactly one element of the leftmost column with $0 < a < b < c$. Empty cells mean zeros.

for all momenta \mathbf{p} in Λ . We will now consider these matrices as operators without changing the notation so for example $[\tilde{\mathcal{U}}]_{\mathbf{p}', \mathbf{p}} = \langle \mathbf{p}' | \tilde{\mathcal{U}} | \mathbf{p} \rangle$ for $\mathbf{p}', \mathbf{p} \in \Lambda$.

Let us construct a representation \mathfrak{R} of the cubic group \mathcal{O}_h on \mathbb{C}^Λ which maps a rotation $R \in \mathcal{O}_h$ to the matrix $D(R)$ such that $D(R)|\mathbf{p}\rangle = |R \cdot \mathbf{p}\rangle$ for all \mathbf{p} in Λ .

The set of momenta Λ can be partitioned twice as

$$\Lambda = \bigcup_{p \in |\Lambda|} \Lambda_p, \quad \Lambda_p = \bigcup_{\lambda=1}^{N(p)} \Lambda_p^\lambda. \quad (4.106)$$

The first partition is over the norm of the momenta, with

$$|\Lambda| = \{|\mathbf{p}| \in \mathbb{R} \mid \mathbf{p} \in \Lambda\}, \quad \Lambda_p = \{\mathbf{p}' \in \Lambda \mid p = |\mathbf{p}'|\}. \quad (4.107)$$

The second partition is over the orbit of the momenta under the action of the cubic group. Define the equivalence relation such that two momenta in \mathbf{p}, \mathbf{p}' in Λ_p are equivalent if there is a rotation $R \in \mathcal{O}_h$ for which $\mathbf{p}' = R \cdot \mathbf{p}$. Then Λ_p^λ for $\lambda = 1, \dots, N(p)$ are defined as the equivalence classes of that relation. For example $\frac{2\pi}{L}(1, 2, 2)$ and $\frac{2\pi}{L}(3, 0, 0)$ are both in $\Lambda_{\frac{6\pi}{L}}$ but not in the same equivalence class.

These partitions of Λ are stable under the action of the cubic group and therefore induce the following decomposition of the representation \mathfrak{R}

$$\mathfrak{R} = \bigoplus_{p \in |\Lambda|} \mathfrak{R}_p, \quad \mathfrak{R}_p = \bigoplus_{\lambda=1}^{N(p)} \mathfrak{R}_p^\lambda, \quad \mathfrak{R}_p^\lambda = \bigoplus_{\Gamma} N(\Gamma, p\lambda) \times \Gamma. \quad (4.108)$$

The last relation is simply the decomposition of \mathfrak{R}_p^λ over the irreducible representations of the cubic group $\Gamma = A_1^\pm, A_2^\pm, E^\pm, T_1^\pm, T_2^\pm$ with multiplicities $N(\Gamma, p\lambda)$. These multiplicities are summed up in table 4.1.

The decomposition (4.108) of \mathfrak{R} implies the existence of a basis of \mathbb{C}^Λ in which the matrices $D(R)$ are block-diagonal with identical blocks for each occurrence of an irreducible representations Γ in the decomposition of \mathfrak{R} . The elements of this basis are noted $|p\lambda\Gamma\nu\alpha\rangle$ with $p \in |\Lambda|$ the norm of a finite-volume momentum, $\lambda \in \{1, \dots, N(p)\}$ an equivalence class for momenta with this norm, Γ an irreducible representation, $\nu \in \{1, \dots, N(\Gamma, p\lambda)\}$ an index for the multiplicity of Γ in \mathfrak{R}_p^λ and $\alpha \in \{1, \dots, d_\Gamma\}$ where d_Γ is the dimension of Γ . They are such that

$$\langle p'\lambda'\Gamma'\nu'\alpha' | D(R) | p\lambda\Gamma\nu\alpha \rangle = \delta_{p', p} \delta_{\lambda', \lambda} \delta_{\Gamma', \Gamma} \delta_{\nu', \nu} [D^\Gamma(R)]_{\alpha', \alpha}, \quad (4.109)$$

where $R \in \mathcal{O}_h \mapsto D^\Gamma(R)$ is some representation of \mathcal{O}_h isomorphic to Γ .

Let \mathbf{p} be a momentum in Λ . It belongs to some equivalence class Λ_p^λ , where $p = |\mathbf{p}|$, which contains in total $N(p\lambda) = \sum_\Gamma N(\Gamma, p\lambda) d_\Gamma$ elements. These elements can be canonically enumerated as $\mathbf{p}_1, \mathbf{p}_2, \dots, \mathbf{p}_{N(p\lambda)}$ starting from $\mathbf{p}_1 = (a, b, c)$ with $0 \leq a \leq b \leq c$ then using permutations and sign changes on the coordinates. Denote i the index such that $\mathbf{p} = \mathbf{p}_i$. The mixing of the two bases introduced so far necessarily takes the form

$$\langle p' \lambda' \Gamma \nu \alpha | \mathbf{p} \rangle = \delta_{p', p} \delta_{\lambda', \lambda} [\Theta^{p\lambda}]_{\Gamma \nu \alpha, i}. \quad (4.110)$$

The matrices $\Theta^{p\lambda}$ are unitary with finite size $N(p\lambda) \times N(p\lambda)$. Note that the particular values of the momenta in Λ_p^λ are not relevant for the structure of the representation, only the way they transform under the action of the cubic group is. Therefore, it can be shown that for a fixed choice of canonical enumeration we only need 7 matrices $\Theta^{p\lambda}$, corresponding to the shape of \mathbf{p}_1 described by the rows of table 4.1. The dimensions $N(p\lambda)$ of $\Theta^{p\lambda}$ associated to these rows from top to bottom are 1, 6, 12, 8, 24, 24 and 48.

Enumerate the elements of $|\Lambda|$ as $q_1 = 0, q_2 = \frac{2\pi}{L}, \dots$ by increasing value. Let $q = q_i$ one such element, i.e. the norm of some momentum in Λ , and define the matrices \mathcal{R}_q and $\tilde{\mathcal{U}}_q$ by

$$[\mathcal{R}_q]_{p', p} = \delta_{q, |p|} [\mathcal{R}]_{p', p} \quad \text{and} \quad \tilde{\mathcal{U}}_q = \frac{1}{1 + \tilde{\mathcal{U}}(\mathcal{R} - \mathcal{R}_q)} \tilde{\mathcal{U}}, \quad (4.111)$$

so that the relation (4.103) can be written

$$\tilde{\mathcal{G}}_{4L} = -\tilde{\mathcal{U}} \left[1 - (\mathcal{R} - \mathcal{R}_q) \tilde{\mathcal{U}}_q \right] \frac{1}{1 + \mathcal{R}_q \tilde{\mathcal{U}}}. \quad (4.112)$$

The matrix \mathcal{R}_q vanishes except for momenta with norm q and it is easy to show that both $\mathcal{R} - \mathcal{R}_q$ and $\tilde{\mathcal{U}}_q$ are analytic in the region⁹ $\omega_{q_{i-1}} + \omega_q \leq \text{Re } W < \omega_q + \omega_{q_{i+1}}$. We deduce that any pole of the finite-volume 4-point function $\tilde{\mathcal{G}}_{4L}$ in this region satisfies the condition

$$\det(1 + \mathcal{R}_q \tilde{\mathcal{U}}_q) = 0. \quad (4.113)$$

This condition is equivalent to (4.104) and the determinant is still that of an infinite matrix but we can use the fact that \mathcal{R}_q is zero outside of Λ_q to give it a finite value.

Finally, the spherical symmetry of the Bethe-Salpeter kernel can be used to show¹⁰ that the matrices $\tilde{\mathcal{U}}$ and $\tilde{\mathcal{U}}_q$ transform covariantly under the action of the cubic group in the sense that they commute with the matrices $D(R)$ for any rotation $R \in \mathcal{O}_h$. Using Schür's lemma, this ensures the expression

$$\langle q \lambda' \Gamma' \nu' \alpha' | \tilde{\mathcal{U}}_q | q \lambda \Gamma \nu \alpha \rangle = \delta_{\Gamma', \Gamma} \delta_{\alpha', \alpha} [\tilde{\mathcal{U}}_q^\Gamma]_{\lambda' \nu', \lambda \nu}, \quad (4.114)$$

for some finite matrices $\tilde{\mathcal{U}}_q^\Gamma$. We conclude that (4.113) implies the existence of an irreducible representation Γ such that

$$\det\left(1 + \frac{1}{L^3} R(q) \tilde{\mathcal{U}}_q^\Gamma\right) = 0. \quad (4.115)$$

This is the determinant a finite matrix and it is a well-defined characterization of the finite-volume eigenenergies in the region $\omega_{q_{i-1}} + \omega_q \leq \text{Re } W < \omega_q + \omega_{q_{i+1}}$. Similar conditions can of course be derived for the whole energy region $0 \leq \text{Re } W < 4m$ by changing q . Note that in the simple case of $q \leq \sqrt{8} \cdot 2\pi/L$ and $\Gamma = A_1^+$, $\tilde{\mathcal{U}}_q^\Gamma$ is a 1×1 matrix and this condition is equivalent to Eq. (3.32) of ref. [8].

⁹ For $i = 1$, take $\omega_{q_0} = -m$.

¹⁰ If the 3-projections $\mathcal{P}_{L,R}$ are rotationally invariant, which is the case here.

Residues

Let W_n be any eigenenergy in the elastic energy region. Assuming that it is not “accidentally” a pole of \mathcal{R} , i.e. $W_n = 2\omega_{\mathbf{p}}$ for some momentum \mathbf{p} in Λ , it satisfies the condition (4.115) for some momentum norm q in $|\Lambda|$ and some irreducible representation Γ of the cubic group. The nullspace of $1 + \frac{1}{L^3}R(q)\tilde{\mathcal{U}}_q^\Gamma$ taken at W_n is therefore non-empty. Let $u_1, \dots, u_{N(n\Gamma)}$ be an orthonormal basis of this nullspace. Each vector u_a of the basis, with elements $[u_a]_{\lambda\nu}$, is such that the following holds at the energy W_n ,

$$[u_a]_{\lambda\nu} + \frac{1}{L^3}R(q) \sum_{\lambda'=1}^{N(q)} \sum_{\nu'=1}^{N(\Gamma, q\lambda)} [\tilde{\mathcal{U}}_q^\Gamma]_{\lambda\nu, \lambda'\nu'} [u_a]_{\lambda'\nu'} = 0. \quad (4.116)$$

For any α in $\{1, \dots, d_\Gamma\}$, use this vector to define two elements of \mathbb{C}^Λ

$$|u_a^\alpha\rangle = \sum_{\lambda=1}^{N(q)} \sum_{\nu=1}^{N(\Gamma, q\lambda)} [u_a]_{\lambda\nu} |q\lambda\Gamma\nu\alpha\rangle, \quad |v_n^{\Gamma\alpha\alpha}\rangle = \left(1 - (\mathcal{R}^{(n)} - \mathcal{R}_q^{(n)})\tilde{\mathcal{U}}_q^{(n)}\right) |u_a^\alpha\rangle, \quad (4.117)$$

where we use a superscript (n) to denote that the matrices \mathcal{R} , etc. are taken at the energy W_n . Inserting the definitions of \mathcal{R}_q and $\tilde{\mathcal{U}}_q$ leads to the two relations

$$(1 + \mathcal{R}_q^{(n)}\tilde{\mathcal{U}}_q^{(n)})|u_a^\alpha\rangle = 0, \quad (1 + \mathcal{R}^{(n)}\tilde{\mathcal{U}}^{(n)})|v_n^{\Gamma\alpha\alpha}\rangle = 0. \quad (4.118)$$

This gives sense to the two conditions (4.104) and (4.113): the determinant of these infinite matrices is zero because their nullspace is not empty. Let \mathcal{P}_n be the orthogonal projector on Σ_N , the nullspace of $1 + \mathcal{R}^{(n)}\tilde{\mathcal{U}}^{(n)}$. It may be expressed as

$$\mathcal{P}_n = \sum_{\Gamma} \sum_{\alpha=1}^{d_\Gamma} \mathcal{P}_n^{\Gamma\alpha}, \quad \mathcal{P}_n^{\Gamma\alpha} = \sum_{a=1}^{N(n\Gamma)} |v_n^{\Gamma\alpha\alpha}\rangle \langle v_n^{\Gamma\alpha\alpha}|, \quad (4.119)$$

where the first sum is over the irreducible representations Γ of the cubic group, the second is over the dimension of Γ and the third is over the basis of the nullspace of $1 + \frac{1}{L^3}R(q)\tilde{\mathcal{U}}_q^\Gamma$ at $W = W_n$ (it may be empty for some Γ , in which case $\mathcal{P}_n^{\Gamma\alpha} = 0$, but not all so that $\mathcal{P}_n \neq 0$). All these sums are finite.

The projector \mathcal{P}_n can be used to characterize the residue $\tilde{\mathcal{X}}_n$ of $(1 + \mathcal{R}\tilde{\mathcal{G}}_{4L})\mathcal{R}$ at the pole $W = W_n$. Note that $\tilde{\mathcal{U}}$ is analytic at this energy due to Theorem 4.1 so we have the expansion

$$\tilde{\mathcal{U}} = \tilde{\mathcal{U}}^{(n)} + (W - W_n)\tilde{\mathcal{U}}^{(n)'} + O((W - W_n)^2), \quad (4.120)$$

for some matrix $\tilde{\mathcal{U}}^{(n)'}$. We can also work out the expansion of \mathcal{R} around $W = W_n$,

$$\mathcal{R} = \mathcal{R}^{(n)} \left[1 + (W - W_n) \frac{W_n L^3}{2m} \mathcal{R}^{(n)} + O((W - W_n)^2) \right]. \quad (4.121)$$

Combining the last two expansions, we obtain around the pole

$$1 + \mathcal{R}\tilde{\mathcal{U}} = \left(1 + \mathcal{R}^{(n)}\tilde{\mathcal{U}}^{(n)}\right) + (W - W_n)\mathcal{R}^{(n)} \left(\frac{W_n L^3}{2m}\mathcal{R}^{(n)}\tilde{\mathcal{U}}^{(n)} + \tilde{\mathcal{U}}^{(n)'}\right) + O((W - W_n)^2). \quad (4.122)$$

The first term $1 + \mathcal{R}^{(n)}\tilde{\mathcal{U}}^{(n)}$ is zero when left- or right-multiplied by any vector of Σ_n and non-zero otherwise. Consider $1 + \mathcal{R}\tilde{\mathcal{U}}$ as a 2×2 block matrix with blocks separating Σ_n and its orthogonal complement, the upper-left block A being its restriction from Σ_n to Σ_n , etc. The inverse of a 2×2 block matrix is given by

$$\begin{bmatrix} A & B \\ C & D \end{bmatrix}^{-1} = \begin{bmatrix} (A - BD^{-1}C)^{-1} & -A^{-1}B(D - CA^{-1}B)^{-1} \\ -D^{-1}C(A - BD^{-1}C)^{-1} & (D - CA^{-1}B)^{-1} \end{bmatrix}. \quad (4.123)$$

From the previous observation A , B and C scale like $W - W_n$ around the pole while D converges towards an invertible matrix. Only the upper-left part of the inverse matrix is singular and equivalent to A^{-1} around the pole. We deduce that

$$\frac{1}{1 + \mathcal{R}\tilde{\mathcal{U}}} = \frac{1}{W - W_n} \mathcal{P}_n \frac{1}{\mathcal{R}^{(n)} \left(-\frac{W_n L^3}{2m} + \mathcal{P}_n \tilde{\mathcal{U}}^{(n)'} \mathcal{P}_n \right)} \mathcal{P}_n + O(1), \quad (4.124)$$

where we used $\mathcal{R}^{(n)} \tilde{\mathcal{U}}^{(n)} \mathcal{P}_n = -\mathcal{P}_n$. Given (4.103), the residue $\tilde{\mathcal{X}}_n$ is then directly given by

$$\tilde{\mathcal{X}}_n = \mathcal{P}_n \frac{1}{-\frac{W_n L^3}{2m} + \mathcal{P}_n \tilde{\mathcal{U}}^{(n)'} \mathcal{P}_n} \mathcal{P}_n. \quad (4.125)$$

Note that if the kernel \tilde{U} is not energy-dependent, $\tilde{\mathcal{U}}^{(n)'}$ vanishes and the residue is proportional to the projection \mathcal{P}_n .

With the expression (4.125) of the residue $\tilde{\mathcal{X}}_n$, we can show that the function $\hat{\psi}_n$ defined in (4.102) satisfies

$$- [R^{(n)}]^{-1}(\mathbf{p}) \hat{\psi}_n(\mathbf{p}) = \frac{1}{L^3} \sum_{\mathbf{p}' \in \Lambda} \tilde{U}_\eta^{(n)}(\mathbf{p}, \mathbf{p}') \hat{\psi}_n(\mathbf{p}'), \quad (4.126)$$

where $\mathbf{p} \in \Lambda$ and the rescaled kernel \tilde{U}_η is

$$\tilde{U}_\eta(\mathbf{p}, \mathbf{p}') = e^{\eta \frac{\mathbf{p}^2 - \mathbf{p}'^2}{2m^2}} \tilde{U}(\mathbf{p}, \mathbf{p}'), \quad (4.127)$$

with $\hat{U}_\eta^{(n)}$ its value at the energy W_n as before. Remember that η was introduced in (4.95) to ensure that some integrals do not exhibit UV divergences. Since η can be taken arbitrarily close to zero, the deviation between \tilde{U}_η and \tilde{U} is only for asymptotically large $\frac{\mathbf{p}^2 - \mathbf{p}'^2}{m^2}$. This corresponds to the interaction between intermediate states of vastly different energies. For the present study of energies of the order of the mass m , we will consider that we may replace \tilde{U}_η by \tilde{U} for η small enough.

Defining $\psi_n(\mathbf{r})$ the inverse Fourier transform of $\hat{\psi}_n(\mathbf{p})$, the previous equation reads in position space, up to correction vanishing exponentially with the volume as usual,

$$\frac{1}{m} (\Delta + q_n^2) \psi_n(\mathbf{r}) = \int_{\text{FV}} d^3 \mathbf{r}' U^{(n)}(\mathbf{r}, \mathbf{r}') \psi_n(\mathbf{r}'), \quad (4.128)$$

where $\mathbf{r}, \mathbf{r}' \in [-\frac{L}{2}, \frac{L}{2}]^3$ and q_n is such that $W_n = 2\omega_{q_n}$.

The previous equation is quite similar to (4.70) satisfied by $\psi_\infty^{(n)}$ in infinite volume. However, it becomes exactly the same if we replace U by the compactly supported U_R where $R = 0.4L$ in both (4.70) and (4.128). As discussed for the infinite-volume equation, this only results in additional corrections vanishing exponentially with the volume. In summary, up to such corrections, ψ_n and $\psi_\infty^{(n)}$ satisfy the exact same Schrödinger equation on the ball $B(0, \frac{L}{2})$. This implies in particular that in the region $0.4L < r < 0.5L$, ψ_n is determined by the scattering phase shifts $\delta_l(q_n)$ in the same way as (4.79)¹¹.

¹¹ With possibly different coefficients α_{lm} .

Another quantization condition

We have seen that the poles of the 4-point function \tilde{G}_{4L} below the inelastic threshold correspond¹² to the finite-size spectrum and we have expressed a characterization of these poles through (4.104). Another characterization can be directly derived using the relation (4.89) between the finite- and the infinite-volume 4-point functions. Indeed, since the infinite-volume amputated 4-point function G_4 has no singularity in the elastic energy region (in the absence of bound states and resonances), the pole must satisfy

$$\det(1 + \mathcal{M}^{\bullet\bullet}\tilde{\mathcal{G}}_4^{\bullet\bullet}) = 0, \quad (4.129)$$

where the determinant is over all angular momenta (l, m) .

Remember that $\tilde{\mathcal{G}}_4^{\bullet\bullet}$ corresponds to \tilde{G}_4 being taken on-shell on both arguments and this is proportional to the T-matrix by (4.57). Therefore, we have for a pole at $W_n = 2\omega_{q_n}$,

$$[\tilde{\mathcal{G}}_4^{\bullet\bullet}]_{lm, l'm'} = \frac{1}{2mW_n} [T]_{lm, l'm'} = \delta_{l, l'} \delta_{m, m'} \frac{8\pi^2}{imq_n} \left(e^{2i\delta_l(q_n)} - 1 \right), \quad (4.130)$$

where m in the denominators is the particle mass. Equation (4.129) is then equivalent to the finite-size formula derived by Lüscher in ref. [9].

Once again, this condition involves the determinant of an infinite matrix, which may be interpreted as the fact that $1 + \mathcal{M}^{\bullet\bullet}\tilde{\mathcal{G}}_4^{\bullet\bullet}$ has a non-zero nullspace at some eigenenergy W_n . For the rest of this subsection, we take all energy-dependent matrices and functions at this energy W_n (or $W_n + i\epsilon$ when necessary) and omit the usual superscript (n) to avoid too heavy notations. Let u_1, u_2, \dots be an orthonormal basis of the nullspace of $1 + \mathcal{M}^{\bullet\bullet}\tilde{\mathcal{G}}_4^{\bullet\bullet}$. Each vector u_a of the basis, with elements $[u_a]_{lm}$, is such that

$$[u_a]_{lm} + \sum_{l'=0}^{\infty} \sum_{m'=-l'}^{l'} [\mathcal{M}^{\bullet\bullet}]_{lm, l'm'} [\tilde{\mathcal{G}}_4^{\bullet\bullet}]_{l'm', lm'} [u_a]_{l'm'} = 0. \quad (4.131)$$

For any position $\mathbf{r} \in \mathbb{R}^3$ and any on-shell momentum $\mathbf{q} = q_n \hat{\mathbf{q}}$, we introduce the difference

$$\Delta_L(\mathbf{r}, \hat{\mathbf{q}}) \equiv \int \frac{d^3\mathbf{p}}{(2\pi)^3} e^{i\mathbf{p}\cdot\mathbf{r}} R(\mathbf{p}) \tilde{G}_4(\mathbf{p}, \mathbf{q}) - \frac{1}{L^3} \sum_{\mathbf{p} \in \Lambda} e^{i\mathbf{p}\cdot\mathbf{r}} R(\mathbf{p}) \tilde{G}_4(\mathbf{p}, \mathbf{q}). \quad (4.132)$$

With the methods discussed in appendix B.2 which lead to the relation (4.89), we can show that this difference has the following expression

$$\Delta_L(\mathbf{r}, \hat{\mathbf{q}}) = \sum_{lm} \sum_{l'm'} 4\pi i^l j_l(q_n r) Y_{lm}(\hat{\mathbf{r}}) [\mathcal{M}^{\bullet\bullet}]_{lm, l'm'} [\tilde{\mathcal{G}}_4^{\bullet\bullet}]_{l'm', l'm'} Y_{l'm'}^*(\hat{\mathbf{q}}). \quad (4.133)$$

Due to the similarity with (4.131), we define for any vector u_a a function of the angle $\hat{\mathbf{q}}$

$$f_a(\hat{\mathbf{q}}) = \sum_{l=0}^{\infty} \sum_{m=-l}^l [u_a]_{lm} Y_{lm}(\hat{\mathbf{q}}). \quad (4.134)$$

These functions all satisfy the relation

$$\int d\hat{\mathbf{q}} \Delta_L(\mathbf{r}, \hat{\mathbf{q}}) f_a(\hat{\mathbf{q}}) = - \int d\hat{\mathbf{q}} e^{i\mathbf{q}\cdot\mathbf{r}} f_a(\hat{\mathbf{q}}). \quad (4.135)$$

¹² Except for “accidental” eigenenergies $W_n = 2\omega_{\mathbf{q}}$ with \mathbf{q} in Λ .

We can use the functions f_a to take some specific combinations of the infinite-volume “wave functions” $\hat{\psi}_\infty^q$ defined in (4.68),

$$\hat{\psi}_\infty^{q_n,a}(\mathbf{p}) = \int d\hat{\mathbf{q}} \hat{\psi}_\infty^q(\mathbf{p}) f_a(\hat{\mathbf{q}}). \quad (4.136)$$

Then, the previous discussion leads to the remarkable¹³ property that up to corrections vanishing exponentially with the volume, these generalized functions satisfy

$$[\mathcal{F}_\infty^{-1} \cdot \hat{\psi}_\infty^{q_n,a}](\mathbf{r}) = [\mathcal{F}_L^{-1} \cdot \hat{\psi}_\infty^{q_n,a}](\mathbf{r}), \quad (4.137)$$

for any $\mathbf{r} \in [-\frac{L}{2}, \frac{L}{2}]^3$, where the infinite- and finite-volume inverse Fourier transforms are defined as usual by

$$[\mathcal{F}_\infty^{-1} \cdot \hat{h}](\mathbf{r}) = \int \frac{d\mathbf{p}}{(2\pi)^3} e^{i\mathbf{p}\cdot\mathbf{r}} \hat{h}(\mathbf{p}), \quad [\mathcal{F}_L^{-1} \cdot \hat{h}](\mathbf{r}) = \frac{1}{L^3} \sum_{\mathbf{p} \in \Lambda} e^{i\mathbf{p}\cdot\mathbf{r}} \hat{h}(\mathbf{p}), \quad (4.138)$$

for a function \hat{h} defined on \mathbb{R}^3 .

4.3.3 Description of the method

In the previous section, we have derived two quantization conditions allowing to characterize the finite-volume energy spectrum below the inelastic threshold. The two conditions are of course equivalent and they are related by equation (4.89).

The second condition (4.129) is the well-known finite-size formula first derived by Lüscher in ref. [9]. While it was derived in a purely quantum-field-theoretical setting using the 4-point function, we also gave an interpretation in terms of “wave functions”. The idea is that some functions $\hat{\psi}_\infty^{q_n,a}$ defined in infinite-volume can “fit” in a finite box, in the sense of (4.137), which was the starting point of Lüscher’s derivation for a quantum mechanical system. The condition itself can be directly exploited to relate the finite-size spectrum to the scattering phase shifts. However, the existence of the functions $\hat{\psi}_\infty^{q_n,a}$ does not seem to have any practical use since they are defined from the unknown functions $\hat{\psi}_\infty^q$.

The first quantization condition (4.104) is a generalization of the work by Lüscher in ref. [8]. It states that the functions

$$\psi_n(\mathbf{r}) = \frac{1}{L^3} \int_{\text{FV}} d^3\mathbf{x} \langle 0 | \phi(\mathbf{x} + \mathbf{r}, 0) \phi(\mathbf{x}, 0) | n \rangle, \quad (4.139)$$

defined for any eigenstate $|n\rangle$ of the finite-volume Hamiltonian with an energy under the inelastic threshold, satisfy the same Schrödinger equation (4.70) as the infinite-volume “wave functions” ψ_∞ . This is significant because the functions ψ_n can actually be evaluated using lattice simulations and the functions ψ_∞ are directly related to the scattering phase shifts by (4.79). It implies that the scattering phase shifts can similarly be extracted from ψ_n but also opens the way to approximate the Schrödinger equation at nearby energies. We will explore that possibility in this section.

Kernel approximation

We come back to the Schrödinger equation (4.70) satisfied by the infinite-volume functions ψ_∞ in the elastic energy region. As discussed previously, it still holds if we

¹³ Considering their singularities.

replace U by the compactly supported U_R up to corrections decaying exponentially with R . At an energy $W_n < 4m$ of the finite-volume spectrum, taking $R = 0.4L$ it also satisfied in the ball $B(0, \frac{L}{2})$ by the finite-volume function ψ_n up similar corrections, which we will neglect since $R \sim L$. Let us write it again

$$\frac{1}{m}(\Delta + q_n^2)\psi(\mathbf{r}) = \int d^3\mathbf{r}' U_R^{(n)}(\mathbf{r}, \mathbf{r}')\psi(\mathbf{r}'), \quad (4.140)$$

valid with $\mathbf{r} \in \mathbb{R}^3$ for $\psi = \psi_\infty^{(n)}$ and $\mathbf{r} \in B(0, \frac{L}{2})$ for $\psi = \psi_n$.

Due to its spherical symmetry, the kernel $U_R^{(n)}$ can be expanded on the spherical harmonics as

$$U_R^{(n)}(\mathbf{r}, \mathbf{r}') = \sum_{l=0}^{\infty} \sum_{m=-l}^l [U_R^{(n)}]_{l}(r, r') Y_{lm}(\hat{\mathbf{r}}) Y_{lm}^*(\hat{\mathbf{r}}'), \quad (4.141)$$

while the function ψ , which is either $\psi_\infty^{(n)}$ or ψ_n , is expanded as

$$\psi(\mathbf{r}) = \sum_{l=0}^{\infty} \sum_{m=-l}^l [\psi]_{lm}(r) Y_{lm}(\hat{\mathbf{r}}). \quad (4.142)$$

For any angular momentum channel (l, m) , this leads to the radial Schrödinger equation

$$\frac{1}{m} \left(\frac{d^2}{dr^2} + \frac{2}{r} \frac{d}{dr} - \frac{l(l+1)}{r^2} + q_n^2 \right) [\psi]_{lm}(r) = \int_0^R dr' r'^2 [U_R^{(n)}]_{l}(r, r') [\psi]_{lm}(r'), \quad (4.143)$$

valid at least for $r < \frac{L}{2}$.

It may seem surprising that the functions ψ_n satisfy uncoupled radial Schrödinger equations while the angular momentum is not conserved in finite volume. However, remember that the Schrödinger equation (4.128) for ψ_n is only valid up to corrections decaying exponentially with the volume. It would be exact if we replaced $U^{(n)}$ by a kernel defined from the finite-volume Bethe-Salpeter kernel K_L using sums over momenta in Λ instead of integrals for loops, Fourier transforms, etc. This kernel would only transform covariantly under the cubic symmetry and therefore it would mix the different angular momentum components of ψ_n in the Schrödinger equation. We deduce that these mixings decay exponentially with the volume and may be neglected. This is in stark contrast with the finite-size formula (4.129) for which the mixing of the angular momentum channels in finite volume is essential.

If the function $[\psi]_{lm}$ is analytic at r and its Taylor expansion around r has a radius of convergence larger than R , the right-hand side of the radial Schrödinger equation can be shown¹⁴ to read

$$\int_0^R dr' r'^2 [U_R^{(n)}]_{l}(r, r') [\psi]_{lm}(r') = \sum_{j=0}^{\infty} V_{l,j}^{(n)}(r) \left(\frac{1}{m} \partial_r \right)^j [\psi]_{lm}(r), \quad (4.144)$$

where the series converges absolutely and the functions $V_{l,j}$ are given by

$$V_{l,j}(r) = \frac{m^j}{j!} \int_0^R dr' (r - r')^j r'^2 [U_R]_{l}(r, r'), \quad (4.145)$$

with the usual superscript $^{(n)}$ to denote that they are taken at the energy W_n . We use the derivative $(\frac{1}{m} \partial_r)^j$ so that the functions $V_{l,j}$ all have the dimension of an energy.

¹⁴ Using the compact support of U_R , the Fourier transform of $g(r - r') = r'^2 [U_R^{(n)}]_{l}(r, r')$ is entire and its expression as a power series can be used to obtain the derivatives of $[\psi]_{lm}$.

Since $[U_R^{(n)}]_l$ is smooth, the functions $[\psi]_{lm}$ are also smooth by elliptic regularity but they may not be analytic, let alone have a large radius of convergence. However, if we set an arbitrary UV momentum cutoff¹⁵, i.e. make their Fourier transform compactly supported, the functions $[\psi]_{lm}$ become entire and the expansion (4.144) holds. Another way to have a well-defined expansion is if the kernel $[U_R^{(n)}]_l(r, r')$ has some particular decay properties in $|r - r'|$. For example if $[U_R^{(n)}]_l(r, r') \propto \delta(r - r')$, the functions $V_{l,j}^{(n)}$ vanish for $j > 0$ and expansion is a finite sum. Either way, we will assume in the following that the expansion converges absolutely.

Due to Theorem 4.1, the functions $[U_R^{(n)}]_l$ and therefore $V_{l,j}$ are analytic in the energy region $0 \leq \text{Re } W < 4m$. It follows that the coefficients $V_{l,j}(r)$ seen as functions of real W are equal to their Taylor series around $W = 2m$ in the open interval $I_{\text{el}} =]0, 4m[$ ¹⁶. For any finite-volume eigenenergy W_n in I_{el} , the following expansion converges absolutely

$$\int_0^R dr' r'^2 [U_R^{(n)}]_l(r, r') [\psi]_{lm}(r') = \sum_{j=0}^{\infty} \sum_{k=0}^{\infty} V_{l,j,k}(r) \left(\frac{W_n}{2m} - 1\right)^k \left(\frac{1}{m} \partial_r\right)^j [\psi]_{lm}(r), \quad (4.146)$$

where the functions $V_{l,j,k}$ defined by

$$V_{l,j,k}(r) = \frac{(2m)^k}{k!} \partial_W^k V_{l,j}(r)|_{W=2m}, \quad (4.147)$$

are again scaled to have the dimension of an energy.

Note how the coefficients $V_{l,j,k}(r)$ have no superscript (n) in the previous equation since they are energy-independent. The energy dependence is now made completely explicit in the terms $\left(\frac{W_n}{2m} - 1\right)^k$. While that equation is satisfied by the functions $[\psi_n]_{lm}$ at energies W_n in the intersection of the finite-size spectrum and I_{el} (a finite set), it is also satisfied with the same set of coefficients $V_{l,j,k}(r)$ by the infinite-volume functions $[\psi_\infty]_{lm}$ at *all* energies W in I_{el} , replacing W_n by W , q_n by $\sqrt{m\mathcal{E}(W)}$ and ψ by ψ_∞ .

Since the expansion (4.146) converges absolutely, it can be approximated by truncation. In other terms, the radial Schrödinger equation for $[\psi]_{lm}$ at an energy W_n in the interval I_{el} reads

$$\frac{1}{m} \left(\frac{d^2}{dr^2} + \frac{2}{r} \frac{d}{dr} - \frac{l(l+1)}{r^2} + q_n^2 \right) [\psi]_{lm}(r) \simeq \sum_{j=0}^{N_j} \sum_{k=0}^{N_k} V_{l,j,k}(r) \left(\frac{W_n}{2m} - 1\right)^k \left(\frac{1}{m} \partial_r\right)^j [\psi]_{lm}(r), \quad (4.148)$$

for large N_j, N_k and as usual large box size L . This truncation is simple but may not have the optimal convergence rate.

In general, consider any basis $\{\Theta^b\}_{b=1,2,\dots}$ of the set of vectors indexed by \mathbb{N}^2 . Denote their components $\Theta_{j,k}^b$ where $(j, k) \in \mathbb{N}^2$. At fixed r and l , the coefficients $V_{l,j,k}(r)$ can be seen as the components of a vector and therefore expanded as

$$V_{l,j,k}(r) = \sum_{b=1}^{\infty} \Theta_{j,k}^b V_l^b(r), \quad (4.149)$$

for some functions $V_l^b(r)$. This relation is invertible so that the knowledge of all the coefficients $V_{l,j,k}(r)$ or all the coefficients $V_l^b(r)$ is equivalent. If the vectors Θ^b all have

¹⁵ Lattice simulations will naturally set a UV cutoff.

¹⁶ We can also consider the Taylor series around any real energy $W_* \in [0, 4m[$ which would converge in the interval $I_* =]W_* - \delta_W, W_* + \delta_W[$ where $\delta_W = \min(W_*, 4m - W_*)$. The choice of $W_* = 2m$ will be the most useful for computations.

a finite number of non-zero components, each choice of basis leads to a sequence of truncations

$$\begin{aligned} \frac{1}{m} \left(\frac{d^2}{dr^2} + \frac{2}{r} \frac{d}{dr} - \frac{l(l+1)}{r^2} + q_n^2 \right) [\psi]_{lm}(r) \\ \simeq \sum_{b=1}^B V_l^b(r) \sum_{j=0}^{\infty} \sum_{k=0}^{\infty} \Theta_{j,k}^b \left(\frac{W_n}{2m} - 1 \right)^k \left(\frac{1}{m} \partial_r \right)^j [\psi]_{lm}(r), \end{aligned} \quad (4.150)$$

such that we recover the radial Schrödinger equation (4.143) as $B \rightarrow \infty$. The previous truncation (4.148) is the particular choice of $B = (N_j + 1)(N_k + 1)$ and $\Theta_{j',k'}^{j+(N_j+1)k} = \delta_{j,j'} \delta_{k,k'}$.

Kernel computation

As discussed previously, the functions ψ_n can be evaluated by lattice simulations. Select a certain number of finite-volume operators \mathcal{O}_i ($i = 1, \dots, N_{\text{src}}$), not necessarily in the form described by (4.91). Discretizing the finite-volume theory on a regular lattice with spacing a (where $L \in a\mathbb{N}$), one may compute the correlators

$$\Psi_{\mathbf{r},i}(t) \equiv e^{2mt} \frac{1}{L^3} \sum_{\mathbf{x}} \langle \phi(\mathbf{x} + \mathbf{r}, t) \phi(\mathbf{x}, t) \mathcal{O}_i^\dagger \rangle_a. \quad (4.151)$$

where $i = 1, \dots, N_{\text{src}}$ and the brackets $\langle \dots \rangle_a$ denote the Euclidean correlation functions in the discretized theory. The index \mathbf{r} and the sum on \mathbf{x} are over the grid positions $a\mathbb{Z}^3 \cap [-\frac{L}{2}, \frac{L}{2}]$ while the Euclidean time t may be discretized with another spacing proportional to a . The factor e^{2mt} will be useful later.

These correlators have the usual expansion over the eigenstates with energies W_n^a of the Hamiltonian of the discretized theory

$$\Psi_{\mathbf{r},i}(t) = \sum_{n \geq 1} \psi_n^a(\mathbf{r}) A_{n,i} e^{-(W_n^a - 2m)t}, \quad (4.152)$$

for some coefficients $A_{n,i}$ and where $\psi_n^a(\mathbf{r})$ and W_n^a have the limit

$$\lim_{\substack{a \rightarrow 0 \\ \mathbf{r} \in a\mathbb{Z}^3}} \psi_n^a(\mathbf{r}) = \psi_n(\mathbf{r}), \quad \lim_{a \rightarrow 0} W_n^a = W_n. \quad (4.153)$$

The correlators $\Psi_{\mathbf{r},i}(t)$ are defined for \mathbf{r} on the discrete lattice. They can be interpolated linearly in \mathbf{r} on the whole ball $B(0, \frac{L}{2})$, projected on specific angular momenta channels (l, m) then convolved with a normalized gaussian function with width of the order of a . The resulting correlators are denoted $\Psi_{lm,i}(r, t)$ and can be expressed as

$$\Psi_{lm,i}(r, t) = \sum_{n \geq 1} [\psi_n^a]_{lm}(r) A_{n,i} e^{-(W_n^a - 2m)t}, \quad (4.154)$$

where $r \in [0, \frac{L}{2}[$ is continuous (but t is discretized) and we have the limits

$$\lim_{a \rightarrow 0} \partial_r^j [\psi_n^a]_{lm}(r) = \partial_r^j [\psi_n]_{lm}(r), \quad (4.155)$$

for any $j \geq 0$. The asymptotic rate of convergence is linear with a practical convergence rate expected to be the slowest at small r (compared to L) and/or large angular momenta

l. We take the convolution with a gaussian so that the functions $[\psi_n^a]_{lm}(r)$ and $\Psi_{lm,i}(r, t)$ are smooth in r and the limit above also holds for the derivatives.

With a large number N_{src} of operators and correlators evaluated at large times t , one can use the variational method to extract the functions $[\psi_n^a]_{lm}(r)$ for a certain set $n \in \mathcal{N}$. For some B such that there are at least B eigenenergies in $\{W_n\}_{n \in \mathcal{N}} \cap I_{\text{el}}$, plug $[\psi_n^a]_{lm}(r)$ at these energies in the truncated radial Schrödinger equation (4.150) to obtain the coefficients $V_l^a(r)$ ¹⁷ up to linear corrections in the lattice spacing, exponentially decaying correction in the box size L and additional corrections due to the truncation. Solving the same Schrödinger equation for any energy in the interval I_{el} leads to solutions proportional to $[\psi_\infty]_{lm}$ which can be used to extract the scattering phase shifts at these energies from the asymptotic behavior (4.79), up to the same order of corrections as described for $V_{l,j,k}(r)$. These corrections vanish as we take $a \rightarrow 0$, $L \rightarrow \infty$ and $B \rightarrow \infty$.

The previous paragraph describes an ideal scenario which is unfortunately unattainable with limited computational resources. In practice, only a few eigenenergies above the ground state may have a decent signal-to-noise ratio and it can be difficult to separate their contributions in the case of a dense finite-size spectrum. Separate the contributions of the inelastic states as

$$\Psi_{lm,i}(r, t) = \sum_{W_n \in I_{\text{el}}} [\psi_n^a]_{lm}(r) A_{n,i} e^{-(W_n^a - 2m)t} + O(e^{-2mt}). \quad (4.156)$$

It is then easy to show that the equation

$$\begin{aligned} & \frac{1}{m} \left(\partial_r^2 + \frac{2}{r} \partial_r - \frac{l(l+1)}{r^2} - \partial_t + \frac{1}{4m} \partial_t^2 \right) \Psi_{lm,i}(r, t) \\ &= \sum_{b=1}^{\infty} \left(\sum_{j=0}^{\infty} \sum_{k=0}^{\infty} \Theta_{j,k}^b \frac{1}{(-2)^k} \frac{1}{m^{j+k}} \partial_t^k \partial_r^j \Psi_{lm,i}(r, t) \right) V_l^b(r) + O(e^{-2mt}), \end{aligned} \quad (4.157)$$

holds up to additional corrections linear in a and exponential in L . At this stage, ∂_t is discretized but not ∂_r since the spatial dependence has already been interpolated.

Suppose that the correlators can be evaluated at times t large enough that the $O(e^{-2mt})$ contributions of the inelastic eigenstates are negligible. The number of finite-volume eigenenergies in the interval I_{el} grows to infinity with L . At finite L suppose that there are at least B such energies. Then choose B arbitrary operators \mathcal{O}_i with linearly independent mixing with the eigenstates corresponding to energies in I_{el} . After truncation of the sum on b , the coefficients $V_l^b(r)$ for $b = 1, \dots, B$ can be approximated by inverting (4.157). These coefficients can be used as previously to approximate the scattering phase shifts at any energy in I_{el} .

Discussion

In practice, it may not be possible to neglect the contribution of the inelastic eigenstates with energies $W_n \geq 4m$. The variational method can be used to face this issue. In the first formulation of this method, we used the fact that the variational method can theoretically be used to extract the contribution of a single eigenstate. This is how the variational method is usually used and it becomes challenging as the volume increases. In the second formulation, we only need to use the variational method to remove as much as possible the contribution of eigenstates with energies $W_n \geq 4m$, for example by adding some operators which couple with these unwanted states.

¹⁷ These coefficients are then the solution of a linear system at each r .

Consider the system of two pions in the isospin $I = 1$ channel at the physical point. The first energy levels are pion-pion scattering states and there are higher energy levels corresponding to the rho resonance. By adding rho-like operators in the variational basis, one can obtain “clean” pion-pion operators with negligible mixing with the rho states. However, there is no need to fine tune the pion-pion operators to mix with exactly one eigenstate as is usually required to extract the associated eigenenergy which will be used in the finite-size formula. At large L where the energies of the pion-pion scattering states are very close, the improvement can be significant. Of course, the focus would be on the elastic scattering and not the properties of the resonance.

Similarly as the variational method, for which one can check the validity of the extracted eigenenergies by the appearance of a plateau, the coefficients $V_{l,j,k}(r)$ should also exhibit a plateau in some time range. Another available test is to check the dependence on the truncation B or the choice of basis. Finally, if the extraction of specific eigenstates by variational method is amenable, one can check that the scattering phase shifts agree at the energies of the finite-size spectrum using the finite-size formula. If these tests pass, one can gain confidence in the value of the scattering phase shifts obtained in the range $[2m, W_{\max}]$ where W_{\max} is the energy of the highest eigenstate which contribute significantly to the correlators. Indeed, at higher energies, the contributions of the truncated terms may become more important.

In summary, the kernel approximation method has two main advantages, in its area of application, compared to the finite-size formula,

- i) there is no need to separate the contribution of each single eigenstates using the variational method, only to “clean” the operators sufficiently from the contribution of the inelastic eigenstates,
- ii) it provides an approximation of the scattering phase shifts in the whole region I_{el} , which converges as $B \rightarrow \infty$ ¹⁸.

¹⁸ Technically, this limit corresponds to $L \rightarrow \infty$ so that the finite-size spectrum would become dense in I_{el} anyway. However, not only would it be impossible to separate the contribution of each eigenstate by the variational method in this limit but we may expect that moderate B are sufficient to obtain the scattering phase shifts at a certain degree of precision.

Numerical applications

5.1 COMPARING THE METHODS IN THE TWO-PION $I = 2$ CHANNEL

The system of two pions in the isospin $I = 2$ channel is arguably the simplest and less computationally expensive to study scattering process in lattice QCD. For this reason, it has been widely investigated (see e.g. ref. [30, 41, 42]) and is the system of choice to serve as the test-bed of new methods. In this section we will present simulation results for the study of this system using the various methods discussed so far in order to analyze the correctness and efficiency of each method.

5.1.1 Simulations details

We have performed simulations of the $I = 2$ $\pi\pi$ channel in full lattice QCD. Our calculations are based on $N_f = 2 + 1$ QCD gauge configurations generated by the PACS-CS collaboration [43] on a $32^3 \times 64$ lattice using the Iwasaki gauge action at $\beta = 1.9$ and clover fermions. The associated lattice spacing is $a = 0.0907$ fm and the sea quark hopping parameters are $\kappa_{ud} = 0.1370$ and $\kappa_s = 0.1364$, making for a pion mass of $m = 0.32242(65) a^{-1}$, or $m = 0.7$ GeV.

We use momentum-wall source fields for all the methods, i.e.

$$\mathcal{S}_j^\dagger(t) = [\bar{u}_w(\mathbf{q}_j, t) \gamma_5 d_w(\mathbf{0}, t)] [\bar{u}_w(-\mathbf{q}_j, t) \gamma_5 d_w(\mathbf{0}, t)] \quad (5.1)$$

at the Euclidean time t , where the momentum-wall quarks are defined from the quark fields as

$$\bar{u}_w(\mathbf{q}_j, t) = \sum_{\mathbf{x}} e^{-i\mathbf{q}_j \cdot \mathbf{x}} \bar{u}(\mathbf{x}, t). \quad (5.2)$$

We use 5 momenta, chosen as $\mathbf{q}_1 = \mathbf{0}$, $\mathbf{q}_2 = (0, 0, q)$, $\mathbf{q}_3 = (0, q, q)$, $\mathbf{q}_4 = (q, q, q)$ and $\mathbf{q}_5 = (0, 0, 2q)$, with $q = \frac{2\pi}{L}$.

For the HAL QCD, effective potential and kernel approximation method, we use local pion fields with fixed separation as sink fields

$$\mathcal{O}_r^{\text{wf}} = \frac{1}{48} \sum_{R \in \mathcal{O}_h} \sum_{\mathbf{x}} [u \gamma_5 \vec{d}] (\mathbf{x}) [u \gamma_5 \vec{d}] (\mathbf{x} + R \cdot \mathbf{r}) \quad (5.3)$$

where the lattice sites \mathbf{x} and \mathbf{r} run over one periodicity cell. The first sum is on the rotations R of the cubic group \mathcal{O}_h and serves as a projection on the A_1^+ irreducible representation. The sink operators for the variational method are then constructed by projecting the previous fields on momenta \mathbf{q}_i ,

$$\mathcal{O}_i^{\text{var}} = \sum_{\mathbf{r}_k} e^{-i\mathbf{q}_i \cdot \mathbf{r}_k} \mathcal{O}_k^{\text{wf}}, \quad (5.4)$$

which are chosen similarly as for the source fields.

5.1.2 HAL QCD method

We use the time-dependent HAL QCD method described in section 3.3.2. The starting point is the evaluation of the following correlators on the lattice

$$R_i(\mathbf{r}, t) \equiv e^{2mt} \langle \mathcal{O}_{\mathbf{r}}^{\text{wf}}(t) \mathcal{S}_i^\dagger(0) \rangle, \quad (5.5)$$

where the index i refers to source operator used in the correlator. We show in fig. 5.1 some of these correlators. As expected, they take contributions at small times t from the BS wave functions $\psi_{L,n}$ of the energy eigenstates $|n\rangle$, cf. (3.98), in such a way that their shapes somehow resemble their free values (the projection of $\cos(\frac{2\pi}{L} \mathbf{q}_i \cdot \mathbf{r})$ on A_1^+ for R_i). At large t , the contribution of the ground state dominates so that the shape of the correlators becomes independent of the source operator (here indexed by i). We see that this ground state saturation is more or less complete by $t = 25$ for all our sources but $i = 1$.

Assuming Hermiticity, rotational invariance and time-reversal invariance of the potential U_{HAL} for a system of two mesons, it can be expressed as

$$U_{\text{HAL}}(\mathbf{r}, \mathbf{r}') = V(r, \mathbf{v}^2, \mathbf{L}^2) \delta(\mathbf{r} - \mathbf{r}'), \quad (5.6)$$

for some function V , where $\mathbf{v} = 2\mathbf{p}/m$, $\mathbf{L} = \mathbf{r} \times \mathbf{p}$ and $\mathbf{p} = -i\nabla$ are differential operators. The velocity expansion at the next-to-leading order then reads

$$U_{\text{HAL}}(\mathbf{r}, \mathbf{r}') = \left[V_0(\mathbf{r}) + \frac{1}{2} \{V_{v^2}(\mathbf{r}), \mathbf{v}^2\} + V_{l^2}(\mathbf{r}) \mathbf{L}^2 + O(\mathbf{v}^4) \right] \delta(\mathbf{r} - \mathbf{r}'), \quad (5.7)$$

where $O(\mathbf{v}^4)$ is to be understood as a decaying behavior when the potential is applied to functions varying asymptotically slowly.

In order to analyze the validity of the velocity expansion, we show in fig. 5.2 the effect of the operators \mathbf{L}^2 and \mathbf{v}^2 on the correlators R_i at $t = 12$ for $i = 0$ to 4. The functions $\mathbf{v}^2 R_i$ are seen to be large, compared to R_i , and almost radial at small radii while the functions $\mathbf{L}^2 R_i$ are negligible up to $r \gtrsim 0.8$ fm then become large and highly multi-valued in the radial direction. The effect of \mathbf{L}^2 is as expected since the correlators R_i transforming as the A_1^+ representation of the cubic group contains angular momentum components $l = 0, l = 4, l = 6$ and above. The application of \mathbf{L}^2 makes the $l = 0$ component vanish while the $l \geq 4$ components, suppressed at small radii by the centrifugal effect, are enhanced.

As we will see, the range of the interaction at the energies considered here is $r \simeq 0.8$ fm. The functions $\mathbf{L}^2 R_i$ have a very small signal-to-noise ratio in the interacting region so that the \mathbf{L}^2 dependence of V cannot be extracted reliably from our simulations. However, this \mathbf{L}^2 dependence of V is expected to be much less relevant than its \mathbf{v}^2 dependence when applied on the correlators R_i , for the very same reason. We are thus lead to analyze the expansion

$$U_{\text{HAL}}(\mathbf{r}, \mathbf{r}') = \left[V_0(\mathbf{r}) + \frac{1}{2} \{V_{v^2}(\mathbf{r}), \mathbf{v}^2\} + \frac{1}{2} \{V_{v^4}(\mathbf{r}), \mathbf{v}^4\} + O(\mathbf{L}^2) + O(\mathbf{v}^4) \right] \delta(\mathbf{r} - \mathbf{r}'), \quad (5.8)$$

which would be reasonable for functions with the features of the correlators R_i described above.

We plot in fig. 5.3 (left) the function $\mathbf{v}^4 R_0$ and $t = 12$. Contrary to expectations, it is much larger than R_0 and seems less regular than $\mathbf{v}^2 R_i$. Looking at fig. 5.3

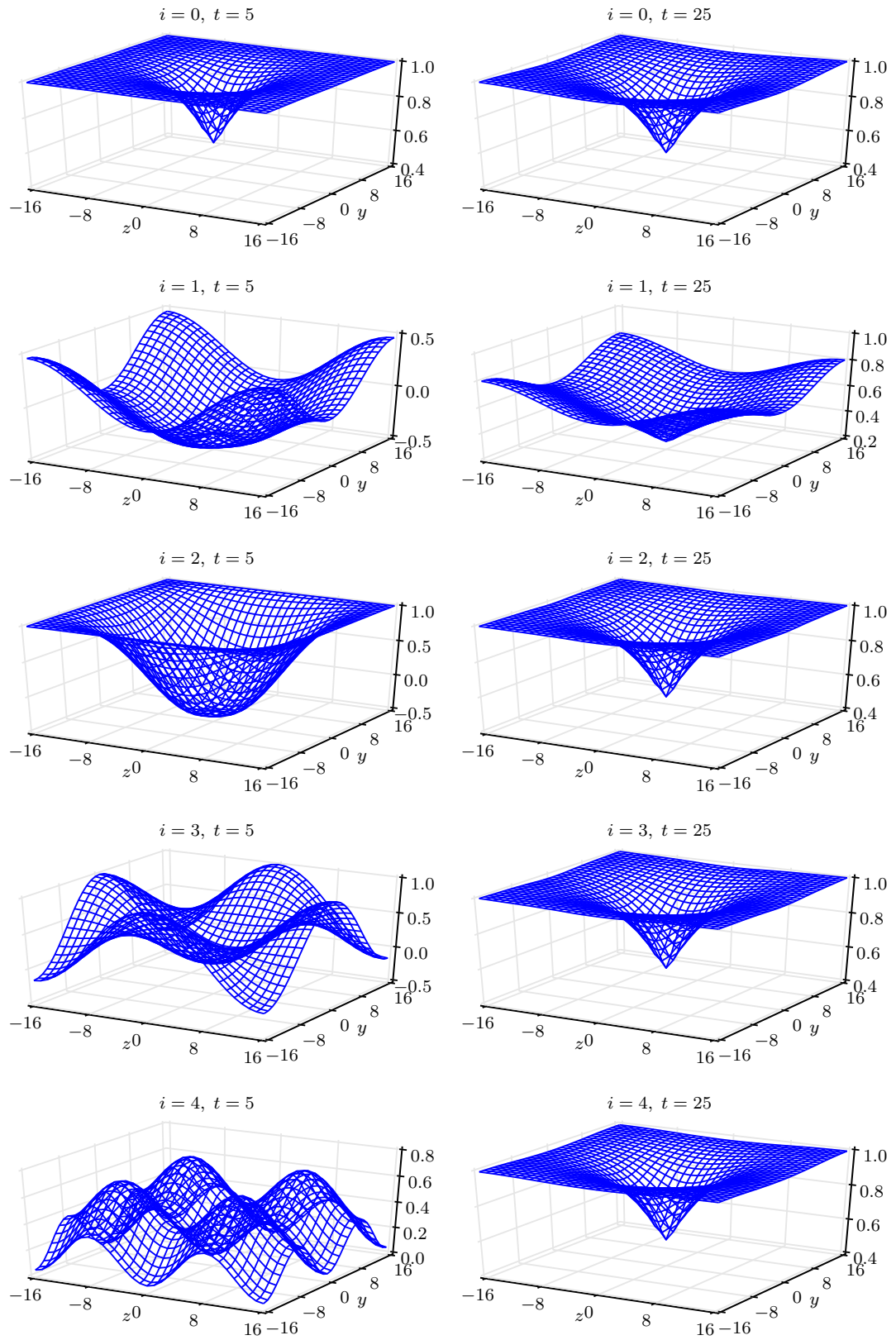


Figure 5.1: In the $(i + 1)$ -th row from the top, the correlators $R_i(\mathbf{r}, t)$, normalized by their global maximum value, are shown in the plane $x = 0$ at the times $t = 5$ (left) and $t = 25$ (right).

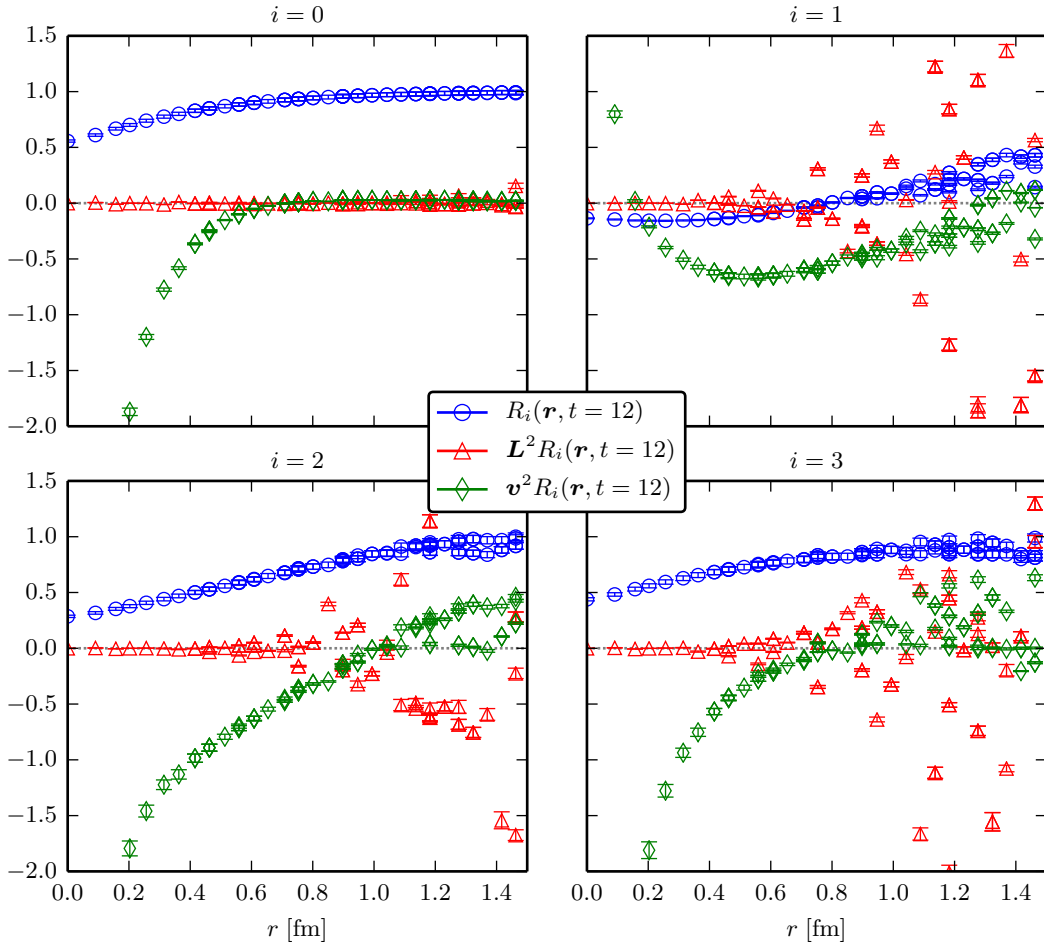


Figure 5.2: The correlators R_i at $t = 12$ for $i = 0$ to 4 and the effect of the operators v^2 and L^2 on them. The normalization of R_i is the same as in fig. 5.1.

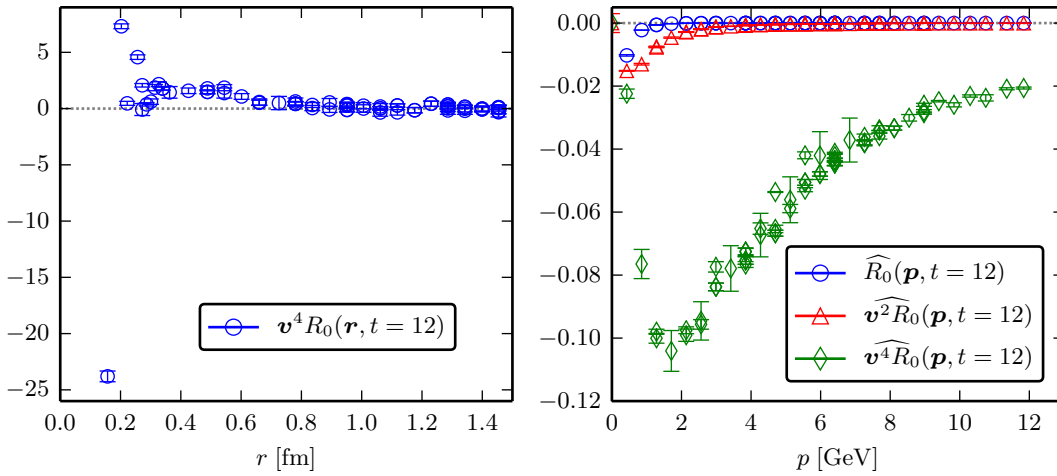


Figure 5.3: (Left) effect of v^4 on the correlator R_0 at $t = 12$. (Right) the Fourier transform of $v^{2k} R_0$ at $t = 12$ for $k = 0, 1, 2$. The normalization of R_0 is the same as in fig. 5.1.

(right), this can be explained directly by the lattice discretization effect. We see that R_0 and $\mathbf{v}^2 R_0$ contain contributions for momenta mostly below 1 GeV and 3 GeV respectively. However, $\mathbf{v}^4 R_0$ takes sizeable contributions for momenta up to the lattice cutoff $\frac{2\pi}{a} \sim 12$ GeV and therefore cannot be reliably used without reducing the lattice spacing a . The same remarks stand for $\mathbf{v}^4 R_i$ with different sources i .

Given the previous discussion, we will consider the following approximations of the potential U_{HAL} ,

$$U_{\text{HAL}}(\mathbf{r}, \mathbf{r}') \simeq V_0(\mathbf{r})\delta(\mathbf{r} - \mathbf{r}'), \quad (5.9)$$

at the leading order (LO) and

$$U_{\text{HAL}}(\mathbf{r}, \mathbf{r}') \simeq \left[V_0(\mathbf{r}) + \frac{1}{2}\{V_{v^2}(\mathbf{r}), \mathbf{v}^2\} \right] \delta(\mathbf{r} - \mathbf{r}'), \quad (5.10)$$

at the next-to-leading order (NLO). Remember that these approximations are only expected to be valid when the potential is applied to the correlators R_i or functions with similar features.

For $i = 0, \dots, 4$ define the functions

$$V_A^i(\mathbf{r}, t) \equiv \frac{1}{R_i(\mathbf{r}, t)} \left(\frac{1}{4m} \frac{\partial^2}{\partial t^2} - \frac{\partial}{\partial t} + \frac{\Delta}{m} \right) R_i(\mathbf{r}, t). \quad (5.11)$$

Using the Schrödinger equation (3.113), the LO approximation is equivalent to

$$V_0(r) \simeq V_A^i(\mathbf{r}, t), \quad (5.12)$$

for any source i provided that the contribution of the inelastic eigenstates are negligible at the time t . The previous analysis of the correlators shows that only the two lowest energy eigenstates are non-negligible at $t = 25$. Looking at more time slices, it seems reasonable to neglect the contribution of the inelastic eigenstates at times $t \gtrsim 10$.

Fig. 5.4 presents the leading order (LO) potentials $V_A^i(\mathbf{r}, t)$ for our 5 sources at times $t = 12$ and $t = 25$. Projected in the radial direction, these are multi-valued functions. At $t = 12$, we can see that they coincide completely for $i = 0$, $i = 3$ and $i = 4$. The ground state saturation can be considered complete at $t = 12$ for the source $i = 0$ but not for $i = 3$ and $i = 4$ where the third and fourth excited states still contribute as we will see in the discussion of the variational method. The agreement between these three leading order potentials is therefore encouraging. The same can be said for the sources $i = 2$ at $t = 12$ and $i = 1$ at $t = 25$. In both cases (as can be seen in fig. 5.1 for the latter), the correlators are still far from achieving a complete ground state saturation but the leading order potentials are very close to their asymptotic values. The slight deviations can be the result of either the contributions of inelastic states or the truncation of the potential. As discussed previously we would incline for the latter so that this observation suggest that the truncation effects are rather small. The singularity of V_A^1 is due to the correlator $R_1(\mathbf{r}, t)$ crossing zero around $r = 0.8$ fm at $t = 12$, see fig. 5.2 (upper right).

For any pair of source indices $i_1 \neq i_2$, define the functions $V_A^{i_1, i_2}(\mathbf{r}, t)$ and $V_B^{i_1, i_2}(\mathbf{r}, t)$ as the solutions of the system

$$\left(\frac{1}{4m} \frac{\partial^2}{\partial t^2} - \frac{\partial}{\partial t} + \frac{\Delta}{m} \right) \cdot \begin{bmatrix} R_{i_1}(\mathbf{r}, t) \\ R_{i_2}(\mathbf{r}, t) \end{bmatrix} = \begin{bmatrix} R_{i_1}(\mathbf{r}, t) & \frac{1}{2}\mathbf{v}^2 R_{i_1}(\mathbf{r}, t) \\ R_{i_2}(\mathbf{r}, t) & \frac{1}{2}\mathbf{v}^2 R_{i_2}(\mathbf{r}, t) \end{bmatrix} \begin{bmatrix} V_A^{i_1, i_2}(\mathbf{r}, t) \\ V_B^{i_1, i_2}(\mathbf{r}, t) \end{bmatrix}, \quad (5.13)$$

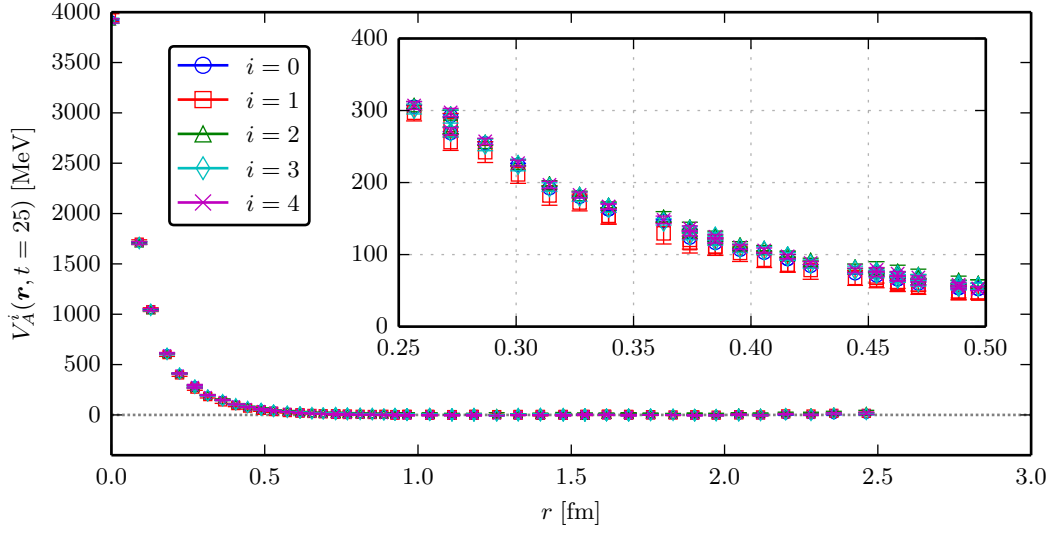
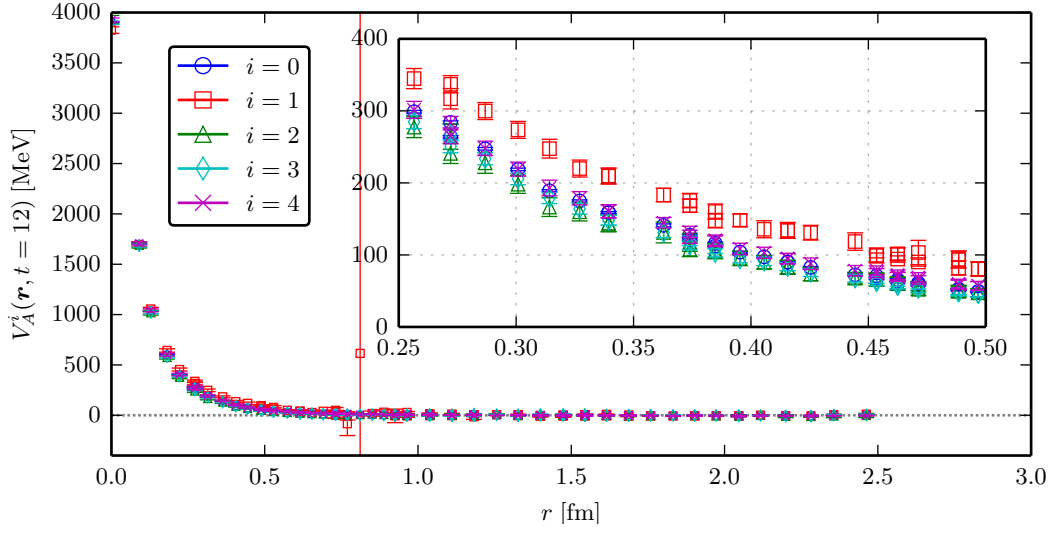


Figure 5.4: The LO potentials V_A^i computed for each source i separately at the times $t = 12$ (upper) and $t = 25$ (lower).

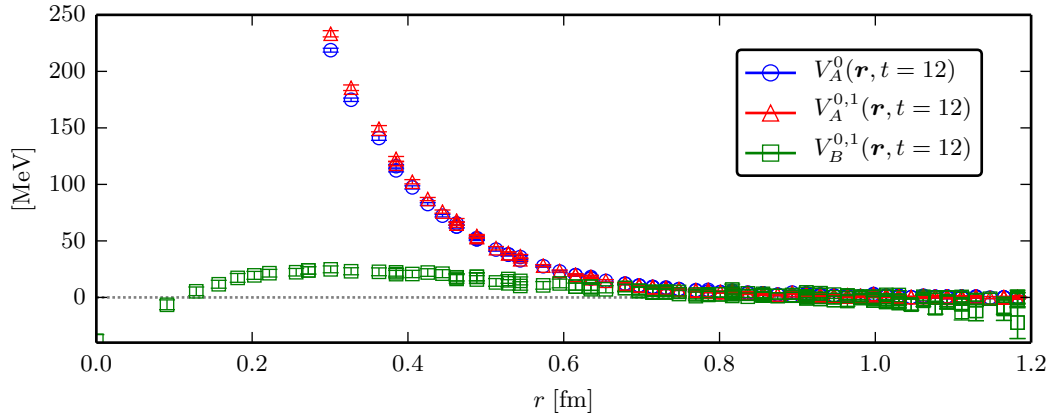


Figure 5.5: The components $V_A^{i_1, i_2}$ and $V_B^{i_1, i_2}$ of the NLO potential, at $t = 12$ for the choice of sources $(i_1, i_2) = (0, 1)$. The LO potential V_A^i computed from the source $i = 0$ is shown for comparison.

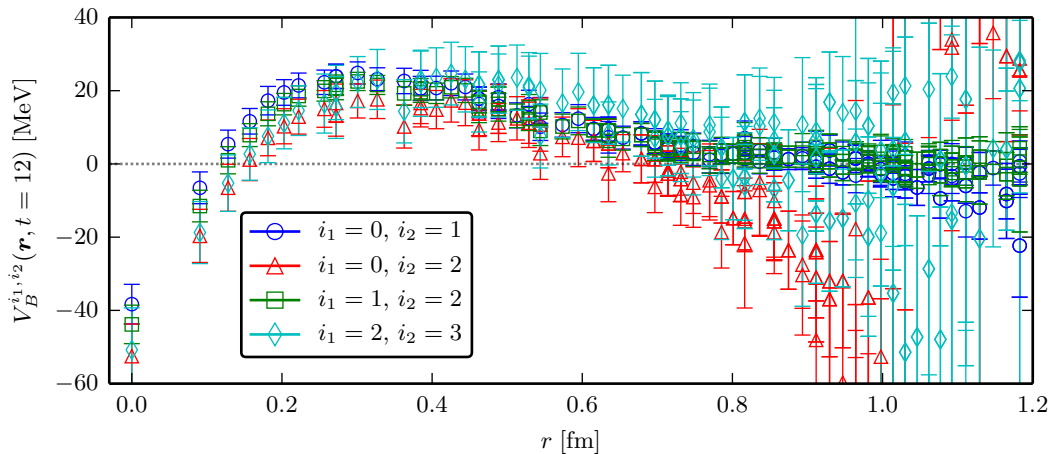


Figure 5.6: Comparison of the component $V_B^{i_1, i_2}$ of the NLO potential, at $t = 12$ for different choices of sources (i_1, i_2) .

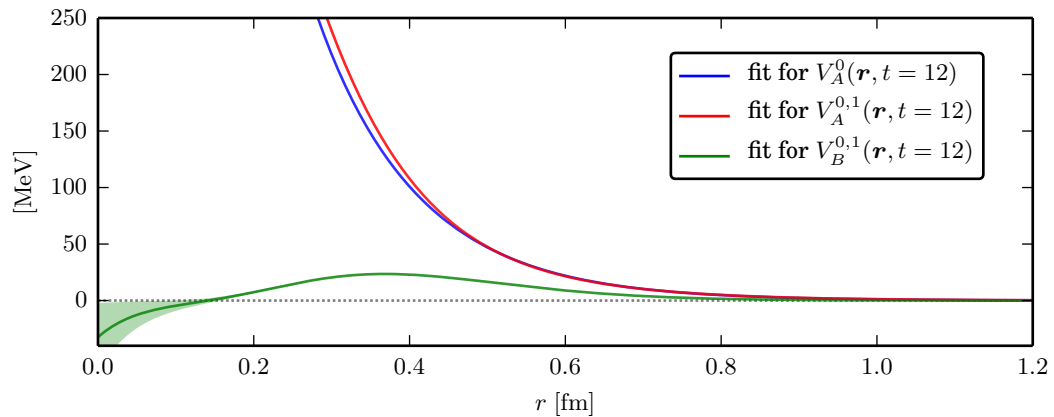


Figure 5.7: Fit functions for the components of the LO and NLO potentials corresponding to fig. 5.5. Bands at one standard deviation are shown for each fit function.

at all positions \mathbf{r} . Then, the Schrödinger equation (3.113) implies that the NLO approximation is equivalent to

$$V_0(r) \simeq V_A^{i_1, i_2}(\mathbf{r}, t) + \frac{1}{2} \mathbf{v}^2 V_B^{i_1, i_2}(\mathbf{r}, t), \quad V_{v_2}(r) \simeq V_B^{i_1, i_2}(\mathbf{r}, t), \quad (5.14)$$

at a time t where the inelastic states contributions are negligible.

Fig. 5.5 shows the functions $V_A^{i_1, i_2}$ and $V_B^{i_1, i_2}$ that we extract with the choice $(i_1, i_2) = (0, 1)$ and $t = 12$. We observe that $V_B^{i_1, i_2}$ is small and $V_A^{i_1, i_2}$ is close to the LO potential $V_0^{i_1}$. This is consistent with the fact that the truncation effects at the LO level were expected to be small from the previous discussion. To confirm this fact, we compute the NLO potential for several other choices (i_1, i_2) . The agreement of the results in fig. 5.6 is remarkable. Note that at the NLO, the fact that the correlator $R_1(\mathbf{r}, t = 12)$ crosses zero around $r = 0.8$ fm does not induce a singularity because $\mathbf{v}^2 R_1(\mathbf{r}, t = 12)$ is non-zero in this region.

We now fit the components of the potential by radial analytic functions. For the

components V_A^i and $V_A^{i_1, i_2}$, we use a sum of one Gaussian and two exponentials

$$f(r) = a_1 e^{-a_2 r^2} + a_3 e^{-a_4 r} + a_5 e^{-a_6 r}, \quad (5.15)$$

and for the component $V_B^{i_1, i_2}$, we use

$$f(r) = a_1 (r^{a_2} - a_3) e^{-a_4 r}, \quad (5.16)$$

as fit functions with parameters a_1, a_2, \dots . We show in fig 5.7 the results of the fits corresponding to the potentials previously shown in fig. 5.5.

We then solve the radial Schrödinger equation in infinite volume in the S-wave at any energy using the fit to the potentials obtained by lattice input. These potentials approximate U_{HAL} and therefore the solutions approximate the infinite-volume BS wave functions given the relation (3.105). An numerical estimation of the scattering phase can thus be extracted from the asymptotic behavior of the solutions. Using either the LO or the NLO potential, we obtain two estimations which we will present in fig. (5.9) along with the results of the kernel approximation method.

5.1.3 Kernel approximation method

The kernel approximation method is in practice quite similar to the HAL QCD method, with some advantages that we will see. It relies on the same correlators $R_i(\mathbf{r}, t)$, but projected on angular momentum channels as described in section 4.3.3. First, the correlators $R_i(\mathbf{r}, t)$, defined for discrete \mathbf{r} on the lattice, are interpolated linearly to obtain $R_i^{\text{lin}}(\mathbf{r}, t)$ defined for continuous \mathbf{r} in the ball $B(0, \frac{L}{2})$. Then, these interpolations are projected on the angular momentum channels by the spherical harmonics as

$$[R_i^{\text{lin}}]_{lm}(r, t) = \int d\hat{\mathbf{r}} Y_{lm}^*(\hat{\mathbf{r}}) R_i^{\text{lin}}(\mathbf{r}, t), \quad (5.17)$$

for $0 \leq r < \frac{L}{2}$. Finally, we use a convolution with a Gaussian function or its derivatives to obtain the following smooth radial functions

$$\partial_r^j [R_i]_{lm}(r, t) = \int_0^{\frac{L}{2}} dr' [R_i^{\text{lin}}]_{lm}(r - r', t) \frac{1}{\sqrt{2\pi}} \left[\frac{d}{dr'} \right]^j e^{-\frac{r'^2}{2\sigma}}, \quad (5.18)$$

for any $j \geq 0$, where the differentiation in the integral can be performed analytically.

An important difference with the HAL QCD method is that the existence of a rapidly-decaying, spherically symmetric potential which can be approximated by truncation is not assumed but proven. However, it is energy-dependent and may not satisfy Hermiticity and time-reversal invariance. Its general form is therefore

$$U(\mathbf{r}, \mathbf{r}') = V(r, \mathbf{r} \cdot \mathbf{v}, \mathbf{v}^2, \mathbf{L}^2, W - 2m_\pi) \delta(\mathbf{r} - \mathbf{r}'), \quad (5.19)$$

where the dependence in all the arguments of V but r can be expanded in a power series as seen in (4.148).

In this work, we are interested in the S-wave $(l, m) = (0, 0)$. The dependence of the potential in \mathbf{L}^2 is therefore irrelevant. As for the other dependences, the analysis made for the HAL QCD method suggests that an expansion of U similar to U_{HAL} is adequate. We therefore directly consider the NLO expression 5.10 for $U(\mathbf{r}, \mathbf{r}')$ and define the functions $\tilde{V}_A^{i_1, i_2}(r, t)$ and $\tilde{V}_B^{i_1, i_2}(r, t)$ by

$$\left(\frac{1}{4m} \frac{\partial^2}{\partial t^2} - \frac{\partial}{\partial t} + \frac{\Delta}{m} \right) \cdot \begin{pmatrix} [R_{i_1}]_{00}(r, t) \\ [R_{i_2}]_{00}(r, t) \end{pmatrix} = \begin{pmatrix} [R_{i_1}]_{00}(r, t) & \frac{1}{2} \mathbf{v}^2 [R_{i_1}]_{00}(r, t) \\ [R_{i_2}]_{00}(r, t) & \frac{1}{2} \mathbf{v}^2 [R_{i_2}]_{00}(r, t) \end{pmatrix} \begin{pmatrix} \tilde{V}_A^{i_1, i_2}(r, t) \\ \tilde{V}_B^{i_1, i_2}(r, t) \end{pmatrix}, \quad (5.20)$$

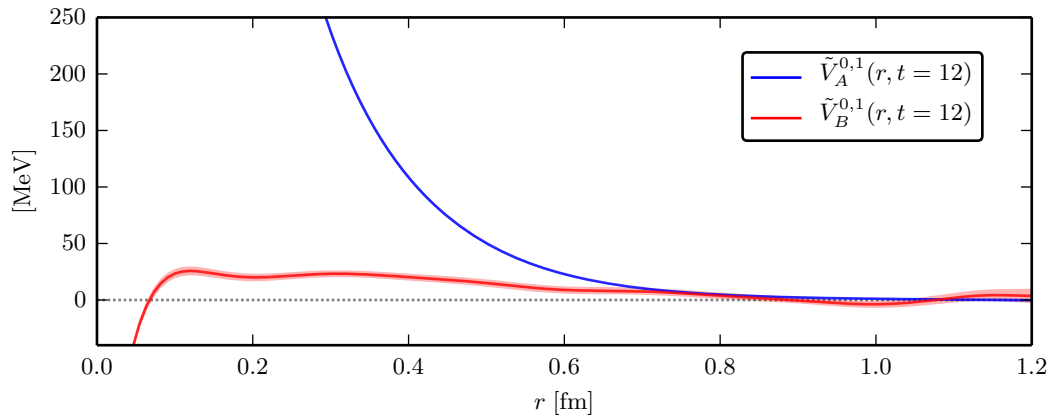


Figure 5.8: The components $\tilde{V}_A^{i_1, i_2}$ and $\tilde{V}_B^{i_1, i_2}$ of the potential obtained using the kernel approximation method, at $t = 12$ for the choice of sources $(i_1, i_2) = (0, 1)$. Bands at one standard deviation are shown for each component.

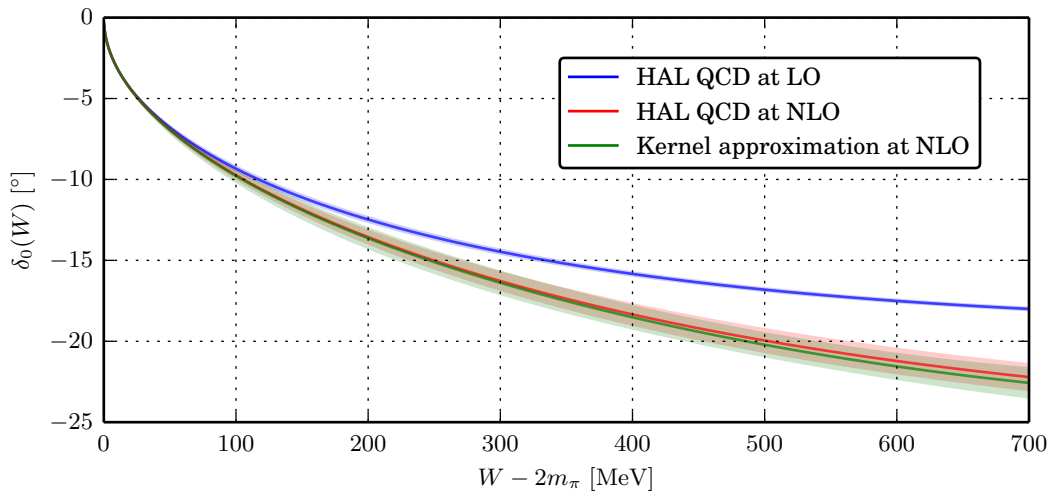


Figure 5.9: Comparison of the S-wave scattering phase shifts obtained with the HAL QCD method and the kernel approximation method. Corresponds to the potentials shown in fig. (5.7) and fig. (5.8) respectively.

for any pair of source indices (i_1, i_2) . We show in fig. 5.8 the results for $t = 12$ and $(i_1, i_2) = (0, 1)$. Note that the radial derivatives are computed using the convolution (5.18) and we chose $\sigma = 0.8a$.

Once the potential is extracted, we can solve the Schrödinger equation (4.70) to approximate the S-wave component of the infinite-volume functions ψ^∞ in the elastic region and consequently the scattering phase shifts from their asymptotic behavior. We show in fig. 5.9 a comparison of the scattering phase shifts obtained using the HAL QCD method and the kernel approximation method. As expected, the two methods give very close results at the NLO. Furthermore, the interaction is more attractive at the NLO than at the LO which is consistent with the sign of the NLO components V_B and \tilde{V}_B . We see that the NLO starts to deviate from the LO at around 150 MeV above the two-particle threshold.

Although the final results are quite similar for the current numerical application, it is important to stress the advantages of the kernel approximation method.

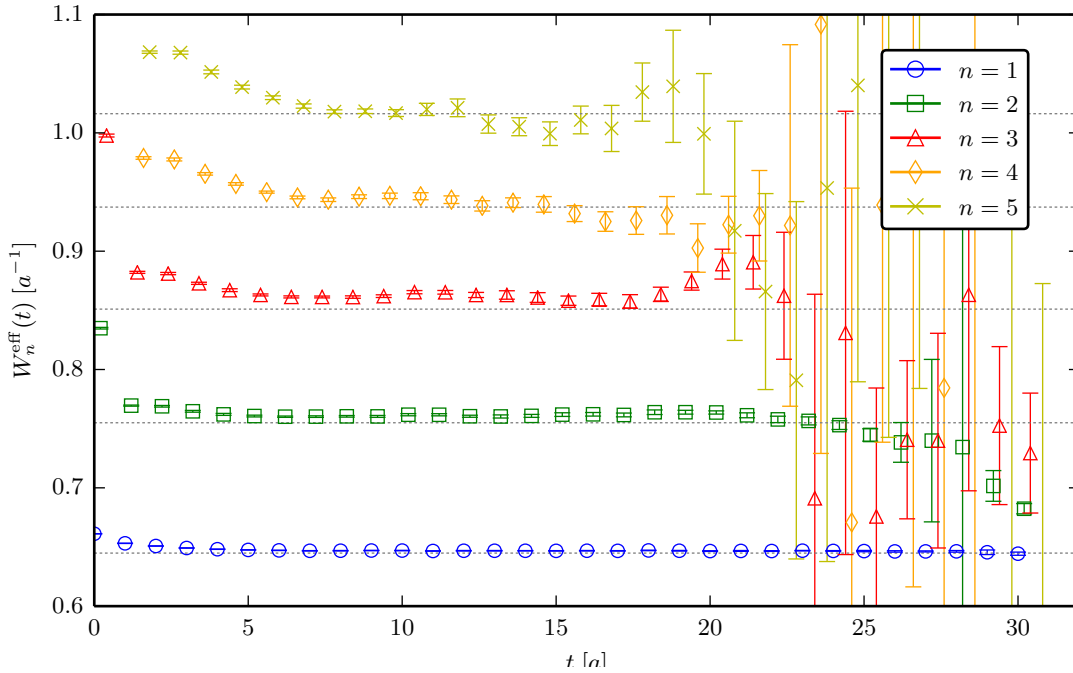


Figure 5.10: Effective energies obtained using the variational method at $N_{\text{src}} = 5$. The dashed lines show the location of the eigenenergies in the absence of interaction.

- i) In the HAL QCD method, the existence of an energy-independent potential is shown but the existence of an energy-dependent potential with Hermiticity, rotational invariance, time-reversal invariance and some analyticity properties is assumed. In the kernel approximation method, these properties are explicitly proven if we relax the energy-independence, Hermiticity, and time-reversal invariance requirements.
- i) By projecting on the partial waves, the kernel approximation method treats correctly the fact lattice correlators contain an infinity of angular momentum components due to the cubic symmetry of the lattice. This is not particularly relevant for correlators in the A_1^+ representation because the contributions for $l \geq 4$ are small but it can make an important difference for the study of the P- or D-waves.
- i) Because the correlators are interpolated to continuous radii, the kernel approximation method does not require the choice of fit functions for the potentials, thereby reducing systematic uncertainties. For example, the form (5.16) is motivated by the observed results but has no particular physical meaning.

5.1.4 Variational and effective potential methods

As discussed in section 2.3.2, the variational method is based on the computation of correlation matrices defined by

$$C_{ij}(t) = \langle \mathcal{O}_i^{\text{var}}(t) \mathcal{S}_j^\dagger(0) \rangle, \quad i, j = 1, \dots, N_{\text{src}}. \quad (5.21)$$

For the current calculations we use the $N_{\text{src}} = 5$ sources described in (5.4). By solving the generalized eigenvalue problem (2.64), some effective energies $W_n^{\text{eff}}(t)$ can be extracted, which converge towards the energies of the Hamiltonian eigenstates at large

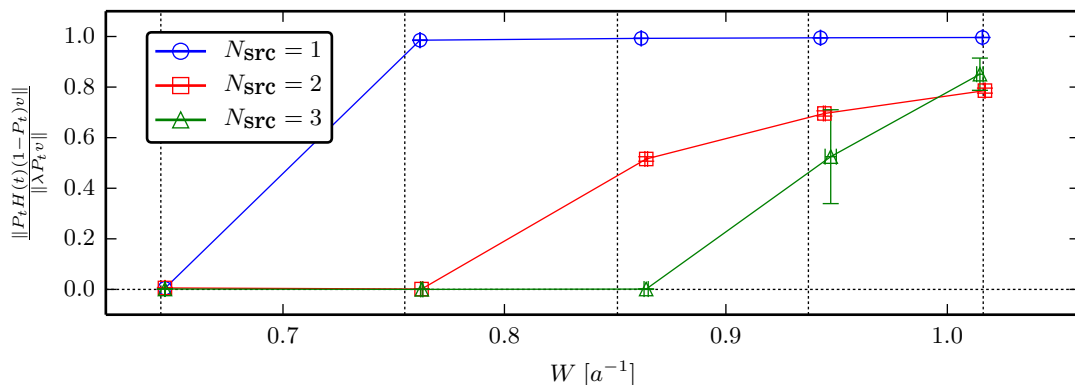


Figure 5.11: Left-hand side of the condition (4.39) corresponding the first 5 eigenvalues of the effective Hamiltonian in the effective potential method, depending on the number of sources. Vertical dashed lines show the location of the eigenenergies in the absence of interaction.

times t . Using the fixed difference $t - t_0 = 5$, the asymptotic behavior of the effective energies is given by (2.66). The results of our calculations are shown in fig. 5.10 for the first 5 eigenstates.

For the effective potential method, the starting point is again the correlators $R_i(\mathbf{r}, t)$ where \mathbf{r} runs over the lattice sites. However, instead of seeing these correlators as the discretization of functions in the continuum, they are seen as rectangular correlation matrices of size $(L/a)^3 \times N_{\text{src}}$ with indices \mathbf{r} and i . Then, an effective Hamiltonian is constructed which satisfies eq. (4.49). As was proven in section 4.2, this implies that some of its eigenvalues approximate the eigenenergies with the asymptotic behavior (4.48). These eigenvalues can be identified by the condition (4.39). We use the construction of the effective Hamiltonian as described in appendix A.3.2. The effective Hamiltonian is then moderately non-local but not Hermitian. The effective potential is set to zero at distances greater than $aN_s/2$ from the origin and the non-locality cutoff R_{max} is set to 0, 1 and $\sqrt{2}$ for $N_{\text{src}} = 1, 2$ and 3 respectively.

For the variational method, exactly N_{src} effective energies can be extracted when N_{src} sources are used. For the effective potential method, the effective Hamiltonian has $(L/a)^3 \gg N_{\text{src}}$ eigenvalues but only those satisfying the condition (4.39) can be reliably identified to the eigenenergies. We can see in fig. 5.11 how the condition is satisfied in practice. For N_{src} sources, the first N_{src} clearly satisfy the condition, which makes it at least equivalent to the variational method. For $N_{\text{src}} = 2$ and 3, the condition is moderately satisfied for a few more eigenenergies but not enough to be conclusive. However, remember that the condition is sufficient but not necessary so more than N_{src} may indeed in practice be extracted as we will see.

We show in fig. 5.12 a comparison between the effective energies obtained using the variational (left) and the effective potential method (right). For the variational method, we only show $N_{\text{src}} = 5$. Using less than 5 sources, less eigenenergies are accessible but for a given eigenenergy increasing the number of sources has little effect. A first remark is that even from $N_{\text{src}} = 1$, the estimation for the first 5 eigenenergies using the effective potential method are reasonable and as N_{src} increases, these estimations improve. Compared to $N_{\text{src}} = 2$ and 3 the energies above the ground state for $N_{\text{src}} = 1$ are underestimated. This can be related to the strengthening of the repulsion between the LO and NLO in the HAL QCD and kernel approximation method. Between $N_{\text{src}} = 2$ and 3, the same remark applies for the energies above the second excited state.

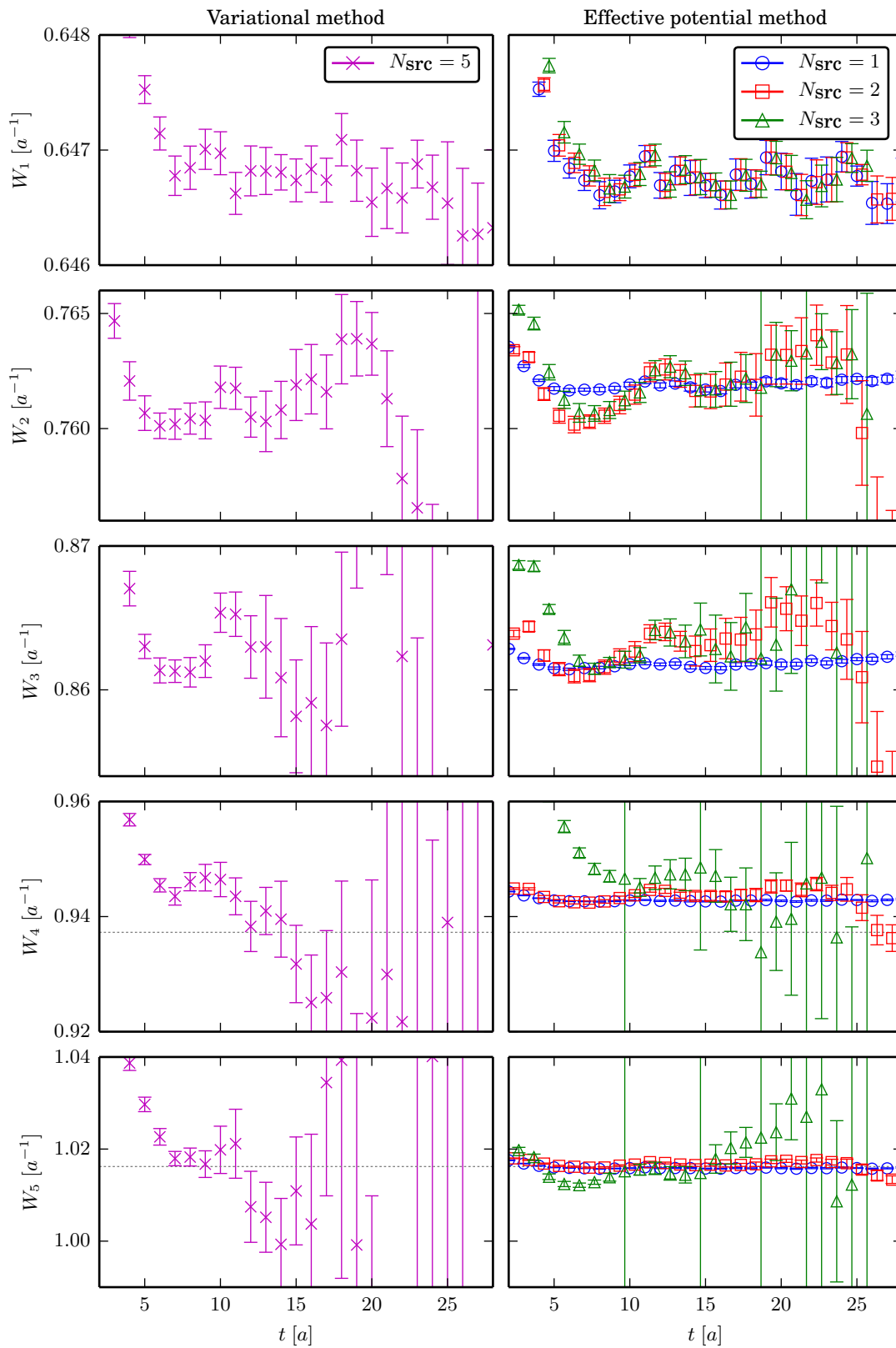
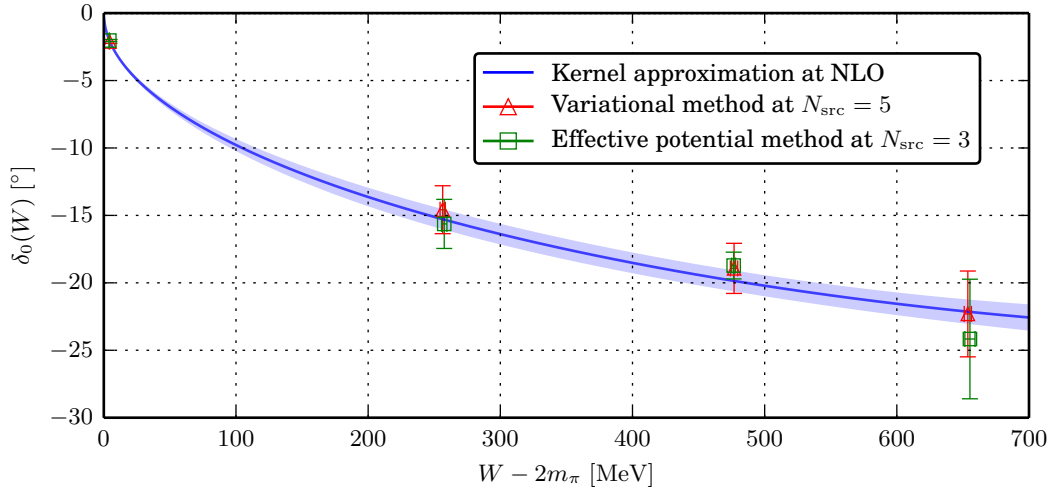


Figure 5.12: Effective energies obtained using the variational method or the effective potential method depending on the number of sources N_{src} .

n	Variational method	Effective potential method
1	[7, 23]	[8, 25]
2	[15, 21]	[19, 24]
3	[10, 17]	[11, 19]
4	[6, 10]	[10, 16]

Table 5.1: Fit ranges used for the variational and effective potential method.**Figure 5.13:** Comparison of the S-wave scattering phase shifts obtained with the variational method and the effective potential method. The estimation from the kernel approximation method corresponding to fig. 5.9 is shown for reference.

Furthermore, the effective energies exhibit significantly cleaner and longer plateaus in the effective potential method than in the variational method. For the latter it can be difficult to choose an adequate fitting range.

In order to obtain the scattering phase shifts, the effective energies are fitted to a constant for both methods and the finite-size formula is applied, neglecting the contribution of angular momenta $l \geq 4$. We use $N_{\text{src}} = 5$ for the variational method and $N_{\text{src}} = 3$ for the effective potential method, with fitting ranges summarized in table 5.1 for the first 4 eigenstates. The results are shown in fig. 5.13. We can see a very good agreement between all the methods discussed so far.

5.2 STUDY OF THE RHO MESON CHANNEL

In recent years, the $I = 1$ two-pion system has attracted a lot of attention in lattice QCD. The increase in computational power has finally allowed to generate fully dynamical QCD gauge configurations at quark masses low enough for the rho resonance to be observed, promising a better understanding of complex hadron processes from first principles. Recent studies [44–47] all use the finite-size formula [9] or its extension to moving frames [21], in order to relate the finite-size energy spectrum to the infinite volume phase shifts. The main difficulty faced by this method is that one can only extract the phase shifts at a few energies on the lattice, making it difficult to reconstruct the continuous energy range and thus the physical parameters of the system, especially

around the resonance where the phase shifts vary rapidly.

This section reports on our first attempt to apply the HAL QCD method to the $I = 1$ two-pion system. The meson masses considered here do not allow for the rho meson to decay, the goal being to test the viability of the method in this channel before applying it to the study of the resonance.

5.2.1 Computation method

Decay condition

In the physical world, the rho meson is a resonance in the two-pion channel with isospin $I = 1$. It has a mass of roughly 770 MeV which is well above the lowest two-pion states at an energy of $2m_\pi \sim 280$ MeV. In typical calculations, the situation on the lattice is quite different. As discussed previously, computational limitations imply that we are for the moment restricted to quark masses above their physical values. Large quark masses induce larger pion masses and larger rho masses but not proportionately. It results that the mass ratio m_π/m_ρ is typically much larger than its experimental value of ~ 0.18 . If this ratio is larger than 0.5, as was the case until a few years ago, the ρ meson does not decay into two pions and the dynamics is completely different from the physical world.

Recent calculations have been realized at mass ratios under 0.5 but face another challenge on the lattice. Indeed, the rho meson is a resonance appearing in the P-wave of the two pions channel, which means that the pions cannot be at rest. On the lattice, the smallest non-zero momenta have norm $2\pi/L$ so that the lowest pion-pion state in the center of mass frame has an energy close to

$$W_{\pi\pi} = 2\sqrt{m_\pi^2 + (2\pi/L)^2}. \quad (5.22)$$

The rho meson can decay if $W_{\pi\pi} < W_\rho = m_\rho$, which happens if $L \gtrsim 3.5$ fm at the physical values of the masses. While such configurations are beginning to be available, they were not at the time of this study and still require huge computational resources. A workaround, which has been used extensively in the past studies, is to study the system in a moving frame, i.e. consider two pions with non-zero total momentum. In this case, one of the pions can be set at rest in the lattice frame so that the two-pion states' energy decreases while the rho meson gains a non-zero momentum and its energy increases, making it easier to satisfy the decay condition $W_{\pi\pi} < W_\rho$.

The HAL QCD method is only defined in the center of mass frame so that the direct study of the decay of the rho meson is impossible. In the wait of larger computational power, we here lay the ground for future simulations by considering how the HAL QCD method can be applied to this system, even in the case of unphysical dynamics. Indeed, this channel has several features which make it particularly challenging.

Variational basis

To describe two pions in the center of mass frame and isospin $I = 1$ channel, we use the following operator

$$\pi\pi(\mathbf{q}) = \frac{1}{\sqrt{2}} \left[\pi^-(\mathbf{q})\pi^+(-\mathbf{q}) - \pi^+(\mathbf{q})\pi^-(-\mathbf{q}) \right], \quad (5.23)$$

$$\begin{aligned}
\langle \pi\pi(\mathbf{q}; t) \bar{\pi}\pi(\mathbf{p}; t_0) \rangle &= \begin{array}{c} \mathbf{q} \quad -\mathbf{q} \\ \curvearrowright \quad \curvearrowleft \\ -\mathbf{p} \quad \mathbf{p} \end{array} - \begin{array}{c} \square \\ \rightarrow \quad \leftarrow \\ \leftarrow \quad \rightarrow \end{array} - \begin{array}{c} \square \\ \leftarrow \quad \rightarrow \\ \rightarrow \quad \leftarrow \end{array} - (\mathbf{q} \leftrightarrow -\mathbf{q}) \\
\langle \pi\pi(\mathbf{q}; t) \bar{\rho}(t_0) \rangle &= \begin{array}{c} \mathbf{q} \quad -\mathbf{q} \\ \triangle \\ \mathbf{0} \end{array} - (\mathbf{q} \leftrightarrow -\mathbf{q})
\end{aligned}$$

Figure 5.14: Decomposition in Wick contractions of the correlation functions corresponding to $\pi\pi \rightarrow \pi\pi$ and $\rho \rightarrow \pi\pi$, appearing both in the correlation matrix (with $\mathbf{q} = \mathbf{p}$) and the BS wave function. Time goes upward.

where π^\pm are local interpolating operators for the pions. The Bethe-Salpeter (BS) wave functions are then defined in this channel as

$$\Psi_n(\mathbf{r}) = \int \frac{d^3\mathbf{q}}{(2\pi)^3} e^{i\mathbf{r}\cdot\mathbf{q}} \langle 0 | \pi\pi(\mathbf{q}) | n \rangle \quad (5.24)$$

with $|n\rangle$ an eigenstate of QCD with the required quantum numbers.

As discussed previously, the considered channel contains both pion-pion scattering states and the rho meson. Furthermore, in the pion mass region we investigate, we expect the ground state to be the rho meson and the first excited state to be the pion-pion scattering state with back-to-back momenta with a norm close to $2\pi/L$. Due to the presence of the rho state, we cannot use the time-dependent HAL QCD method. We will therefore combine the HAL QCD method with the variational method to extract the contribution of the rho and the pion-pion states in the lattice correlators.

To approximate the pion-pion state we use the operator $\pi\pi(\mathbf{p})$ with momentum $\mathbf{p} = \frac{2\pi}{L}\mathbf{e}_z$ and for the rho meson the operator

$$\rho \equiv \frac{1}{\sqrt{2}} \sum_{\mathbf{x}} \left[\bar{u}(\mathbf{x}) \mathbf{a} \cdot \boldsymbol{\gamma} u(\mathbf{x}) - \bar{d}(\mathbf{x}) \mathbf{a} \cdot \boldsymbol{\gamma} d(\mathbf{x}) \right] \quad (5.25)$$

with a polarization taken parallel to that of the relative momentum of the pions, $\mathbf{a} = \mathbf{e}_3$.

As described in section 2.3.2, the variational method relies on the computation of the correlation matrices

$$C(t, t_0) = \begin{pmatrix} \langle \pi\pi(\mathbf{p}; t) \bar{\pi}\pi(\mathbf{p}; t_0) \rangle & \langle \pi\pi(\mathbf{p}; t) \bar{\rho}(t_0) \rangle \\ \langle \rho(t) \bar{\pi}\pi(\mathbf{p}; t_0) \rangle & \langle \rho(t) \bar{\rho}(t_0) \rangle \end{pmatrix}. \quad (5.26)$$

Neglecting the contributions of the higher eigenstates, the variational method provides the mixing between the states $\bar{\pi}\pi(\mathbf{p})|0\rangle$ and $\bar{\rho}|0\rangle$ and the eigenstates $|n\rangle$ corresponding to the lowest pion-pion state and the rho meson. Once this mixing is known, we can choose optimal sources to extract the BS wave functions $\Psi_n(\mathbf{r})$.

Wick contractions

We have seen in equation (2.51) how to compute correlation functions in lattice QCD. The correlation functions are expanded in all the possible ways to pair the quark and antiquark fields, called Wick contractions, and each pair is associated a weight given by the Dirac propagator. We illustrate in Fig. 5.14 some of the correlation functions necessary to our calculations as well as their Wick contractions. The computational

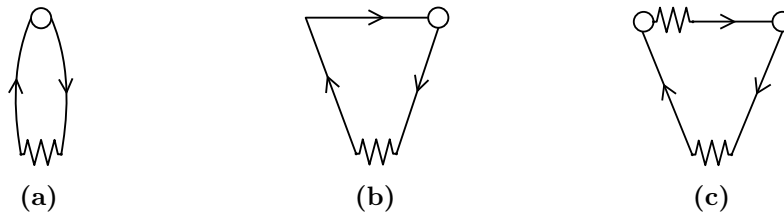


Figure 5.15: Computation method for some Wick contractions. Springs link pairs of points which are projected one on the other by summing over stochastic noises. Open circles are explicit summations. Straight (resp. broken) arrows are direct (sequential) propagators.

difficulty of the $I = 1$ pion-pion channel arises from the presence of the square and triangle diagrams, which do not appear in the $I = 2$ channel. These diagrams represent the possibility of a pair creation and annihilation between the quark and antiquarks at the time t . They require the computation of the Dirac propagator $D^{-1}(\mathbf{x}, t; \mathbf{y}, t)$ between any two points at the sink time t , which is prohibitively expensive. Following [44], we use stochastic noises as a workaround.

At each spatial point \mathbf{x} of the lattice, generate a sequence of random values $\xi_j(\mathbf{x}) \in U(1)$ for $j = 1, \dots, N$. These noises are such that

$$\lim_{N \rightarrow \infty} \frac{1}{N} \sum_{j=1}^N \xi_j^*(\mathbf{x}) \xi_j(\mathbf{y}) = \delta_{\mathbf{x}, \mathbf{y}}. \quad (5.27)$$

We can therefore use them to approximate the Dirac propagators as

$$D^{-1}(\mathbf{x}, t; \mathbf{y}, t) = \frac{1}{N} \sum_{j=1}^N \xi_j^*(\mathbf{y}) \left[\sum_{\mathbf{z}} D^{-1}(\mathbf{x}, t; \mathbf{z}, t) \xi_j(\mathbf{z}) \right], \quad (5.28)$$

which converges as $N \rightarrow \infty$. Instead of computing the Dirac propagator for each starting point \mathbf{y} , we invert the Dirac matrix with a random source and then “project” it to effectively start at the point \mathbf{y} using the conjugate noise $\xi_j^*(\mathbf{y})$. Fig. 5.15 shows some examples of the process.

Numerical setup

The results presented here were computed using the $N_f = 2 + 1$ full QCD gauge configurations of ILDG/JLDG generated by the CP-PACS and JLQCD collaborations [48] on a $28^3 \times 56$ lattice with a RG improved gauge action at $\beta = 2.05$ and a $O(a)$ improved Wilson quark action with $c_{SW} = 1.628$. The lattice spacing is $a = 0.0685$ fm which makes for a lowest non-zero momentum of $p = 2\pi/L = 0.65$ GeV. The light quark hopping parameters are $\kappa_{ud} = 0.1347$ and $\kappa_s = 0.1351$, leading to meson masses $m_\pi = 1.05$ GeV and $m_\rho = 1.37$ GeV. The lowest energy of two free pions in the center of mass frame, $W_{\pi\pi}$, is therefore significantly larger than that of the rho meson at rest.

The quark propagators are computed with temporal Dirichlet boundary condition. We use $U(1)$ stochastic noises, 6 at the source and 20 at the sink. Wave functions are projected in the T_1^- representation of the cubic group which contains the P-wave. Statistical errors are computed using the jackknife technique although 2-dimensional plots are shown without error bars for clarity.

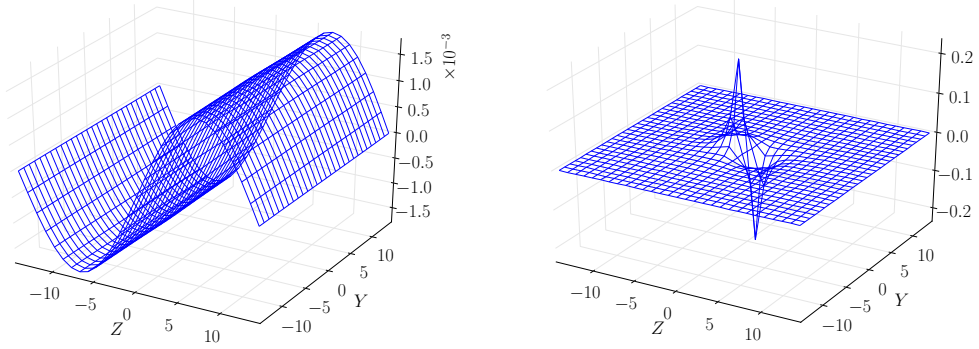


Figure 5.16: Contribution to the wave functions for the first (left) and second (right) diagrams of the $\pi\pi \rightarrow \pi\pi$ correlation function in Fig. 5.14 (upper). Normalized such that the total wave function has a norm 1. Computed at $t - t_0 = 12$.

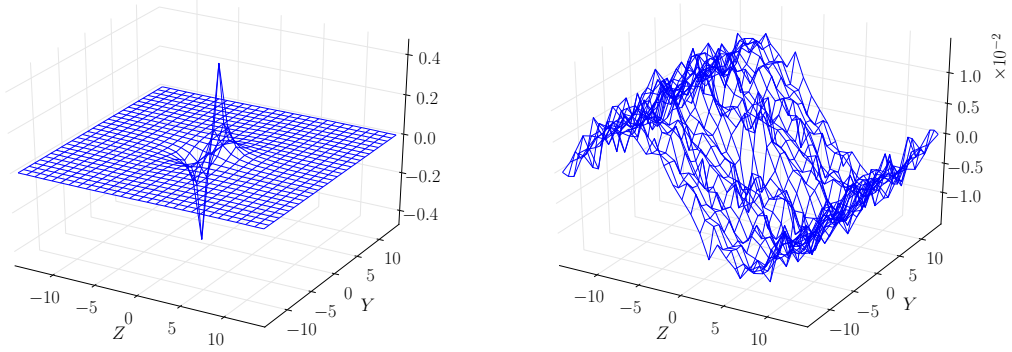


Figure 5.17: $I = 1$ pion-pion wave functions on the ground (left) and first excited (right) states. Normalized to 1. Computed at $t - t_0 = 10$.

5.2.2 Simulation results

Wave functions

We have seen that the BS wave functions are obtained as combinations of the wave functions computed with the source operators $\pi\pi(\mathbf{p})$ and ρ , themselves computed as sum of Wick contractions ("diagrams"). The combinations are obtained using the variational method from the correlation matrices $C(t)$.

Figure 5.16 shows the contribution of the two kind of diagrams appearing in the $\pi\pi \rightarrow \pi\pi$ wave function. The left one, corresponding to the "parallel" diagram (the first one in fig. 5.14), is close to the free wave function. The right one, corresponding to the box diagram, exhibits a very peaked and short-ranged behaviour. The triangle diagram is found to lead to a wave function very similar (up to a normalization) to that of the rectangle one. The rho meson being the ground state, the quark-antiquark pair propagating in the rectangle and triangle diagrams from t_0 to t can be thought of as forming a rho meson, which could explain why the two diagrams' wave functions are similar and short-ranged.

The ground state's wave function, Fig. 5.17 (left), can be obtained using either source operator by saturation at large enough time separation. Taking $\pi\pi(\mathbf{p})$ as source

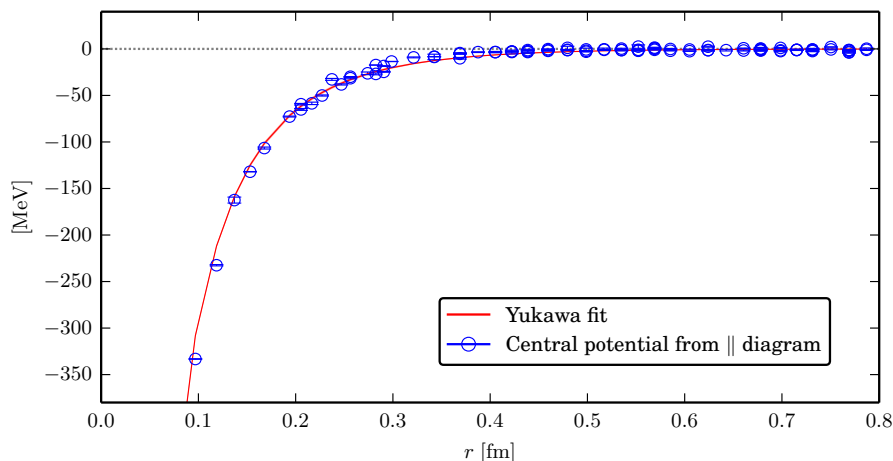


Figure 5.18: Central potential using only the parallel diagrams at $t - t_0 = 12$. Fit by a Yukawa potential (the statistical error is shown but very small).

operator, we see that the dominant contribution as time separation increases is from the rectangle diagram.

The first excited state's wave function is shown Fig. 5.17 (right). We see that the dominant contribution is this time coming from the parallel diagram. The wave function is obtained with a linear combination of the two source operators, which has for effect the cancellation of the peaked short-range contribution between the rectangle and triangle diagrams. However, while the signal from the ground state wave function is cancelled, the statistical noise remains and grows as $e^{\Delta W(t-t_0)}$ with ΔW the energy difference between the two lowest eigenstates.

Potential

An approximate potential is obtained by inverting the Schrödinger equation with the BS wave functions computed on the lattice as input. The wave functions in Fig. 5.17 unfortunately do not allow such a computation. The ground state wave function (left) is sharply peaked around the origin, leading to huge discretization errors when taking finite-difference Laplacian operator. The first excited state wave function (right) is extremely noisy due to large energy separation between the two lowest eigenstates and the noise is further enhanced by taking the Laplacian.

Using the fact that the main contribution to the first excited state wave function is from the parallel diagram and that the other diagrams should only contribute to the short-range part of the potential, we show in Fig. 5.18 the effective central potential computed using only the parallel diagrams, on both sets of hopping parameters. We see that a simple Yukawa fit is in very good agreement to the data even at surprisingly short range. The mass in the Yukawa fit is $1.53(9)$ GeV.

Discussion

We have shown results of the first application of the HAL QCD method to the $I = 1$ pion-pion system. The method, which has been successful in the study of baryon-baryon systems and the $I = 2$ pion-pion channel, encountered difficulties in this particular setup. First, the ground state being the rho meson, the wave function is very short-ranged and the computation of the potential leads to large discretization errors. Then,

while the first excited state is a scattering state and likely to be well described by a potential, it is difficult to extract due to the large energy difference.

However, approaching the problem from a different perspective compared to the other studies, the present results shed a new light on the qualitative understanding of the system. Furthermore, the above problems may be solved in the region where the rho meson is a resonance and not the ground state, since the scattering state will be simply extracted by saturation and the short-ranged component should become less important. In this case, the potential method could lead to competitive quantitative results. Further study at smaller pion masses will confirm or invalidate this expectation.

5.3 SEARCH FOR TETRAQUARK BOUND STATES

In this section, we describe the application of the HAL QCD method to another exciting problem, the search for tetraquark bound states from lattice QCD.

5.3.1 Quark model predictions

Due to confinement, particles in QCD must be composed of quarks and anti-quarks in a color-singlet configuration. The simplest examples and the only to have been unambiguously observed so far are mesons $q\bar{q}$ and baryons qqq . However, it is possible to form color-singlet states with more than three quarks. Jaffe famously predicted [49] using the quark bag model that the dibaryon H ($udsuds$) could be stable against strong decay. Since then, several other possibly stable multiquark states have been proposed.

In this section we are interested in tetraquark states of the form $qq\bar{q}\bar{q}$ with a diquark pair qq in the color $\mathbf{3}$ representation and an anti-diquark $\bar{q}\bar{q}$ in the color $\mathbf{3}^*$ representation. It has long been suggested from model calculations [50, 51] that such states should be stable in the case where the two quarks are much heavier than the two anti-quarks. We will briefly present the diquark picture [52], which is a simple phenomenological model that could explain the stability of such states. This model describes the mass difference of hadrons by a color-spin interaction between the constituent quarks

$$-C_H \sum_{i>j} \mathbf{s}_i \cdot \mathbf{s}_j \frac{1}{m_i m_j}, \quad (5.29)$$

where \mathbf{s}_i and m_i are the spin and mass of the quarks. The constant C_H takes the value C_M for $q\bar{q}$ pairs and C_B for qq diquarks. As the names suggest, these two constants are respectively fitted from the mass difference of mesons and baryons, resulting in $C_M \simeq 3C_B$. With only one parameter in each case, this model is found to reproduce the experimental data for the hadron differences quite well. It can then be used to predict the binding energy of tetraquark states.

Let $Q_{1,2}$ be two heavy quarks and $\bar{q}_{1,2}$ two light anti-quarks. The interaction (5.29) is suppressed for large quark masses, attractive for $S = 0$ and repulsive for $S = 1$ $q\bar{q}$ pairs or qq diquarks. Therefore, a tetraquark $Q_1 Q_2 \bar{q}_1 \bar{q}_2$ composed of an $O(1)$ attractive $\bar{q}_1 \bar{q}_2$ anti-diquark and a $O(1/m_Q^2)$ attractive or repulsive $Q_1 Q_2$ diquark could be bound compared to the threshold given by the two mesons with $O(1/m_Q)$ attractive or repulsive pairs $Q_1 \bar{q}_1$ and $Q_2 \bar{q}_2$. Candidate tetraquarks with charm (but no bottom) quarks would be

- T_{cc} ($J^P = 1^+, I = 0$) with a strongly attractive scalar $\bar{u}\bar{d}$ and a weakly repulsive axial vector cc could be bound with respect to the $D - D^*$ threshold,
- T_{cs} ($J^P = 1^+, I = 0$) with a strongly attractive scalar $\bar{u}\bar{d}$ and a weakly repulsive axial vector cs could be bound with respect to the $\bar{K} - D^*$ threshold,

- T_{cs} ($J^P = 0^+, I = 0$) with a strongly attractive scalar $\bar{u}\bar{d}$ and a weakly attractive scalar cs could be bound with respect to the $\bar{K} - D$ threshold.

Phenomenological models give wildly varying predictions for the existence of such bound states and if applicable their binding energies. In the wait of experimental verification, a definite conclusion could only be drawn with fully dynamical lattice QCD simulations at the physical point. Our work is a first step in this direction.

5.3.2 Simulation details

Heavy quarks on the lattice

We have presented in section 2.2 how to perform lattice simulations of QCD for an arbitrary number of quark flavors. However, typical corrections of the order $O(m^f a)$ become problematic when we consider quark flavors with particularly heavy masses such as the charm and bottom quarks. The earliest attempts to treat heavy quarks on the lattice included taking the static approximation $m^{c,b} \rightarrow \infty$ [53], using a non-relativistic action for these flavors [54] or lattices with large anisotropy parameters [55]. Each of these approaches leads to sizable corrections and cannot be used in precision calculations.

A more careful approach was proposed in ref. [56] by introducing a relativistic heavy-quark (RHQ) action designed to avoid corrections in powers of $m^f a$. Following the Symanzik improvement program [57], the lattice theory is described by a local effective action

$$S_{\text{eff}} = S_0 + \sum_{k \leq 1, i} a^k \int d^4x c_{4+k, i}(g) \mathcal{O}_{4+k, i}(x), \quad (5.30)$$

where S_0 is the continuum action and $\mathcal{O}_{4+k, i}(x)$ are local composite operators of dimension $4 + k$. Considering only operators up to dimension 5 allowed by the symmetries of the theory, the action for a heavy quark Q can be written with the appropriate normalization of the fields as

$$S_Q = \sum_x \left[\bar{\psi}^Q(x) \psi^Q(x) - \kappa_Q \sum_{\pm} \sum_{i=1}^3 \bar{\psi}^Q(x) (r_s \mp \nu \gamma_i) U_{\pm i}(x) \psi^Q(x \pm \hat{i}) \right. \quad (5.31)$$

$$\left. - \kappa_Q \sum_{\pm} \bar{\psi}^Q(x) (r_t \mp \nu \gamma_4) U_{\pm 4}(x) \psi^Q(x \pm \hat{4}) \right] \quad (5.32)$$

$$\left. - \kappa_Q \bar{\psi}^Q(x) \left(c_B \sum_{i, j} F_{ij} \sigma_{ij} + c_E \sum_i F_{i4} \sigma_{i4} \right) \psi^Q(x) \right]. \quad (5.33)$$

using the notations of section 2.2 and lattice units where $a = 1$. The parameter r_t can be set to 1. Then, we see that if $r_s = r_t$ and $c_B = c_E = 0$, we recover the action (2.48) for Wilson fermions. If $r_s = r_t$ and $c_B = c_E (\equiv c_{\text{SW}}) \neq 0$, we obtain the action for clover fermions which are an improvement over the Wilson fermions as discussed in section 2.2.

The parameters of the RHQ action can be determined non-pertubatively to reduce the corrections of order $O((m_Q a)^n)$ with arbitrary n in the Wilson or clover action to corrections of order $O(f(m_Q a)(a\Lambda_{\text{QCD}})^2)$ where f is a function analytic at $m_Q a = 0$. This means that we only require the lattice spacing to satisfy $a\Lambda_{\text{QCD}} \ll 1$, a significant improvement over the usual requirement $am_Q \ll 1$.

Lattice setup

Our calculations are based on $N_f = 2 + 1$ QCD gauge configurations generated by the PACS-CS collaboration [43] on a $32^3 \times 64$ lattice using the Iwasaki gauge action at $\beta = 1.9$ and clover fermions for the sea quarks u, d, s with parameter $c_{\text{SW}} = 1.715$. The associated lattice spacing is $a = 0.0907$ fm making for a spatial extent $L \simeq 2.9$ fm. We use three set of configurations, with three different sea quark hopping parameters (κ_{ud}, κ_s) . The parameter values are $(0.13754, 0.13640)$, $(0.13727, 0.13640)$, and $(0.13700, 0.13640)$ which lead to a pion mass of 410, 570 and 700 MeV respectively.

For the non-dynamical charm quark, we use the RHQ action described previously. The parameters of the action are chosen similarly as in ref. [58], $\kappa_Q = 0.10959947$, $r_s = 1.1881607$, $\nu = 1.1450511$, $c_B = 1.9849139$ and $c_E = 1.7819512$. These were tuned to reproduce the 1S charmonium mass and dispersion relation when the light sea quarks are at the physical point. Note that our three sets of light quark masses are heavier than at the physical point but we can choose the same RHQ action parameters and decrease the light quark masses to get the correct overall trend towards the physical point. Furthermore, the sea quark parameters would only mildly affect the charm quark parameters if the latter were to be tuned for each set.

We investigate the interaction in the following channels

- D - D with $J^P = 0^+$, $I = 1$,
- \bar{K} - D with $J^P = 0^+$, $I = 0$ and $I = 1$,
- D - D^* with $J^P = 1^+$, $I = 0$ and $I = 1$,
- \bar{K} - D^* with $J^P = 1^+$, $I = 0$ and $I = 1$.

The three channels with isospin $I = 0$ are those where the candidate tetraquarks T_{cs} and T_{cc} discussed previously could be bound. We also consider the isospin $I = 1$ channels to have a more general understanding of the interaction.

To study a meson-meson channel $A - B$, we apply the time-dependent HAL QCD method described in section 3.3.2. The correlators (3.112) are computed using local interpolators $q\Gamma q$ for the mesons at the sink and operators $q_w\Gamma q_w$ with quark walls defined as (5.2) at the source. The operators are projected on the desired isospin channel and the A_1^+ representation of the cubic group which principally contains the S-wave.

Assuming that the Schrödinger equation (3.113) is well approximated for $A = 1$, we extract from the correlators the leading term $V_0(\mathbf{r})$ of the potential defined with $M_{0,n} = \delta_{n,0}$. The term $V_0(\mathbf{r})$ corresponds to a central approximation of the potential, which we will note $V_C(\mathbf{r})$.

5.3.3 Numerical results

The central potentials V_C in all the channels considered are computed from the correlators and shown at the time slice $t = 16$ in figures 5.19 and 5.20, along with their statistical error estimated using a jackknife analysis. These potentials reach a relatively time-independent plateau in the region $t = 13 - 18$ and the remaining time-dependence will later be considered as a systematic error.

We can readily observe that all the channels with isospin $I = 0$ present an attraction while all the channels with isospin $I = 1$ present a repulsion. In the diquark model, an isospin $I = 0$ (resp. $I = 1$) enforces a light diquark $\bar{q}q$ with spin $S = 0$ (resp. $S = 1$) which is strongly attractive (resp. repulsive). Therefore, our results are qualitatively in agreement with the predictions of this simple model. The quark mass dependence of the potentials in all channels is rather minor in the pion mass range 410 – 700 MeV

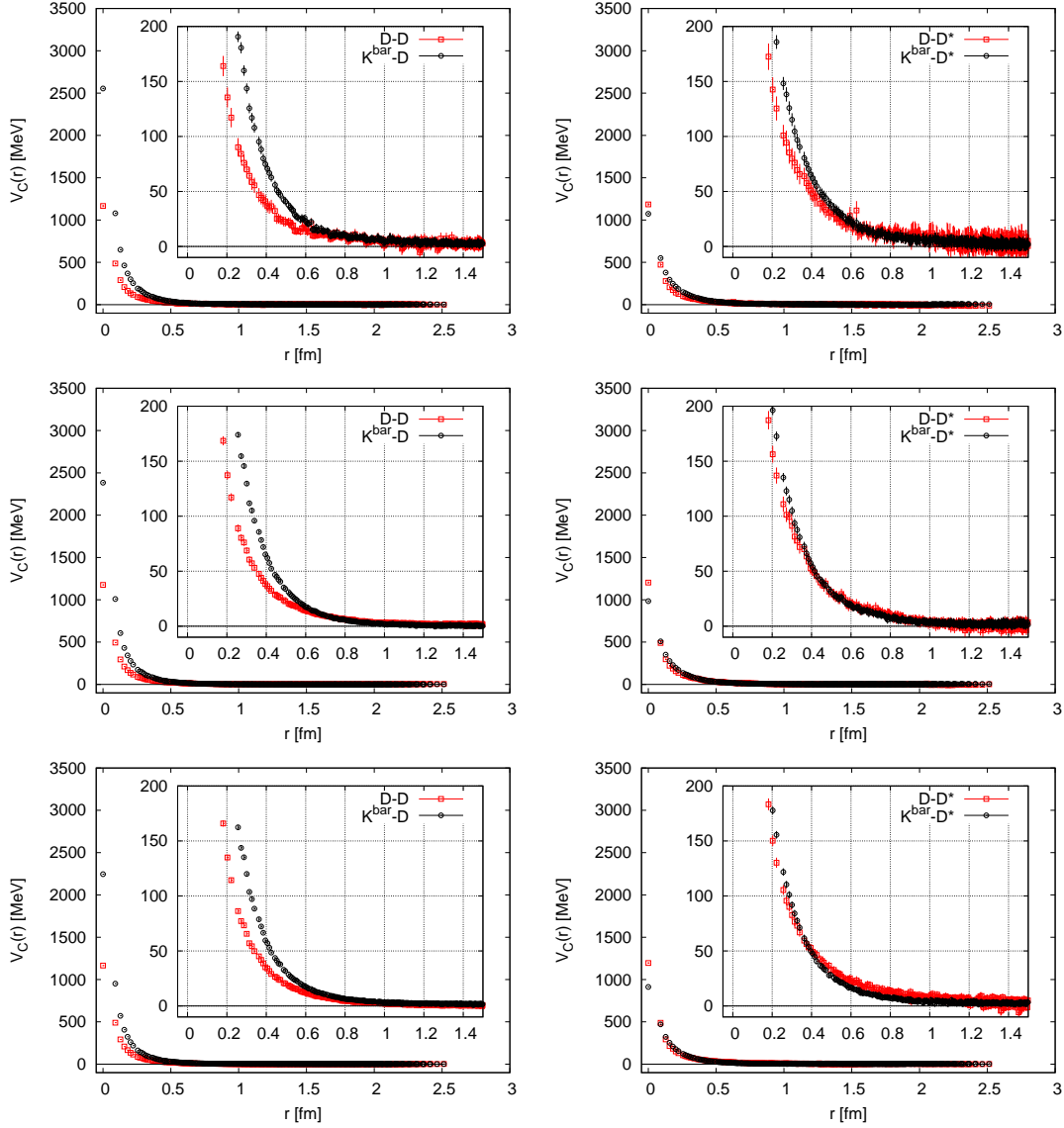


Figure 5.19: Potentials V_C at $t = 16$. Left column for the D - D (square) and \bar{K} - D (circle) channels with $(J^P, I) = (0^+, 1)$. Right column for the D - D^* (square) and \bar{K} - D^* (circle) channels with $(J^P, I) = (1^+, 1)$. Each row corresponds to a set of configuration, with pion masses $m_\pi = 410$ MeV, $m_\pi = 570$ MeV and $m_\pi = 700$ MeV from top to bottom.

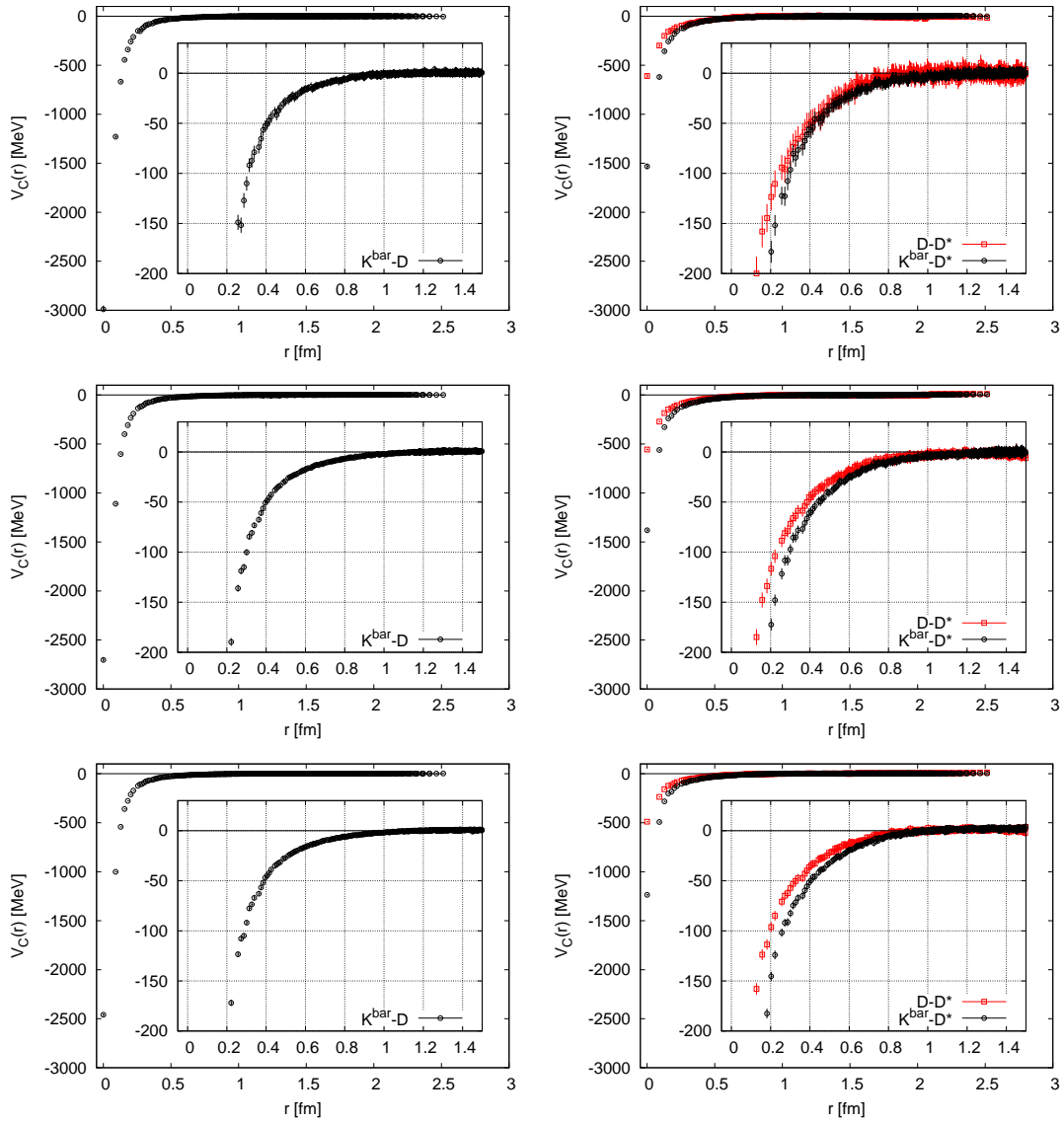


Figure 5.20: Potentials V_C at $t = 16$. Left column for the $\bar{K}-D$ channel with $(J^P, I) = (0^+, 0)$. Right column for the $D-D^*$ (square) and $\bar{K}-D^*$ (circle) channels with $(J^P, I) = (1^+, 0)$. Same layout as fig.5.19 for the rows.

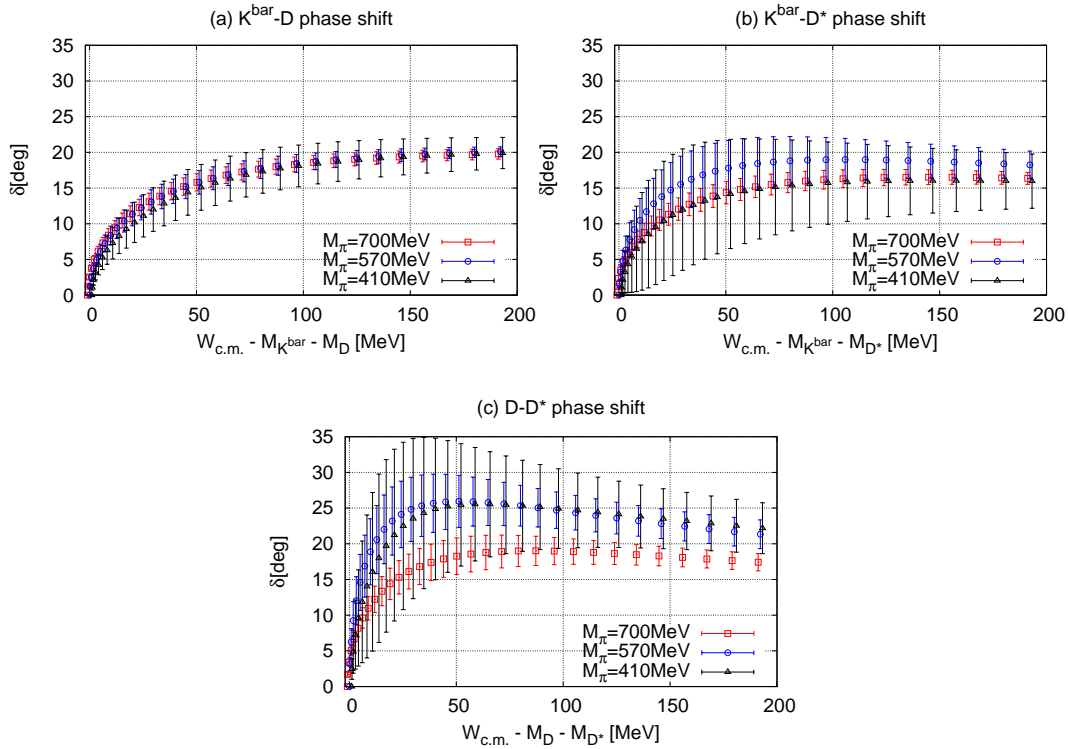


Figure 5.21: S-wave $I = 0$ scattering phase shifts in the (a) $\bar{K}-D$, (b) $\bar{K}-D^*$ and (c) $D-D^*$ channels. Vertical error bars represent the cumulated statistical and systematic errors.

except at very small distances r

In each channel and at each time slice, the potential is fitted by an analytic radial function, neglecting the contribution of partial waves with $l \geq 4$. The fit functions are chosen as multi-range Gaussians, i.e. $g(r) \equiv \sum_{n=1}^{N_{\max}} V_n \cdot \exp(-\nu_n r^2)$, for which we obtain good fits with $N_{\max} = 4$. Using these fit functions as potential, we solve the radial Schrödinger equation in infinite volume to obtain the S-wave scattering phase shifts. For a given channel, our estimation of the phase shift is obtained by fitting a plateau made by the phase shifts obtained from the potentials at different time slices. As discussed earlier, there is a plateau in the time range $t = 13 - 18$ which we use for the fit. A full jackknife analysis is performed to compute the statistical error on this estimation. The statistical error is evaluated using the difference between the estimations obtained from the two fit ranges $t = 13 - 15$ and $t = 16 - 18$.

Our results for the phase shifts are presented in fig. 5.21. We can see that the attraction is the strongest in the $I = 0 D - D^*$ channel, which is consistent with the diquark model. However, we do not observe bound states or resonances in any of the studied channels. The phase shifts seem to increase as the quark masses decrease, a sign of the attraction becoming stronger. This leaves open the possibility that a bound state could be present at the physical point, especially in the $I = 0 D - D^*$ channel for which the tetraquark T_{cc} ($J^P = 1^+, I = 0$) would be a possible explanation.

Although only calculations at the physical point can draw a definite conclusion, we can get some insight by looking at the quark-mass dependence of our results. Fig. 5.22 presents the quark-mass dependence of the scattering length in the attractive channels. The estimation of the statistical and systematic error is the same as for the scattering

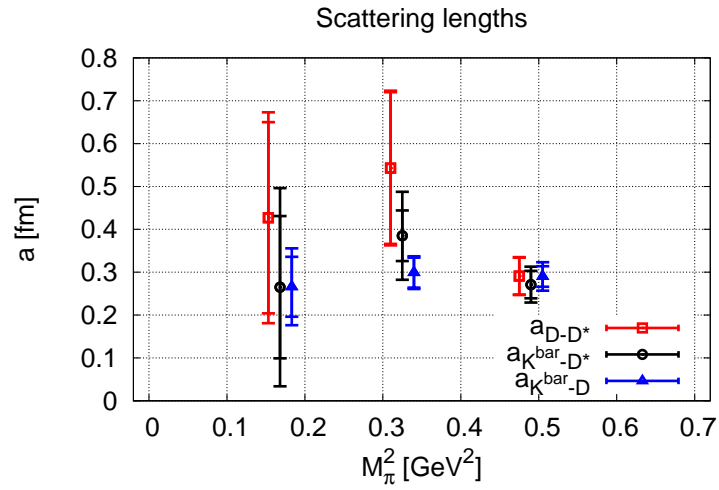


Figure 5.22: Pion mass dependences of scattering lengths in the $I = 0$ $\bar{K}-D$, $\bar{K}-D^*$ and $D-D^*$ channels. Inner vertical error bars represent statistical errors. Both statistical and systematic errors are included in total error bars.

phase shifts. As expected from the direct observation of the potentials, the quark-mass dependence is not significant and casts doubts on the possibility of a bound state at the physical point.

Summary

In this thesis, we have numerically investigated the interaction in two pion-pion channels and searched for tetraquark bound states from first principles using the HAL QCD method. We have also proposed several new methods or extensions to existing methods with the purpose of improving the available tools for the general study of two-particle channels in lattice QCD. We have provided a comprehensive numerical comparison of these tools to the existing ones in order to prove their effectiveness. It is our hope that they will be used in the future in diverse settings and contribute toward an extensive ab-initio description of our world.

In Chapter 5, we have seen how the HAL QCD method could be successfully applied to the pion-pion channel with isospin $I = 2$ and various meson-meson channels in which tetraquark bound states have been predicted by quark model calculations. These results echo the success of the HAL QCD method in the study of various baryon-baryon channels [59–61], including the important nucleon-nucleon channel. However, we have also seen how this method faced difficulties in the rho meson channel. The issues could be mainly explained by the predominance of the inelastic contribution of the rho meson and by the inadequate treatment of sharply-peaked Bethe-Salpeter wave functions due to the lattice discretization. We conclude that the HAL QCD approach may not be generally applicable but can be powerful in the study of channels dominated by low-energy elastic scattering.

While the investigation of the rho meson channel only resulted in a qualitative understanding of the interaction, we could extract numerical predictions for the other two channels. In the $I = 2$ pion-pion channel, we successfully mapped the scattering phase shifts in a large energy region at a pion mass of $m_\pi = 700$ MeV. As the computational power available increases, the very same method will likely lead to precise predictions at the physical point which can be compared to experimental values. Finally, we investigated the presence of bound charmed tetraquark states and did not find any bound state in the pion mass range $m_\pi = 410 \sim 700$ MeV. Our study of the quark mass dependence does not suggest that bound states would appear at the physical point although only future simulations can definitely decide on this matter.

A major shortcoming of the HAL QCD method is its inability to deal with states above the inelastic threshold. In section 4.1, we have proposed an extension of the method to deal with such states. In the general case, we have seen how the formulation of this extension requires a non-relativistic approximation which may not be valid in practice. However, the formulation is simplified and does not require a non-relativistic approximation in the case where the inelastic thresholds correspond to the opening of new two-particle channels. Numerical studies of such coupled two-particle channels

using this extension have already been achieved [62] with successful results.

Even in its area of applicability, the direct application of the HAL QCD method can raise some concerns. While an energy-independent and non-local potential for the BS wave functions has been constructed, it does not satisfy any of the properties required for the velocity expansion, such as Hermiticity, fast decay in non-locality, etc. Since the potential is not unique, the method therefore relies on the assumed existence of another energy-independent and non-local potential which has these properties and can be approximated with a truncation of the velocity expansion. Other concerns include the dependence on a fit function to relate the finite-volume potential to the infinite-volume one. Additionally, the mixing of the angular momentum channels in finite-volume is not properly addressed. Finally, it is not clear how the method can deal with a large number of source operators in lattice simulations, an important aspect for future precision calculations. We have proposed two methods to answer these concerns while retaining the core ideas of the HAL QCD method.

The effective potential method, introduced in section 4.2, is designed to combine the strongest points of the finite-size and the HAL QCD approaches. The scattering phase shifts are computed from the finite-volume spectrum with the finite-size formula as in Lüscher's approach but the spectrum is not extracted with the usual variational method. Inspired by the HAL QCD method, we use the time-dependence of arbitrary rectangular correlation matrices to construct an effective Hamiltonian operator in a certain subspace of the Hilbert space of physical states. This is in contrast with the variational method which relies on square correlation matrices to determine the mixing of the source states and the Hamiltonian eigenstates. Our approach has two main advantages: (i) rectangular correlation matrices allow to use more information from lattice simulation at little additional cost in several practical situations and (ii) the effective subspace treated by the method is larger than for square matrices so that more eigenstates may be accessible for the same number of source operators. The effective potential method is a particular case of this approach where the correlation matrices can be interpreted as wave functions and the effective Hamiltonian is given the form of the quantum mechanical Hamiltonian with a non-local potential. In this case, the effective potential has no particular interpretation, it is merely used as a fit to obtain the spectrum. Furthermore, it is not related to any infinite-volume quantity, the formulation being purely restricted to the finite lattice. In doing so, we avoid most of the assumptions of the HAL QCD method.

We have proposed in section 4.3 another approach called the kernel approximation method. This method provides an alternative to the HAL QCD method based on an extensive theoretical study of the finite-volume correlators. The BS wave functions are found to satisfy a Schrödinger equation with a non-local and energy-dependent potential. This potential is directly related to the Bethe-Salpeter kernel so that its properties are explicitly proven. It is found that it can be expanded as a power series in both non-locality and energy, enabling to approximate it by truncation. Furthermore, the method relies on the spatial interpolation of the lattice wave function which allows to project them on specific angular momentum channels and avoid any dependence on fit functions. We prove that the mixing of the angular momentum channels by the cubic group is exponentially suppressed with the volume so that the interaction in each channel can be treated separately as in infinite volume. These properties lead to a well-defined strategy to extract the scattering phase shifts from lattice simulations.

In section 5.1, the two newly proposed methods have been compared numerically to the existing finite-size and HAL QCD methods in the context of the two-pion channel

with isospin $I = 2$. We found that the theoretical advantages of our methods are well supported by practical results and we are confident that similar advantages would be encountered in the application to other systems. We hope that this efficiency, combined with the rigorous theoretical basis presented in this thesis, will convince other researchers to adopt these methods.

For lattice practitioners, Moore's law does not mean that we can keep the same methods and the computer will progressively give better results. An increase in computer power represents new opportunities along with new challenges and the methods of yesterday may not measure up to the challenges of tomorrow.

* * *

The publication status and attribution of the work presented in this thesis is as follows.

- Section 4.1 is the result of a collaboration lead by S. Aoki, who introduced the original idea. I helped improving the formalism and proposed alternative constructions of the potential. It was published in ref. [3] although the version given here is freely adapted from the published one.
- Sections 4.2 to 5.2 are personal projects. A preliminary version of the content of section 4.2 was published in ref. [2] and a more complete article is in the works. The content of the sections 4.3 and 5.1 is yet unpublished but corresponding articles are in preparation. The results of section 5.2 have been reported in ref. [1].
- Section 5.3 is the fruit of a collaboration lead by Y. Ikeda. He instigated this research and performed simulations for the two sets at the heaviest quark masses. I developed code to tackle the more computationally challenging set with the lightest quark mass, performed the associated simulations and designed a scheme for the evaluation of the statistical and systematic errors. The results have been published in ref. [4], of which some figures have been used in this thesis.

Acknowledgments

First of all, I would like to thank my supervisor Prof. Tetsuo Hatsuda for his continuous support and guidance during these three years. I am particularly indebted to Dr. Takumi Doi for his warm encouragements and so many helpful discussions which often got me back on the right track. Thanks also go to the other members of the HAL QCD Collaboration, particularly Prof. Sinya Aoki for his interesting comments at the monthly meetings and Dr. Yoichi Ikeda for a fruitful collaboration. Thank you also to the members of the research group in Hongo and then Wako for a nice working environment.

I would like to thank the staff at the University of Tokyo and RIKEN, most notably Masayo Imahori and Yoko Fujita, for their very helpful administrative support. I am also grateful for the financial support provided by the Japanese government (MEXT) in the form of a scholarship for the length of my studies.

Last but not least, I would like to express my deep gratitude to my family and friends for their moral support and constant encouragements.

Details for the effective potential method

A.1 EFFECTIVE HAMILTONIAN PERTURBATION

A.1.1 Notations and preliminary result

For two integers $M \geq N$, let $\{v_n\}_{n=1}^N$ be a basis of an N -dimensional subspace Σ of \mathbb{R}^M . Define V the matrix representing this basis in the canonical basis and V^+ its Moore-Penrose pseudoinverse. Then the columns $\{\bar{v}_n\}_{n=1}^N$ of $[V^+]^\dagger$ form the dual basis of $\{v_n\}_{n=1}^N$, i.e. $\langle \bar{v}_n, v_p \rangle = \delta_{np}$ where $\langle \cdot, \cdot \rangle$ is the canonical inner product.

For any two non-zero vectors a and b of \mathbb{R}^M , we will show that if $P_V b \neq 0$,

$$\min_{n, \langle \bar{v}_n, b \rangle \neq 0} \left| \frac{\langle \bar{v}_n, a \rangle}{\langle \bar{v}_n, b \rangle} \right| \leq \kappa(V) \frac{\|P_V a\|}{\|P_V b\|}, \quad (\text{A.1})$$

where $\kappa(V) = \|V\| \|V^+\|$ is the condition number of V and $P_V = VV^+$ is the orthogonal projector on the column space of V , i.e. Σ .

First, define the coefficients

$$\beta_n = \frac{\langle \bar{v}_n, a \rangle}{\langle \bar{v}_n, b \rangle}, \quad n = 1, \dots, N. \quad (\text{A.2})$$

with $\beta_n = \epsilon^{-1}$ for some $\epsilon > 0$ if $\langle \bar{v}_n, b \rangle = 0$. If there is an n such that $\beta_n = 0$, (A.1) is trivial. If all β_n are non-zero, we have

$$VD(\beta^{-1})V^+P_V a = P_V b + O(\epsilon), \quad (\text{A.3})$$

where $D(\beta^{-1})$ is the N -dimensional diagonal matrix with elements $[D(\beta^{-1})]_{nn} = \beta_n^{-1}$.

Using the properties of the operator norm, it follows that

$$\|VD(\beta^{-1})V^+P_V a\| \leq \kappa(V) \|D(\beta^{-1})\| \|P_V a\|, \quad (\text{A.4})$$

$$\|D(\beta^{-1})\| = \max_n |\beta_n^{-1}|. \quad (\text{A.5})$$

and after rearrangement,

$$\min_n |\beta_n| \leq \kappa(V) \frac{\|P_V a\|}{\|VD(\beta^{-1})V^+P_V a\|}. \quad (\text{A.6})$$

In the limit of $\epsilon \rightarrow 0$, we obtain (A.1).

A.1.2 General case

Consider the *full* generalized eigenvalue problem (GEVP) for two $M \times N$ matrices A and B ,

$$Bw = \lambda Aw, \quad (\text{A.7})$$

with $M \geq N$. These matrices are such that they can be decomposed as

$$A = A^{(0)} + A^{(1)}, \quad B = B^{(0)} + B^{(1)}, \quad (\text{A.8})$$

and there are N linearly-independent solutions to the *reduced* GEVP

$$B^{(0)}w_n^{(0)} = \lambda_n^{(0)}A^{(0)}w_n^{(0)}, \quad n = 1, \dots, N, \quad (\text{A.9})$$

while there may not be any solution to the full GEVP.

Now, suppose there exist an $M \times M$ matrix H such that

$$HA = B. \quad (\text{A.10})$$

Assuming that $A^{(0)}$ has full column rank, we can decompose the matrix H as,

$$H = H^{(0)} + H^{(1)}, \quad (\text{A.11})$$

$$H^{(0)} = B^{(0)}A^{(0)+} + H(1 - A^{(0)}A^{(0)+}), \quad (\text{A.12})$$

$$H^{(1)} = (B^{(1)} - HA^{(1)})A^{(0)+}, \quad (\text{A.13})$$

so that we obtain a reduced form of eq. (A.10),

$$H^{(0)}A^{(0)} = B^{(0)}. \quad (\text{A.14})$$

It follows from the decomposition of H that for $n = 1, \dots, N$

$$HA^{(0)}w_n^{(0)} = \lambda_n^{(0)}A^{(0)}w_n^{(0)} + H^{(1)}A^{(0)}w_n^{(0)}. \quad (\text{A.15})$$

Denote by $\{v_m\}_{m=1}^M$ a basis of normalized eigenvectors of the matrix H , $\{\lambda_m\}_{m=1}^M$ their associated eigenvalues, $\{\bar{v}_m\}_{m=1}^M$ its dual basis and V its matrix representation. We can expand the previous relation on this basis to obtain for $n = 1, \dots, N$

$$\lambda_m = \lambda_n^{(0)} + \frac{\langle \bar{v}_m, H^{(1)}A^{(0)}w_n^{(0)} \rangle}{\langle \bar{v}_m, A^{(0)}w_n^{(0)} \rangle}. \quad (\text{A.16})$$

Using the preliminary result (A.1) and the expression (A.13),

$$\min_{\substack{m=1, \dots, M \\ \langle \bar{v}_m, A^{(0)}w_n^{(0)} \rangle \neq 0}} \left| \frac{\langle \bar{v}_m, H^{(1)}A^{(0)}w_n^{(0)} \rangle}{\langle \bar{v}_m, A^{(0)}w_n^{(0)} \rangle} \right| \leq \kappa(V) \frac{\|(B^{(1)} - HA^{(1)})w_n^{(0)}\|}{\|A^{(0)}w_n^{(0)}\|}. \quad (\text{A.17})$$

Assuming A has full column rank and since the vectors $\{w_n^{(0)}\}_{n=1}^N$ are linearly-independent, the vectors $\{u_n = Aw_n^{(0)} / \|A^{(0)}w_n^{(0)}\|\}_{n=1}^N$ form a basis of the column space of A . Let $\{\bar{u}_n\}_{n=1}^N$ be its dual basis and U its matrix representation. For $n = 1, \dots, N$ we have

$$Hu_n = \lambda_n^{(0)}u_n + \frac{(B^{(1)} - \lambda_n^{(0)}A^{(1)})w_n^{(0)}}{\|A^{(0)}w_n^{(0)}\|}. \quad (\text{A.18})$$

Now, take any eigenvector v of H and λ its associated eigenvalue. It can be expanded as

$$v = \sum_{n=1}^N \langle \bar{u}_n, v \rangle u_n + (1 - P_A)v \quad (\text{A.19})$$

where $P_A = AA^+$ is the orthogonal projector on the column space of A . From this, we obtain for any $n = 1, \dots, N$

$$\lambda \left[1 - \frac{\langle \bar{u}_n, H(1 - P_A)v \rangle}{\langle \bar{u}_n, \lambda v \rangle} \right] = \lambda_n^{(0)} + \frac{\langle \bar{u}_n, (B^{(1)} - \lambda_n^{(0)} A^{(1)})w_n^{(0)} \rangle}{\|A^{(0)}w_n^{(0)}\|}, \quad (\text{A.20})$$

and, as previously, we have the upper bound

$$\min_{\substack{n=1, \dots, N \\ \langle \bar{u}_n, v \rangle \neq 0}} \left| \frac{\langle \bar{u}_n, H(1 - P_A)v \rangle}{\langle \bar{u}_n, \lambda v \rangle} \right| \leq \kappa(U) \frac{\|P_A H(1 - P_A)v\|}{\|\lambda P_A v\|}. \quad (\text{A.21})$$

Finally, it follows from the Cauchy-Schwartz inequality and the definition of $\kappa(U)$ that

$$\frac{|\langle \bar{u}_n, (B^{(1)} - \lambda_n^{(0)} A^{(1)})w_n^{(0)} \rangle|}{\|A^{(0)}w_n^{(0)}\|} \leq \kappa(U) \frac{\|(B^{(1)} - \lambda_n^{(0)} A^{(1)})w_n^{(0)}\|}{\|Aw_n^{(0)}\|}. \quad (\text{A.22})$$

A.1.3 Effective Hamiltonian

For the study of an effective Hamiltonian operator, we set

$$A = C(t), \quad A^{(0)} = C^{(0)}(t), \quad B = -\partial_t C(t), \quad B^{(0)} = -\partial_t C^{(0)}(t), \quad (\text{A.23})$$

with $C(t)$ the correlation matrix at some time t and $C^{(0)}(t)$ the same correlation matrix but only including the contributions of the N lower energy eigenstates. The solutions to the reduced GEVP (A.9) are $w_n^{(0)} = Q^{(0)-1} e_n$ and $\lambda_n^{(0)} = W_n$ for $n = 1, \dots, N$ and at all times t (e_n is the n -th vector of the canonical basis and see section 4.2.1 for other notations). We have the following large time behaviours

$$A^{(1)} = O(e^{-W_{N+1}t}), \quad B^{(1)} = O(e^{-W_{N+1}t}), \quad (\text{A.24})$$

due to the contributions of eigenstates with energies higher than W_N and for any $n = 1, \dots, N$,

$$A^{(0)}w_n^{(0)} = e^{-W_n t} P^{(0)} e_n, \quad u_n = \frac{P^{(0)} e_n}{\|P^{(0)} e_n\|} + O(e^{-W_{N+1}t}). \quad (\text{A.25})$$

where $P^{(0)} e_n$ is a constant. We do not write explicitly the time-dependence of the objects introduced in the previous subsection, e.g. $A^{(0)}$, for notational consistency.

The construction of the effective Hamiltonian H is abstracted as the result of a function $f(A, B)$ such that $f(A, B)A = B$. Assuming that the construction is such that $f(A^{(0)}, B^{(0)})$ is constant in time, the asymptotic behaviour of H in time is $O(1)$, and so is that of $\kappa(V)$. Combining this and the asymptotic behaviours previously mentioned, we deduce that the right-hand sides of eq. (A.17) and (A.22) are $O(e^{-(W_{N+1} - W_n)t})$.

For each time t and eigenstate index $n = 1, \dots, N$, define $\lambda_n^*(t)$ the eigenvalue λ_m of $H(t)$ associated to the index m which realizes the minimum on the left-hand side of eq. (A.17). All previous results lead to the asymptotic behaviours

$$\lambda_n^*(t) = W_n + O(e^{-(W_{N+1} - W_n)t}). \quad (\text{A.26})$$

This ensures that the Hamiltonian eigenstates energies are included amongst the eigenvalues of the matrix H , up to corrections exponentially decreasing with t . Since the matrix H has $M \geq N$ eigenvalues, there may be other eigenvalues which are not related to the eigen-energies.

At each time t , let $\{(\lambda_m(t), v_m(t))\}_{m=1}^M$ be pairs of eigenvalues and eigenvectors of $H(t)$, ordered by eigenvalue. For each index $m = 1, \dots, M$, define $\nu_m(t)$ the index n which realizes the minimum on the left-hand side of eq. (A.21) with $\lambda = \lambda_m(t)$ and $v = v_m(t)$. With $\nu_m = \lim_{t \rightarrow \infty} \nu_m(t)$, these satisfy the inequality

$$\left| 1 - \frac{\lambda_{\nu_m}^*}{\lambda_m(t)} \right| \leq \kappa(U) R_m(t), \quad R_m(t) = \frac{\|P_A H(1 - P_A)v_m(t)\|}{\|\lambda_m(t) P_A v_m(t)\|} + O(e^{-(W_{N+1} - W_{\nu_m})t}). \quad (\text{A.27})$$

where it is clear from its definition that $\kappa(U) = O(1)$.

We can interpret (A.26) and (A.27) as follows for asymptotic t , i.e. for t large enough. Assuming $M > N$, the spectrum of H contains some eigenvalues which are associated to the N first eigen-energies, and some which are not, i.e. $\{\lambda_n^*(t)\}_{n=1}^N \subsetneq \{\lambda_m(t)\}_{m=1}^M$. If an eigenvalue $\lambda_m(t)$ of H is associated to an eigen-energy, i.e. $\lambda_m(t) = \lambda_n^*(t)$ for some n , we have $\nu_m = n$. As a sort of weak converse, if a pair $(\lambda_m(t), v_m(t))$ is such that

$$\frac{\|P_A H(1 - P_A)v_m(t)\|}{\|\lambda_m(t) P_A v_m(t)\|} \ll 1, \quad (\text{A.28})$$

then $\lambda_m(t) = \lambda_{\nu_m}^*(t)$, i.e. it is associated to the ν_m -th eigen-energy. The condition (A.28) thus gives a way to identify which eigenvalues of H are associated to eigen-energies. It is a sufficient condition but not necessary in general.

We finally note that the convergence rate of the effective energies $\lambda_n^*(t)$ is influenced by $\kappa(V)$, which is minimal when H is Hermitian.

A.2 LATTICE OPERATORS AND CUBIC SYMMETRY

A.2.1 Open boundary conditions

Let $\Lambda = \{(x, y, z) \mid x, y, z \in \{-N, \dots, N\}\}$ be the set of the sites of a lattice of volume $V = (2N + 1)^3$ with open boundary conditions and u a bijection from Λ to the set of integers $\{1, \dots, V\}$. Then for any lattice wave function Φ , i.e. a function from Λ to \mathbb{R} , we can define the vector ϕ with elements $\phi_r = \Phi \circ u^{-1}(r)$ for $r = 1, \dots, V$. Any operator acting on lattice wave function can then be represented by a $V \times V$ matrix.

Each rotation g of the cubic group O_h is associated to a permutation matrix R^g . Define the action of g on the indices $r = 1, \dots, V$ by writing the elements of R^g as $(R^g)_{r,r'} = \delta_{r,gr'}$. Then, an operator transforms covariantly under the action of the cubic group if its associated matrix U commutes with all the matrices R^g , which is equivalent to

$$U_{gr,gr'} = U_{r,r'} \text{ for any } g \in O_h, (r, r') \in \{1, \dots, V\}^2. \quad (\text{A.29})$$

The matrices R^g define a representation \mathcal{R} of the cubic group on \mathbb{R}^V . For any index $r = 1, \dots, V$ define \bar{r} its orbit under the action of the cubic group, i.e. $\bar{r} = \{gr \mid g \in O_h\}$. It is trivial that we have the following decomposition of \mathcal{R} on the irreducible representations of the cubic group

$$\mathcal{R} = \bigoplus_{\bar{r} \in \bar{\Lambda}} \bigoplus_{\Gamma} N(\Gamma, \bar{r}) \times \Gamma, \quad (\text{A.30})$$

with a direct sum over $\bar{\Lambda}$, the set of all unique orbits, and $N(\Gamma, \bar{r})$ the number of occurrences of the irreducible representation Γ in the subrepresentation of \mathcal{R} associated

\bar{r}	A_1^+	A_2^+	E^+	T_1^+	T_2^+	A_1^-	A_2^-	E^-	T_1^-	T_2^-
(0, 0, 0)	1									
(0, 0, a)	1		1						1	
(0, a, a)	1		1		1				1	1
(a, a, a)	1				1		1		1	
(0, a, b)	1	1	2	1	1				2	2
(a, b, b) or (a, a, b)	1		1	1	2		1	1	2	1
(a, b, c)	1	1	2	3	3	1	1	2	3	3

Table A.1: Number of occurrences $N(\Gamma, \bar{r})$ of the irreducible representation Γ of the cubic group appearing in the decomposition (A.30). Empty cells mean zeros. The first column shows the kind of the representative of the orbit \bar{r} , with $0 < a < b < c$.

to \bar{r} . Each orbit \bar{r} contains an unique element $\bar{r} = (x, y, z)$ with $0 \leq x \leq y \leq z$, which will be taken as the representative of the orbit. Table A.1 summarizes the coefficients $N(\Gamma, \bar{r})$ depending on the representative of \bar{r} .

Each occurrence of an irreducible representation Γ is associated to a pair $\tilde{r} = (\bar{r}, \nu)$ for $\bar{r} \in \bar{\Lambda}$ and $\nu = 1, \dots, N(\Gamma, \bar{r})$. Let $\tilde{\Lambda}_\Gamma$ be the set of all those pairs so that

$$\mathcal{R} = \bigoplus_\Gamma \bigoplus_{\tilde{r} \in \tilde{\Lambda}_\Gamma} \Gamma. \quad (\text{A.31})$$

The decomposition (A.31) implies the existence of an orthonormal basis of \mathbb{R}^V consisting of vectors $\psi^{\Gamma\alpha\tilde{r}}$ with $\alpha = 1, \dots, d_\Gamma$ (d_Γ is the dimension of the irreducible representation Γ) and $\tilde{r} \in \tilde{\Lambda}_\Gamma$. Let Ψ be the unitary matrix whose columns are the vectors $\psi^{\Gamma\alpha\tilde{r}}$. For any matrix U satisfying (A.29), one can use Schur's lemma to show that

$$[\psi^{\Gamma\alpha\tilde{r}}]^\dagger U \psi^{\Gamma'\alpha'\tilde{r}'} = \delta_{\Gamma\Gamma'} \delta_{\alpha\alpha'} \tilde{U}_{\tilde{r}, \tilde{r}'}^\Gamma. \quad (\text{A.32})$$

Therefore, the matrix $\tilde{U} = \Psi^\dagger U \Psi$ is block-diagonal with blocks \tilde{U}^Γ each appearing d_Γ times. The elements of \tilde{U}^Γ for each irreducible representation Γ are the actual degrees of freedom of U . Compare

$$[\sum_\Gamma d_\Gamma \sum_{\bar{r}} N(\Gamma, \bar{r})]^2 = V^2 = (2N + 1)^6 \sim 64N^6, \quad (\text{A.33})$$

the dimension of the set of all matrices of \mathbb{R}^V , to

$$\sum_\Gamma N(\Gamma)^2 \sim \frac{4}{3}N^6, \quad (\text{A.34})$$

the dimension of the subset of those which satisfy (A.29). Here, \sim denotes the equivalence at large N and $N(\Gamma) = \sum_{\bar{r}} N(\Gamma, \bar{r}) \sim \frac{d_\Gamma}{6} N^2$ is the number of degrees of freedom for each irreducible representation.

A.2.2 Periodic boundary conditions

In this subsection, we consider a cubic lattice with periodic boundary conditions containing $(2N)^3$ sites in each periodicity cell. A lattice wave function Φ can still be represented by a V -dimensional vector ϕ , using notations from the previous subsection, with the following constraint imposed by the boundary conditions:

$$\forall \mathbf{n} \in \mathbb{Z}^3, \forall \mathbf{r} \in \Lambda, \quad \mathbf{r} + 2N\mathbf{n} \in \Lambda \implies \phi_{u(\mathbf{r})} = \phi_{u(\mathbf{r}+2N\mathbf{n})}. \quad (\text{A.35})$$

\bar{r}	A_1^+	A_2^+	E^+	T_1^+	T_2^+	A_1^-	A_2^-	E^-	T_1^-	T_2^-
$(0, 0, N)$ or $(0, N, N)$	1		1							
(N, N, N)	1									
(a, N, N)	1		1						1	
$(0, a, N)$	1	1	2						1	1
(a, a, N)	1		1		1				1	1
(a, b, N)	1	1	2	1	1				2	2

Table A.2: Number of occurrences $N(\Gamma, \bar{r})$ of the irreducible representation Γ of the cubic group appearing in the decomposition (A.30) when periodic boundary are enforced and the orbit \bar{r} contains sites at the boundary. Empty cells mean zeros. The first column shows the kind of the representative of the orbit \bar{r} , with $0 < a < b < N$.

Define the functions $\tau_{\mathbf{n}}$ for $\mathbf{n} \in \mathbb{Z}^3$ such that for $r = 1, \dots, V$, $\tau_{\mathbf{n}}(r) = u(u^{-1}(r) + 2N\mathbf{n})$ if $u^{-1}(r) + 2N\mathbf{n} \in \Lambda$ and $\tau_{\mathbf{n}}(r) = r$ otherwise. These functions implement the translations by vectors $2N\mathbf{n}$ on the indices in $\{1, \dots, V\}$ through the bijection u . Now, define the matrices $T^{\mathbf{n}}$ with elements $T_{rr'}^{\mathbf{n}} = \delta_{r, \tau_{\mathbf{n}}(r')}$ for $\mathbf{n} \in \mathbb{Z}^3$. Then, the vectors of \mathbb{R}^V which can be identified with lattice wave functions are those left invariant by the matrices $T^{\mathbf{n}}$ for $\mathbf{n} \in \{-1, 0, 1\}^3$.

An operator acting on lattice wave functions can again be represented by a $V \times V$ matrix U which acts similarly on the V -dimensional-vector representations of the wave functions. To transform covariantly both under the cubic group rotations and the translations by $2N\mathbb{Z}^3$ required by the periodic boundary conditions, the matrix U must, in addition to (A.29), commute with the matrices $T^{\mathbf{n}}$, which is equivalent to

$$U_{\tau_{\mathbf{n}}(r), \tau_{\mathbf{n}}(r')} = U_{r, r'} \text{ for any } \mathbf{n} \in \{-1, 0, 1\}^3, (r, r') \in \{1, \dots, V\}^2. \quad (\text{A.36})$$

The matrices R^g combined with the matrices $T^{\mathbf{n}}$ define a representation \mathcal{R}' on \mathbb{R}^V of the direct sum of the cubic group and some other group. For the purpose of this paper, it suffice to say that this representation is equivalent to a representation \mathcal{R} of the cubic group, which has the decomposition described in (A.30), albeit with a different function $N(\Gamma, \bar{r})$ when \bar{r} is an orbit associated to lattice sites at the boundary. The changes are summarized in Table A.2.

All results from the previous subsection can then be transposed to the case of periodic boundary conditions, including the asymptotic behaviours in N since the boundary has a negligible effect. Note that the number of occurrences $N(\Gamma, \bar{r})$ at the boundary, and thus the number of actual degrees of freedom of U are logically decreased due to the additional constraint (A.36). Furthermore, the open or periodic boundary conditions make no difference for $N(\Gamma, \bar{r})$ when Γ is A_1^+ , A_2^+ or E^+ .

A.3 INVERSION PROBLEMS

A.3.1 Basic strategy

Suppose that we are given N_{src} pairs of lattice wave functions (Φ^i, X^i) . We wish to find an operator \hat{U} transforming covariantly under cubic symmetry such that $\hat{U}\Phi^i = X^i$ for $i = 0, \dots, N_{\text{src}}$.

Let (ϕ^i, χ^i) be the associated pairs of vectors of \mathbb{R}^V as defined in sec. A.2. The goal is then to find a $V \times V$ matrix U in \mathcal{C} such that

$$\forall i \in \{1, \dots, N_{\text{src}}\}, \quad U\phi^i = \chi^i. \quad (\text{A.37})$$

The lattice wave functions are assumed to transform as an irreducible representation (Γ, α) of the cubic group (with α in $1, \dots, d_\Gamma$), i.e.

$$\forall i \in \{1, \dots, N_{\text{src}}\}, \quad P^{\Gamma, \alpha} \phi^i = \phi^i, \quad P^{\Gamma, \alpha} \chi^i = \chi^i, \quad (\text{A.38})$$

using the orthogonal projectors $P^{\Gamma, \alpha} = \sum_{\tilde{r} \in \tilde{\Lambda}_\Gamma} \psi^{\Gamma \alpha \tilde{r}} [\psi^{\Gamma \alpha \tilde{r}}]^\dagger$. This means that the vectors can be expanded as

$$\forall i \in \{1, \dots, N_{\text{src}}\}, \quad \phi^i = \sum_{\tilde{r} \in \tilde{\Lambda}_\Gamma} \tilde{\phi}_{\tilde{r}}^i \psi^{\Gamma \alpha \tilde{r}}, \quad \chi^i = \sum_{\tilde{r} \in \tilde{\Lambda}_\Gamma} \tilde{\chi}_{\tilde{r}}^i \psi^{\Gamma \alpha \tilde{r}}, \quad (\text{A.39})$$

and the constraint (A.37) is reduced to

$$\forall i \in \{1, \dots, N_{\text{src}}\}, \quad \tilde{U}^\Gamma \tilde{\phi}^i = \tilde{\chi}^i, \quad (\text{A.40})$$

where \tilde{U}^Γ is the $N(\Gamma) \times N(\Gamma)$ matrix defined in (A.32). This matrix is $\sim (\frac{48}{d_\Gamma})^2$ times smaller than U . The purpose of appendix A.2 which led to this reduction is not only to drastically reduce the computational cost of the inversion but also to identify the independent degrees of freedom of the lattice wave functions in order to facilitate the inversion.

We propose a matrix \tilde{U}^Γ of the form

$$\tilde{U}^\Gamma = \sum_{j=1}^{N_{\text{dof}}} V_j M^j, \quad (\text{A.41})$$

for some unknown coefficients V_j and a predetermined set of linearly independent matrices M^j . $N_{\text{dof}} = N_{\text{src}} \times N(\Gamma)$ is the number of degrees of freedom fixed by the constraint (A.40).

The coefficients V_j needed to satisfy (A.40) are then found as solutions of the linear system

$$\forall i \in \{1, \dots, N_{\text{src}}\}, \quad \forall \tilde{r} \in \tilde{\Lambda}_\Gamma, \quad \sum_{j=1}^{N_{\text{dof}}} K_{i\tilde{r}, j} V_j = \tilde{\chi}_{\tilde{r}}^i, \quad (\text{A.42})$$

where the $N_{\text{dof}} \times N_{\text{dof}}$ matrix K is defined by its elements

$$K_{i\tilde{r}, j} = \sum_{\tilde{r}' \in \tilde{\Lambda}_\Gamma} M_{\tilde{r}, \tilde{r}'}^j \tilde{\phi}_{\tilde{r}'}^i. \quad (\text{A.43})$$

There is now a freedom to chose a set of matrices M^j such that

- \hat{U} inherits some desired properties,
- K has a moderate condition number to allow a stable numerical solution of (A.42).

A.3.2 Inversion with locality constraint

In this subsection, we discuss choices for matrices M^j such that the operator \hat{U} is only moderately non-local. We translate the non-locality of the operator to the non-locality of the matrix \tilde{U}^Γ using the indicator $R[\tilde{U}^\Gamma]$ which is defined as

$$R[A] = \max \left\{ d(\tilde{r}, \tilde{r}') \mid \tilde{r}, \tilde{r}' \in \tilde{\Lambda}_\Gamma, \tilde{A}_{\tilde{r}, \tilde{r}'} \neq 0 \right\}. \quad (\text{A.44})$$

where the distance between $\tilde{r} = (\bar{r}, \nu)$ and $\tilde{r}' = (\bar{r}', \nu')$ in $\tilde{\Lambda}_\Gamma$ is $d(\tilde{r}, \tilde{r}') = \|\bar{r} - \bar{r}'\|$, the distance between the representatives of the orbits \bar{r} and \bar{r}' .

For each \tilde{r} in $\tilde{\Lambda}_\Gamma$, define a bijection $l \mapsto \omega_l^{\tilde{r}}$ from $\{1, \dots, N(\Gamma)\}$ to $\tilde{\Lambda}_\Gamma$ such that $d(\tilde{r}, \omega_l^{\tilde{r}})$ is increasing with l . We can then define matrices $M^{(\tilde{r}, l)}$ for $l = 1, \dots, N(\Gamma)$ with elements $M_{\tilde{r}', \tilde{r}''}^{(\tilde{r}, l)} = \delta_{\tilde{r}', \tilde{r}} \delta_{\tilde{r}'', \omega_l^{\tilde{r}}}$ for which the non-locality $R[M^{(\tilde{r}, l)}]$ increases with l .

With some irrelevant numbering \tilde{r}_k of the elements of $\tilde{\Lambda}_\Gamma$, a natural choice of matrices M^j for $j = 1, \dots, N_{\text{dof}}$ is $M^{LN(\Gamma)+k} = M^{(\tilde{r}_k, l)}$. As the number of wave functions N_{src} increases, this set includes matrices with increasing non-locality. The elements of the matrix K are then

$$K_{i\tilde{r}, lN(\Gamma)+k} = \delta_{\tilde{r}, \tilde{r}_k} \tilde{\phi}_{\omega_l^{\tilde{r}}}^i, \quad (\text{A.45})$$

so that K is block diagonal with a block for each element of $\tilde{\Lambda}_\Gamma$. The linear system (A.42) can thus be solved efficiently block by block.

In practice, this construction is found to be numerically unstable due to large condition numbers for some blocks of K . To overcome this problem, we allow slightly more non-locality in order to find an optimal set of matrices M^j . For each \tilde{r} in $\tilde{\Lambda}_\Gamma$, we have previously only considered matrices $M^{(\tilde{r}, l)}$ with l up to N_{src} . Instead, we now consider all indices l up to $N(\tilde{r}, R_{\text{max}}) = \max \{l \in \{1, \dots, N(\Gamma)\} \mid d(\tilde{r}, \omega_l^{\tilde{r}}) \leq R_{\text{max}}\}$, i.e. all matrices with a non-locality less than or equal to R_{max} . We then build the $N_{\text{src}} \times N(\tilde{r}, R_{\text{max}})$ matrix $K^{\tilde{r}}$ with elements

$$K_{i,l}^{\tilde{r}} = \tilde{\phi}_{\omega_l^{\tilde{r}}}^i. \quad (\text{A.46})$$

Note that R_{max} must be large enough that $N(\tilde{r}, R_{\text{max}}) \geq N_{\text{src}}$ for all \tilde{r} . Now, consider the singular value decomposition (SVD) of $K^{\tilde{r}}$ as $K^{\tilde{r}} = A^{\tilde{r}} D^{\tilde{r}} [B^{\tilde{r}}]^\dagger$ with the diagonal elements of $D^{\tilde{r}}$ in decreasing order. The coefficients in the N_{src} first columns of $B^{\tilde{r}}$ allow to chose a set of matrices M^j with a non-locality bounded by R_{max} and such that K has a minimal condition number. This choice is

$$M^{LN(\Gamma)+k} = \sum_{l'=1}^{N(\tilde{r}_k, R_{\text{max}})} [B^{\tilde{r}_k}]_{l', l} M^{(\tilde{r}_k, l')}. \quad (\text{A.47})$$

so that the elements of K become $K_{i\tilde{r}, lN(\Gamma)+k} = \delta_{\tilde{r}, \tilde{r}_k} [A^{\tilde{r}} D^{\tilde{r}}]_{il}$.

With $R_{\text{max}} \ll N$, as is usually the case, all the considered matrices are sparse, which allows fast implementations of this method.

A.3.3 Inversion with Hermiticity and locality constraints

In this subsection, we add a constraint of Hermiticity on the operator \hat{U} . For this, we choose a set of matrices M^j which are symmetric and moderately non-local. Consider the set of unordered pairs $(\tilde{r}_l, \tilde{r}'_l) \in \tilde{\Lambda}_\Gamma^2$ indexed by $l = 1, \dots, \frac{1}{2}N(\Gamma)(N(\Gamma)+1)$ such that $d(\tilde{r}_l, \tilde{r}'_l)$ increases with l . Then, a choice of matrices M^j are the matrices with elements $M_{\tilde{r}, \tilde{r}'}^j = \delta_{\tilde{r}, \tilde{r}'_j} \delta_{\tilde{r}', \tilde{r}_j} + (\tilde{r} \leftrightarrow \tilde{r}')$. These matrices are symmetric and their non-locality increases with j . The matrix K then has elements

$$K_{i\tilde{r}, j} = \delta_{\tilde{r}, \tilde{r}_l} \tilde{\phi}_{\tilde{r}'_l}^i + \delta_{\tilde{r}, \tilde{r}'_l} \tilde{\phi}_{\tilde{r}_l}^i. \quad (\text{A.48})$$

Contrary to the previous section, the matrix K is not block diagonal so that the system (A.42) must be solved as a whole. Furthermore, this leads in practice to very high condition numbers for K .

As previously, a way to reduce the condition number of K is to allow more non-local matrices and select the optimal ones. This can be done by enlarging K as a

rectangular matrix with elements $K_{i\tilde{r},j}$ for $j > N_{\text{dof}}$. The SVD of this rectangular matrix K leads the optimal set of matrices M^j . However, it is found in practice that even such a construction suffers from large condition numbers for K . Hopefully, another construction might lead to a practical way to extract an Hermitian operator \hat{U} with locality constraints.

Details for the kernel approximation method

B.1 FOURIER TRANSFORM OF A 3D COMPACTLY SUPPORTED FUNCTION

In this section, we prove Proposition 4.2 which is mostly a corollary of the Paley-Wiener theorem. The expansion of the Fourier transform \hat{h} on the spherical harmonics is written by

$$\hat{h}(\mathbf{p}) = \sum_{l=0}^{\infty} \sum_{m=-l}^l [\hat{h}]_{lm}(p) Y_{lm}(\hat{\mathbf{p}}), \quad (\text{B.1})$$

where the radial functions are related to those of h by

$$[\hat{h}]_{lm}(p) = 4\pi(-i)^l \int_0^R dr r^2 j_l(pr) [h]_{lm}(r) \quad \text{for } p \in [0, \infty[, \quad (\text{B.2})$$

and reciprocally

$$[h]_{lm}(r) = \frac{i^l}{2\pi^2} \int_0^{\infty} dp p^2 j_l(pr) [\hat{h}]_{lm}(p) \quad \text{for } r \in [0, \infty[. \quad (\text{B.3})$$

Take $l \geq 0$ any angular momentum and any $m = -l, \dots, l$. Since h is smooth, $[\hat{h}]_{lm}(p)$ decays at large p faster than any power of p^{-1} . We can then use Lebesgue's dominated convergence theorem and the well-known behavior of j_l at the origin to show that

$$\lim_{r \rightarrow 0} r^{-l} [h]_{lm}(r) = \frac{i^l}{2\pi^2} \int_0^{\infty} dp \frac{p^{l+2}}{(2l+1)!!} [\hat{h}]_{lm}(p) < \infty. \quad (\text{B.4})$$

Using Rayleigh's formula for j_l , we can rewrite (B.2) as

$$[\hat{h}]_{lm}(p) = 4\pi(-ip)^l \left(-\frac{1}{p} \frac{d}{dp} \right)^l \frac{1}{2ip} I_{lm}(p) \quad (\text{B.5})$$

with the integral

$$I_{lm}(p) = 2ip \int_0^R dr j_0(pr) r^{2-l} [h]_{lm}(r). \quad (\text{B.6})$$

Extend the function $[h]_{lm}$ to $[-R, R]$ by $[h]_{lm}(-r) = (-1)^l [h]_{lm}(r)$ so that

$$I_{lm}(p) = \int_{-R}^R dr e^{ipr} r^{1-l} [h]_{lm}(r). \quad (\text{B.7})$$

$[h]_{lm}$ is continuous on $[0, R]$ and given its behavior at the origin (B.4), $r^{1-l}[h]_{lm}(r)$ is square-integrable on $[-R, R]$. We can then use the Paley-Wiener theorem to conclude that $I_{lm}(p)$ can be extended on the complex plane to an entire function of p of exponential type R .

Since $I_{lm}(p)$ is odd, let

$$I_{lm}(p) = \sum_{n=0}^{\infty} a_n p^{2n+1}. \quad (\text{B.8})$$

Using (B.5) we obtain for any real $p > 0$,

$$f_{lm}(p) \equiv p^{-l}[\hat{h}]_{lm}(p) = -\pi(2i)^{l+1} \sum_{n=0}^{\infty} \frac{(n+l)!}{n!} a_{n+l} p^{2n}. \quad (\text{B.9})$$

Given the properties of $I_{lm}(p)$, it is straightforward to conclude that f_{lm} can also be extended to an (even) entire function of p of exponential type R .

Combining results for all pairs (l, m) , we obtain the desired result

$$\hat{h}(\mathbf{p}) = \sum_{l=0}^l \sum_{m=-l}^l p^l f_{lm}(p) Y_{lm}(\hat{\mathbf{p}}). \quad (\text{B.10})$$

B.2 RELATION BETWEEN THE FINITE- AND INFINITE-VOLUME 4-POINT FUNCTIONS

The ‘‘projected’’ infinite-volume 4-point function \tilde{G}_4 is composed of the following integrals

$$I_n(\mathbf{p}', \mathbf{p}) \equiv \int \prod_{i=1}^n \frac{d^3 \mathbf{k}_i}{(2\pi)^3} \tilde{U}(\mathbf{p}', \mathbf{k}_1) R(\mathbf{k}_1) \tilde{U}(\mathbf{k}_1, \mathbf{k}_2) \cdots R(\mathbf{k}_n) \tilde{U}(\mathbf{k}_n, \mathbf{p}) \quad (\text{B.11})$$

where $n \geq 1$, \mathbf{p}' and \mathbf{p} in \mathbb{R}^3 . For $n = 0$, we set $I_0 = \tilde{U}$. Using (4.88), we can define the infinite matrices \mathcal{I}_n , \mathcal{I}_n° , \mathcal{I}_n^\bullet and $\mathcal{I}_n^{\bullet\bullet}$.

We first analyze the integral for $n = 1$, i.e. with integration over only one momentum, following [38] and [63]. Expand the dependence on the integrated momentum over the spherical harmonics as

$$I_1(\mathbf{p}', \mathbf{p}) \equiv \int \frac{d^3 \mathbf{k}}{(2\pi)^3} \tilde{U}(\mathbf{p}', \mathbf{k}) R(\mathbf{k}) \tilde{U}(\mathbf{k}, \mathbf{p}) = \sum_{lm} \int \frac{d^3 \mathbf{k}}{(2\pi)^3} f_{lm}(k) \frac{k^l Y_{lm}(\hat{\mathbf{k}})}{k^2 - q^2 - i\epsilon}, \quad (\text{B.12})$$

for some radial functions f_{lm} related to \tilde{U} . Remember that $W = 2\omega_q + i\epsilon$.

Add and subtract a function then reorganize the terms to obtain

$$I_1(\mathbf{p}', \mathbf{p}) = \sum_{lm} f_{lm}(q) \int \frac{d^3 \mathbf{k}}{(2\pi)^3} \frac{k^l Y_{lm}(\hat{\mathbf{k}}) e^{\alpha(q^2 - k^2)}}{k^2 - q^2 - i\epsilon} + \sum_{lm} \int \frac{d^3 \mathbf{k}}{(2\pi)^3} \left[f_{lm}(k) - f_{lm}(q) e^{\alpha(q^2 - k^2)} \right] \frac{k^l Y_{lm}(\hat{\mathbf{k}})}{k^2 - q^2 - i\epsilon}, \quad (\text{B.13})$$

where $\alpha > 0$. This function is chosen such that the integrands in the second term are not singular anymore. Relating them to \tilde{U} , we can work out from Theorem 4.1 their analyticity domain and use Proposition 4.3 to convert the integral into a sum, up to

corrections decaying exponentially with the volume. Neglecting these corrections, we get

$$I_1(\mathbf{p}', \mathbf{p}) = \frac{iqf_{00}(q)}{8\pi^{3/2}} + \sum_{lm} f_{lm}(q) \text{PV} \int \frac{d^3\mathbf{k}}{(2\pi)^3} k^l Y_{lm}(\hat{\mathbf{k}}) \frac{e^{\alpha(q^2-k^2)}}{k^2-q^2} + \sum_{lm} \frac{1}{L^3} \sum_{\mathbf{k} \in \Lambda} \left[f_{lm}(k) - f_{lm}(q) e^{\alpha(q^2-k^2)} \right] \frac{k^l Y_{lm}(\hat{\mathbf{k}})}{k^2-q^2}, \quad (\text{B.14})$$

where PV denotes the principal value. To obtain the first two terms, we used $\frac{1}{k^2-q^2-i\epsilon} = i\pi\delta(k^2-q^2) + \text{PV} \frac{1}{k^2-q^2}$ on the first term of (B.13). Rearranging the terms we finally obtain

$$I_1(\mathbf{p}', \mathbf{p}) = \frac{1}{L^3} \sum_{\mathbf{k} \in \Lambda} \sum_{lm} f_{lm}(k) \frac{k^l Y_{lm}(\hat{\mathbf{k}})}{k^2-q^2} + \frac{iqf_{00}(q)}{8\pi^{3/2}} + \sum_{lm} f_{lm}(q) c_{lm}(1; q), \quad (\text{B.15})$$

where

$$c_{lm}(s; q) = \left[\text{PV} \int \frac{d^3\mathbf{k}}{(2\pi)^3} - \frac{1}{L^3} \sum_{\mathbf{k} \in \Lambda} \right] \frac{k^l Y_{lm}(\hat{\mathbf{k}}) e^{\alpha(q^2-k^2)^s}}{(k^2-q^2)^s} \quad (\text{B.16})$$

is defined for $\text{Re } s > 0$. Note that $c_{lm}(s; q)$ does not actually depend on $\alpha > 0$ (derive by α to see this). Furthermore, in the complex region $\text{Re } 2s > l + 3$, we can take the limit $\alpha \rightarrow 0$ to obtain¹

$$c_{lm}(s; q) = -\frac{1}{L^3} \left(\frac{2\pi}{L} \right)^{l-2s} \mathcal{Z}_{lm} \left(s; \frac{qL}{2\pi} \right), \quad (\text{B.17})$$

with the Zeta function

$$\mathcal{Z}_{lm}(s; x) = \sum_{\mathbf{k} \in \mathbb{Z}^3} \frac{k^l Y_{lm}(\hat{\mathbf{k}})}{(k^2-x^2)^s}. \quad (\text{B.18})$$

In the rest of the complex plane for s , $\mathcal{Z}_{lm}(s; x)$ can be analytically continued so that (B.17) still holds at $s = 1$.

We can now express f_{lm} back in terms of \tilde{U} in (B.15) to get

$$I_1(\mathbf{p}', \mathbf{p}) = \frac{1}{L^3} \sum_{\mathbf{k} \in \Lambda} \tilde{U}(\mathbf{p}', \mathbf{k}) R(\mathbf{k}) \tilde{U}(\mathbf{k}, \mathbf{p}) + \sum_{l_1 m_1} \sum_{l_2 m_2} \left[\int d\hat{\mathbf{q}} \tilde{U}(\mathbf{p}', \hat{\mathbf{q}}) Y_{l_1 m_1}(\hat{\mathbf{q}}) \right] [\mathcal{M}^{\bullet\bullet}]_{l_1 m_1, l_2 m_2} \left[\int d\hat{\mathbf{q}} Y_{l_2 m_2}^*(\hat{\mathbf{q}}) \tilde{U}(\hat{\mathbf{q}}, \mathbf{p}) \right], \quad (\text{B.19})$$

where $\mathbf{q} = q\hat{\mathbf{q}}$ is on-shell and the matrix $\mathcal{M}^{\bullet\bullet}$ has elements

$$[\mathcal{M}^{\bullet\bullet}]_{l_1 m_1, l_2 m_2} = \frac{imq}{(4\pi)^2} \left[\delta_{l_1 m_1, l_2 m_2} + \sum_{lm} \frac{(4\pi)^2}{iq^{l+1}} c_{lm}(1; q) \int d\hat{\mathbf{q}} Y_{l_1 m_1}^*(\hat{\mathbf{q}}) Y_{lm}^*(\hat{\mathbf{q}}) Y_{l_2 m_2}(\hat{\mathbf{q}}) \right]. \quad (\text{B.20})$$

Note that $\mathcal{M}^{\bullet\bullet} = \frac{imq}{(4\pi)^2} (1 + iM)$ where M is the matrix used in eq. (4.10) of ref. [9].

Equation (B.19) may be summarized in terms of matrices as

$$\mathcal{I}_1 = \tilde{U} \mathcal{R} \tilde{U} + \tilde{U}^{\bullet\bullet} \mathcal{M}^{\bullet\bullet} \tilde{U}^{\bullet\bullet} = \mathcal{I}_0 \mathcal{R} \mathcal{I}_0 + \mathcal{I}_0^{\bullet\bullet} \mathcal{M}^{\bullet\bullet} \mathcal{I}_0^{\bullet\bullet}. \quad (\text{B.21})$$

and similar relations for $\mathcal{I}_1^{\bullet\bullet}$, etc.

¹ It is straightforward for $l \geq 1$ but more involved for $l = 0$.

For $n \geq 2$, \mathcal{I}_n is an integral over several continuous momenta. We can choose any one of these momenta and apply the same argument as before to replace its integration by a sum and an on-shell projection, while leaving the integration over the other momenta unchanged. This leads to the relation

$$\mathcal{I}_{m+n+1} = \mathcal{I}_m \mathcal{R} \mathcal{I}_n + \mathcal{I}_m^{\circ\bullet} \mathcal{M}^{\bullet\bullet} \mathcal{I}_n^{\circ\bullet}, \quad (\text{B.22})$$

and similar ones for $\mathcal{I}_n^{\circ\bullet}$, etc.

The “projected” finite-volume 4-point function $\tilde{\mathcal{G}}_{4L}$ is composed of the following sums over Λ

$$\mathcal{J}_n \equiv \tilde{\mathcal{U}}(\mathcal{R}\tilde{\mathcal{U}})^n = \mathcal{I}_0(\mathcal{R}\mathcal{I}_0)^n. \quad (\text{B.23})$$

Using (B.22), it is easy to prove by recurrence the following expression of \mathcal{J}_n in terms of the integrals \mathcal{I}_n

$$\mathcal{J}_n = \mathcal{I}_n + \sum_{m=1}^n (-1)^m \sum_{\substack{n_0+\dots+n_m=n-m \\ n_i=0,1,\dots}} \mathcal{I}_{n_0}^{\circ\bullet} \mathcal{M}^{\bullet\bullet} \mathcal{I}_{n_1}^{\circ\bullet} \mathcal{M}^{\bullet\bullet} \dots \mathcal{I}_{n_{m-1}}^{\circ\bullet} \mathcal{M}^{\bullet\bullet} \mathcal{I}_{n_m}^{\circ\bullet}. \quad (\text{B.24})$$

Note that this relation still holds if we replace \mathcal{I}_n by $\hat{\mathcal{I}}_n = (-1)^{n+1} \mathcal{I}_n$ and \mathcal{J}_n by $\hat{\mathcal{J}}_n = (-1)^{n+1} \mathcal{J}_n$. Summing over n , we finally get

$$\sum_{n=0}^{\infty} \hat{\mathcal{J}}_n = \sum_{n=0}^{\infty} \hat{\mathcal{I}}_n + \sum_{m=1}^{\infty} (-1)^m \left[\sum_{n=0}^{\infty} \hat{\mathcal{I}}_n^{\circ\bullet} \right] \left\{ \mathcal{M}^{\bullet\bullet} \sum_{n=0}^{\infty} \hat{\mathcal{I}}_n^{\circ\bullet} \right\}^{m-1} \mathcal{M}^{\bullet\bullet} \left[\sum_{n=0}^{\infty} \hat{\mathcal{I}}_n^{\circ\bullet} \right], \quad (\text{B.25})$$

which is nothing but

$$\tilde{\mathcal{G}}_{4L} = \tilde{\mathcal{G}}_4 + \sum_{m=1}^{\infty} (-1)^m \tilde{\mathcal{G}}_4^{\circ\bullet} \left\{ \mathcal{M}^{\bullet\bullet} \tilde{\mathcal{G}}_4^{\circ\bullet} \right\}^{m-1} \mathcal{M}^{\bullet\bullet} \tilde{\mathcal{G}}_4^{\circ\bullet}. \quad (\text{B.26})$$

We have thus proven equation (4.89).

Bibliography

- [1] B. Charron (HAL QCD Collaboration), PoS **LATTICE2012**, 258 (2012), arXiv:1212.6333
- [2] B. Charron (HAL QCD Collaboration), PoS **LATTICE2013**, 223 (2013), arXiv:1312.1032 [hep-lat]
- [3] S. Aoki, B. Charron, T. Doi, T. Hatsuda, T. Inoue, *et al.*, Phys.Rev. **D87**, 034512 (2013), arXiv:1212.4896 [hep-lat]
- [4] Y. Ikeda, B. Charron, S. Aoki, T. Doi, T. Hatsuda, *et al.*, Phys.Lett. **B729**, 85 (2014), arXiv:1311.6214 [hep-lat]
- [5] D. J. Gross and F. Wilczek, Phys.Rev.Lett. **30**, 1343 (1973)
- [6] K. G. Wilson, Phys.Rev. **D10**, 2445 (1974)
- [7] S. Durr, Z. Fodor, J. Frison, C. Hoelbling, R. Hoffmann, *et al.*, Science **322**, 1224 (2008), arXiv:0906.3599 [hep-lat]
- [8] M. Luscher, Commun.Math.Phys. **105**, 153 (1986)
- [9] M. Luscher, Nucl.Phys. **B354**, 531 (1991)
- [10] N. Ishii, S. Aoki, and T. Hatsuda, Phys.Rev.Lett. **99**, 022001 (2007), arXiv:nucl-th/0611096 [nucl-th]
- [11] S. Aoki, T. Hatsuda, and N. Ishii, Comput.Sci.Dis. **1**, 015009 (2008), arXiv:0805.2462 [hep-ph]
- [12] S. Aoki, T. Hatsuda, and N. Ishii, Prog.Theor.Phys. **123**, 89 (2010), arXiv:0909.5585 [hep-lat]
- [13] T. Kurth, N. Ishii, T. Doi, S. Aoki, and T. Hatsuda, JHEP **1312**, 015 (2013), arXiv:1305.4462 [hep-lat]
- [14] K. Murano, N. Ishii, S. Aoki, and T. Hatsuda, Prog.Theor.Phys. **125**, 1225 (2011), arXiv:1103.0619 [hep-lat]
- [15] I. Montvay and G. Munster, *Quantum fields on a lattice* (1994)
- [16] M. Creutz(1984)
- [17] H. Rothe, *Lattice gauge theories: An Introduction*, Vol. 43 (1992) pp. 1–381

- [18] C. Gattringer and C. B. Lang, *Quantum chromodynamics on the lattice*, Vol. 788 (2010) pp. 1–343
- [19] M. Luscher and U. Wolff, Nucl.Phys. **B339**, 222 (1990)
- [20] B. Blossier, M. Della Morte, G. von Hippel, T. Mendes, and R. Sommer, JHEP **0904**, 094 (2009), arXiv:0902.1265 [hep-lat]
- [21] K. Rummukainen and S. A. Gottlieb, Nucl.Phys. **B450**, 397 (1995), arXiv:hep-lat/9503028 [hep-lat]
- [22] X. Li and C. Liu, Phys.Lett. **B587**, 100 (2004), arXiv:hep-lat/0311035 [hep-lat]
- [23] S. Ozaki and S. Sasaki, Phys.Rev. **D87**, 014506 (2013), arXiv:1211.5512 [hep-lat]
- [24] R. A. Briceno, Phys.Rev. **D89**, 074507 (2014), arXiv:1401.3312 [hep-lat]
- [25] M. T. Hansen and S. R. Sharpe, Phys.Rev. **D86**, 016007 (2012), arXiv:1204.0826 [hep-lat]
- [26] R. A. Briceno and Z. Davoudi, Phys.Rev. **D87**, 094507 (2013), arXiv:1212.3398 [hep-lat]
- [27] M. Luscher, Commun.Math.Phys. **104**, 177 (1986)
- [28] S. Aoki *et al.* (HAL QCD Collaboration), PTEP **2012**, 01A105 (2012), arXiv:1206.5088 [hep-lat]
- [29] C. D. Lin, G. Martinelli, C. T. Sachrajda, and M. Testa, Nucl.Phys. **B619**, 467 (2001), arXiv:hep-lat/0104006 [hep-lat]
- [30] S. Aoki *et al.* (CP-PACS Collaboration), Phys.Rev. **D71**, 094504 (2005), arXiv:hep-lat/0503025 [hep-lat]
- [31] W. Zimmermann, “COMPOSITE FIELD OPERATORS IN QUANTUM FIELD THEORY,” (1987)
- [32] S. Okubo and R. Marshak, Annals of Physics **4**, 166 (1958), ISSN 0003-4916, <http://www.sciencedirect.com/science/article/pii/0003491658900319>
- [33] N. Ishii *et al.* (HAL QCD Collaboration), Phys.Lett. **B712**, 437 (2012), arXiv:1203.3642 [hep-lat]
- [34] T. Doi, “Time-dependent Schrödinger equation for unequal mass case,” unpublished (2011)
- [35] S. Aoki, N. Ishii, T. Doi, Y. Ikeda, and T. Inoue, Phys.Rev. **D88**, 014036 (2013), arXiv:1303.2210 [hep-lat]
- [36] S. Aoki *et al.* (HAL QCD Collaboration), Proc.Japan Acad. **B87**, 509 (2011), arXiv:1106.2281 [hep-lat]
- [37] C. D. Lin, G. Martinelli, C. Sachrajda, and M. Testa, Nucl.Phys.Proc.Suppl. **109A**, 218 (2002), arXiv:hep-lat/0111033 [hep-lat]
- [38] C. Kim, C. Sachrajda, and S. R. Sharpe, Nucl.Phys. **B727**, 218 (2005), arXiv:hep-lat/0507006 [hep-lat]

-
- [39] A. Klein and T.-S. H. Lee, Phys.Rev. **D10**, 4308 (1974)
- [40] C. Schwartz, Journal of Mathematical Physics **23**, 2266 (1982), <http://scitation.aip.org/content/aip/journal/jmp/23/12/10.1063/1.525317>
- [41] J. J. Dudek, R. G. Edwards, and C. E. Thomas, Phys.Rev. **D86**, 034031 (2012), arXiv:1203.6041 [hep-ph]
- [42] S. Beane *et al.* (NPLQCD Collaboration), Phys.Rev. **D85**, 034505 (2012), arXiv:1107.5023 [hep-lat]
- [43] S. Aoki *et al.* (PACS-CS Collaboration), Phys.Rev. **D79**, 034503 (2009), arXiv:0807.1661 [hep-lat]
- [44] S. Aoki *et al.* (CS Collaboration), Phys.Rev. **D84**, 094505 (2011), arXiv:1106.5365 [hep-lat]
- [45] C. Lang, D. Mohler, S. Prelovsek, and M. Vidmar, Phys.Rev. **D84**, 054503 (2011), arXiv:1105.5636 [hep-lat]
- [46] J. Frison *et al.* (Budapest-Marseille-Wuppertal Collaboration), PoS **LATTICE2010**, 139 (2010), arXiv:1011.3413 [hep-lat]
- [47] X. Feng, K. Jansen, and D. B. Renner, Phys.Rev. **D83**, 094505 (2011), arXiv:1011.5288 [hep-lat]
- [48] T. Ishikawa *et al.* (JLQCD Collaboration), Phys.Rev. **D78**, 011502 (2008), arXiv:0704.1937 [hep-lat]
- [49] R. L. Jaffe, Phys.Rev.Lett. **38**, 195 (1977)
- [50] H. J. Lipkin, Phys.Lett. **B172**, 242 (1986)
- [51] J. Carlson, L. Heller, and J. Tjon, Phys.Rev. **D37**, 744 (1988)
- [52] S. H. Lee and S. Yasui, Eur.Phys.J. **C64**, 283 (2009), arXiv:0901.2977 [hep-ph]
- [53] E. Eichten, Nucl.Phys.Proc.Suppl. **4**, 170 (1988)
- [54] G. Lepage and B. Thacker, Nucl.Phys.Proc.Suppl. **4**, 199 (1988)
- [55] F. Karsch, Nucl.Phys. **B205**, 285 (1982)
- [56] S. Aoki, Y. Kuramashi, and S.-i. Tominaga, Prog.Theor.Phys. **109**, 383 (2003), arXiv:hep-lat/0107009 [hep-lat]
- [57] K. Symanzik, Nucl.Phys. **B226**, 187 (1983)
- [58] Y. Namekawa *et al.* (PACS-CS Collaboration), Phys.Rev. **D84**, 074505 (2011), arXiv:1104.4600 [hep-lat]
- [59] H. Nemura, N. Ishii, S. Aoki, and T. Hatsuda, Phys.Lett. **B673**, 136 (2009), arXiv:0806.1094 [nucl-th]
- [60] T. Inoue *et al.* (HAL QCD collaboration), Prog.Theor.Phys. **124**, 591 (2010), arXiv:1007.3559 [hep-lat]

- [61] N. Ishii (PACS-CS Collaboration, HAL-QCD Collaboration), PoS **LAT2009**, 019 (2009), arXiv:1004.0405 [hep-lat]
- [62] K. Sasaki (HAL QCD collaboration), PoS **LATTICE2010**, 157 (2010), arXiv:1012.5685 [hep-lat]
- [63] R. A. Briceno, *On the Determination of Elastic and Inelastic Nuclear Observables from Lattice QCD*, Ph.D. thesis (2013), arXiv:1311.6032 [hep-lat]